

平成 29 年度博士学位論文

Studies on geranylgeranoic acid-induced cell death: with special attention
to pyroptosis in human hepatoma cells

ゲラニルゲラノイン酸誘導性細胞死に関する研究
-特にヒト肝癌細胞におけるパイロトーシスについて-

D3215001

藪田末美

2018 年 3 月
長崎県立大学大学院
人間健康科学研究科 栄養科学専攻

専攻分野 細胞生化学

指導教員 四童子好廣

印



Contents

Chapter 0: Foundation research	1
Abstract.....	2
0-1. Introduction	3
0-1-1. Telomeres	3
0-1-2. Nutritional perturbation of telomere length shortening	3
0-1-3. β-Carotene metabolism-related genes	4
0-2. Results	6
0-2-1. Characteristics of subjects	6
0-2-2. Circulating β-carotene levels in each genotype group	7
0-2-3. Buccal RTLs and FFQ	8
0-2-4. Measurement of transcribed telomere repeats	10
0-2-5. Retinoids downregulated <i>TERRA</i>	12
0-3. Discussion	13
Chapter I: General Introduction	16
I-1. Diterpenoid acids or acyclic retinoids	17
I-2. Geranylgeranoic acid (GGA)	18
I-3. GGA-induced cell death	19
I-3-1. GGA-induced mitochondrial impairment	21
I-3-2. GGA-induced nuclear translocation of the mutant p53	21
I-3-3. GGA-induced incomplete autophagic response	24
I-3-4. Lipid-induced unfolded protein responses	27
I-3-5. Rapid downregulation of cyclin D1	30
I-4. Programmed cell death	34
I-5. Brief outline of the thesis	38
Chapter II: Pyroptotic cell death with GGA through canonical inflammasome	39
Abstract.....	40
II-1. Introduction	41
II-1-1. Pyroptosis	41

II-1-2. Canonical inflammasomes: NLR and ALR inflammasomes	42
II-1-3. Mechanisms of NLRP3 inflammasome activation	44
II-1-4. NLRP3 inflammasome priming: first hit	47
II-1-5. NLRP3 inflammasome activation: second hit	48
II-1-6. Expression of NLRP3 through NF- κ B.....	49
II-1-7. Downstream signals of TLRs.....	50
II-1-8. Pyroptosis interacts with UPR	55
II-1-9. Gasdermin D is emerging as executors of pyroptosis	57
II-1-10. GSDMD-N forms functional pores	59
II-2. Results	60
II-2-1. Activation of caspase-1 activity after GGA treatment	60
II-2-2. GGA induced priming of inflammasome activation in HuH-7 cells	62
II-2-3. NF- κ B relocates from the cytoplasm to the nucleus after GGA treatment	64
II-2-4. Translocation for plasma membrane of GSDMD after GGA treatment	66
II-2-5. Morphological alterations and membrane damages after GGA treatment	68
II-2-6. GGA-induced cell death via TLR4 signaling	70
II-2-7. GGA-induced UPR upregulates TLR2 expression.....	76
II-2-8. ATRA did not induce pyroptotic cell death.....	80
II-3. Discussion	82
Chapter III: Pyroptotic cell death with GGA through noncanonical inflammasome.....	87
Abstract.....	88
III-1. Introduction	89
III-1-1. Non-canonical inflammasome pathway.....	89
III-1-2. Priming of the non-canonical inflammasome.....	90
III-1-3. Non-canonical pathway interacts with UPR	91
III-2. Results.....	93
III-2-1. GGA-induced pyroptosis via non-canonical inflammasome pathway in HuH-7 cells.....	93

III-2-2. UPR induces the activation of caspase-4	95
III-2-3. Increase of intracellular calcium concentration via UPR in HuH-7 cells	97
III-3. Discussion	102
Chapter IV: Epigenetic aspect of cancer chemoprevention with GGA	105
Abstract	106
IV-1. Introduction	107
IV-1-1. Epigenetic regulatory mechanisms	107
IV-1-2. Histone modification	107
IV-1-3. Lysine-specific demethylase 1A (LSD1/KDM1A)	109
IV-1-4. Another lysine-specific demethylase for histone H3 (KDM5A)	112
IV-1-5. Aim of the present study in this chapter	112
IV-2. Results	114
IV-2-1. Cytoplasmic translocation of nuclear KDM1A induced by GGA or TCP	114
IV-2-2. Specificity for KDM1A inhibitors and nuclear KDMs	116
IV-2-3. Subcellular distribution of KDM1A in M-phase cells	118
IV-2-4. Release of nuclear KDM1A by GGA or TCP under cell-free conditions	120
IV-3. Discussion	122
Chapter V: General Discussion	126
V-1. How does GGA induce cell death in HuH-7 cells?	127
V-1-1. Previous studies on GGA-induced cell death in HuH-7 cells	127
V-1-2. Anti-tumorigenic effects of GGA other than inflammatory cell death	128
V-2. Inflammation	129
V-2-1. GGA-induced inflammatory response with UPR and autophagy	130
V-2-2. GGA-induced pyroptosis occurred in hepatoma cells	131
V-2-3. GGA in comparison with LPS, in terms of TLR4 signaling	132
V-3. How does GGA work in highly TLR4-expressing cells such as macrophage?	133
V-4. To be, or not to be in inflammation	134
V-5. Cancer prevention with GGA	135
V-5-1. Between secondary and tertiary prevention by using GGA	135

V-5-2. Primary prevention with GGA	136
Chapter VI: Materials and methods	139
VI. Materials and methods	140
VI-1. Materials	140
VI-1-1. Instruments	140
VI-1-2. Chemical reagents	142
VI-1-3. Cell culture compounds	144
VI-1-4. Kits	145
VI-1-5. Antibodies	145
VI-1-6. Cell line	146
VI-1-7. Solutions and Buffers	147
VI-2. Methods	149
VI-2-1. Study population	149
VI-2-2. Food frequency questionnaire (FFQ)	149
VI-2-3. DNA-preparation	150
VI-2-4. RTLs determination	151
VI-2-5. Genotyping	152
VI-2-6. Measurement of serum β-carotene	152
VI-2-7. Cell culture	153
VI-2-8. Sodium dodecyl sulfate polyacrylamide gel electrophoresis (SDS-PAGE) and immunoblotting	153
VI-2-9. Cell-free analysis	155
VI-2-10. Isolation of total cellular RNA	155
VI-2-11. Reverse transcription for cDNA synthesis	155
VI-2-12. Real-time PCR	156
VI-2-13. ROS detection	159

VI-2-14. Ca²⁺ fluorescence imaging	159
VI-2-15. Fluorescent immunostaining	159
VI-2-16. Caspase-Glo1 assay	160
VI-2-17. Cell viability assay	160
VI-2-18. LDH assay	161
VI-2-19. Statistical analysis	161
Notes	162
Acknowledgments	163
References	164

List of abbreviations

9CRA	9- <i>cis</i> retinoic acid
AD	allele discrimination
ADP	adenosine diphosphate
AIM	absent in melanoma
ALR	AIM-like receptor
AM	acetoxymethyl
AMP	adenosine monophosphate
AP	activator protein
APAF	apoptotic protease activating factor
APS	ammonium peroxydisulfate
ASC	apoptosis-associated speck-like protein containing a caspase recruitment domain
ATF	activating transcription factor
ATG	autophagy-related gene
ATP	adenosine triphosphate
ATRA	all- <i>trans</i> retinoic acid
BBC	BCL2 binding component
BCL	B-cell lymphoma
BCO1	β -carotene oxygenase 1
BiP	binding immunoglobulin protein
BH-3	bcl-2 homology domain 3
CIITA	class II transcription activator
CARD	caspase activation and recruitment domain
CASP	caspase
CD14	cluster of differentiation 14
CDK	cyclin-dependent kinase
CDKN1A	CDK inhibitor 1
cDNA	complementary DNA
CoA	coenzyme A
Cont	control
CoREST	corepressor for element 1-silencing transcription factor
CP	control peptide
CRABP	cellular retinoic acid binding protein
CREB	cyclic AMP-responsive element-binding protein
Ct	threshold cycle
CTL	c-type lectin
CUL	cullin

DAMP	damage-associated molecular pattern
DDIT3/CHOP	DNA-damage-inducible transcript 3
DIC	differential interference contrast
$\Delta\Psi_m$	mitochondrial inner membrane potential
D-MEM	Dulbecco's modified Eagle's medium
DMSO	dimethyl sulfoxide
DNA	deoxyribonucleic acid
DP	DNA-binding partner of E2Fs
DRAM	DNA damage-regulated autophagy modulator
dsDNA	double-stranded DNA
DSS	disuccinimidyl suberate
ECSIT	evolutionarily conserved signaling intermediate in Toll pathway
eIF	eukaryotic initiation factor
ER	endoplasmic reticulum
ES	embryonic stem
FA	farnesoic acid
FAD	flavin adenine dinucleotide
FBS	fetal bovine serum
FFQ	food frequency questionnaire
G1	gap phase 1 in cell cycle
G2	gap phase 2 in cell cycle
GBP	guanylate-binding protein
GGA	geranylgeranoic acid
GGOH	geranylgeraniol
GGPP	geranylgeranyl diphosphate
GGPPase	geranylgeranyl diphosphatase
GPX	glutathione peroxidase
GRP	glucose-regulated protein 78
GSDM	gasdermin
H3K4	histone H3 lysine-4
HDAC	histone deacetylase
HET-E	heterokaryon incompatibility
HGNC	HUGO nomenclature committee
HIN	hematopoietic interferon-inducible nuclear protein
HOX	homeobox
HPA	Human Protein Atlas
HPLC	high-performance liquid chromatography
HRP	horseradish peroxidase

HSC	hepatic stellate cell
HUGO	human genome organization
IC ₅₀	inhibitory concentration at a half maximum
ICE	IL-1 β -converting enzyme
IFN	interferon
IgG	immunoglobulin G
IL	interleukin
IL-1R	IL-1 receptor
I κ B	inhibitor of NF- κ B
IKK	I κ B kinase
IPAF	interstitial pneumonia with autoimmune feature
IRAK	IL-1R-associated kinase
IRE	inositol requiring
IRF	interferon-regulatory factor
IRGB	immunity-related GTPase family member B
ISX	intestine-specific homeobox
JARID	Jumonji, At rich interactive domain
JNK	c-jun N-terminal kinase
kDa	kilodalton
KDM	lysine (K)-specific demethylase
LC	microtubule-associated protein 1 light chain
LDH	lactate dehydrogenase
LBP	LPS-binding protein
LPS	lipopolysaccharide
LRR	leucine-rich repeat
LSD1/KDM1A	histone lysine demethylase 1
LTA	lipoteichoic acid
LTL	leukocyte telomere length
M	mitosis phase in cell cycle
MAF	minor allele frequency
MAL	MyD88 adaptor-like
MAP	mitogen-activated protein
MAPK	MAP kinase
MD	myeloid differentiation protein
MDa	megadalton
MHC	major histocompatibility complex
MKK	MAP kinase kinase
MLKL	mixed lineage kinase domain like pseudokinase

MMqPCR	monochrome multiplex qPCR
mRNA	messenger RNA
mTOR	mammalian target of rapamycin
mtROS	mitochondrial ROS
MyD	myeloid differentiation primary-response protein
NADH	β -nicotinamide adenine dinucleotide, reduced
NAIP	neuronal apoptosis inhibitory protein
NBD	nucleotide-binding domain
N.D.	not determined
NEMO	NF- κ B essential modulator
NET	neutrophil extracellular trap
NF- κ B	nuclear factor of kappa-light polypeptide gene enhancer in B-cells
NIK	NF- κ B-inducing kinase
NLRC	NLR family CARD domain-containing protein
NLRP	NOD-like receptor containing pyrin domain
nm	nanometer
NOD	nucleotide-binding oligomerization domain
NR2E1/TLX	nuclear receptor subfamily 2 group E
OA	oleic acid
OCT	octamer-binding transcription factor
OD	optical density
ORC	origin recognition complex
P2X7	purinergic receptor P2X 7
P2X7R	P2X7 receptor
PA	palmitic acid
PAD	peptidylarginine deiminase
PAMP	pathogen-associated molecular pattern
PARC	p53-associated parkin-like cytoplasmic protein
PBS	phosphate buffered saline
PBS (-)	phosphate buffered saline, Ca-free
PBS-T	phosphate buffered saline with Tween 20
PCR	polymerase chain reaction
PERK	PKR-like ER kinase
PFA	paraformaldehyde
pHH3	phospho-histone H3
PI3K	phosphoinositide 3-kinase
PKR	protein kinase RNA
POU	Pit-1, Oct-1, Oct-2 and unc-86

POU5F1	POU domain, class 5, transcription factor 1
PRR	pattern-recognition receptor
PTEN	phosphatase and tensin homolog
PTM	post-translational modification
PUMA	p53 upregulated modulator of apoptosis
PYD	pyrin domain
PYHIN	pyrin and HIN domain family
PYRIN	PYD or PADD/DAPIN domain
PVDF	polyvinylidene difluoride
QNZ	quinazolinediamine
qPCR	quantitative PCR
RAR	retinoic acid receptor
RB	retinoblastoma protein
RIP	receptor-interacting protein
RIPA	radio immunoprecipitation assay
RIPK	receptor interacting protein kinase
RhoA	Ras homolog gene family member A
RNA	ribonucleic acid
RNase	endoribonuclease
ROI	regions-of-interest
ROS	reactive oxygen species
rRNA	ribosomal RNA
RT	reverse transcription
RTL	relative telomere length
RT-qPCR	reverse transcription and quantitative polymerase chain reaction
RXR	retinoid X receptor
S	DNA synthesis phase
SCD	stearoyl-CoA desaturase
scg	single copy gene
SCO2	synthesis of cytochrome c oxidase 2
SD	standard deviation
SDS-PAGE	sodium dodecyl sulfate-polyacrylamide gel electrophoresis
siRNA	small interfering RNA
SLC7A11	solute carrier family 7 member 11
SNP	single nucleotide polymorphism
SQSTM	sequestosome
ssRNA	single-stranded RNA
SUMO	small ubiquitin-related modifier

T3SS	type III secretion system
TAB	TAK1-binding protein
TAK	TGF- β -activated kinase
tBID	truncated p15 BH3 interacting-domain death agonist
TCP	<i>trans</i> -2-phenylcyclopropylamine
TE	10 mM Tris-HCl, pH 7.4 and 1 mM EDTA buffer
TERRA	telomeric repeat-containing RNA
TERT	telomerase reverse transcriptase
TG	thapsigargin
TGF	transforming growth factor
TIGAR	TP53-induced glycolysis and apoptosis regulator
TIR	toll-IL-1 receptor
TIRAP	TIR domain-containing adaptor protein
TLR	toll-like receptor
TM	tunicamycin
TNF	tumor necrosis factor
TNFR	TNF receptor
TP	tumor protein
TP1	telomerase-associated protein 1
TRAF	TNF-receptor-associated factor
TRAM	TRIF-related adaptor molecule
TRF	terminal restriction fragment
TRIF	TIR-domain-containing adaptor-inducing interferon
UPR	unfolded protein response
UV	ultra violet
XBP1	X-box binding protein 1
xCT	cysteine transporter

List of tables and figures

Tables

Table 0-1 Subjects characteristics.....	6
Table 0-2 Circulating β -carotene levels in each genotype group.....	8
Table 0-3 Association between buccal cell RTL and β -carotene intakes.....	9
Table II-1 Toll-like receptors and their ligands.....	53
Table VI-1 The nucleotide sequences of each primers used for real time RT-PCR.....	157

Figures

Fig.0-1. ISX binds regulatory SNP site (rs6564851) of the <i>BCO1</i> gene.....	5
Fig.0-2. Alternative method of <i>TERRA</i> measurement.....	11
Fig.0-3. GGA time-dependently downregulated <i>TERRA</i>	12
Fig.I-1. Chemical structure of geranylgeranoic acid.....	19
Fig.I-2. Diverse function of p53 through multiple target genes.....	22
Fig.I-3. The formation of phagolysosomes.....	25
Fig.I-4. Canonical unfolded protein responses.....	28
Fig.I-5. Cell cycle.....	31
Fig.I-6. Genes related G1/S transition.....	32
Fig.I-7. Suppression of growth by the UPR.....	33
Fig.I-8. Programmed cell death.....	36
Fig.I-9. Autophagy, apoptosis, necroptosis, pyroptosis and necrosis pathways.....	37
Fig.II-1. Canonical inflammasomes.....	43
Fig.II-2. Mechanisms of NLRP3 inflammasome activation.....	45

Fig.II-3. Mammalian TLR signaling pathways.....	54
Fig.II-4. Schematic representation of the pyroptosis pathways.....	58
Fig.II-5. GGA activated caspase-1 in HuH-7 cells.....	61
Fig.II-6. GGA induced priming of inflammasome in HuH-7 cells.....	63
Fig.II-7. NF- κ B is relocated from the cytoplasm to the nucleus by GGA.....	65
Fig.II-8. Translocate for plasma membrane of GSDMD after GGA treatment.....	67
Fig.II-9. Morphological alterations and membrane damages after GGA treatment.....	69
Fig.II-10. GGA-induced cell death via TLR4.....	73
Fig.II-11. GGA-induced UPR upregulates TLR2.....	78
Fig.II-12. ATRA was not induced pyroptotic cell death.....	81
Fig.III-1. The role of GSDMD in pyroptosis driven by non-canonical and canonical inflammasomes.....	90
Fig.III-2. GGA-induced pyroptosis via non-canonical inflammasome pathway in HuH-7 cells.....	94
Fig.III-3. UPR induces the activation caspase-4.....	96
Fig.III-4. Increase intracellular calcium via UPR in HuH-7 cells.....	99
Fig.IV-1. Characteristic of histone H3K4 demethylase KDM1A.....	110
Fig.IV-2. Cytoplasmic translocation of nuclear KDM1A induced by either GGA or TCP treatment.....	115
Fig.IV-3. Nuclear localization of KDM1A and KDM5A after 3 h treatment with non-inhibitory isoprenoids and KDM1A-inhibitors.....	116
Fig.IV-4. Subcellular distribution of KDM1A in M-phase cells.....	119
Fig.IV-5. Release of nuclear KDM1A after incubation of the nuclear fraction with GGA or TCP..	121

Chapter 0

Foundation research

Suemi Yabuta

*Molecular and Cellular Biology, Graduate School of Human Health Science,
University of Nagasaki, Nagasaki, Japan*

Abstract

Telomere length shortening is modulated not only by aging, but also by both genetic and environmental factors. The aim of this study was to investigate the interactions between antioxidant nutrient metabolism-related gene single nucleotide polymorphisms (the genetic factors) and nutrient intake (the environmental factors) in their effects on telomere length shortening. Data were collected on the relative telomere lengths (RTLs) of buccal cells and the habitual food intake of 70 healthy Japanese adults. All subjects were genotyped for two common single nucleotide polymorphisms: rs6564851 in the β -carotene oxygenase 1 (*BCO1*) gene and rs362090 in the intestine-specific homeobox (*ISX*) gene. We subdivided the study population into four groups based on combinations of the rs6564851 and rs362090 genotypes. After this subdivision, we showed a positive effect of daily α - or β -carotene intake on buccal RTL in the *ISX* rs362090 G-allele carrier + *BCO1* rs6564851 GG-genotype group. In contrast, negative association of the buccal RTL with β -carotene intakes was unexpectedly detected in *ISX* G-carrier + *BCO1* T-carrier genotype. We speculated telomere length maintenance might be affected by retinoids, so we next showed retinoids time-dependently downregulated *TERRA* (telomere repeat-containing RNA) that joined telomere regulation. In conclusion, retinoids may be involved in maintenance of telomere length through downregulation of *TERRA* expression.

0-1. Introduction

0-1-1. Telomeres

It is well established that cellular telomere length reflects the replication number of chromosomal DNA, such that telomere length is the most reliable indicator of mitotic history and acts as a biomarker of cellular aging [1]. Indeed, a systematic review reveals that a decrease of leukocyte telomere length (LTL) with age is out of question [2]. Hence, it may be important to measure the telomere length of non-invasive samples to assess the aging degree in public health service.

Several years ago, Cawthon developed a singleplex quantitative polymerase chain reaction (qPCR) assay for “relative” average telomere lengths [3], which uses far less DNA and requires much less time to perform than the traditional Southern blot method for measuring terminal restriction fragment (TRF) lengths. Furthermore, Cawthon has recently improved his previous method in a monochrome multiplex qPCR (MMqPCR) [4,5].

0-1-2. Nutritional perturbation of telomere length shortening

Telomere length is likely shortened not only by cell proliferation, but also by environmental factors through an effect of oxidative stress and inflammation, which is the major causes of accelerated telomere erosion [6]. Both oxidative stress and inflammation form a pathogenic mechanism of lifestyle-related diseases and it is well known that dietary intervention can modulate oxidative stress and inflammation. In this context, one can easily speculate that dietary intervention with anti-oxidative nutrients may protect the

cells from accelerated telomere erosion. Recently, strong evidence for this speculation has been repeatedly brought by Blackburn's group that LTL increased with decreasing n-6:n-3 ratios in polyunsaturated fatty acid supplementation for 4 months in human clinical trial [7], comprehensive lifestyle changes significantly increased telomerase activity in peripheral immune cells [8] and an inverse relationship between baseline blood levels of marine omega-3 fatty acids and the rate of telomere shortening over 5 years [9]. Another evidence was very recently appended to demonstrate that telomere shortening in elderly individuals with mild cognitive impairment could be attenuated with n-3 fatty acid supplementation [10].

0-1-3. β -Carotene metabolism-related genes

The metabolism of antioxidant nutrients can be affected by genetic background. For example, several common SNPs of β -carotene oxygenase 1 (*BCO1*) gene are associated with β -carotene metabolism [11]. Indeed, a common promoter SNP (rs6564851) was associated with higher circulating β -carotene level. Other common nonsynonymous SNPs (rs12934922; rs7501331) in the *BCO1* gene, occurring at frequencies similar to those of the poor converter trait, reduced catalytic activity of *BCO1* by down to 69% in female [12].

BCO1 is an intestinal enzyme responsible for the symmetrical cleavage of β -carotene into retinal. Recently, the gut specific homeodomain transcription factor ISX (intestine specific homeobox) has been identified as a putative repressor of intestinal *BCO1* gene expression (**Fig.0-1**) [13]. Furthermore, ISX also suppresses the gene expression of membrane transporter scavenger receptor class B type 1, which manages

intestinal lipid absorption including anti-oxidant lipids, carotenoids and vitamin E [14].

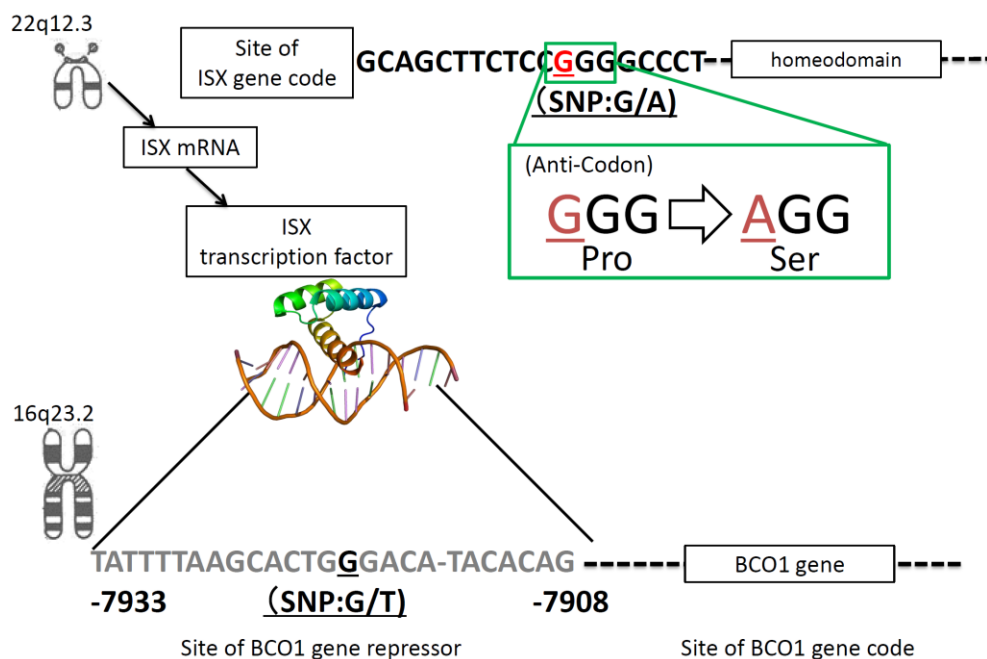


Fig.0-1. ISX binds regulatory SNP site (rs6564851) of the *BCO1* gene.

BCO1 is an intestinal enzyme responsible for the cleavage of β -carotene into retinal. Several years ago, the gut-specific homeodomain transcription factor ISX has been identified as a putative repressor of intestinal *BCO1* gene expression. ISX has been shown to bind to *BCO1* SNP-containing 26-bp DNA fragment; G-allele-containing fragment has more affinity to ISX than T-allele fragment. Yabuta S, Masaki M, and Shidoji Y. *Atlas of Science* (2016) <https://atlasofscience.org/%CE%B2-carotene-requirement-for-anti-aging-depends-on-genetic-background/> [15]

The current study addresses a basic question. Are there any interactions between nutrient intake (environment factor) and common SNPs of the *BCO1* and *ISX* genes (genetic factor) in their effects on telomere length shortening? The approach used in this study is the measurement of buccal cell telomere length with the analysis of food frequency questionnaires (FFQs) and genotyping of 2 common SNPs (rs6564851 of *BCO1* and rs362090 of *ISX*).

0-2. Results

0-2-1. Characteristics of subjects

The demographic characteristics, and *BCO1* and *ISX* common SNPs allele frequencies of the participants analyzed in the present study are shown in **Table 0-1**. There was no difference in the buccal cell relative telomere lengths (RTLs) in between males and females, whereas the average concentration of serum β -carotene was significantly higher in females than that in males.

As for rs6564851, a major allele (frequency, 84.1%) was G in the subjects and no difference of the allele frequency was found in between males and females. A minor allele (30.7%) of rs362090 was G, which frequency was higher in females than males.

Table 0-1. Subjects characteristics

Characteristics	All	male	female	P-trend
n	70	43	27	-
Age, y	40.9 \pm 11.2*	42.3 \pm 11.3	38.7 \pm 10.5	0.19
RTL	0.89 \pm 0.15	0.89 \pm 0.13	0.89 \pm 0.19	0.95
Serum BC, μ g/dL	58.7 \pm 47.6	49.2 \pm 47.8	72.7 \pm 43.6	0.04**
SNPs for BCO1 or ISX gene	Allele frequency (%)			
rs6564851 (G allele; T allele)	84.1; 15.9	82.1; 17.9	87.0; 13.0	
rs362090 (A allele; G allele)	69.3; 30.7	78.6; 21.4	57.4; 42.6	

*Data are mean \pm SD.

**Significantly different by gender analyzed using Student *t*-test ($p < 0.05$).

0-2-2. Circulating β -carotene levels in each genotype group

A genome-wide association study revealed that a common SNP rs6564851 near the *BCOI* gene affects the circulating levels of carotenoids in three Caucasian population [16], thus we evaluated the effects of SNPs and serum carotenoid levels in Japanese population. Because the two polymorphisms (rs6564851 in *BCOI*, rs362090 in *ISX*) tested herein are common SNPs with a minor allele frequency (MAF) of 0.05 or more, two groups of homozygotes carrying major alleles and the other minor-allele carriers were analyzed below for comparison (**Table 0-2**). The average concentrations of serum β -carotene in the rs6564851 GG homozygotes (the SNP of the *BCOI* gene) in total, males and females were significantly higher than those in the T allele carriers ($p = 0.003, 0.039$ and 0.027 , respectively), showing that the GG homozygotes had a 2-fold higher serum β -carotene level compared with that of T allele carriers. In contrast, it was no significant difference in the serum β -carotene concentration between the major homozygotes and the minor allele carriers in the other SNPs rs362090 (the SNP of the *ISX* gene).

Table 0-2. Circulating β -carotene levels in each genotype group

Genotype	n(M/F)	Total	Male	Female	
<i>BCO1</i> rs6564851		Serum β -carotene ($\mu\text{g/dL}$, mean \pm SD)			p(Male vs. Female)
GG	59 (37/22)	63.9 \pm 52.6	52.9 \pm 54.7	82.4 \pm 43.2	0.002**
GT;TT	27 (20/7)	31.2 \pm 23.4	25.9 \pm 20.9	46.2 \pm 23.6	0.056
p(GG vs. T-carrier)		0.0032**	0.0394*	0.0271*	
<hr/>					
<i>ISX</i> rs362090					
AA	35 (27/8)	57.4 \pm 51.9	49.2 \pm 52.9	85.1 \pm 28.7	0.030*
AG;GG	52 (31/21)	50.8 \pm 44.5	38.3 \pm 40.8	74.9 \pm 43.4	0.001**
p(AA vs. G-carrier)		0.6815	0.3659	0.3453	

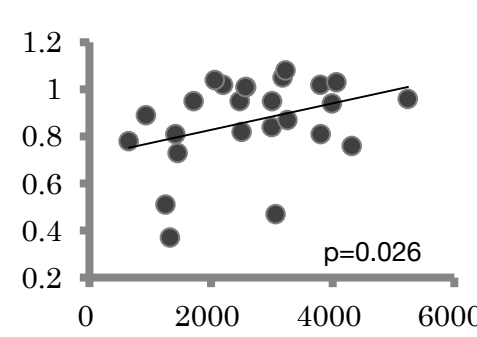
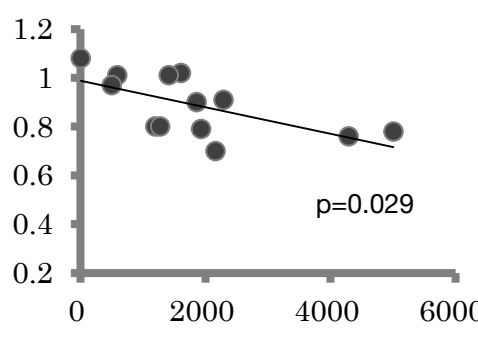
*, **: Significantly different by gender or genotype group, analyzed using the Student's *t*-test (*, **: $p < 0.05, 0.01$, respectively)

0-2-3. Buccal RTLs and FFQ

To further analyze genotype effects on the buccal RTLs, the *BCO1* genotype groups (categorized into 2 groups of rs6564851 GG and T-carrier) were crossed with the *ISX* genotype groups (rs362090 AA and G-carrier) to make 4 combinations for statistical analysis. Multiple regression modeling depicted that daily β -carotene intake in the *ISX* G-allele carriers with the *BCO1*-GG genotype was significantly and positively associated with the buccal RTLs as illustrated in **Table 0-3**. On the other hand, in the remaining T-carriers of the *BCO1* genotype, the G-carriers of the *ISX* gene showed significant and negative association between

RTLs and daily intake of β -carotene (Table 0-3).

Table 0-3. Association between buccal cell RTL and β -carotene intakes.

<i>BCO1</i>	GG	GT; TT
<i>ISX</i>		
AA	no association	no association
AG; GG	 <p>$p=0.026$</p>	 <p>$p=0.029$</p>

0-2-4. Measurement of transcribed telomere repeats

Why are *ISX* G-carrier and *BCO1* T-carrier genotype groups taking toxic levels of β -carotene, in terms of telomere shortening protection? In this group, intestinal expression of the *BCO1* gene must be high, so that ingested β -carotene may be efficiently converted to retinoids [17]. Hence, we speculated telomere length maintenance might be affected by not carotene itself, but rather retinoids.

So, we next conducted the following experiment to understand how retinoids regulate telomere length. Besides shelterin as mentioned initially, telomeric repeat-containing RNA (*TERRA*) has recently joined in telomere regulation. Its transcription by RNA polymerase II starts within subtelomere regions and proceeds toward each chromosome ends. Although its function is still unclear, some studies reported that *TERRA* might act on negative control of telomere length through telomerase sequestration. First, introduce measurement of *TERRA* family in this study, the pro-terminal DNA sequences associated with the long-arm telomeres of human chromosomes XqYq and 10q were named TelBam and TelSau, respectively. BLAST search analysis demonstrated. Because measurement used with random hexamer measure including non-subtelomere region, we measured with cDNA has been used by telomere motif primer (CCCTAA)₅. **Fig.0-2A** shows PCR amplification curves. The delta Ct between with and without RT reaction clearly indicates to be derived from the amount of telomeric repeat-containing RNA, or expression level of *TERRA*. Although it shown Ct of without RT reaction increased, we show difference in the melting points of amplicons with or without RT (**Fig.0-2B, upper**), and Fig.0-2B, **bottom** showed match melting points of between RT (-) and cDNA used by random hexamer. Furthermore, the delta Ct, similar to RT

(+/-), difference in primer of telomere motif or random hexamer (**Fig.0-2C**), suggesting that it can measure *TERRA* used by telomere motif primer.

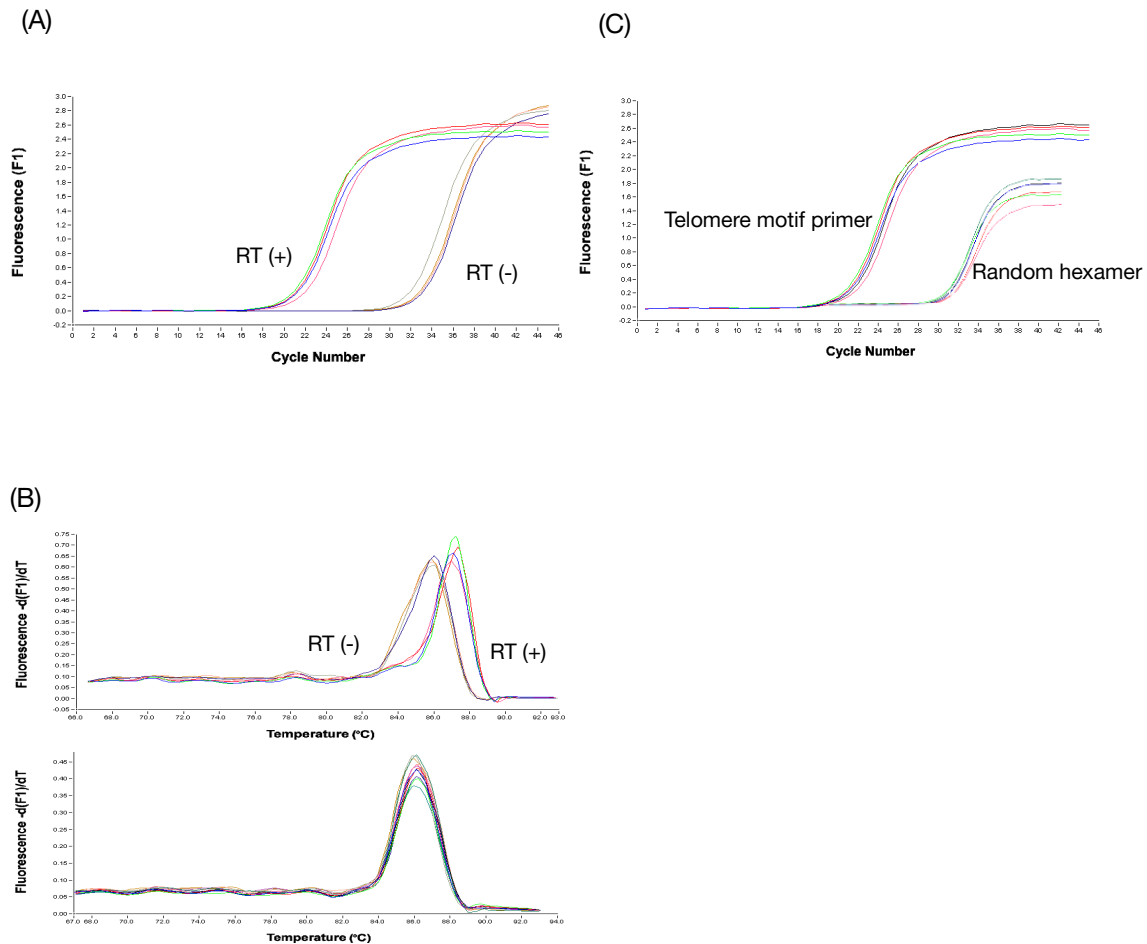


Fig.0-2. Alternative method of *TERRA* measurement.

Total RNA or RNA was extracted to analyze the TelSau in *TERRA* by RT-qPCR in HuH-7 cells. (A) PCR amplification curves of the delta C_t between with and without RT reaction. (B) Melting curves of amplicons with or without RT (upper), random hexamer (bottom). (C) PCR amplification curves of telomeric repeat sequence or random hexamer.

0-2-5. Retinoids downregulated *TERRA*

Next, we speculated telomere maintenance might be affected with retinoid, measured the cellular *TERRA* level after treatment with 20 μ M GGA of acyclic retinoids (**Fig.0-3**). GGA apparently showed a time-dependent downregulation of the cellular *TERRA* level from 8 to 24 h.

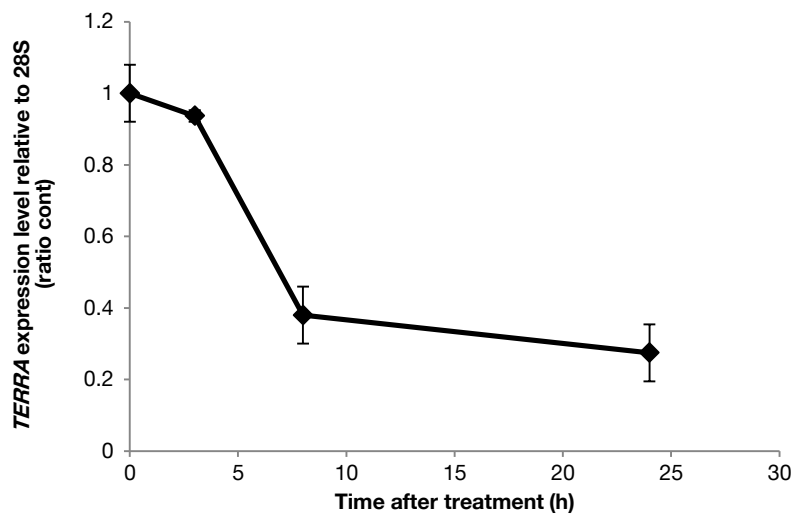


Fig.0-3. GGA time-dependently downregulated *TERRA*.

HuH-7 cells were treated with 20 μ M GGA for 0, 3, 8 and 24 h. Total RNA was extracted to analyze the cellular levels of TelSau in *TERRA* mRNA by RT-qPCR (unpublished observation).

0-3. Discussion

In the present study, we addressed a basic question whether any associations exist between daily nutrient intakes and buccal cell RTLs. As a result, we found that the RTLs in buccal cells measured in 70 Japanese samples by MMqPCR method were associated with dietary intakes of β -carotene in specified genotype groups.

In the present investigation, we again failed to find any protective roles of vegetables, fats and oils, and antioxidant nutrients including carotenoids, tocopherol and vitamin C against telomere shortening in buccal cells, unless the study population was subdivided into 4-genotype groups by a combination of SNPs (rs6564851 and rs362090) of the antioxidant vitamin metabolism-related genes such as the *BCOI* and *ISX* genes. Interestingly, the positive influence of daily α - or β -carotene intake on buccal RTLs was shown only in [*BCOI* rs6564851 GG-genotype + *ISX* rs362090 G-carrier] group. *BCOI* rs6564851 GG-genotype has been established to provide higher circulating β -carotene concentrations than *BCOI* rs6564851 T-carrier. In *BCOI* rs6564851 GG-genotype group, cellular expression of the *BCOI* gene is thought to be low in intestine, so that the ingested β -carotene may be poorly converted to retinoids, indicating that the higher β -carotene intake is, the higher serum β -carotene concentration is in this genotype group. Hence, we speculate that in [*BCOI* rs6564851 GG-genotype + *ISX* rs362090 G-carrier] group, anti-oxidative protection of telomere length shortening may be highly dependent on the daily intake of β -carotene. On the contrary, we found that buccal cell RTL was also negatively associated with β -carotene intake in *ISX* G-allele carriers who carry the *BCOI* T-allele. In this group, intestinal expression of the *BCOI* gene must

be high, so that ingested β -carotene may be abundant converted to retinoids, and is independent of daily β -carotene intake in *BCOI* rs6564851 T-carriers. However, the least β -carotene intakes in *ISX* G-allele carriers who carry the *BCOI* T-allele than the other group, this group might be already taking too much β -carotene, so that their buccal RTL is negatively associated with the present β -carotene intake.

It is interesting that GGA time-dependently downregulated *TERRA* in HuH-7 cells. Here, it is well known that retinoids repressor of telomerase, associate with elongation of telomere length. Some study reported retinoids downregulated both telomerase reverse transcriptase (*TERT*) mRNA expression and telomerase activity [18,19]. It has been repeatedly reported that retinoids treatment decreases telomerase activity, but the effect requires 3 to 5 days. In contrast, we showed GGA treatment downregulated *TERRA* level in 24 h, suggesting that GGA might affect by telomere instability for short time in downregulation of *TERRA*, and by telomere shortening for long term in downregulation of telomerase. All these results suggested that retinoids including GGA might be effect cancer cells, for example, HuH-7 cells in hepatoma.

These results strongly suggested that GGA might associate with transcriptional regulation of *TERRA*. Recently, we reported that GGA directly inhibits histone lysine-specific demethylase-1 (KDM1A/LSD1) activity [20], and to our knowledge, the cellular expression of *TERRA* is known to be regulated via a specific binding of KDM1A to *TERRA* [21]. Here, we will show GGA can inhibit hepato-carcinogenesis by acting at the gene level, because we were noticed that it is important to establish cancer prevention mechanism operated by GGA. Therefore, the present study aims to scrutinize cellular mechanisms of

GGA-induced cell death in human hepatoma cells as shown in the following chapters.

Chapter I

General Introduction

Suemi Yabuta

*Molecular and Cellular Biology, Graduate School of Human Health Science,
University of Nagasaki, Nagasaki, Japan*

I-1. Diterpenoid acids or acyclic retinoids

Retinoids including all-*trans* retinoic acid (ATRA), 9-*cis* retinoic acid (9CRA) and other retinoic acid derivatives are clinically applied as chemotherapeutic agents for acute promyelocytic leukemia. However, their side effects are sometimes so severe that it becomes difficult to continue administration of the retinoids [22]. Thus, synthetic retinoids without serious side effects are now certainly desired especially in cancer prevention field. In this regard, of note, a promising synthetic retinoid with few side effects has been developed in Japan.

The clinical efficacy of a chemically synthetic 20-carbon polyprenoic acid (all-*trans* 3,7,11,15-tetramethyl-2,4,6,10,14-hexadecapentaenoic acid or 4,5-didehydrogeranylgeranoic acid) on prevention of second primary hepatoma has been proven in a placebo-controlled, double-blinded and randomized phase II clinical trial with postoperative hepatoma patients with few side effects [23], and later, it was revealed that the polyprenoic acid significantly increased a 5-year survival rate after a radical therapy of primary hepatoma in these patients [24].

As for a mechanism how the polyprenoic acid prevents second primary hepatoma, it has been shown that the polyprenoic acid binds to cellular retinoic acid binding protein (CRABP) [25], activates nuclear retinoid receptors including retinoic acid receptor- β (RAR β) and retinoid-X receptor- α (RXR α) [26], exerts transcriptional activation of some hepatocyte-specific genes in hepatoma cells [27], and has preventive actions in chemical and spontaneous hepatocarcinogenesis [28]. Considering that it is similar to the action of retinoids, the polyprenoic acid was named “acyclic retinoid” [29]. However, there was a big

difference in cell death-including activity between acyclic retinoid and natural retinoids such as retinoic acid. In other words, acyclic retinoid efficiently induced cell death in human hepatoma HuH-7 cells, but 5-times more ATRA did not [30]. So, in cell-death induction against hepatoma cells, “acyclic retinoid” was considered not to be retinoid.

If the cell-death inducing activity of acyclic retinoid is not the property of natural retinoids, what kind of cellular metabolites does “acyclic retinoid” mimic in terms of cancer-killing activity? In this context, we paid attention to a chemical structure of “acyclic retinoid”, which is a 4, 5-didehydro derivative of geranylgeranoic acid. C₂₀ geranylgeranyl diphosphate (GGPP) is a substrate for biosynthesis of diterpenoids including taxol (cyclic) and GGA (acyclic). Indeed, Shidoji and Ogawa found natural GGA in medicinal herbs [31]. Furthermore, de novo GGPP synthesis has been established in mammalian hepatocytes [32]. Consequently, one can reasonably speculate that mammalian cells may be able to produce GGA from endogenous or even exogenous GGPP [33]. Therefore, Mitake and Shidoji examined 1) bioavailability of plant GGA in humans [34], 2) possible conversion of ingested GGPP to GGA in mammalian cells [35], and 3) possibility of synthesis of GGA from GGPP in mammalian cells [35].

I-2. Geranylgeranoic acid (GGA)

More than two decades ago, Bansal and Vaidya [36] reported geranylgeranyl pyrophosphatase (GGPPase) found in rat liver, which catalyzed a conversion of GGPP to geranylgeraniol (GGOH). Once GGOH is produced through dephosphorylation of GGPP by the specific GGPPase, it seems reasonable to

assume that the non-specific fatty alcohol dehydrogenase/ fatty aldehyde dehydrogenase system might produce GGA in mammalian hepatocytes.

GGA, **Fig. I-1** is a natural diterpenoid found in several medicinal herbs including turmeric [31]. GGA and its derivatives have been repeatedly reported to induce cell death in human hepatoma cells [30,37]. While ‘Peretinoin’ (4, 5-didehydroGGA) has been utilized for clinical trials, it has so far not been identified in natural resources.

GGA was much less toxic than natural retinoids in a human hepatoma cell line in the presence of fetal bovine serum (FBS) [38], and one-year intake of 4,5-didehydroGGA (600 mg/day) gave no apparent side effects in the above-mentioned clinical trial [39].

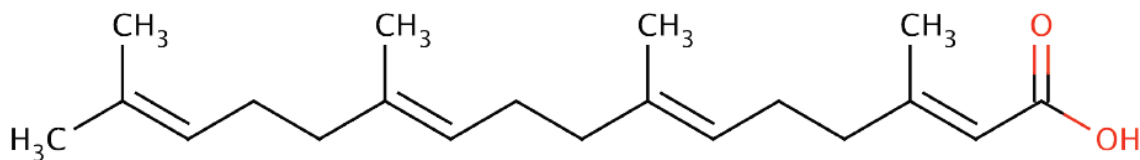


Fig.I-1. Chemical structure of geranylgeranoic acid.

I-3. GGA-induced cell death

In human hepatoma-derived HuH-7 cells, we have demonstrated GGA-induced cell death by large-scale DNA fragmentations, nucleosomal-scale ladder formation and dissipation of mitochondrial inner membrane potential ($\Delta\Psi_m$) [40,41]. It has been also reported that caspase-1 or -3 inhibitors blocked or delayed GGA-induced cell death, respectively, and, furthermore, α -tocopherol prevented HuH-7 cells from dissipation of $\Delta\Psi_m$ as well as cell death in the presence of GGA.

GGA-induced cell death was first characterized by apoptosis, which was evidenced by chromatin condensation and nucleosomal ladder formation [30]. During apoptotic cell death, cytosolic cysteine protease family including interleukin (IL)-1 β -converting enzyme (ICE or caspase-1) have repeatedly been confirmed to be activated and the active CPP32 (caspase-3) cleaves poly-ADP-ribosyl polymerase, a nuclear enzyme responsible for DNA repair and integrity of nucleosomes, and sterol response element-binding protein [42,43]. Although a molecular mechanism for activation of caspase family protease cascade is fully solved at present, dysfunction of mitochondrion is now one of the most effective organelles to trigger the protease cascade through apoptosome [44,45]. Diterpenoids such as retinoids are well-established to disturb mitochondrial electron transport and oxidative phosphorylation system [46]. Hence, we were very much interested to know whether GGA cause a loss of the mitochondrial membrane potential and activation of caspase family protease cascade. Pretreatment with synthetic tetrapeptide cysteine protease inhibitor, acetyl-Tyr-Val-Ala-Asp-chloromethylketone (caspase-1 inhibitor) blocked GGA induced cell death, but acetyl-Asp-Glu-Val-Asp-aldehyde (caspase-3 inhibitor) was not completely blocked [37]. Several years ago, we investigated another form of programmed cell death, autophagic cell death, after GGA treatment. Then, we have found that GGA at its micromolar concentrations induces an incomplete autophagic response, which is characterized as massive accumulation of initial/early autophagosomes and defect of autolysosome formation or fusion of autophagosome with lysosome [47].

I-3-1. GGA-induced mitochondrial impairment

Furthermore, GGA-induced cell death was accompanied all the time by increased production of reactive oxygen species (ROS), superoxide, in mitochondria [47] and delayed dissipation of $\Delta\Psi_m$ [37]. Interestingly, wortmannin, a broad-specific inhibitor of phosphoinositide 3-kinases (PI3Ks), prevented GGA-induced incomplete autophagic response as well as hyperproduction of superoxide in mitochondria [47], suggesting that hyperproduction of superoxide in mitochondria might be mediated through signal transduction rather than direct action of GGA on mitochondria. As for GGA-induced mitochondrial impairment, it is also noteworthy that α -tocopherol, an antioxidant vitamin, efficiently prevents $\Delta\Psi_m$ dissipation and cell death induced with GGA [37], suggesting that hyperproduction of mitochondrial superoxide might be indispensable for GGA-induced cell death.

I-3-2. GGA-induced nuclear translocation of the mutant p53

First we investigated GGA effects on p53, because it has been well established that HuH-7 cells harbor the mutant *TP53* gene [48]. *TP53* is the first tumor suppressor gene linked to apoptosis [49], inhibits tumor growth through activation of both cell cycle arrest- and apoptosis-related genes, and is thought to be central to tumor-suppressor activity [50,51]. It seems likely that activation of p53-dependent cell death can contribute to inhibition of cancer development at several stages during tumorigenesis [49]. Therefore, the p53 pathway is crucial for effective tumor suppression in humans [52].

The structure, function, and clinical significance of the p53 tumor suppressor protein in oncology have

been clarified in detail [53,54]. The p53 transcription factor is known to regulate many target genes that induce cell-cycle arrest (e.g., *p21* or *CDKN1A* as provided by the HUGO Nomenclature Committee [HGNC]), cell death (e.g., *PUMA* <p53 upregulated modulator of apoptosis>, or *BBC3* <BCL2 binding component 3>, as indicated by HGNC), respiration (e.g., *SCO2* <synthesis of cytochrome c oxidase-2>), autophagy (e.g., *DRAM* <DNA damage regulated autophagy modulator>), and inhibition of glycolysis (e.g., *TIGAR* <TP53-induced glycolysis and apoptosis regulator>) [55]. Therefore, it responds to diverse stress (including DNA damage, overexpressed gene and various metabolic restrictions). All of these p53 targets are associated with p53-mediated cancer prevention (**Fig.I-2**).

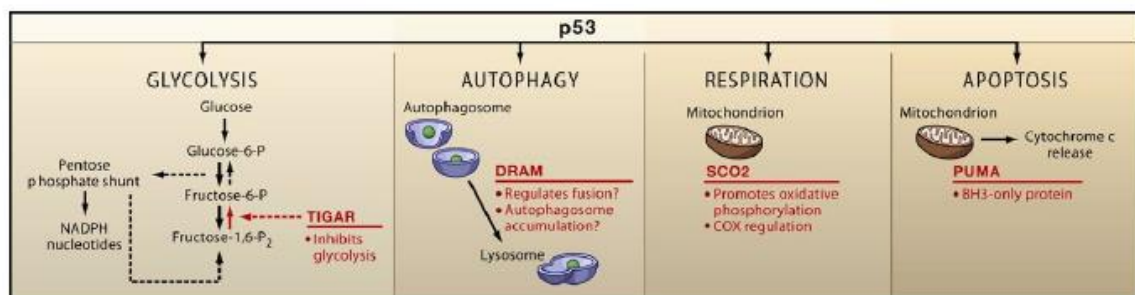


Fig.I-2. Diverse function of p53 through multiple target genes.

Adopted from Green DR and Chipuk JE: *Cell*, 126: 30-32 (2006) [56]

Among these targets, the *PUMA* gene is particularly interesting, in terms of cancer prevention. This is because *PUMA* has been identified as a potent inducer of p53-dependent mitochondrial-mediated cell death in various tissues and cells [57]. *PUMA* is one of the BH-3-only proteins, which induce the mitochondrial inner membrane permeability transition. Therefore, overexpression of *PUMA* causes hyperproduction of mitochondrial ROS, leading to mitochondria-mediated cell death. *PUMA* is essential

for p53-mediated apoptosis [57], but it also contributes to induce autophagy during p53-dependent cell death [58].

Several p53-interacting proteins are known to be involved in its cytoplasmic sequestration, blocking it from degradation as well as restricting its access to the nuclear compartment, where p53 plays a role in transcription. Among the p53-interacting proteins, the 250-kDa CUL9 (previously named PARC, p53-associated, parkin-like cytoplasmic protein, by HGNC), a member of the cullin family and a potential E3 ubiquitin ligase [59], is one of the proteins playing a major role in sequestering p53 into the cytoplasm. The CUL9 N-terminus binds the C-terminus of p53 to form about 1-MDa multiprotein complex. Then, p53 is retained in the cytoplasm by inhibiting the transport of cytoplasmic p53 to the nucleus [60].

GGA-induced cell death in HuH-7 cells is accompanied by $\Delta\Psi_m$ dissipation [37,47]. This mitochondria-involved cell death revealed features of apoptosis, such as chromatin condensation as revealed by Hoechst staining. However, as will be described later, it was impossible to completely prevent GGA-induced cell death with caspase-3 inhibitor [37].

p53 plays dual distinct roles in autophagy and has attracted attention in the field of autophagy in recent years [61]. p53 *trans*-activates the autophagy-related gene *DRAM* [62], as an ability of p53 to induce autophagy [63]. In contrast, cytoplasmic p53 suppresses autophagy, but its mechanism has not been elucidated [64]. In our laboratory we have found a rapid nuclear translocation of p53 after GGA treatment in HuH-7 cells [65]. In this context, GGA-induced nuclear translocation of the cytoplasmic p53 shows that it provides an easy intracellular environment to induce autophagy.

I-3-3. GGA-induced incomplete autophagic response

Mizushima, Ohsumi and Yoshimori explained their concept of autophagy in detail as follows [66]; although most intracellular short-lived proteins are selectively degraded by ubiquitin-proteasome pathway [67], most long-lived proteins are degraded in lysosomes [68]. In general, the mechanism that carries cytoplasmic components to the lysosomes is also called autophagy. Three types of autophagy have been proposed: macroautophagy, microautophagy and chaperone-mediated autophagy [69]. Among them, macroautophagy is believed to be responsible for the majority of the intracellular protein degradation and in the case of starvation-induced proteolysis in particular [68]. In macroautophagy (simply referred to as ‘autophagy’ hereafter), cytoplasmic constituents including cellular organelles such as mitochondrion and peroxisome, are enveloped by a membrane so called “isolation membrane” and later “phagophore” (**Fig.I-3**). Thereafter, the isolated membrane closes and forms double membrane structure called “autophagosomes”. Autophagosome fuses with endosome to become amphisomes, and further it becomes autolysosome produced by the fusion of autophagosome (or amphisomes) outer membrane and lysosomal membrane [66].

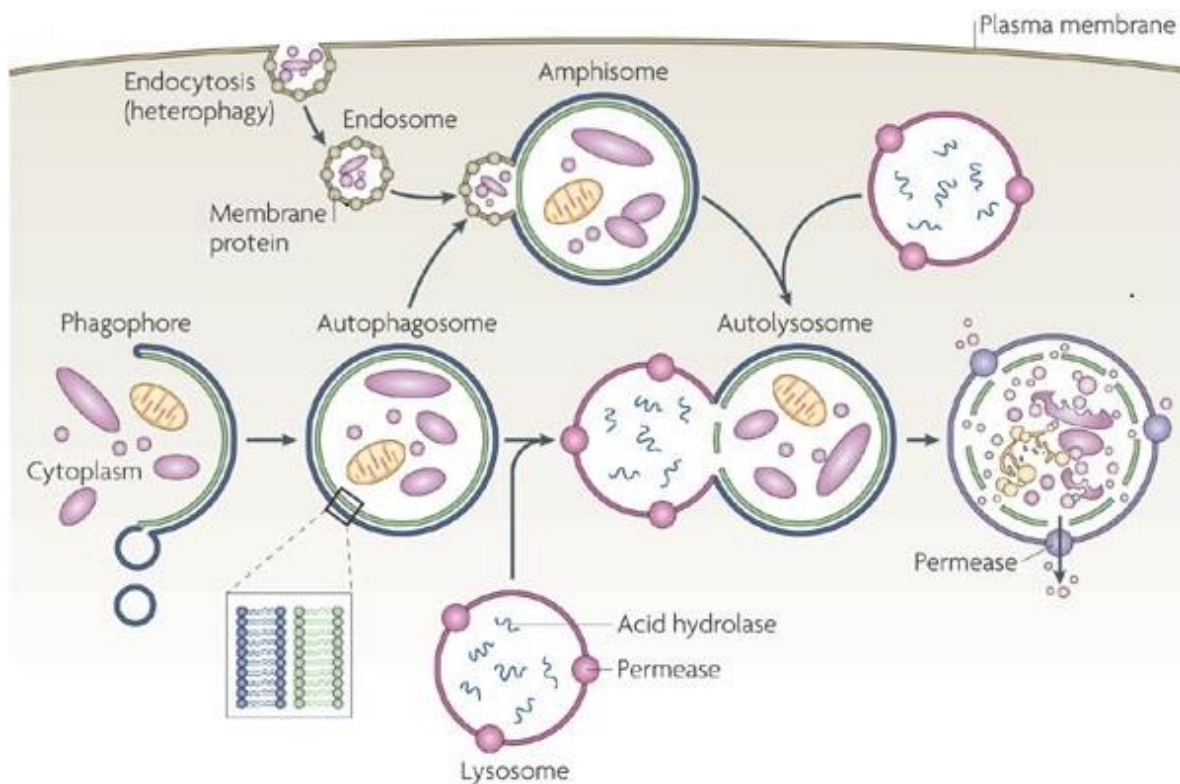


Fig.I-3. The formation of phagolysosomes.

Klionsky D J. *Nature Reviews Molecular Cell Biology* 8: 931-937 (2007) [70]

LC3 (microtubule-associated protein 1 light chain 3) is specific to autophagy marker. LC3 was originally discovered as one of three light chains complexed with microtubule-associated proteins 1A and 1B. LC protein consists of 3 members, but unlike LC1 and LC2, LC3 are transcribed and translated as a single protein and conserved in fungi, plants and animals. In humans, there are three genes encoding protein such as highly homologous LC3 α , β , and γ . For example, LC3 γ is an ortholog of the yeast autophagosome protein autophagy-related gene-8 (ATG8), and it has been demonstrated that all three proteins are involved in autophagosome biogenesis, while LC3 β has been exclusively used by mammals as a feature of autophagosome formation in cells. Hence, in this manuscript, we use a word of LC3 in place of LC3 β . LC3 is a homolog of ATG8 essential for autophagy in yeast, and is associated to the

autophagosome membranes after processing. LC3 can be converted post-translationally into two forms called LC3-I and LC3-II in various cells. LC3-I (an apparent molecular size of approximately 18 kDa on SD-PAGE gel) is cytosolic soluble and non-lipidated, whereas LC3-II (approximately 16 kDa) is autophagosome membrane bound and lipidated with phosphatidylethanolamine at its C-terminal glycine [71].

In recent years, autophagy is also popular because of winning the Nobel Prize, but it is also obvious that it plays an important role in various physiological responses as follows: starvation, development, differentiation, tumorigenesis, immunity, inflammation and neurodegeneration [72]. Autophagy, in particular when it occurs in response to starvation, is generally thought to non-selectively degrade cellular cytoplasmic components [72]. This extensive decomposition contributes to the survival of cells during starvation by recycling resources degradation products in energy production and macromolecule synthesis. In addition to the importance of basal autophagy that plays a constant role at low rates even under nutrient-rich environments and plays an important role in maintaining cellular homeostasis is also emphasized [66,69,71–76]. Indeed, studies using mouse genetics have indicated that autophagy-deficient mice have shown a prominent accumulation of ubiquitinated protein aggregates and furthermore have produced hepatocytes and neuronal cell death without starvation [73,74,76].

HuH-7 cells undergo an incomplete autophagic response following GGA treatment [47], which may also contribute to GGA-induced cell death. What is an incomplete autophagic response? The answer is that GGA causes the initial phase of autophagy, but the late stage of autophagy such as maturation of

autolysosomes or late stage of autophagy fail to proceed, leading to cell death in HuH-7 cells [47]. The GGA-induced incomplete autophagic response results in massive accumulation of initial/early autophagosomes and cell death, because the defects in autophagic response could be linked to defects in energy supply.

I-3-4. Lipid-induced unfolded protein responses

Next, we focused on what kind of cellular events GGA initially induces as an upstream signal for the incomplete autophagic response. And as a result, we found that GGA at micromolar concentrations immediately induces so-called “lipid-induced endoplasmic reticulum (ER) stress response/unfolded protein response (UPR)”, which is essentially linked to its lipotoxicity in human hepatoma cells [77].

In general, Kitai et al. [78] explained the conventional UPR is an adaptive stress response that responds to the accumulation of misfolded proteins in ER lumen (ER stress) and regulates protein folding capability via chaperones to the needs of the cell [79,80]. The UPR is sensed by a chaperone of the binding immunoglobulin protein (BiP)/glucose-regulated protein 78 (GRP78). The accumulation of unfolded proteins requires to recruit BiP/GRP78, so it dissociates from three ER-transmembrane transducers leading to their activation. These transducers are inositol requiring 1 α (IRE1 α), protein kinase RNA (PKR)-like ER kinase (PERK), and activating transcription factor 6 α (ATF6 α) (**Fig.I-4**).

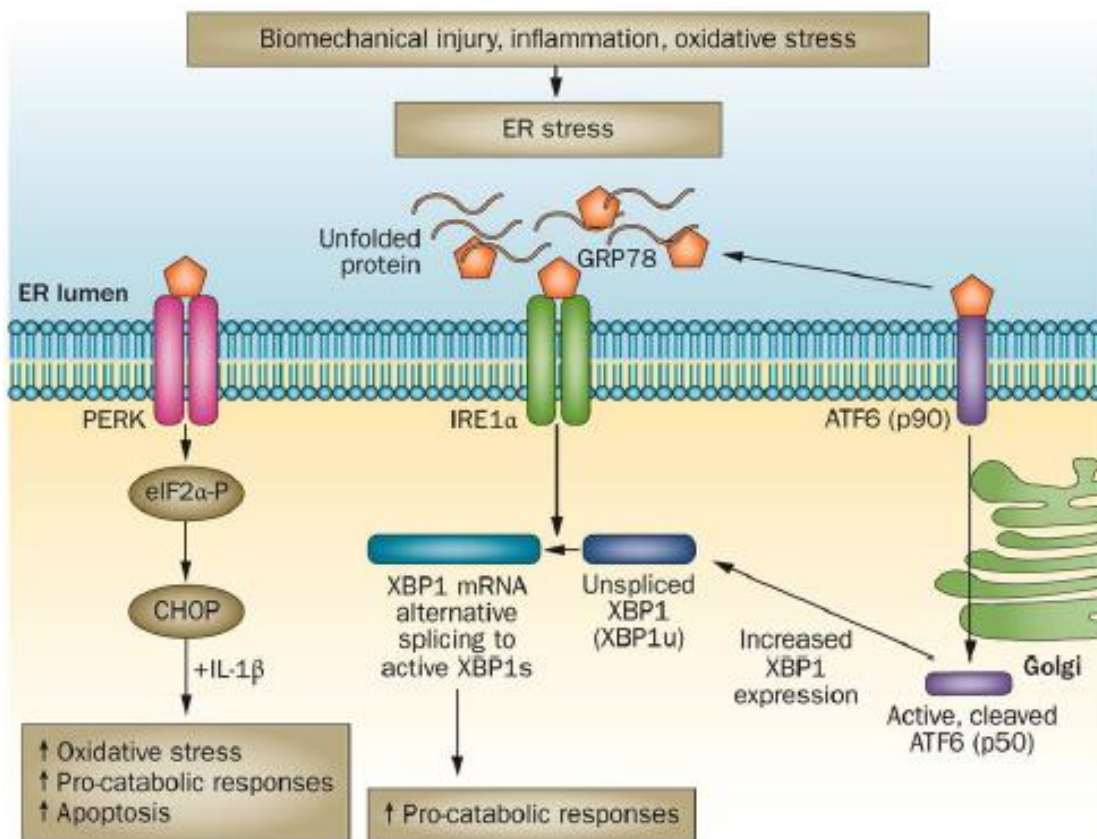


Fig.I-4. Canonical unfolded protein responses.

Liu-Bryan R and Terkeltaub R. *Nature Reviews Rheumatology* 11: 35-44 (2015) [81]

PERK attenuates overall mRNA translation by phosphorylating the eukaryotic initiation factor 2 alpha (eIF2 α). At the same time, it selectively increases the translation of a small number of mRNAs including the transcription factor *ATF4* and its downstream target gene DNA damage inducible transcript 3 (*DDIT3* or previously named *CHOP*). IRE1 α has kinase and endoribonuclease (RNase) activities. IRE1 α autophosphorylation activates RNase, splices X-box binding protein 1 (*XBPI*) mRNA on the ER membrane, and then produces the active transcription factor *XBPIs* m Furthermore, activation of IRE1 α kinase recruits and activates the stress kinase c-jun N-terminal kinase (JNK). When ER stress occurs, ATF6 α shifts to the Golgi apparatus. When it is degraded by Golgi intramembrane proteins, a soluble

truncated ATF6 α is produced and transported to the nucleus. These three UPR pathways act in concert to reduce the density of new proteins entering the ER by extending the ER space, expanding the folding capacity of the ER protein, and degrading the misfolded protein. When ER stress persists and adaptive process starts to fail, cell death occurs, possibly mediated through calcium perturbations, ROS, and the proapoptotic transcription factor DDIT3 [82].

As a general characteristic of lipid-induced UPR, GGA-induced UPR is also suppressed by co-treatment with equimolar oleic acid, which prevents GGA-induced cell death as well [77]. Currently, at least two different hypotheses have been argued as a mechanism for suppressing lipid-induced UPR by oleic acid co-treatment. One is that phospholipids containing oleic acid inserted in the ER membrane inhibit lipid (e.g., palmitic acid)-induced UPR by increasing the membrane fluidity [78,83]. Another is that oleic acid promotes lipid droplet formation, thereby sequestering UPR-causing lipids from the ER membrane to lipid droplets [84,85]. In either case, oleic acid must be at first thio-esterified with coenzyme A (CoA)-SH to become oleyl-CoA that is the only substrate of the enzymatic reaction into which oleic acid is introduced to either membrane phospholipids or triacylglycerols in lipid droplets. However, even though the carboxyl group of oleic acid was blocked with methyl group, the inhibitory effect of the resultant methyl oleate on GGA-induced UPR was exactly similar to the effect of oleate [77]. Furthermore, the preventive effect of oleic acid on GGA-induced UPR was not observed when it was added before GGA treatment [77]. Hence, we speculated that oleic acid might directly or competitively block GGA-mediated signals to induce UPR and cell death.

I-3-5. Rapid downregulation of cyclin D1

Finally, to evaluate chemoprevention targets to clarify the molecular mechanism of hepatoma chemoprevention with GGA. Over the past 20 years, our laboratory have reported various cell-death related effects of GGA at micromolar concentrations in several cell culture systems: loss of $\Delta\Psi_m$ in HuH-7 cells [37], hyper-production of superoxide in transformed fibroblastic 104C1 cells [86], and rapid downregulation of cyclin D1 in three human hepatoma-derived cell lines [87].

Normal cells as they are proliferating and renewing are going through different phase, in a process referred as the cell cycle (**Fig.I-5**). Diploid cells go from G1 phase with double genomes through DNA synthesis (S phase) to G2 phase, its DNA content doubles its original content. Finally, the cell enters the mitosis, M-phase to give and become two daughter cells with identical genome. During their lifetime cells may be exposed to various DNA damaging agents such as UV irradiation and genotoxic drugs. Interestingly, after DNA damage, cells have been observed to arrest at either G1/S transition or G2/M and repair DNA by stopping cell cycle progression [88]. The role of these 2 checkpoints is to avoid the propagation of mutagenic lesions to the daughter cells by providing an efficient time in order to survey DNA damages and to repair them. Cyclin D1 is known to be involved in G1/S checkpoint, as described below in detail.

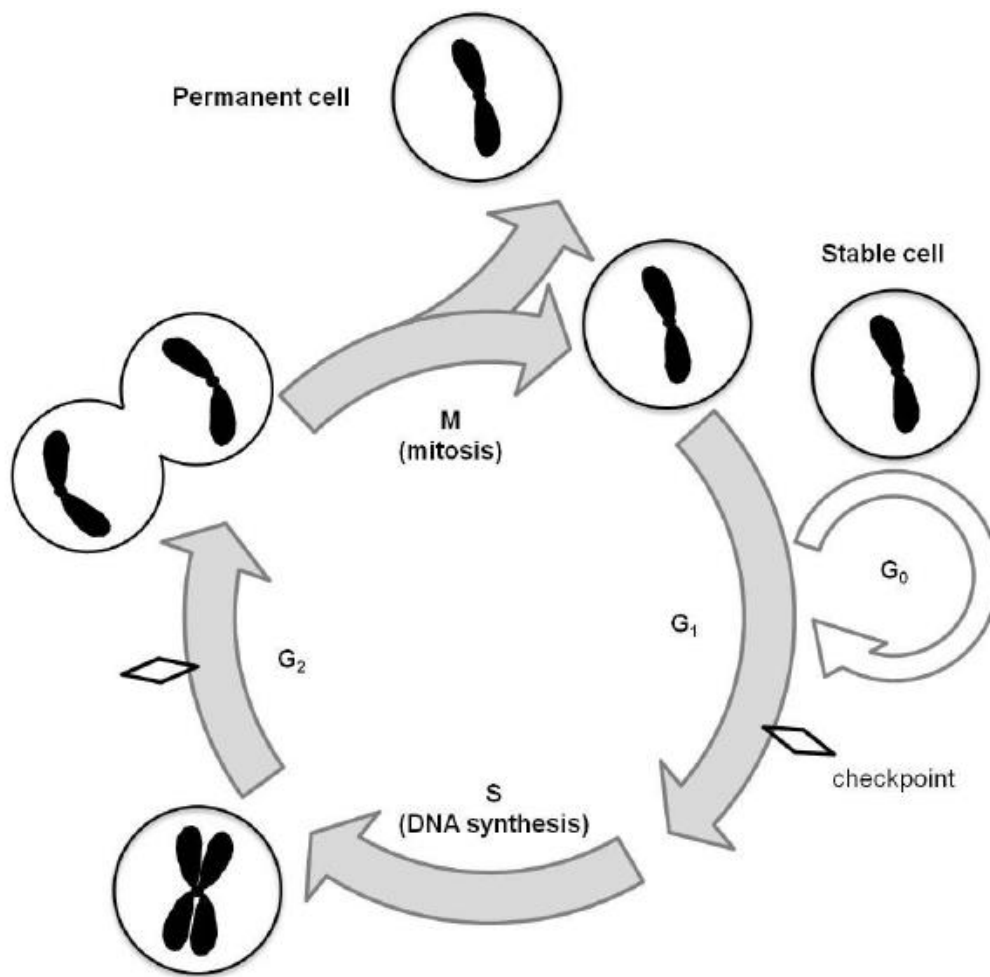


Fig.I-5. Cell cycle.
Sakane's Doctral thesis [89]

Regulation of the cell cycle has complex interaction with cell-cycle related proteins. Cell-cycle related protein of cyclin D1 that regulates G₁/S transition is shown in **Fig.I-6**. The G₁/S transition in the cell cycle leads to the S phase by inducing the expression of cyclin D1 by the dividing signal and its binding to cdk4/6 (cyclin dependent kinase 4/6) in the G₁ phase. It can be described that cyclin D1 promotes cell division by regulating critical regulator genes involved in the G₁/S transition [90].

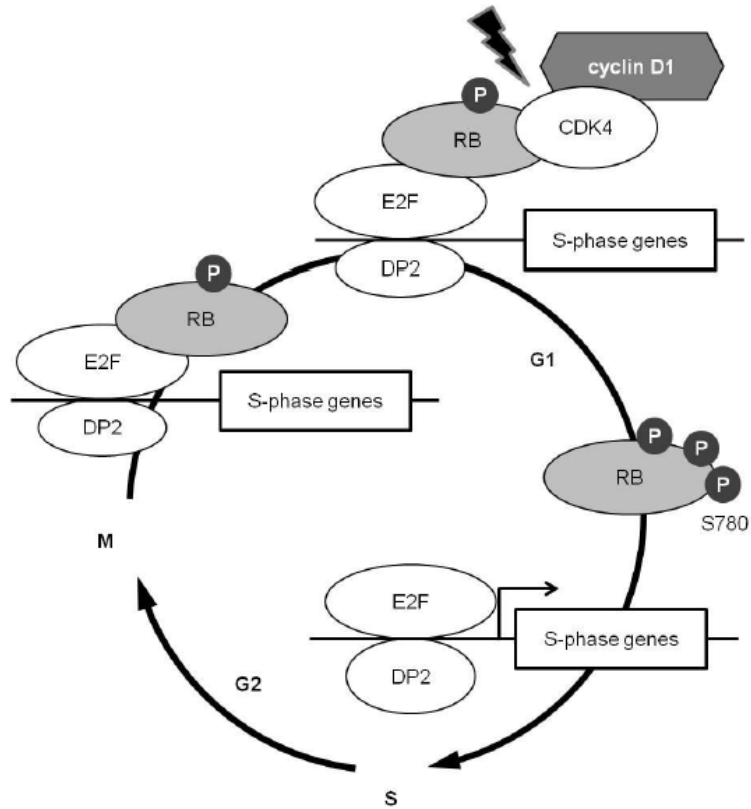


Fig.I-6. Genes related G1/S transition.

Sakane's Doctral thesis [89]

Our prior study proposed that HuH-7 cells undergo an incomplete autophagic response following GGA treatment [47], which may contribute to GGA-induced cell death. Here, while the initial phase of autophagy occurs, the maturation of autolysosomes or later stages of autophagy fail to proceed, leading to substantial accumulation of early/initial autophagic vacuoles, LC3-II, and p62/sequestosome (SQSTM) in HuH-7 cells [47].

Possible mechanisms by which GGA could induce autophagy include impairing mTOR-mediated suppression of autophagy through starvation stress such as amino acid depletion [91], activation of autophagy-initiating gene product, ATG4, which is induced by oxidative stress [92], and the ER stress-mediated UPR as an upstream signal from lipotoxicity with fatty acids [93]. Among these three

potential triggering mechanisms, our laboratory revealed UPR-mediated induction of autophagy, confirming our previous data identified that GGA induced rapid translational downregulation of cyclin D1 [87]. This strongly suggests upregulation of the PERK pathway, which is one branch of the mammalian UPR should be involved in rapid blocking of cyclin D1 translation, providing G1 arrest in cells (**Fig.I-7**) [94].

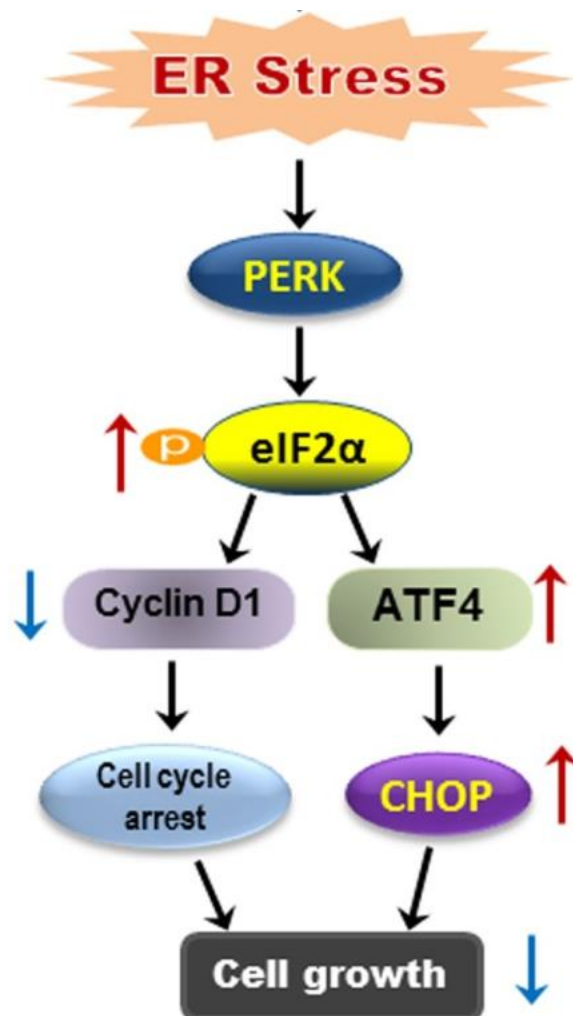


Fig.I-7. Suppression of growth by the UPR.
Liu R, et al. *PLoS ONE* 10 (5): e0125928. (2015) [95]

I-4. Programmed cell death

Programmed cell death is recently classified as apoptosis, necroptosis, pyroptosis, ferroptosis, autophagy and netosis (**Fig.I-8** and **9**). Apoptosis, a non-inflammatory cell death, can be triggered through an extrinsic or intrinsic pathway leading to effector caspase activation and apoptotic body formation [96]. Apoptosis is a form of programmed cell death characterized morphologically by chromatin condensation, membrane blebbing, and cytoplasm compaction, and molecularly by the activation of caspase proteases such as caspases-3, -7, -8, and -9, which are named apoptotic caspase [96]. Necroptosis is induced by ligand binding to tumor necrosis factor (TNF) family death domain receptors, pattern recognizing receptors and virus sensors [97]. Pyroptosis is an inflammatory cell death mechanism, which is triggered by damage-associated molecular patterns (DAMPs), leading to ROS production and inflammasome activation resulting in production of pro-inflammatory cytokines (for example, IL-1 β and IL-18) and caspase-1 activation with consequent cell lysis. As shown in Fig.I-8, inflammatory caspase includes caspase-4, -5, and -11 (a rodent ortholog of human caspase-4/5) besides caspase-1 [98]. Ferroptosis is dependent on iron and ROS and is characterized by lipid peroxidation. Ferroptosis is induced by inhibition of cysteine uptake transporter (SLC7A11 or xCT) or inactivation of the lipid repair enzyme glutathione peroxidase 4 (GPX4) [99]. Autophagy is a lysosome-dependent cellular degradation mechanism in eukaryotic cells, which allows bulk recycling of superfluous cytoplasmic aggregate proteins or dysfunctional organelles [100]. Autophagic cell death was originally defined as a type of cell death-with massive autophagic vacuolization of the cytoplasm and a resulting vacuolated appearance. As mentioned

earlier, autophagic response is not only induced by starvation-stress, but also induced under other stress conditions such as hypoxia, heat, and drug treatment. Netosis is one of the mechanisms underlying programmed cell death that occurs with the release of a scaffold of chromatin associated with different granular and intracellular proteins, named Neutrophil Extracellular Traps (NETs) [101]. Netosis, different from apoptosis and necrosis, is a complex process that occurs in a dramatic change in the morphology of neutrophilic cells that differ in detail depending on the stimulus.





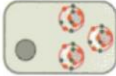

Form	Characteristics	factor/executor
Apoptosis 	<ul style="list-style-type: none"> • Aggregation of chromatin • Fragmentation of cytoplasm 	Caspase-3, 6, 7
Necroptosis 	<ul style="list-style-type: none"> • Swelling of cell • Normal nuclear 	RIPK1, PIRK3, MLKL
Pyroptosis 	<ul style="list-style-type: none"> • Production of cytokine • Rupture of cell 	Caspase-1, 4/5, 11 Gasdermin D
Ferroptosis 	<ul style="list-style-type: none"> • Dependent on iron • Peroxidation of fatty acid 	xCT, GPx1
Autophagy 	<ul style="list-style-type: none"> • Normal nuclear/organella • Excessive autophagy 	Atg5, Beclin1, JNK
netosis 	<ul style="list-style-type: none"> • Release of NET 	NADPH oxidase, PAD4

Fig.I-8. Programmed cell death.

Tanaka M. *Experimental Medicine* 34, (2016) [102]

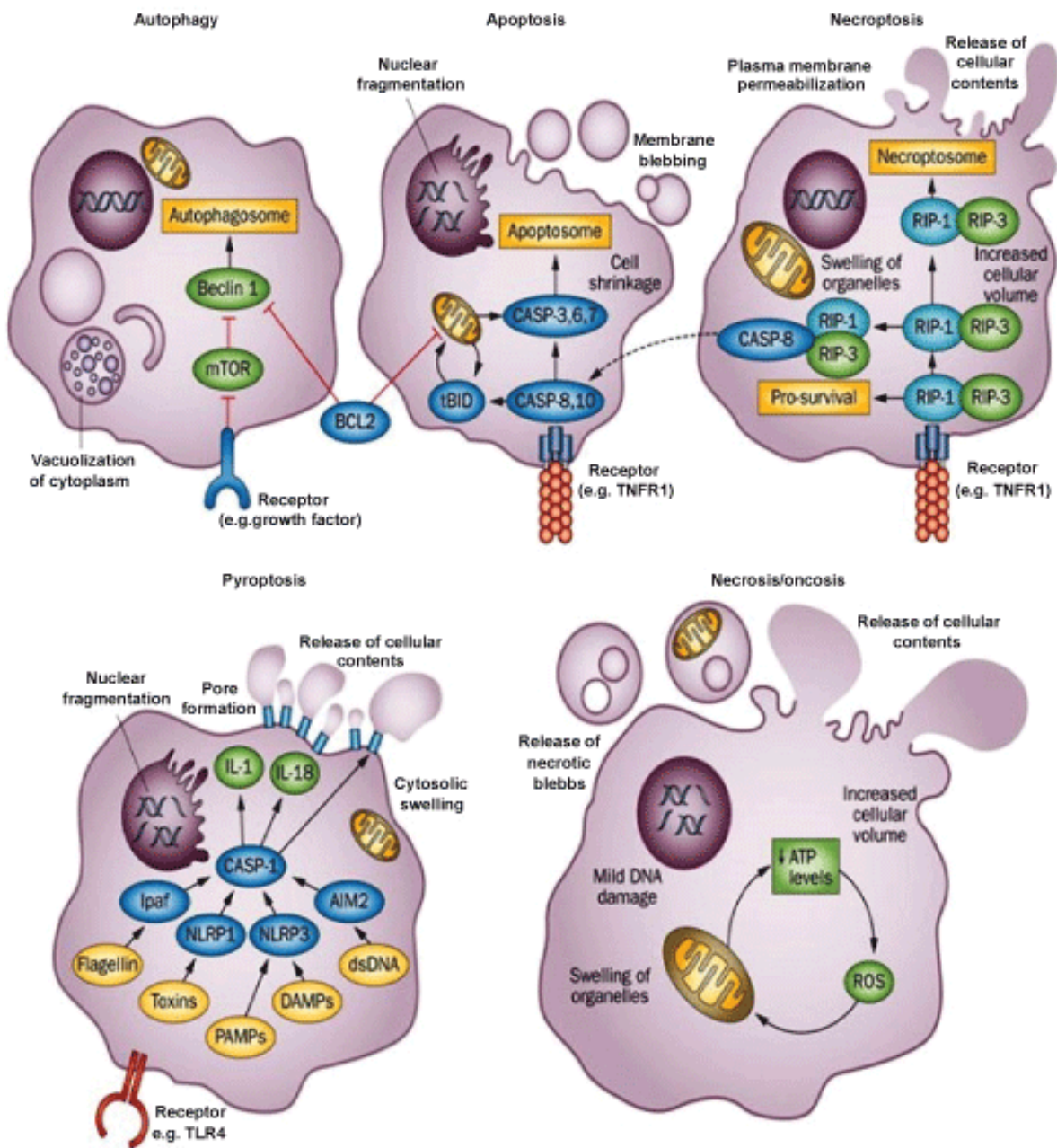


Fig.I-9. Autophagy, apoptosis, necroptosis, pyroptosis and necrosis pathways.

Wree A et al., Nature Reviews Gastroenterol and Hepatology 11, 627-636 (2013) [103]

I-5. Brief outline of the thesis

In this thesis, I describe possible cellular mechanisms of GGA-induced cell death in detail. Particularly, here we propose that toll-like receptor 4 (TLR4)-mediated pyroptosis plays a pivotal role in GGA-induced cell death through canonical inflammasome activation (**Chapter II**) and non-canonical inflammasome signaling (**Chapter III**). In addition to cellular mechanisms of GGA-induced cell death, it is worthwhile to note epigenetic effects of GGA through KDM1A (or formerly named as LSD1) (**Chapter IV**).

Chapter II

Pyroptotic cell death with GGA through canonical inflammasome

Suemi Yabuta

Molecular and Cellular Biology, Graduate School of Human Health Science,

University of Nagasaki, Nagasaki, Japan

Abstract

A branched-chain polyunsaturated fatty acid of GGA (C_{20:4}), which is present in some medicinal herbs, has been reported to induce cell death in human hepatoma cells. So far, we have shown so-called “lipid-induced UPR” as an upstream cellular process of an incomplete response of autophagy, which may be involved in GGA-induced cell death. Here, we show that TLR4-mediated pyroptosis occurs by GGA treatment. The TLR4-specific inhibitor peptide, VIPER, prevented both GGA-induced cell death and GGA-induced UPR. The cellular mRNA levels of the NOD-like receptor containing pyrin domain 3 (*NLRP3*) and *IL1B* genes were upregulated with concomitant translocation of cytoplasmic nuclear factor-kappa B (NF-κB) to the nuclei immediately after GGA treatment, suggesting that GGA induces priming of NLRP3 inflammasome. Furthermore, GGA upregulated the cellular caspase-1 activity, indicating that GGA induces activation of the inflammasome. The activation of caspase-1 activity was completely blocked by either VIPER or MCC950 (a selective inhibitor of NLRP3). Immunofluorescence technique revealed that gasdermin D (GSDMD) was translocated to the plasma membrane after GGA treatment. GGA-induced pyroptosis was also morphologically confirmed by bleb-formation on time-series live-cell imaging. Taken together, the present results indicate that GGA causes pyroptotic cell death in human liver cancer cells via TLR4.

II-1. Introduction

II-1-1. Pyroptosis

As briefly introduced in the previous chapter, pyroptosis is an inflammatory programmed cell death. Multicellular organisms not only prevent infection of pathogenic bacteria and microorganisms but can also cause sepsis and lethal septic shock if over-activated [104]. It is a lytic type of cell death that is initiated by inflammatory caspases. Inflammatory caspases (caspase-1, 4, and 5 in humans) are a group of cysteine-dependent aspartate-directed proteases that are essential for host innate immune defense. Caspase-1 is activated within large multiprotein complexes termed ‘inflammasomes’, which are assembled by the protein pyrin or members of both nucleotide-binding oligomerization domain-like receptor (NLR) and pyrin and HIN (hematopoietic interferon-inducible nuclear protein) domain family (PYHIN) protein families [1, 2].

Sborgi et al described the downstream signaling pathways after inflammasome activation as follows [107]. It is not yet clear enough to see how the downstream signaling pathways following activation of inflammatory caspases and activated caspases initiate these events [108]. Initial study identified the pro-inflammatory cytokine IL-1 β as an important substrate for caspase-1 [109]. Subsequently, it was found that caspase-1, as well as caspase-4 and caspase-5 (human orthologs to rodent caspase-11), induce a novel programmed cell death pathway characterized by cell swelling, lysis, and the release of cytoplasmic content [110–112], presumably as a result of the formation of plasma membrane pores [113]. This type of cell death was named ‘pyroptosis’ from the Greek *pyro* (fire or fever) and *ptosis* (to fall), as it induces

inflammation and morphologically also essentially differs from apoptosis [98]. The physiological function of pyroptosis is to prevent cells from ~~of~~ intracellular pathogen replication and ~~to~~ is thought to re-expose pathogens to extracellular killing mechanisms [114].

II-1-2. Canonical inflammasomes: NLR and ALR inflammasomes

According to Vanaja et al., NLRs such as NLRP1, NLRP3 and NLR family caspase activation and recruitment domain (CARD) domain-containing protein 4 (NLRC4) as well as the absent in melanoma 2 (AIM2), AIM-like receptor (ALR), constitute the most well characterized inflammasomes (**Fig.II-1**) [115].

Among these, NLRP3 is the most extensively studied [116–118], and it is activated by a vast array of microbial- and host-derived triggers as well as endogenous metabolites such as the extracellular ATP, uric acid and cholesterol or inert materials such as aluminum and silica. Conversely, NLRP1 is activated by anthrax lethal toxin and NLRC4 by bacterial type III secretion system (T3SS) components and flagellin. In contrast, AIM2 is activated by bacterial or viral double stranded DNA present in the cytosol. Here, we focus on NLRP3 inflammasome to investigate cellular mechanism of GGA-induced cell death, because GGA is categorized into polyunsaturated branched-chain fatty acid and several saturated fatty acids have been reported to be able to activate NLRP3 inflammasome [119,120]

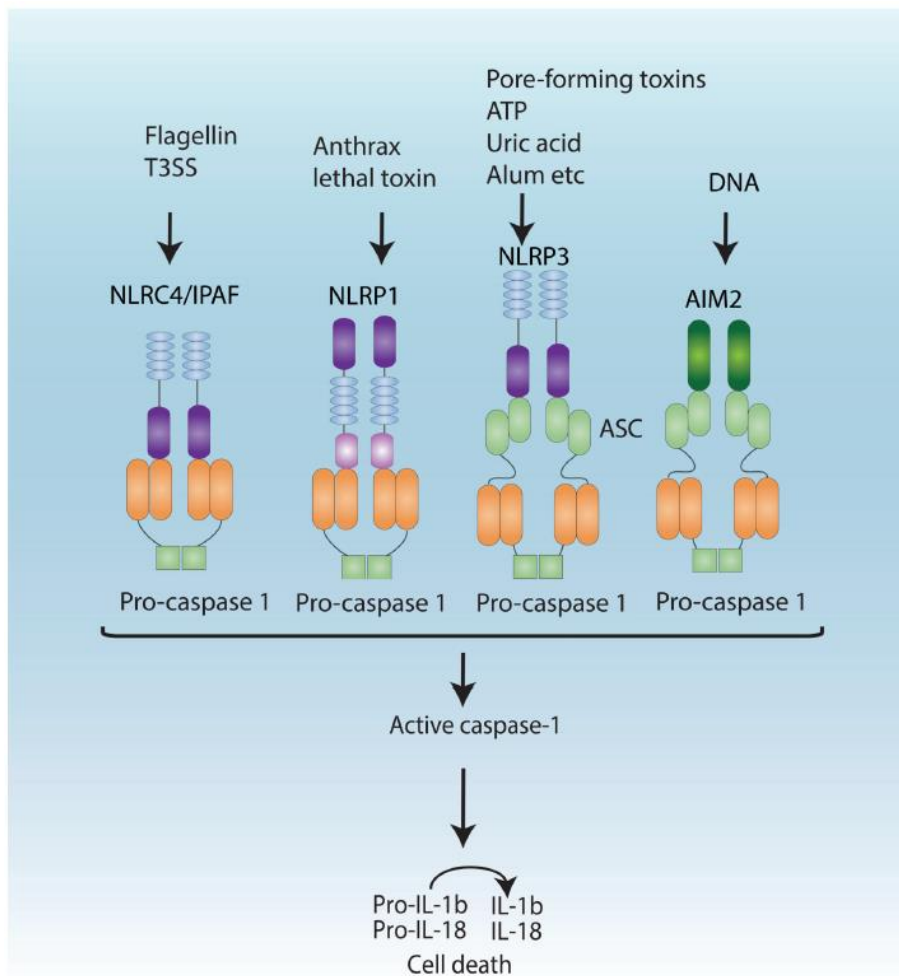


Fig.II-1. Canonical inflammasomes.

Canonical inflammasomes contain sensors belonging to the NLR or ALR family. NLRC4 is activated by bacterial flagellin and T3SS components, NLRP1 is activated by anthrax lethal toxin and AIM2 is activated by cytosolic dsDNA. NLRP3 is activated by a wide variety of signals including pore-forming cytotoxins, ATP, uric acid and alum. Once activated the receptors form an inflammasome complex with or without the adaptor, ASC, and recruit procaspase-1, which is subsequently cleaved into active caspase-1. Caspase-1 cleaves preforms of IL-1 β and IL-18 into their active forms as well as induces cell death. Vanaja et al., *Trends in Cell Biology* 25, 308-315 (2015) [115]

II-1-3. Mechanisms of NLRP3 inflammasome activation

Guo, Callaway and Ting [121] described the most investigated NLRP3 activation mechanism, which includes 1) the relocalization of mitochondrial NLRP3, 2) the generation of mitochondrial ROS and the release of mitochondrial DNA or cardiolipin, 3) potassium efflux out of the cell, and 4) the release of cathepsins into the cytosol after lysosomal destabilization (**Fig.II-2**) [115,122,123]. As mentioned above, the NLRP3 inflammasome is activated in response to the most extensive stimuli, leading to a theory that unusual agonists induce similar downstream events perceived by NLRP3 [123–125].-However, since not all of these events are induced by all NLRP3 agonists including fatty acids, the precise mechanism of NLRP3 inflammasome activation is expected to be a future result. Additionally, increases in intracellular calcium also can activate the NLRP3 inflammasome, although it is not shown in Fig.II-2 [126,127]. But the upregulation of intracellular calcium also cannot be ~~an~~ essentially required for all NLRP3 agonists [128]. Though many published studies support the involvement of lysosomal cathepsins, proteases that degrade internalized proteins, this is an argument in the activation of NLRP3 inflammasome [129].

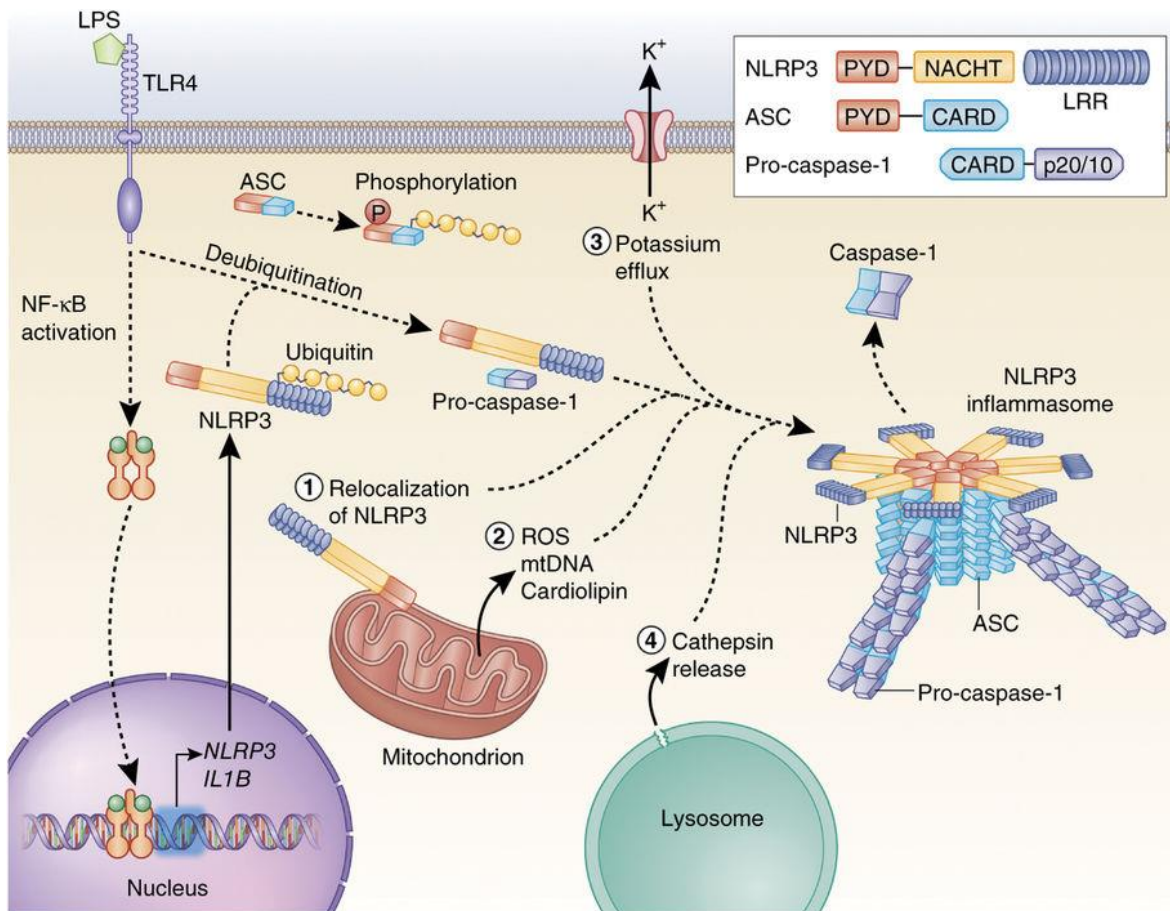


Fig.II-2. Mechanisms of NLRP3 inflammasome activation.

NLRP3 must be primed before activation. Priming involves two distinct steps. First, an NF- κ B-activating stimulus, such as LPS binding to TLR4, induces elevated expression of *NLRP3* (as well as *IL1B*), which leads to increased expression of NLRP3 protein. Additionally, priming immediately licenses NLRP3 by inducing its deubiquitination. The adaptor protein ASC must become linearly ubiquitinated and phosphorylated for inflammasome assembly to occur. After priming, canonical NLRP3 inflammasome activation requires a second, distinct signal to activate NLRP3 and lead to the formation of the NLRP3 inflammasome complex. The most commonly accepted activating stimuli for NLRP3 include relocalization of NLRP3 to the mitochondria, the sensation of mitochondrial factors released into the cytosol (mitochondrial ROS, mitochondrial DNA, or cardiolipin), potassium efflux through ion channels, and cathepsin release following destabilization of lysosomal membranes. Recent studies have determined that activated NLRP3 nucleates ASC into prion-like filaments through PYD-PYD interactions. Pro-caspase-1 filaments subsequently form off of the ASC filaments through CARD-CARD interactions, allowing autoproteolytic activation of pro-caspase-1. Inset shows domain arrangement of the NLRP3 inflammasome components. Pro-caspase-1 and caspase-1 domains are simplified for clarity, the CARD domain is actually removed by cleavage, and two heterodimers form with the p20 and p10 effector domains (p20/10). Guo H, Callaway J. B, and Ting J. P. *Nature Medicine* 21, 677-687 (2015) [130]

As Guo, Callaway and Ting described [121], in most cell types, the NLRP3 inflammasome must be primed prior to inducing pyroptosis. An example of prototype of such a priming event is the activation of TLR4 signaling by gram-negative bacterial lipopolysaccharides (LPS). It has long been known that priming is induced by cellular expression of NLRP3 through NF- κ B signaling [131]. However, recent findings have shown that priming rapidly activates NLRP3 inflammasome by inducing the deubiquitination of NLRP3 independent of new protein synthesis, while inhibition of deubiquitination is activated by NLRP3 activation [132,133]. Upon priming, NLRP3 can assemble the NLRP3 inflammasome in the multiprotein complex in response to its stimulation. In addition, conversely, the adaptor of ASC (apoptosis-associated speck-like protein containing a caspase recruitment domain) must be linearly ubiquitinated ~~for~~ in order to be assembled into NLRP3 inflammasome [134]. The stimulators, also recognized as NLRP3 agonists, induce ATP, pore-forming toxins, crystalline substances such as uric acid and cholesterol, nucleic acids, hyaluron, and fungal, bacterial or viral pathogens [115,122]. These stimuli can be infected with agonists produced by the pathogen or released by the damaged host cells. Furthermore, if there is a pathological condition in the body, it can promote the formation of these stimuli in the absence of infection; an example is the formation of inflammatory cholesterol crystals.

Recent studies have shown that the NLRP3 nucleotide-binding domain (NBD/NACHT*) oligomerizes the NLRP3 pyrin domain (PYD), which acts as a scaffold to nucleate ASC proteins through PYD-PYD interactions (see Fig.II-2) [135,136]. ASC can be transformed into prion-like form and generates long ASC filaments important for activation process. Pro-caspase-1 then interacts with ASC filaments through

CARD-CARD interactions and forms its own prion-like filaments that branch off of the ASC filaments.

The close proximity of pro-caspase-1 proteins then induces auto-proteolytic maturation of pro-caspase-1 into active caspase-1, which is released as soluble protein into the cytosol from NLRP3 inflammasome [121].

* The NACHT is derived from the four plant and animal proteins that initially defined the unique features of this domain: the neuronal apoptosis inhibitory protein (NAIP), class II transcription activator (CIITA) of the MHC, incompatibility locus protein from *Podospora anserina* (HET-E), and telomerase-associated protein 1 (TP1).

II-1-4. NLRP3 inflammasome priming: first hit

Patel et al. have proposed the functional regulation of inflammasome activation in a cell is a ‘two-hit’ process [137]. The ‘first hit’ promotes transcriptional expression of major components of inflammasome. Among all the NLR inflammasomes, NLRP3 is the most widely and extensively studied as aforementioned [116–118]. Without exception, the activation of the NLRP3 inflammasome is also regulated by a two-hit process. The NLRP3 inflammasome is formed after indirect sensing of both non-sterile events derived from pathogens and sterile metabolic stressors. These range from bacterial toxins, host mitochondrial DNA, viral nucleic acids, and extracellular ATP to particulate matter such as crystals (uric acid, cholesterol, silica, aluminum) and amyloids [138,139]. Before a functional NLRP3 inflammasome is formed, however, transcriptional (NF- κ B dependent) and post-translational (deubiquitination and linear ubiquitination dependent) mechanisms are involved in the functioning of NLRP3 and ASC, a reasonable level must be achieved and pro-IL-1 β must also accumulate dependent on NF- κ B—this is a process known as

inflammasome priming, or ‘signal 1’. This is different from cellular priming of B or T cells after first encountered by an antigen, which includes differentiation and maturation processes.

Across species, the expression of both NLRP3 and IL-1 β is known to be transcriptionally regulated, dependent on NF- κ B [131]. This is thought to prime the inflammasome before its activation by second stimuli (second hit). The ‘second hit’, either by the same and/or by additional stimuli, promotes the functional activity of the NLRP3 inflammasome [140]. Although most mammalian cells do not have a ready pool of IL-1 β , IL-18 protein is expressed more constitutively [141], and thus may not have the same requirements for priming between IL-1 β and IL-18.

II-1-5. NLRP3 inflammasome activation: second hit

The second step in activation of the NLRP3 inflammasome, as described by Sutterwala, Haasken, and Cassel, is delivered by one of a variety of agonist groups that cause specific activation of NLRP3 and assembly of the inflammasome complex, and that finally culminates in the activation of caspase-1 [123].

The activators include both exogenous and endogenous molecules such as crystalline molecules requiring phagocytosis for activation, ATP acting through its cell surface receptor P2X7R, and pore-forming toxins such as nigericin. As the activators are structurally distinct and act on the cell in a separate way, it has been suggested that the final activation signal, the binding of a putative ligand directly to NLRP3, must occur downstream from these unrelated upstream activators.

II-1-6. Expression of NLRP3 through NF- κ B

As aforementioned, priming has long been known to upregulate cellular expression of the *NLRP3* gene through nuclear NF- κ B signaling [131]. According to a review by Godwin et al. [142], NF- κ B is a tightly-regulated transcription factor, and consists of homo or heterodimers from a pool of five REL proteins: NF- κ B1 (p50), NF- κ B2 (p52), RelA (p65), RelB, and c-Rel (Rel). However, their biological effects are cell-type dependent, mediating diverse physiological processes. In unstimulated cells, NF- κ B is sequestered in the cytoplasmic space, bound to its regulatory protein, inhibitor of NF- κ B (I κ B). NF- κ B activation is driven by the phosphorylation of I κ B, resulting in the dissociation of the NF- κ B/I κ B complex. As a result, the nuclear localization sequence of NF- κ B is exposed, thereby resulting in its translocation into the nucleus [143]. After homo/heterodimer formation, NF- κ B binds to specific promoter sequences (κ B sites) contained in more than 150 genes, which play important roles in either cell proliferation, cellular adhesion, inflammation or anti-apoptosis [144].

In addition, Godwin et al. described in the same article the downstream pathway of TLR to activate NF- κ B [142]. Traditionally the activation of NF- κ B occurs through phosphorylation. Shortening the long story, binding of a ligand to a cell surface receptor, such as a member of the TLR superfamily, primes the recruitment of adaptor proteins to the cytoplasmic domain of TLRs. Adaptors then recruits and activates the I κ B α kinase (IKK) complex, including the IKK β or IKK α protein and the scaffold protein, NF- κ B essential modulator (NEMO). IKK phosphorylates two serine residues (Ser32/Ser36), in the I κ B α regulatory domain regulating in dissociation of the NF- κ B/I κ B complex, and as a consequence the released

NF- κ B to enter into the nuclear space where NF- κ B acts as transcription factor for its target genes.

Hashimoto, Hudson and Anderson have clearly elucidated NLRP3 is one of the products of NF- κ B-target genes. There is virtually no expression of NLRP3 in primary hepatocytes and stimulation of hepatocytes by LPS in vitro results in a strong activation of NLRP3 expression [145]. They demonstrated that the activation of NLRP3 expression was blocked by the NF- κ B activation inhibitor, N4-[2-(4-phenoxyphenyl) ethyl]-4, 6-quinazolinediamine (QNZ). QNZ blocked NF- κ B-dependent expression of TNF- α , IL-1 β and NLRP3 in liver cells. Moreover, they have found that a 1.3-kbp DNA sequence located in close proximity of the most upstream transcriptional start site (-3968 to -2625) of the human *NLRP3* gene that harbors one putative octamer NF- κ B binding site (-2755 to -2746). Thus, nuclear NF- κ B is a necessary and sufficient factor for activation of the NLRP3 inflammasome in at least in primary hepatocytes [145].

II-1-7. Downstream signals of TLRs

As described above, NLRP3 protein acts as cytosolic pattern-recognition receptors (PRRs) and detect a variety of pathogen-associated molecular patterns (PAMPs) or DAMPs. Hence, cytoplasmic PRRs are the first line of defense against invading microbes and are expressed in a variety of immune cells including macrophages, epithelial cells, dendritic cells, neutrophils, and adaptive immune cells. However, some other non-cytoplasmic types of these PRRs, such as the TLRs, are expressed on the cell surface and can be activated at the extracellular site directly via external pathological signals known as PAMPs, indicating

that TLRs are the most first line of defense.

Akira and Takeda [146] successfully described the discovery of the TLR family began with the identification of Toll, a receptor that is expressed by insects and was found to be essential for establishing dorsoventral polarity during embryogenesis [147]. Subsequent studies revealed that Toll also has an essential role in the ~~insect~~-innate immune response of insects against fungal infection [148]. Homologues of the insect Toll were identified through database searches, and so far, 11 members of the TLR family have been identified in mammals. The TLRs are type I integral membrane glycoproteins, and are members of a larger superfamily that contains the IL-1 receptors (IL-1Rs), based on considerable homology in the cytoplasmic region. In contrast, the extracellular region of the TLRs and IL-1Rs differs markedly: the extracellular region of TLRs contains leucine-rich repeat (LRR) motifs, whereas the extracellular region of IL-1Rs contains three immunoglobulin-like domains. The LRR domains of TLRs form a horseshoe structure, and it is thought that the concave surface of the LRR domains is involved directly in the recognition of various pathogens. The main ligands recognized by different TLRs are summarized in **Table II-1** and **Fig.II-3**. For example, TLR4 homodimers recognize LPS from Gram-negative bacteria. TLR2 recognizes a lipopeptides from *Mycoplasma* or mycobacteria with either TLR6 or TLR1. Notably, despite the conservation between LRR domains, different TLRs can recognize several structurally unrelated ligands [149–151]. The subcellular localization of different TLRs correlates to some extent with the molecular patterns of their ligands. TLR1, TLR2 and TLR4 are located on the cell surface and are supplemented to phagosomes after activation by their respective ligands. By contrast, TLR3, TLR7/8,

TLR9 and TLR13, which are involved in the recognition of nucleic-acid-like structures, are not expressed on the cell surface, as shown in Fig.II-3 [152–154]. For example, TLR9 has been shown to be expressed in the ER, and recruited to endosomal/lysosomal compartments after stimulation with CpG-containing DNA [155].

Table II-1 Toll-like receptors and their ligands

Receptor	Ligand	Origin of ligand
TLR1	Triacyl lipopeptides Soluble factors	Bacteria and mycobacteria <i>Neisseria meningitidis</i>
TLR2	Lipoprotein/lipopeptides Peptidoglycan Lipoteichoic acid Lipoarabinomannan Phenol-soluble modulins Glycoinositolphospholipids Glycolipids Porins Atypical lipopolysaccharide Atypical lipopolysaccharide Zymosan Heat-shock protein 70*	Various pathogens Gram-positive bacteria Gram-positive bacteria Mycobacteria <i>Staphylococcus epidermidis</i> <i>Trypanosoma cruzi</i> <i>Treponema maltophilum</i> <i>Neisseria</i> <i>Leptospira interrogans</i> <i>Porphyromonas gingivalis</i> Fungi Host
TLR3	Double-stranded RNA	Viruses
TLR4	Lipopolysaccharide Taxol Fusion protein Envelope protein Heat-shock protein 60* Heat-shock protein 70* Type III repeat extra domain A of fibronectin* Oligosaccharides of hyaluronic acid* Polysaccharide fragments of heparan sulphate* Fibrinogen*	Gram-negative bacteria Plants Respiratory syncytial virus Mouse mammary-tumour virus <i>Chlamydia pneumoniae</i> Host Host Host Host Host
TLR5	Flagellin	Bacteria
TLR6	Diacyl lipopeptides Lipoteichoic acid Zymosan	<i>Mycoplasma</i> Gram-positive bacteria Fungi
TLR7	Imidazoquinoline Loxoribine Bropirimine Single-stranded RNA	Synthetic compounds Synthetic compounds Synthetic compounds Viruses
TLR8	Imidazoquinoline Single-stranded RNA	Synthetic compounds Viruses
TLR9	CpG-containing DNA	Bacteria and viruses
TLR10	N.D.	N.D.
TLR11	N.D.	Uropathogenic bacteria

*It is possible that these ligand preparations, particularly those of endogenous origin, were contaminated with lipopolysaccharide and/or other potent microbial components, so more-precise analysis is required to conclude that TLRs recognize these endogenous ligands. N.D., not determined. Akira S and Takeda K, *Immunology* 4, 499-511 (2004) [156]

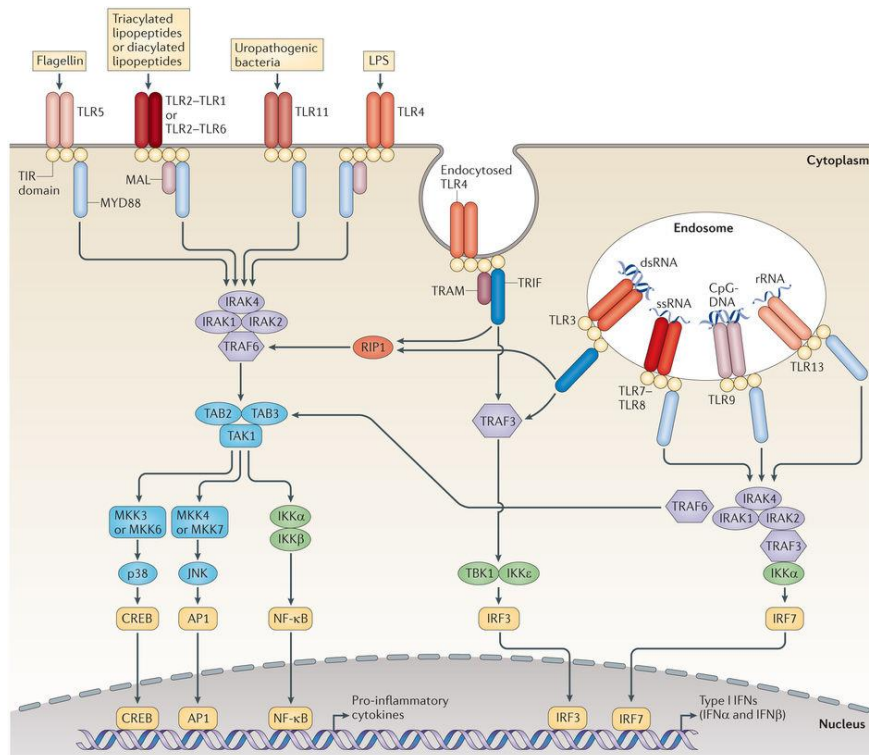


Fig.II-3. Mammalian TLR signaling pathways.

A detailed knowledge of how mammalian TLRs signal has developed over the past 15 years. TLR5, TLR11, TLR4, and the heterodimers of TLR2-TLR1 or TLR2-TLR6 bind to their respective ligands at the cell surface, whereas TLR3, TLR7-TLR8, TLR9 and TLR13 localize to the endosomes, where they sense microbial and host-derived nucleic acids. TLR4 localizes at both the plasma membrane and the endosomes. TLR signaling is initiated by ligand-induced dimerization of receptors. Following this, the TIR domains of TLRs engage TIR domain-containing adaptor proteins (either myeloid differentiation primary-response protein 88 (MyD88) and MyD88-adaptor-like protein (MAL), or TIR domain-containing adaptor protein inducing IFN β (TRIF) and TRIF-related adaptor molecule (TRAM)). TLR4 moves from the plasma membrane to the endosomes in order to switch signaling from MyD88 to TRIF. Engagement of the signaling adaptor molecules stimulates downstream signaling pathways that involve interactions between IL-1R-associated kinases (IRAKs) and the adaptor molecules TNF receptor-associated factors (TRAFs), and that lead to the activation of the mitogen-activated protein kinases (MAPKs) JUN N-terminal kinase (JNK) and p38, and to the activation of transcription factors. Two important families of transcription factors that are activated downstream of TLR signaling are NF- κ B and the interferon-regulatory factors (IRFs), but other transcription factors, such as cyclic AMP-responsive element-binding protein (CREB) and activator protein 1 (AP1), are also important. A major consequence of TLR signaling is the induction of pro-inflammatory cytokines, and in the case of the endosomal TLRs, the induction of IFN. O'Neill L. A, Golenbock D, and Bowie A. G. *Nature Reviews Immunology* 13, 453-460 (2013) [157]

Akira's group have also explained the TLRs/IL-1Rs superfamily signaling cascade as follows [146]. After ligand binding, TLRs/IL-1Rs dimerize and undergo structural change needed for the recruitment of downstream signaling molecules. These include the adaptor molecule myeloid differentiation primary-response protein 88 (MyD88), IL-1R-associated kinases (IRAKs), transforming growth factor- β (TGF β)-activated kinase 1 (TAK1), TAK1-binding protein 1 (TAB1), TAB2 and TNF-receptor-associated factor 3/6 (TRAF3/6) (Fig.II-3) [158,159].

II-1-8. Pyroptosis interacts with UPR

Tufanli et al. [160] have considered from previous studies and then speculated that ER stress might induce inflammasome activation through several mechanisms, including the release of reactive oxygen species from damaged mitochondria (mtROS) [121]. Because previous studies showed that treatment of macrophages with saturated fatty acids activates IRE1 and because these lipids also activated the NLRP3 inflammasome through inducing mtROS production [119,161,162].

Janssens, Pulendran, and Lambrecht [163] described in their article reporter-gene studies *in vivo* have shown constitutive activation of the IRE-1 pathway in specific a certain cell type, such as CD8 α^+ DCs and development of B cells and T cells, suggesting that TLR signaling might induce UPR [164,165]. Indeed, activation of TLRs affects UPR signaling cascades [166,167]. This probably reflects an expected response of the cell to prepare the ER to combat infection or metabolic stress. At this moment, it is still unclear how IRE1 α or other sensors that detect the ER stress are activated ~~in~~ under these conditions; however,

perturbations in the composition of the ER lipid bilayer have been shown to directly induce activation of IRE1 α and PERK independently of their luminal sensor domain [168]. In addition, the flavonoid component quercetin is reported to directly activate IRE1 α by binding to a pocket at to the dimer interface of the RNase domain of IRE1 α [83]. Therefore, there is another way to trigger ER stress sensors may exist. Interestingly, the UPR seems to be closely connected to host immune responses as well as cellular metabolic stress.

Therefore, we addressed that during GGA-induced cell death UPR would be conveyed by TLR4 signaling in human hepatoma cells. To resolve this question, we paid great attention to a paper describing TLR4/ UPR axis [169]. By demonstrating that palmitate-enriched high fat diet-mediated stimulation of TLR4 signaling causes UPR in mice, these authors have indicated the existence of a novel signaling network that links TLR4 activation, ER stress, and mitochondrial dysfunction [169]. Another line of evidence for TLR4/ UPR axis is a report that 7-ketocholesterol-induced inflammation is mediated mostly through the TLR4 receptor and also involves a robust UPR, which seems to be mediated by yet identified kinases activated through the TLR4 receptor [170]. Both lipids of saturated fatty acids and the oxidized cholesterols are well established to induce both UPR [160,171] and TLR4 signaling . Hence, it is quite interesting for us to see whether another novel UPR-inducing lipid of GGA is also able to stimulate TLR4 signaling in order to induce UPR.

II-1-9. Gasdermin D is emerging as executors of pyroptosis

Sborgi et al. introduced in their original paper [107] that some landmark studies recently identified gasdermin D (GSDMD), a member of the gasdermin protein family, as an essential executor of pyroptosis in human cells [172,173]. GSDMD is required for introduction of pyroptosis and is processed by active caspase-1 but not by apoptotic caspases like caspase-3. The N-terminal fragment of GSDMD (GSDMD-N, p20) was found to be sufficient to induce cell death with the morphological features of pyroptosis [173], and overexpression of the C-terminal domain GSDMD-C (p30) was found to block GSDMD-N-dependent cell death [173]. These results led to the hypothesis that caspase-dependent cleavage releases GSDMD-N from an inhibitory interaction with GSDMD-C. Since pyroptosis had long been speculated to involve the formation of a plasma membrane pore, immediate destruction of the electrochemical gradient, and subsequent osmotic lysis of the host cell [108], it is likely that GSDMD-N either promotes the formation of this pore or itself has pore-forming activity (**Fig.II-4**) [174].

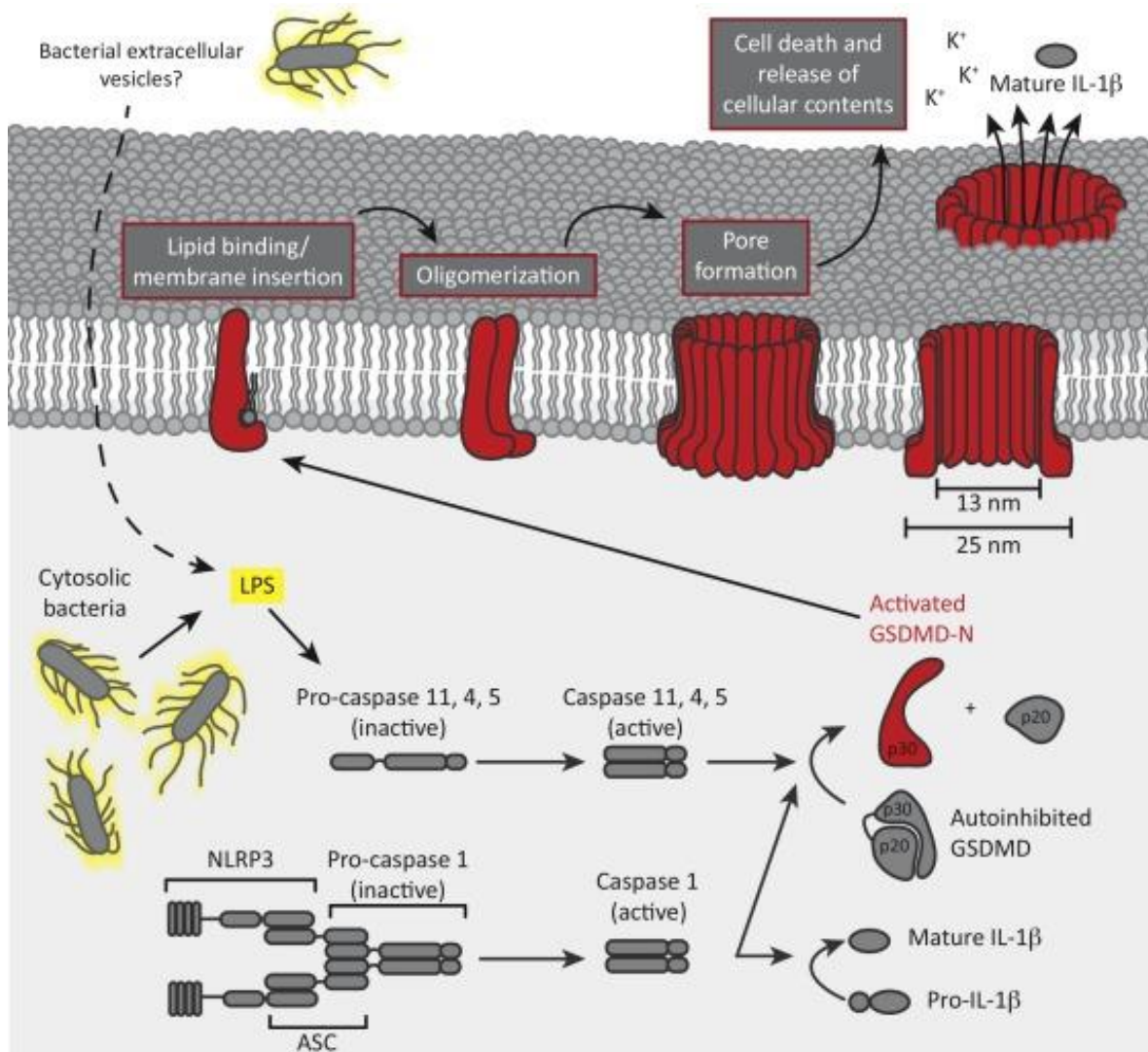


Fig.II-4. Schematic representation of the pyroptosis pathways.

Inflammatory caspases are activated through intracellular LPS binding caspase-11, caspase-4/5 or the inflammasome (caspase-1). Upon activation, the inflammatory caspases cleave Gasdermin D (GSDMD), releasing the N-terminal p30 domain from the autoinhibitory GSDMD-C domain. Activated GSDMD-N (red) then binds to lipids in the plasma membrane and forms large oligomeric pores, leading to release of cellular contents and cell death. Aglietti R. A and Dueber E. C. *Trends in Immunology* 38, 261-271 (2017) [104]

II-1-10. GSDMD-N forms functional pores

The fact that pyroptosis is characterized by pore formation on the plasma membrane strongly suggests that the ring-like structures of GSDMD-N are pores forming on the liposome surface, a hypothesis that has now been confirmed by several studies. Indeed, incubation of cargo-loaded liposomes with GSDMD-N resulted in permeabilization of the liposome membrane and release of the cargo into the surrounding buffer [107,175,176]. Aglietti *et al.* monitored the release of calcium ions using a fluorogenic dye (Fura-2) and demonstrated that GSDMD-N could permeabilize liposomes of multiple lipid compositions, although the kinetics and total calcium release differed depending on the lipids present. Similarly, Ding *et al.* and Liu *et al.* demonstrated that the total release of terbium ion (Tb^{3+} , ionic diameters of 212.6 – 236 pm) also varied with lipid composition. Experiments with different-sized carbohydrate fluorophore conjugates suggested that molecules with a diameter of 10 nm or less pass through the GSDMD-N pore [107,175], consistent with the diameter measured on microscope (see Fig.II-4). Since these experiments were done using recombinant materials with reconstituted liposomes, it is clear that GSDMD-N itself is necessary and sufficient to form these pores by self-assembly on the membrane.

II-2. Results

II-2-1. Activation of caspase-1 activity after GGA treatment

As shown in **Fig.II-5A**, caspase-1 activity was gradually increased immediately after GGA treatment until 5 h, and dramatically enhanced at 8 h and the higher level was maintained until 24 h. However, by immunoblotting, the caspase-1 activation was not able to be detected each time (data not shown). Accordingly, the level of *caspase-1* mRNA was unchanged (**Fig.II-5B**).

A time-dependent change of the cellular *caspase-1* mRNA level was also followed after treatment with 20 μ M GGA in three other human hepatoma cell lines: PLC/PRF/5 (**Fig.II-5C**), HepG2 (**Fig.II-5D**), and Hep3B (**Fig.II-5E**). Three cell lines showed three different behaviors; a transient increase of the cellular *caspase-1* mRNA level was observed in PLC/PRF/5, virtually no change in HepG2, and its immediate downregulation in Hep3B.

Immunofluorescence technique revealed cytoplasmic localization of caspase-1 protein in control HuH-7 cells, but in GGA-treated cells the green fluorescence of caspase-1 protein was mostly co-localized with the blue fluorescence of Hoechst33258 as shown in **Fig.II-5F**.

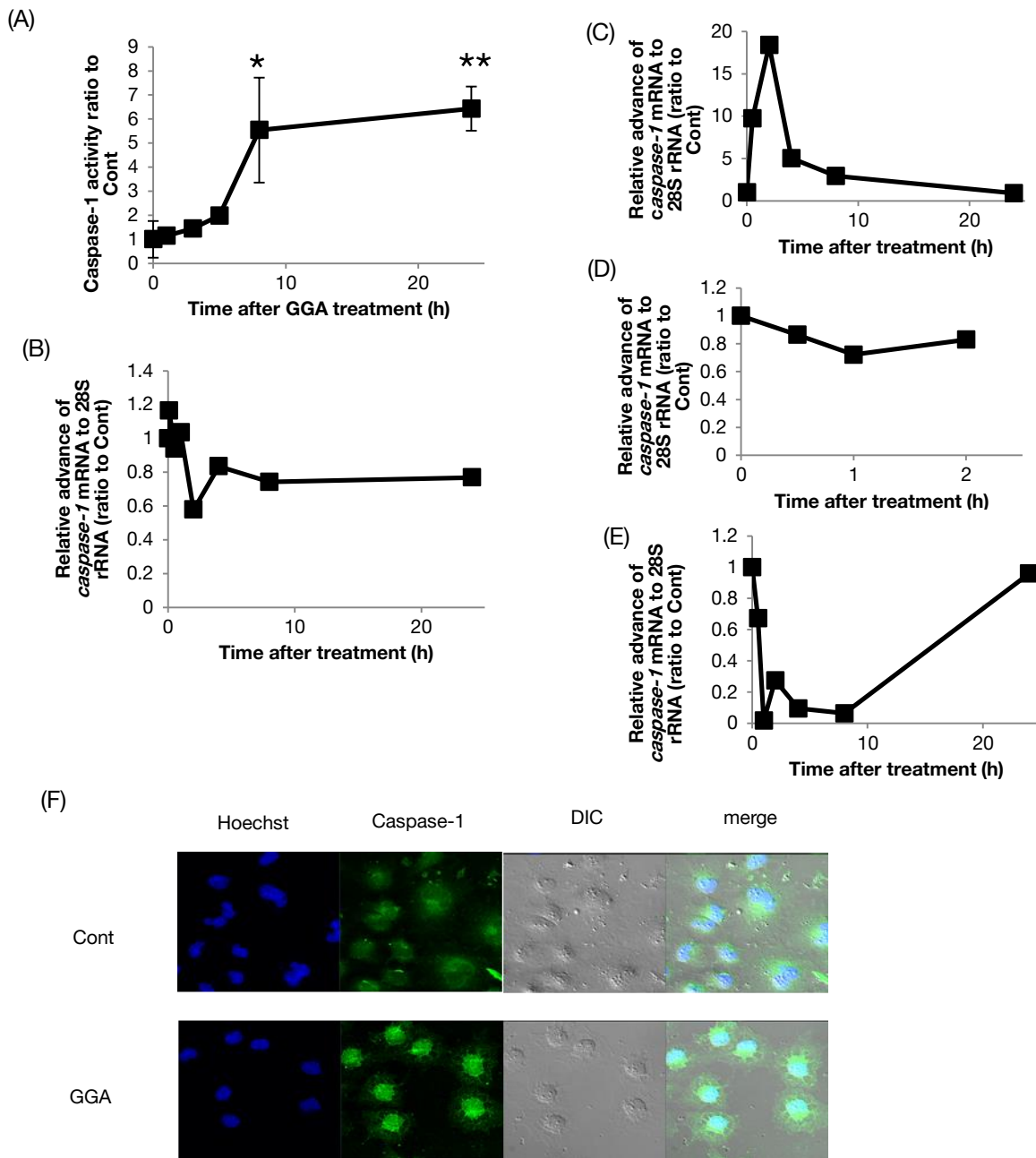


Fig.II-5. GGA activated caspase-1 in HuH-7 cells.

(A) HuH-7 cells were treated with 20 μ M GGA for 0, 1, 3, 5, 8, and 24 h. Caspase-1 activation measurement used with caspase-Glo1 assay. Each point represents the mean \pm SD (n=3). Asterisks (*, **) indicate statistically significant difference from a control sample at 0 h with p value of <0.05, 0.01, respectively, analyzed using the Student's *t*-test. (B) Total RNA was extracted to measure the cellular levels of *caspase-1*. PLC/PRF/5 (C), HepG2 (D) or Hep3B (E) cells were treated with 20 μ M GGA for 0, 0.5, 1, 2, 4, 8, and 24 h (HepG2 was only 0 to 2 h), and total RNA was extracted to analyze *caspase-1* mRNA expression by RT-qPCR. (F) HuH-7 cells were treated with 20 μ M GGA for 3 h. Immunofluorescence images were obtained with caspase-1 (green), and the nuclei were counter-stained with Hoechst 33258 (blue). The merged images (merge) were constructed.

II-2-2. GGA induced priming of inflammasome activation in HuH-7 cells

As described in Introduction section, activation of caspase-1 activity is a sole outcome of inflammasome activation. Next, we decided to determine whether GGA induces priming of inflammasome activation in HuH-7 cells. **Fig.II-6** shows the time-dependent effects of 20 μ M GGA on *NLRP3* or *IL1B* mRNA level as inflammasome priming index in HuH-7 cells. GGA increased *NLRP3* (**Fig.II-6A**) and *IL1B* (**Fig.II-6B**) mRNA levels in a time-dependent manner. At 5 h after GGA treatment, the cellular level of *NLRP3* mRNA rapidly increased to about 20 times the level at 0 h. However, thereafter, the cellular levels of *NLRP3* mRNA gradually decreased 10- and 2.0-fold at 8 and 24 h, respectively (**Fig.II-6A**), indicating that GGA-induced upregulation of the *NLRP3* mRNA expression was transient. On the contrary, the cellular level of *IL1B* mRNA was increased 200-fold over the control level at 8 h and the higher level was maintained until 24 h (**Fig.II-6B**), but the cellular level of *ASC* mRNA was immediately downregulated by adding GGA (**Fig.II-6C**).

Besides early priming of inflammasome such as transcriptional upregulation of *NLRP3* and *IL1B* mRNAs expression, late phase response of inflammation is known as transcriptional upregulation of the *interferon (IFN)* genes. We failed to detect significant *IFN α/β* mRNA upregulation upon treatment with GGA (**Fig.II-6D** and **E**).

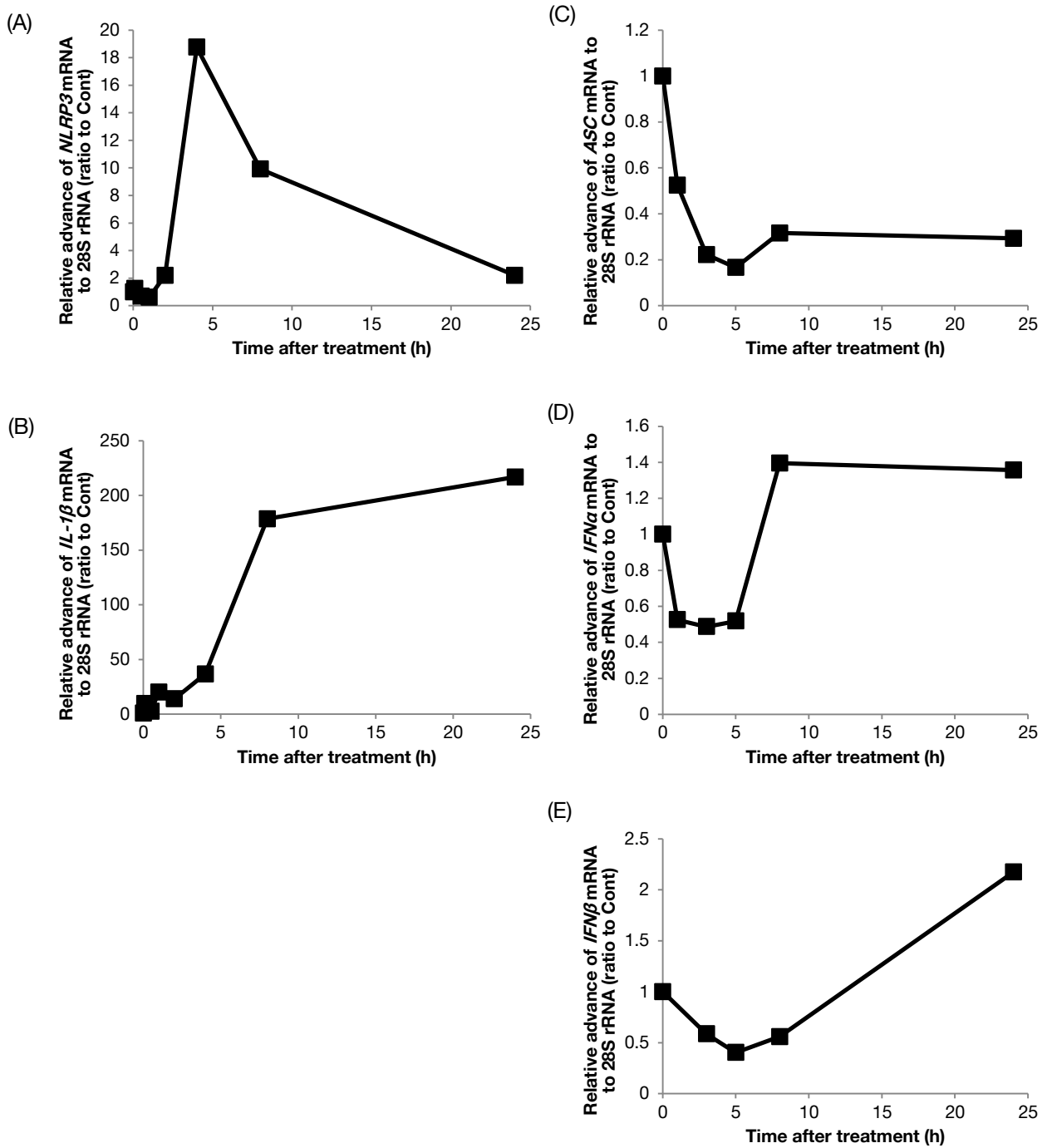


Fig.II-6. GGA induced priming of inflammasome in HuH-7 cells.

HuH-7 cells were treated with 20 μ M GGA for 0, 0.5, 1, 2, 4, 8, and 24 h. Total RNA was extracted to analyze the cellular levels of *NLRP3* (A) and *IL-1β* (B) mRNA by RT-qPCR. (C-E) HuH-7 cells were treated with 20 μ M GGA for 0, 1, 3, 5, 8, and 24 h. Total RNA was extracted to analyze the cellular levels of *ASC* (C), *IFNα* (D) and *IFNβ* (E) mRNA by RT-qPCR.

II-2-3. NF- κ B relocates from the cytoplasm to the nucleus after GGA treatment

We reasonably speculated that the inflammatory transcription factor, NF- κ B, might play a role in GGA-induced priming in HuH-7 cells, because inflammasome priming is performed through NF- κ B signaling [131]. Under normal physiological conditions, NF- κ B complexes remain inactive in the cytoplasm through a direct interaction with proteins of the I κ B family. We observed subcellular localization of NF- κ B, which usually remains in the cytoplasm, but when activated it will move to the nucleus and act as a transcription factor. As clearly shown in **Fig.II-7A**, although NF- κ B protein stayed in the cytoplasm of control HuH-7 cells, GGA conveyed the protein into the nuclear space in 3 h. BAY 11-7082, an irreversible inhibitor of IKK α and phosphorylation of cytokine-inducible I κ B α , evidently prevented GGA-induced nuclear translocation of NF- κ B.

However, GGA-induced cell death was not blocked by co-treatment with BAY-11, but was even enhanced at its 2.5 to 20 μ M (**Fig.II-7B**). Indeed, BAY-11 alone dose-dependently induced cell death (**Fig.II-7C**).

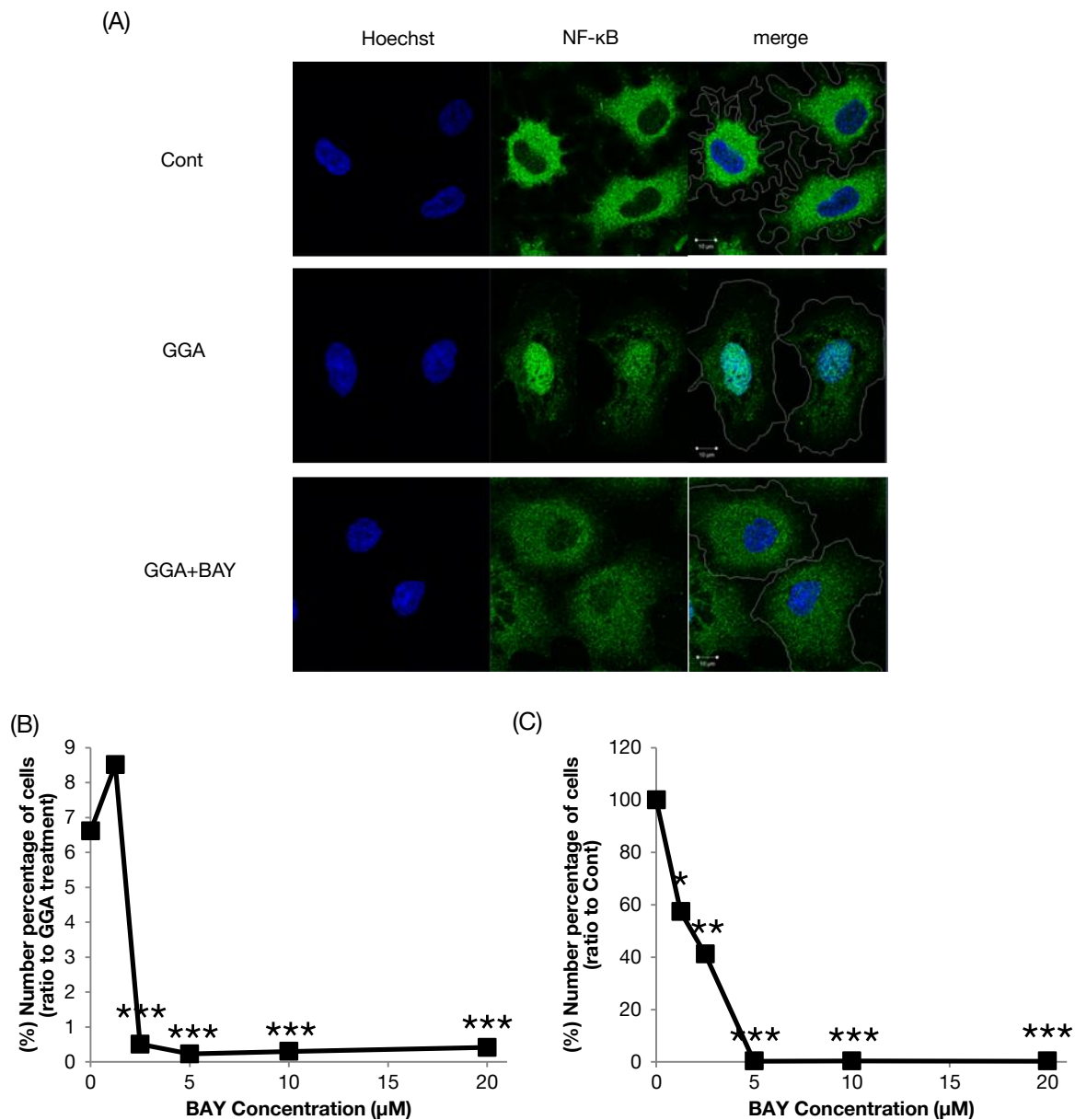


Fig.II-7. NF-κB is relocated from the cytoplasm to the nucleus by GGA.

(A) HuH-7 cells were cultured under the following conditions: no treatment (Cont), 20 μM GGA (GGA), or 20 μM GGA with BAY-11, a specific inhibitor of NF-κB (GGA+BAY), for 3 h. Immunofluorescent images were obtained with anti-NF-κB –anti-rabbit IgG-Alexa488 (green), and the nuclei were counter-stained with Hoechst 33258 (blue). The merged images (merge) were constructed. (B, C) HuH-7 cells were treated with BAY-11 (1.25, 2.5, 5, 10, 20 μM) in the presence (B) or absence (C) 20 μM GGA for 24 h. Viable cells were measured using the Celltiter-Glo assay kit. Asterisks (*, **, ***) indicate statistically significant difference from each relevant control induced by GGA (20 μM) (B) or a control sample at 0 h (C) with p value of <0.05, 0.01, 0.001, respectively, analyzed using the Student's *t*-test.

II-2-4. Translocation for plasma membrane of GSDMD after GGA treatment

GSDMD is one of the established targets of active caspase-1, which is able to produce membrane pore-forming GSDMD-N, a sole executor of pyroptosis [177]. As apparently shown in **Fig.II-8A**, the immunofluorescence technique revealed that most of the GSDMD signals were localized in the nuclear space and the perinuclear region in control HuH-7 cells, which is consistent with the immunofluorescence microscopic data of GSDMD in several human cell lines in Human Protein Atlas (HPA, <http://www.proteinatlas.org/ENSG00000104518-GSDMD/cell>). On the contrary, most of the GSDMD signals were released from the nuclear space and a portion of the signals was clearly detected on the plasma membrane 10 h after GGA treatment, suggesting the GSDMD pore formation was induced by GGA. Indeed, GSDMD-N appeared in a time-dependent manner (**Fig.II-8B**), however, GGA exhibited no detectable effect on the cellular *GSDMD* mRNA levels (see **Fig.II-8C**). We therefore analyzed the oligomerization status of GSDMD (**Fig.II-8D**). Disuccinimidyl suberate (DSS) crosslinking time-dependently increased the size of GSDMD oligomers (dimers and tetramers) on SDS-PAGE.

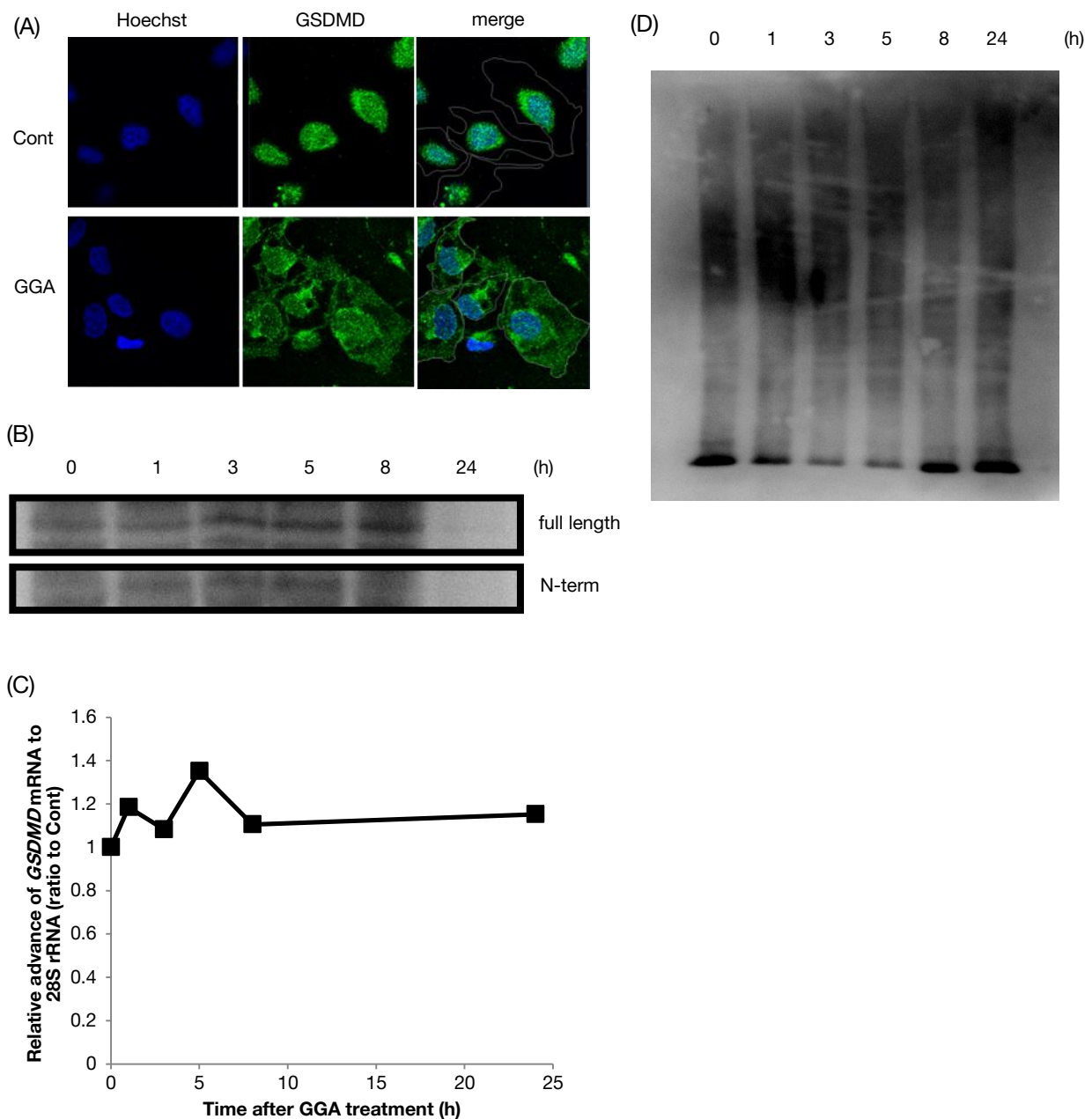


Fig.II-8. Translocation to plasma membrane of GSDMD after GGA treatment.

(A) HuH-7 cells were cultured under the following conditions: vehicle control (Cont), 20 μM GGA for 10 h (GGA). Green fluorescence indicates the distribution of GSDMD. (B) HuH-7 cells were treated with 20 μM GGA for 0, 1, 3, 5, 8, or 24 h. The 600 x g fractions were prepared, 40 μg of total protein per lane and GSDMD levels were analyzed by immunoblotting. (C) HuH-7 cells were treated with 20 μM GGA for 0, 1, 3, 5, 8, or 24 h. Total RNA was extracted to measure the cellular levels of *GSDMD*. (D) HuH-7 cells were treated 20 μM GGA for 0, 1, 3, 5, 8, or 24 h. The culture 600 x g fractions were analyzed after DSS crosslinking. 40 μg of total protein per lane and GSDMD levels were analyzed by immunoblotting.

II-2-5. Morphological alterations and membrane damages after GGA treatment

We conducted the following experiment to obtain morphological evidence for pyroptosis. GGA at 10 μ M induced cell death in HuH-7 cells showed pyroptosis characteristics such as membrane blebbing, which looked a big balloon as large as its cell own size (**Fig.II-9A**).

We next analyzed lactate dehydrogenase (LDH) leakage as an indicator of lytic-type cell death, associated with pyroptosis. We calculate, before GGA treatment in HuH-7 cells, percent cytotoxicity by setting the following two controls, which have to be performed in each experimental setup: low (medium cultured with non-treated cells) and high (medium cultured with Triton X 100-solubilized cells) control, in other words, spontaneous and maximum LDH release, respectively (**Fig.II-9B**). **Fig.II-9C** shows that after addition of 20 μ M GGA to the culture medium, the cellular LDH was leaked in a time dependent manner.

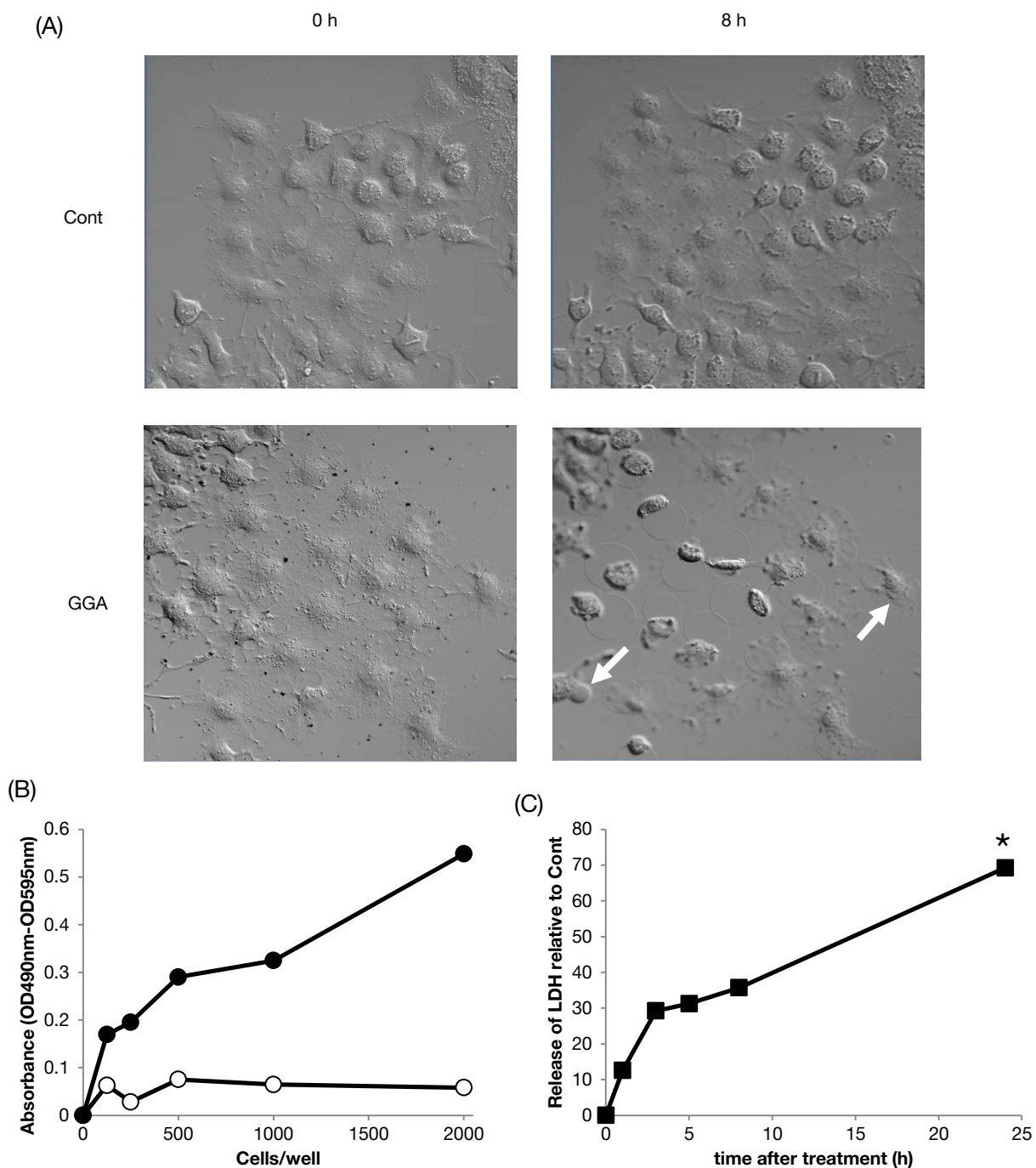


Fig.II-9. Morphological alterations and membrane damages after GGA treatment.

(A) HuH-7 cells were treated 10 μ M GGA in the formation membrane blebbing for 8 h. Live-cell imaging was performed on LSM700 confocal laser-scanning fluorescence microscope. (B) HuH-7 cells were inoculated 125 to 2000 cells/well each low (open square) or high control (closed square) for 24 h. (C) HuH-7 cells were treated with 20 μ M GGA for 0, 1, 3, 5, 8, and 24 h. LDH activity released from the cytosol of damaged cells into the supernatant measured with cytotoxicity detection assay. Asterisks (*) indicate statistically significant difference from a control sample at 0 h with p value of <0.05 , analyzed using the Student's *t*-test.

II-2-6. GGA-induced cell death via TLR4 signaling

Therefore, as some studies reported inflammasome priming occurred through PRRs such as TLRs [178].

As shown on Y axis in **Fig.II-10A**, GGA alone (open circle on Y axis) induced cell death in 90% of HuH-7 cells in 24 h. Then, co-treatment with VIPER peptide (TLR4 inhibitor) prevented GGA-induced cell death in its dose-dependent manner from 1.25 to 5 μ M, but this protective effect was slightly reduced at 10 μ M (closed square and solid line), whereas control peptide CP7 did not rescue the cells from GGA-induced cell death (open circle and broken line).

GGA-induced cell death is known to be rescued by co-treatment with the mono-unsaturated fatty acid oleate (OA) [77] or α -tocopherol, one of vitamin E [37]. The blocking effect of VIPER on GGA-induced cell death was comparable with previously reported inhibitors such as OA and α -tocopherol (**Fig.II-10B**). On the other hand, other TLR4-specific inhibitors C34 and TAK-242 partially prevented GGA-induced cell death (**Fig.II-10C**). In accordance with their preventive effects on GGA-induced cell death, co-treatment with OA, α -tocopherol or VIPER significantly rescued the cells from GGA-induced leakage of the cytosolic LDH (**Fig.II-10D**).

Next, we show that GGA-induced inflammasome priming, caspase-1 activation and NF- κ B nuclear translocation were all suppressed by co-treatment with OA, α -tocopherol or VIPER (**Fig.II-10E-G**). GGA-induced upregulation of the cellular *NLRP3* mRNA level was dramatically blocked by co-treatment with either OA, α -tocopherol, or VIPER (Fig.II-10E). As mentioned above, these 3 organic compounds all prevented GGA-induced cell death, suggesting that NLRP3 inflammasome priming may be tightly linked

to GGA-induced cell death.

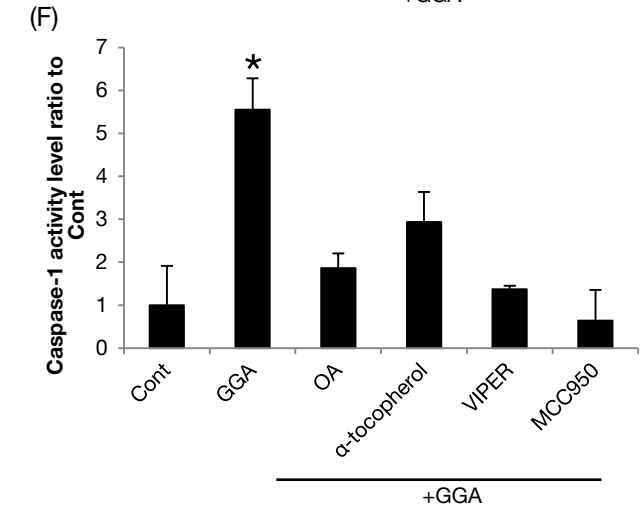
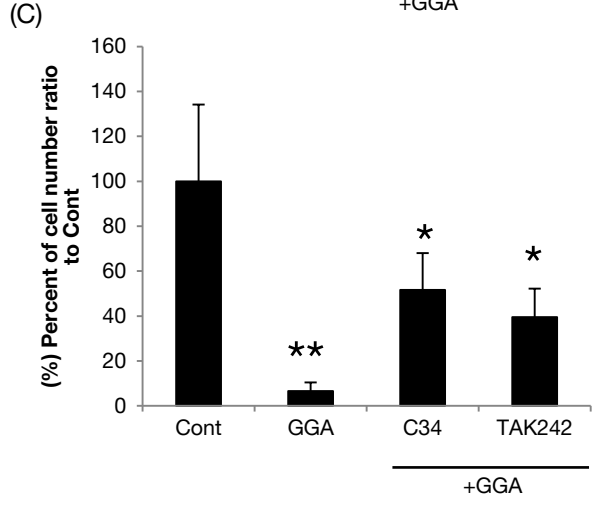
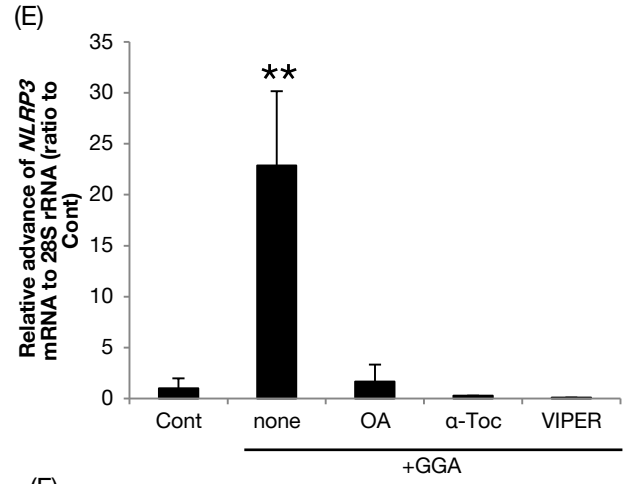
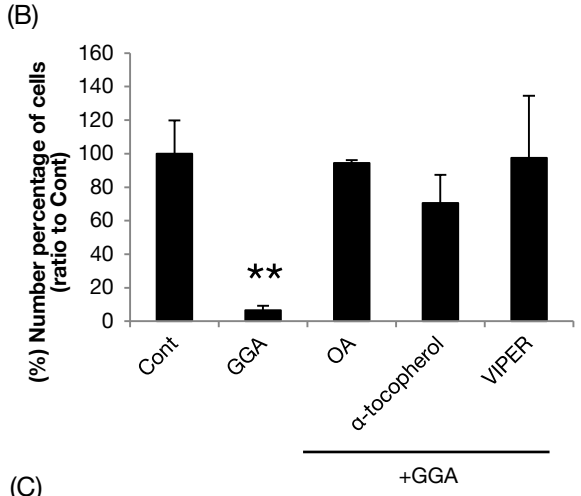
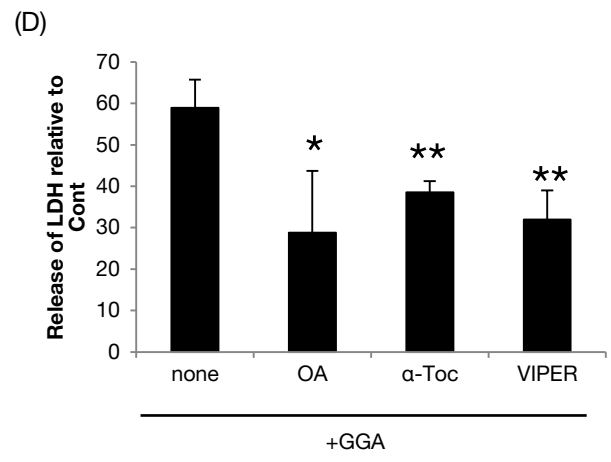
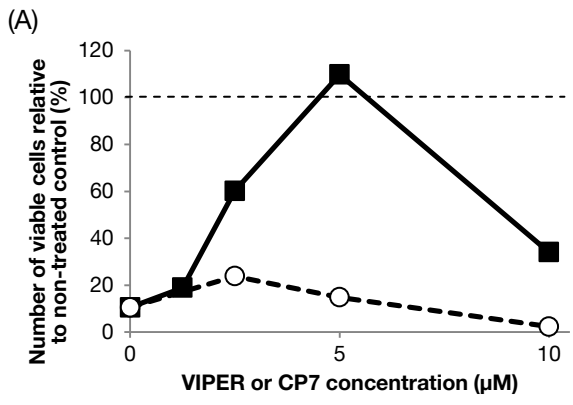
As shown in Fig.II-7F, GGA-induced activation of the cellular caspase-1 activity at 8 h was prevented by co-treatment with either OA, α -tocopherol, VIPER or MCC950 (a selective inhibitor of NLRP3 activation) [179], indicating that a priming step is indispensable for activation of pro-caspase-1.

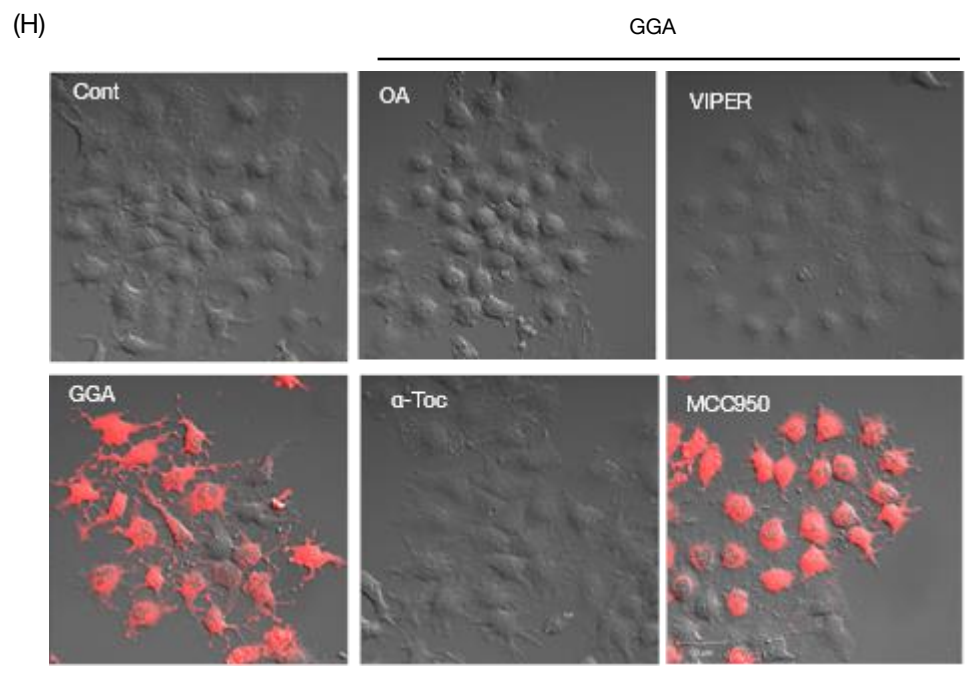
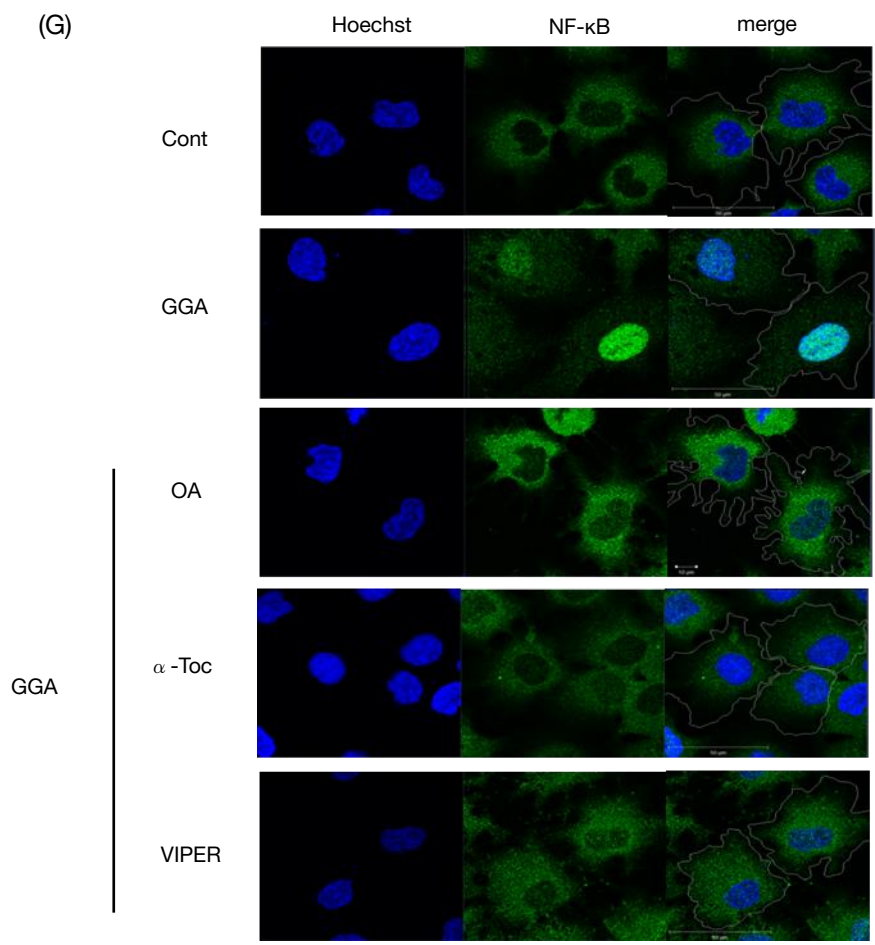
Since the *NLRP3* gene is an NF- κ B-dependent gene, we thought that these inhibitors might keep the cytosolic NF- κ B out of the nucleus in the presence of GGA. As expected, GGA-induced nuclear translocation of NF- κ B was blocked by co-treatment with either VIPER, α -tocopherol or OA (Fig.II-10G).

Furthermore, since we have reported that GGA induces hyperproduction of superoxide in mitochondria in 15 min [47], we considered the mitochondria-mediated hyperproduction of ROS might be important to prime the NLRP3 inflammasome activation. When mitochondria-derived superoxide was observed with fluorogenic reagent of MitoSOX, all of the inhibitors against priming of the NLRP3 inflammasome used in Fig.II-10E extinguished the mitochondrial red fluorescence of MitoSOX in GGA-treated cells, as shown in **Fig.II-10H**, whereas MCC950 did not prevent GGA-induced hyperproduction of mitochondrial superoxide. These results suggest that a burst of mitochondrial superoxide or mitochondrial dysfunction may be essential for a priming step of the NLRP3 inflammasome.

We have recently reported that GGA immediately induces UPR [77]. Therefore, we next observed the effect of VIPER co-treatment on GGA-induced UPR. As a result, VIPER completely suppressed the upregulation of the *XBPIs* and *DDIT3* mRNAs expression (**Fig.II-10I and J**), both of which are hallmarks of GGA-induced UPR [77]. However, α -tocopherol that inhibited GGA-induced cell death as like VIPER

did not suppressed and even enhanced GGA-induced UPR (Fig.II-10I and J). Furthermore, co- treatment OA, α -tocopherol, or VIPER effectively prevented GGA-induced accumulation of LC3-II, a hallmark of autophagosomes (**Fig.II-10K**). These results strongly suggest that TLR4 signaling must be specifically involved in GGA-induced UPR and GGA-induced incomplete autophagy as well as GGA-induced cell death.





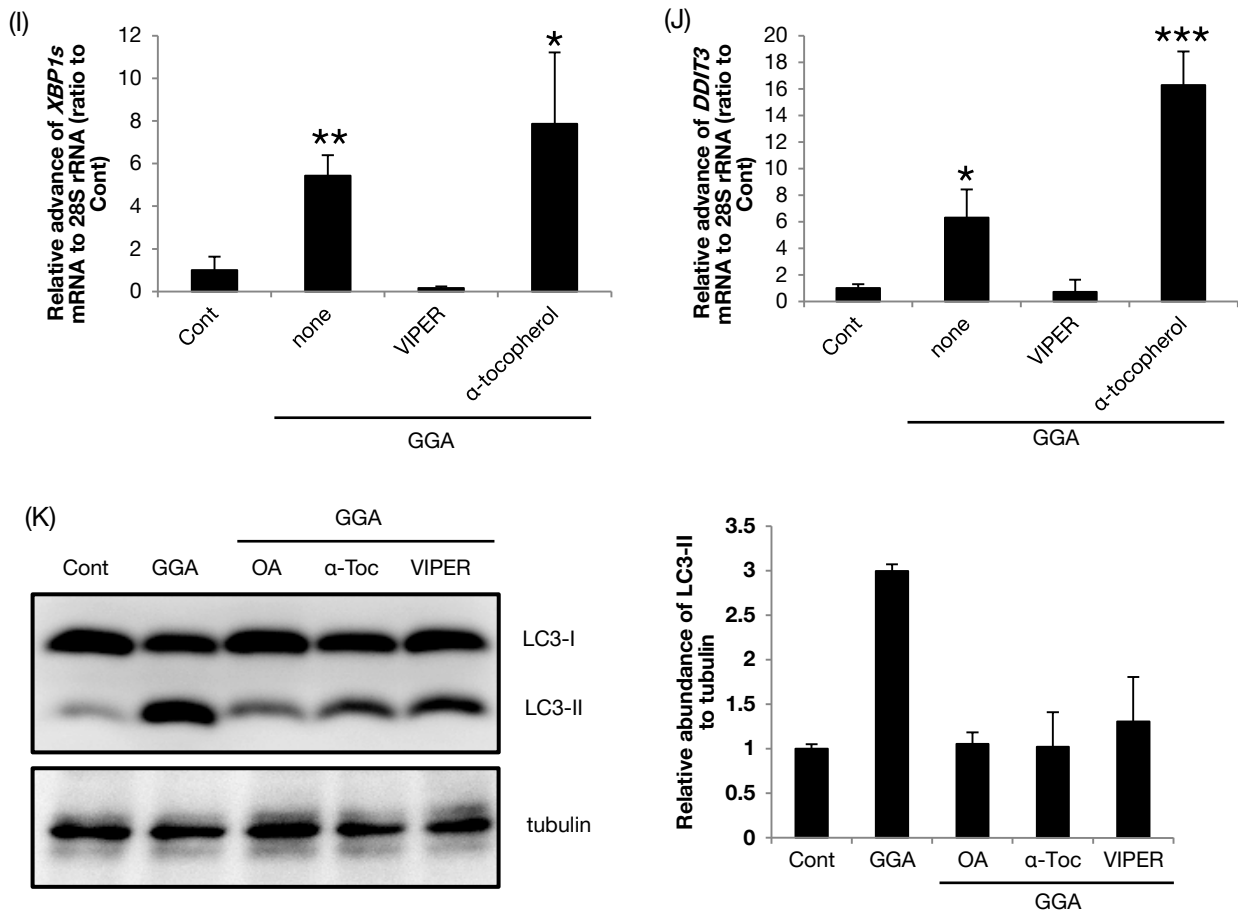


Fig.II-10. GGA-induced cell death via TLR4.

(A) HuH-7 cells were treated with 20 μ M GGA for 24 h in the absence or presence of 1.25, 2.5, 5 or 10 μ M VIPER (closed square) or CP7 (open square). (B) HuH-7 cells were treated with 20 μ M GGA in the presence of oleate, α -tocopherol or VIPER (50, 100 or 5 μ M, respectively) for 24 h. Viable cells were measured using the Celltiter-Glo assay kit. (C) HuH-7 cells were treated with 20 μ M in the absence or presence of 5 μ M C34 or TAK242 for 24 h. (D) HuH-7 cells were treated with 20 μ M GGA in the absent or present of OA, α -tocopherol or VIPER (50, 100 or 5 μ M, respectively) for 24 h. LDH activity released from the cytosol of damaged cells into the supernatant measured with cytotoxicity detection assay. (E) HuH-7 cells were treated with 20 μ M GGA in the absent or present of OA, α -tocopherol or VIPER (50, 100 or 5 μ M, respectively) for 5 h. Total RNA was extracted to measure the cellular level of *NLRP3* mRNA by RT-qPCR. (F) HuH-7 cells were treated with 20 μ M GGA in the presence of oleate, α -tocopherol, VIPER or MCC950 (50, 100, 5 or 5 μ M, respectively) for 8 h. Caspase-1 activation measurement used with caspase-Glo1 assay. (G) HuH-7 cells were treated with 20 μ M GGA in the absent or present of oleate, α -tocopherol or VIPER (50, 100 or 5 μ M, respectively) for 3 h. Immunofluorescent images were obtained with anti-NF- κ B –anti-rabbit IgG-Alexa488 (green), and the nuclei were counter-stained with Hoechst 33258 (blue). The merged images (merge) were constructed. (H) HuH-7 cells were treated with 20 μ M GGA in the absence or presence of oleate, α -tocopherol or VIPER (50, 100, 5 μ M, respectively) for 30 min. Live-cell imaging was performed with the red

fluorescence for MitoSox on the LSM700 confocal laser-scanning fluorescence microscope. (I, J) HuH-7 cells were treated with 20 μ M GGA for 5 h in the absence or presence of VIPER or α -tocopherol (5 or 100 μ M, respectively). Total RNA was extracted to measure the cellular level of *XBP1s* (I) or *DDIT3* (J) mRNA by RT-qPCR. Each point represents the mean \pm SD (n=3). The asterisks (*, **, ***) indicate statistical significance (p<0.05, 0.01, 0.001, respectively), compared with each relevant control as determined by Student's *t*-test. (K) HuH-7 cells were treated with 20 μ M GGA in the absence or presence of oleate, α -tocopherol or VIPER (50, 100, 5 μ M, respectively) for 3 h. Whole-cell lysates (30 μ g/lane) were prepared and LC3 levels were analyzed by immunoblotting. Tubulin- β III was used as a loading control. Levels of LC3-II expression were quantified with ImageJ densitometric analysis (mean \pm SD, n=3). Representative blots and corresponding quantification of LC3-II/Tubulin- β III are shown.

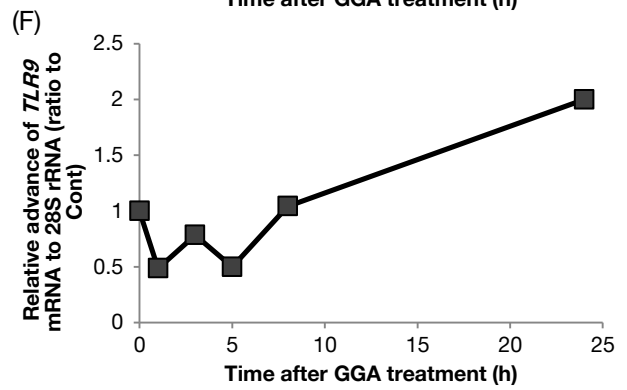
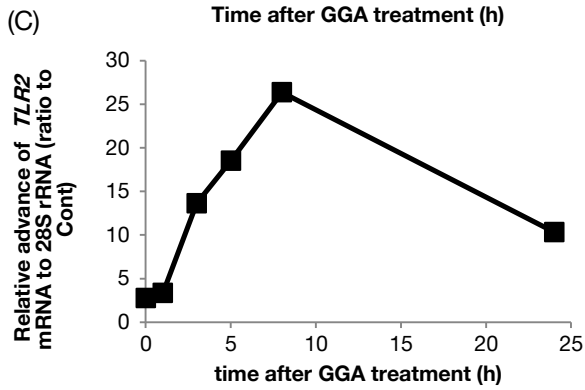
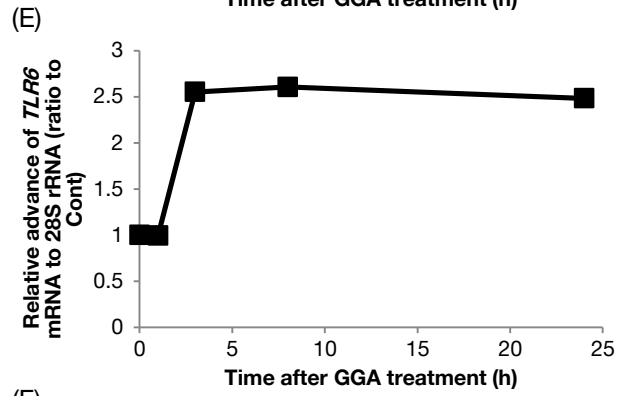
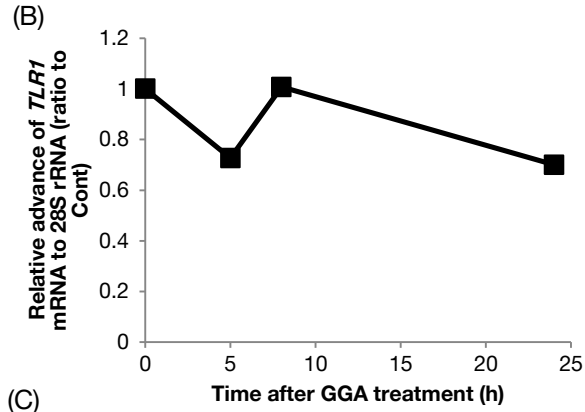
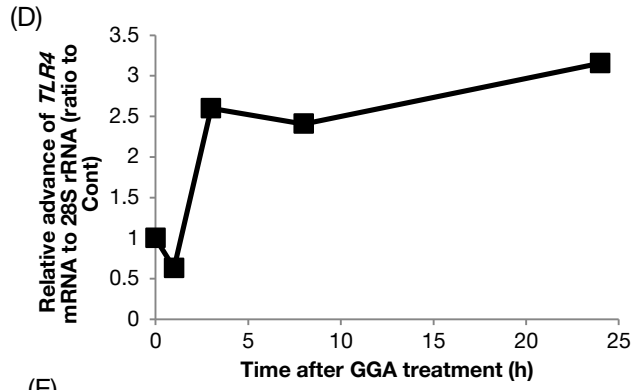
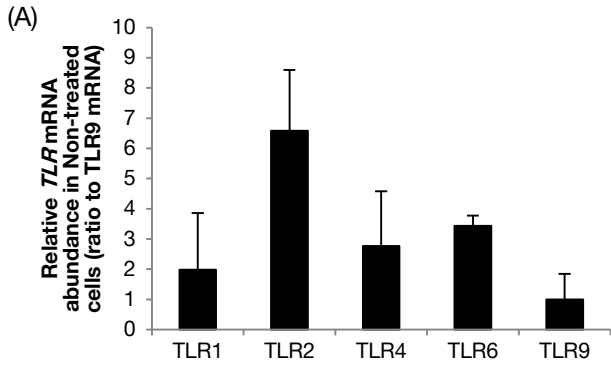
II-2-7. GGA-induced UPR upregulates TLR2 expression

In the literature, the *TLR2* gene expression is known to be upregulated via ATF4, a downstream signal of PERK pathway of UPR [180]. So, we measured the expression of the *TLR2* gene as well as some other TLR family members. To determine whether GGA could upregulate the *TLRs* mRNA level, we treated HuH-7 cells with GGA before measurement *TLRs* (*TLR1*, 2, 4, 6, or 9) mRNA level. **Fig.II-11A** shows the expression level of *TLRs* mRNA in HuH-7 cells prior to GGA treatment. The basal expression level of *TLRs* was as follows: *TLR2* > *TLR6* > *TLR4* > *TLR1* > *TLR9*.

Treatment with 20 μ M GGA upregulated the *TLRs* mRNA level in HuH-7 cells (**Fig.II-11B – F**). The level of *TLR2* mRNA was upregulated in a time dependent manner (Fig.II-11C). *TLR2* mRNA expression was markedly increased 15-fold at 3 h and up to 25-fold at 8 h compared with the control level. From 8-24 h, the cellular levels of *TLR2* mRNA gradually decreased from 25- to 10-fold over the basal level. The cellular level of *TLR4* or *TLR6* mRNA was increased 2.5-fold at 3 h (Fig.II-11D and E), but *TLR1* and *TLR9* mRNA levels were not largely changed after GGA treatment (see Fig.II-11B and F).

In addition to the inhibitory effects of VIPER on GGA-induced cell death and GGA-induced UPR, this TLR4-specific inhibitor also perfectly suppressed GGA-induced upregulation of the *TLR2* gene (**Fig.II-11G**), suggesting that TLR2 may be involved in GGA-induced cell death. It is interesting that co-treatment with OA, an inhibitor of GGA-induced UPR [77], also completely suppressed GGA-induced upregulation of the *TLR2* gene expression (Fig.II-11G), implying that GGA-induced UPR is an upstream signal for the upregulation of *TLR2* gene expression. However, lipoteichoic acid (LTA) (5 μ M) [181], a TLR2-specific agonist, and *o*-vanillin [182], a TLR2-specific antagonist, did not induce cell death without GGA and did not prevent GGA-induced cell death, respectively (**Fig.II-11H**).

Quite a few studies have reported that a dramatic increase of *TLR4* mRNA expression is found in high glucose conditions [183–185]. Hence, we observed how medium shift from low glucose (1000 mg/L) to high glucose (4500 mg/L) affected on the cellular expression of the *TLR4* and *TLR2* genes in HuH-7 cells. As a result, the high glucose medium upregulated the cellular levels of *TLR2* and *TLR4* mRNA in 48 h (**Fig.II-11I and J**), but provided no change in the cellular *TLR6* mRNA level (**Fig.II-11K**).



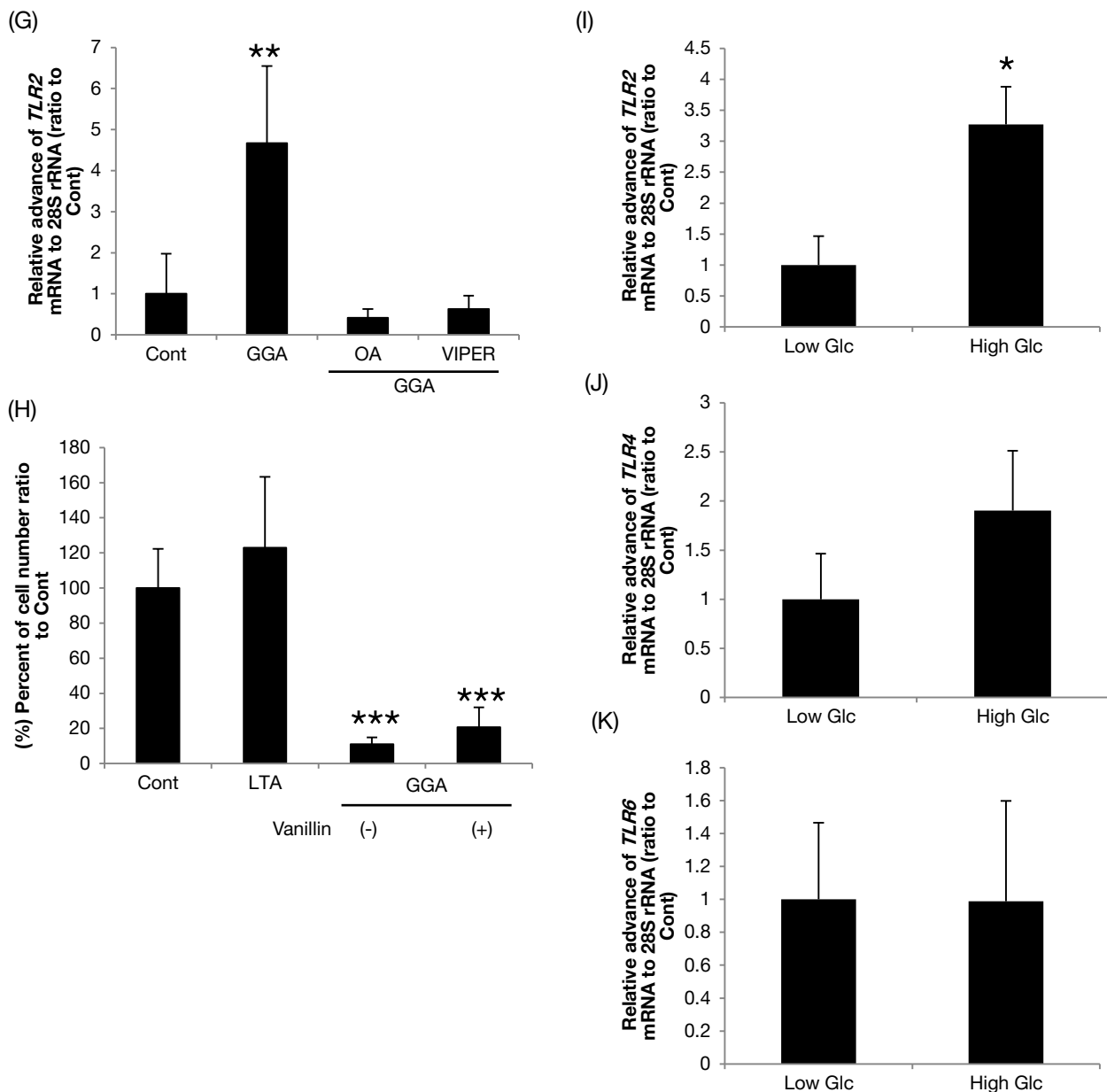


Fig.II-11. GGA-induced UPR upregulates TLR2.

(A) Total RNA was extracted to analyze the cellular levels of TLRs (TLR1, 2, 4, 6, or 9) mRNA by RT-qPCR in HuH-7 cells. (B-F) HuH-7 cells were treated with 20 μ M GGA for 0, 1, 3, 5, 8, and 24 h. total RNA was extracted to measure the cellular levels of *TLR1* (B), *TLR2* (C), *TLR4* (D), *TLR6* (E) and *TLR9* (F) mRNA by RT-qPCR. (G) HuH-7 cells were treated with 20 μ M GGA for 5 h in the absence or presence of VIPER or α -Toc (5 or 100 μ M, respectively). (H) HuH-7 cells were treated with 5 μ M LTA or 20 μ M GGA in the absence or presence of 5 μ M vanillin for 24 h. (I-K) HuH-7 cells were used culture medium by low glucose or high glucose shift for 2 d. Total RNA was extracted to measure the cellular levels of *TLR2* (I), *TLR4* (J) and *TLR6* (K) mRNA by RT-qPCR. Values are the means \pm SD (n=3 or 6). The asterisks (**, ***) indicated statistical significant (p<0.01, 0.001, respectively), as determined by Student's *t*-test.

II-2-8. ATRA did not induce pyroptotic cell death

In contrast to acyclic retinoid of GGA, natural cyclic retinoid of ATRA has been repeatedly reported not to induce cell death in human hepatoma cells, but it induced IRE1-mediated splicing of *XBPI* mRNA. Therefore, the question was what is different in cellular effects on cell death of hepatoma cells between GGA and ATRA. To determine whether ATRA could also induce nuclear translocation of NF- κ B from cytosol, immunofluorescence analysis with anti- NF- κ B antibody was conducted. Contrary to GGA shifting NF- κ B from the cytosol to the nuclear space, the protein still stayed in the cytoplasm of ATRA-treated cells (**Fig.II-12A**). **Fig.II-12B** depicts a time-dependent change in the cellular *NLRP3* mRNA level of HuH-7 cells upon ATRA treatment, in comparison with that after GGA treatment. ATRA, most stronger diterpenoid in the lipid-induced UPR but is not cytotoxic [77], did not induce priming of *NLRP3* inflammasome activation, which is consistent with inability of ATRA to induce nuclear translocation of NF- κ B (**Fig.II-12A**). May cellular mechanism of ATRA-induced UPR is different from that of GGA-induced UPR? We knew that TLR4 signaling was essential for GGA-induced UPR. Therefore, we next observed the effect of VIPER or oleic acid co-treatment on ATRA-induced UPR. Interestingly, both prevented the upregulation of *XBPIs* and *DDIT3* mRNA levels (**Fig.II-12C** and **D**), suggesting ATRA-induced UPR might be also mediated by TLR4 signaling.

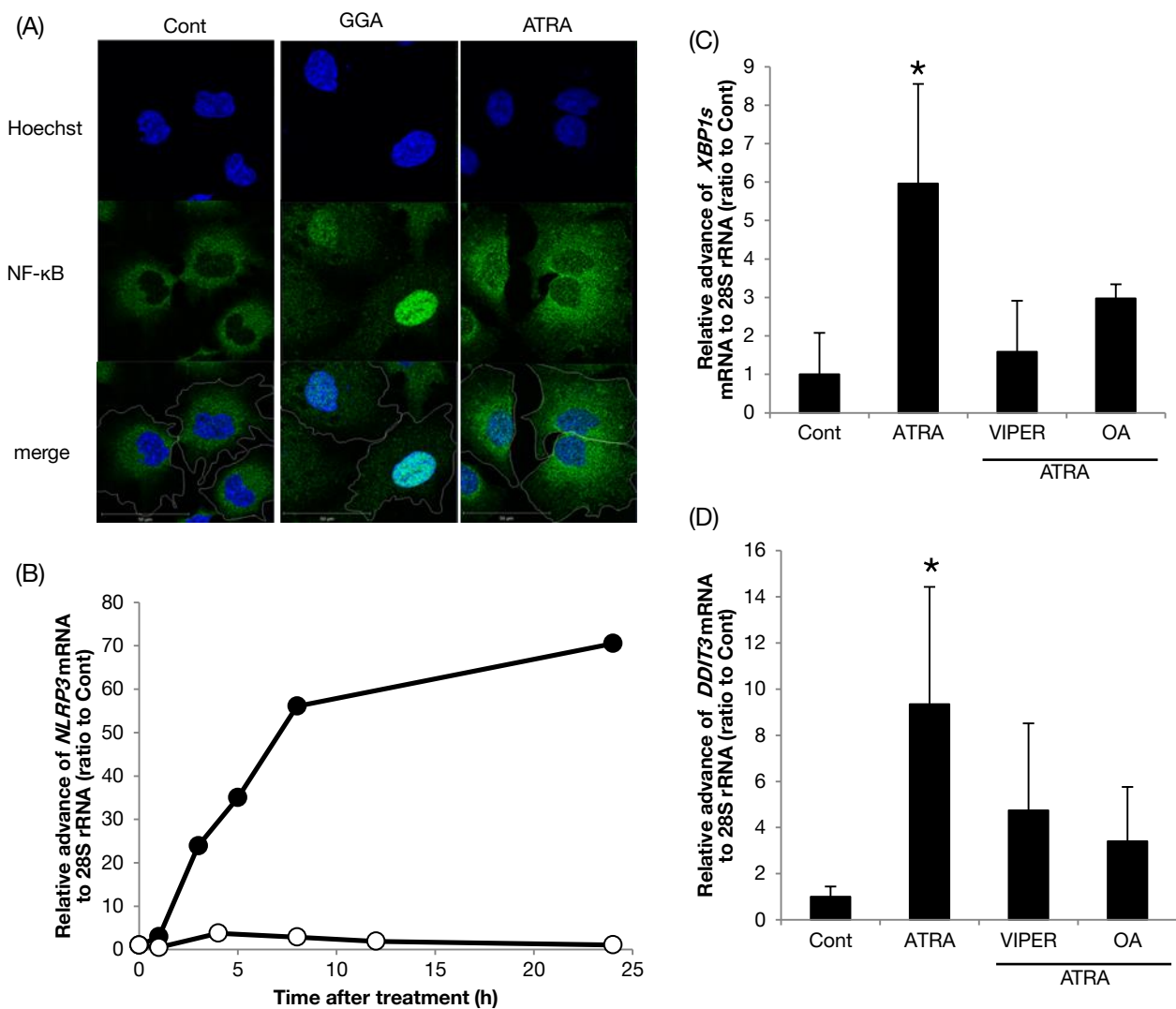


Fig.II-12. ATRA was not induced pyroptotic cell death.

(A) HuH-7 cells were treated with 20 μ M GGA or ATRA for 3 h. Immunofluorescent images were obtained with anti-NF- κ B –anti-rabbit IgG-Alexa488 (green), and the nuclei were counter-stained with Hoechst 33258 (blue). The merged images (merge) were constructed. (B) HuH-7 cells were treated with 20 μ M GGA (●) or ATRA (○) for 0, 1, 3, 5, 8, and 24 h. Total RNA was extracted to analyze the cellular levels of *NLRP3* mRNA by RT-qPCR. (C, D) HuH-7 cells were treated with 20 μ M ATRA for 5 h in the absence or presence of VIPER or OA (5 or 50 μ M, respectively). Total RNA was extracted to measure the cellular level of *XBP1s* (C) or *DDIT3* (D) mRNA by RT-qPCR. The asterisks (*) indicate statistical significance ($p < 0.05$), compared with each relevant control induced by ATRA (20 μ M) alone as determined by Student's *t*-test.

II-3. Discussion

In the present study, we investigated whether TLR4 signaling is involved as an upstream signal for GGA-induced UPR as well as a triggering signal for GGA-induced cell death. As a result, we were able to demonstrate that GGA-induced UPR and GGA-induced cell death are both sensitive to co-treatment with VIPER, a specific inhibitor of TLR4 signaling, and that GGA stimulates NLRP3 inflammasome priming to activate caspase-1 through TLR4 signaling and induce pyroptotic cell death via pore formation in the plasma membrane with the N-terminal fragment of GSDMD, a crucial target of active caspase-1 during pyroptosis. The present results clearly highlight the significance of TLR4-mediated pyroptosis in GGA-induced cell death in hepatoma cells.

GGA was initially reported as an acyclic retinoid inducing apoptosis in HuH-7 hepatoma cells [179], although a caspase-3/7-specific inhibitor, AC-DEVD-CHO, was unable to block GGA-induced cell death [37]. We found that GGA induced an incomplete autophagic response, suggesting GGA might induce autophagic cell death [47]. However, although it was unclear how GGA killed hepatoma cells through autophagic events, we elucidated how GGA triggers the massive accumulation of initial/early autophagosomes via impairment of late-stage processing of autophagy. GGA immediately induces ER stress response or UPR, which forms an upstream signal for the induction of initial stage of autophagy [77]. Thus, we speculated that GGA-induced UPR is linked to its lipotoxicity in human hepatoma cells.

In this context, it is important to understand how GGA induces UPR. To address this, we extensively reviewed previous studies that described the triggering role of TLR4 signaling in UPR induction in several

different cellular systems [166,169,170,186,187], because TLR4 signaling is involved in inflammasome/caspase-1-mediated cell death [188,189]. We reported that GGA-induced cell death in human hepatoma cells was blocked by co-treatment with AC-YVAD-CMK, a caspase-1-specific inhibitor [37]. Therefore, we speculated that GGA stimulates TLR4 signaling, resulting in UPR and cell death. We found that UPR and cell death induced by GGA treatment were completely blocked by VIPER, a specific inhibitor of TLR4, as expected. VIPER is a virus-mimic 11-aa-long peptide fused to a cell penetrating delivery sequence, and is TLR4 specific being inert toward other TLR pathways [190]. VIPER prevents TLR4 signaling by interfering with interactions between TLR4 cytoplasmic domains and adaptor proteins such as TIRAP (Toll/interleukin-1 receptor (TIR) domain-containing adaptor protein/MyD88 adaptor-like (MAL)) and TRAM (Toll-interleukin-1 receptor domain-containing adaptor inducing interferon- β (TRIF)-related adaptor molecule) via masking critical binding sites on TIRAP and TRAM [190]. The TIRAP side of TLR4 signaling mainly leads to the production of proinflammatory cytokines [170], but, the majority of anti-inflammatory cytokines signal via the TRAM side of the TLR4 receptor [191]. Fig.II-10 clearly shows VIPER prevents both GGA-induced cell death and GGA-induced UPR, suggesting that GGA acts upstream from the cytoplasmic domains of TLR4. Another TLR4 inhibitor, C34, inhibits TLR4 signaling by docking with the hydrophobic pocket of the TLR4 co-receptor, myeloid differentiation protein 2 (MD2), which is associated with the extracellular domains of TLR4 [192]. Co-treatment with C34 only partially suppressed cell death induced by GGA, suggesting the action point of GGA might be close to the action point of C34, MD2.

Therefore, we would like to determine how GGA stimulates TLR4 signaling. It is well known that several foreign and endogenous lipophilic materials such as LPS from gram-negative bacteria [193], 7-ketocholesterol [170], oxidized low-density lipoprotein [194], and saturated fatty acids [195] including lauric acid [196], palmitic acid [197] and stearic acid [198] all act as TLR4 agonists/ligands and trigger inflammatory responses. However, the exact molecular mechanisms involved are still elusive, except that under the assistance of LPS-binding protein and CD14, LPS stimulates the TLR4 receptor as a MD2-bound heterodimeric complex in which two MD2-LPS complexes bind two TLR4 extracellular domains resulting in the ligation of two TLR4 molecules [199]. Analogous to the LPS mechanism, Nicholas et al. proposed that 5 molecules of palmitic acid associate with the hydrophobic binding pocket MD2 by hydrophobic protein modeling [197]. Because palmitic acid- and GGA-induced TLR4-mediated cell death are blocked by co-treatment with oleic acid, GGA may be ligand of the TLR4 adaptor MD2, similar to palmitic acid. Another possibility is that GGA may enhance the recruitment of TLR4 into lipid rafts of the plasma membrane. Indeed, Two different research groups reported that TLR4 was recruited into lipid rafts upon palmitic acid treatment [200,201]. Although not discussed in their papers, the palmitic acid-enhanced recruitment of TLR4 into lipid rafts may involve a fatty acid transport scavenger receptor protein, CD36, which is enriched in lipid rafts [202,203]. Because GGA can target lipid rafts during human immunodeficiency virus infection [204], it is reasonable to speculate that GGA might recruit TLR4 receptors into lipid rafts, which can be prevented by oleic acid treatment through CD36.

Besides of TLR4 antagonists used in this study, α -tocopherol also efficiently inhibited GGA-induced

cell death. It is interesting that α -tocopherol also prevented GGA-induced intracellular events such as the hyperproduction of mitochondrial superoxide, nuclear translocation of NF- κ B, and activation of caspase-1 activity, all of which are also prevented by oleic acid or VIPER. However, the anti-oxidative vitamin did not inhibit GGA-induced UPR. These findings strongly suggest that GGA-induced UPR does not satisfy the necessary and sufficient conditions for GGA-induced cell death, but the hyperproduction of mitochondrial ROS does. The GGA-induced hyperproduction of mitochondria superoxide was prevented by VIPER co-treatment., but was not suppressed by co-treatment with MCC950, indicating the signal for ROS production is located downstream of TLR4 and upstream of the NLTP3 inflammasome. West et al. reported that evolutionally conserved signaling intermediate in Toll pathways (ECSIT) after translocation of the TLR signaling adapter, TRAF6 to mitochondria [205]. Recently, an anti-oxidative protein of peroxiredoxin-6 was reported to suppress TLR4-mediated mitochondrial ROS production by interrupting formation of the TRAF6-ECSIT complex induced by TLR4 stimulation [206]. Therefore, we speculate that GGA stimulates TLR4 to form a TRAF6-ECSIT complex, which then results in the ubiquitination and degradation of ECSIT. A loss of ECSIT, a molecular chaperone for complex I of the respiratory chain, produces superoxide in mitochondria.

There are apparent some differences between GGA and retinoids in cellular effects. GGA was initially thought to be an acyclic retinoid, because it has ligand activities for nuclear retinoid receptors of RARB and RXRA and is a cytosolic binding protein for retinoic acid [26]. However, natural retinoids such as ATRA and 9CRA are not effective at killing hepatoma cells, and GGA induces caspase-1-dependent cell

death [30,37,77]. Furthermore, ATRA induces greater *XBPI* splicing and nuclear accumulation of XBPI compared with GGA [77]. In addition, ATRA-induced UPR was prevented by co-treatment with oleic acid or VIPER (Fig.II-12C) suggesting TLR4 signaling is involved in retinoid-induced UPR. Nevertheless, retinoid-induced UPR did not result in cell death, probably because retinoids do not stimulate the hyperproduction of mitochondrial ROS.

In conclusion, we report that micromolar GGA causes inflammatory cell death, pyroptosis, in human hepatoma cells via TLR4 signaling, where mitochondrial superoxide and nuclear translocation of NF- κ B play essential roles to prime the NLRP3 inflammasome. TLR4 was reported to have a pathogenic role during chronic inflammation and may be a cause of human hepatoma [207] and a recent phase II clinical study reported the prevention of hepatoma recurrence with peretinoin or 4,5-didehydroGGA [208], suggesting the further exploration of the preventive roles of GGA in hepatocarcinogenesis.

Chapter III

Pyroptotic cell death with GGA through noncanonical inflammasome

Suemi Yabuta

Molecular and Cellular Biology, Graduate School of Human Health Science,

University of Nagasaki, Nagasaki, Japan

Abstract

In Chapter II, we demonstrated GGA induces TLR4-mediated pyroptosis in human hepatoma cells. Caspase-4 and -5, inflammatory caspases, are known to trigger pyroptosis, and are similar to caspase-1. These caspases also induced cleavage of human GSDMD. In this chapter, we investigated possible roles in GGA-induced pyroptosis, because accumulating evidence suggests the involvement of caspase-4 in ER stress-induced cell death, because caspase-4 is localized mainly to the ER. Here, we show that a non-canonical inflammasome pathway in HuH-7 cells was also activated during GGA-induced pyroptosis via UPR. The enzyme activity of caspase-4 was induced immediately after GGA treatment. Furthermore, the cellular mRNA levels of the *caspase-4* and *-5* genes were upregulated after treatment with GGA, tunicamycin, or thapsigargin, all of which induced UPR. GGA induced calcium release from the endogenous pool, due to GGA-induced UPR. Our results suggest that GGA may be not only able to canonical pathway pyroptosis, but also non-canonical pathway in HuH-7 human hepatoma cells.

III-1. Introduction

III-1-1. Non-canonical inflammasome pathway

Inflammasomes, as described in multiple reviews, are grouped into canonical and noncanonical pathways [209,210]. The functional canonical inflammasome complex is expressed in Chapter II. In contrast, a noncanonical NLRP3 inflammasome activation which depends on caspase-4 and -5, are inflammatory caspases as well as caspase-1, has been described to be pivotal in the maintenance of intestinal immune homeostasis [111]. LPS from Gram-negative bacteria introduced into the cytoplasm of host cells during infection potently activates caspase-4 and -5 [211,212]. Caspase-4 and -5 directly bind LPS [112], and activation of these caspases triggers pyroptosis, similar to caspase-1. Caspase-4 and -5 also induce cleavage of human GSDMD (**Fig.III-1**).

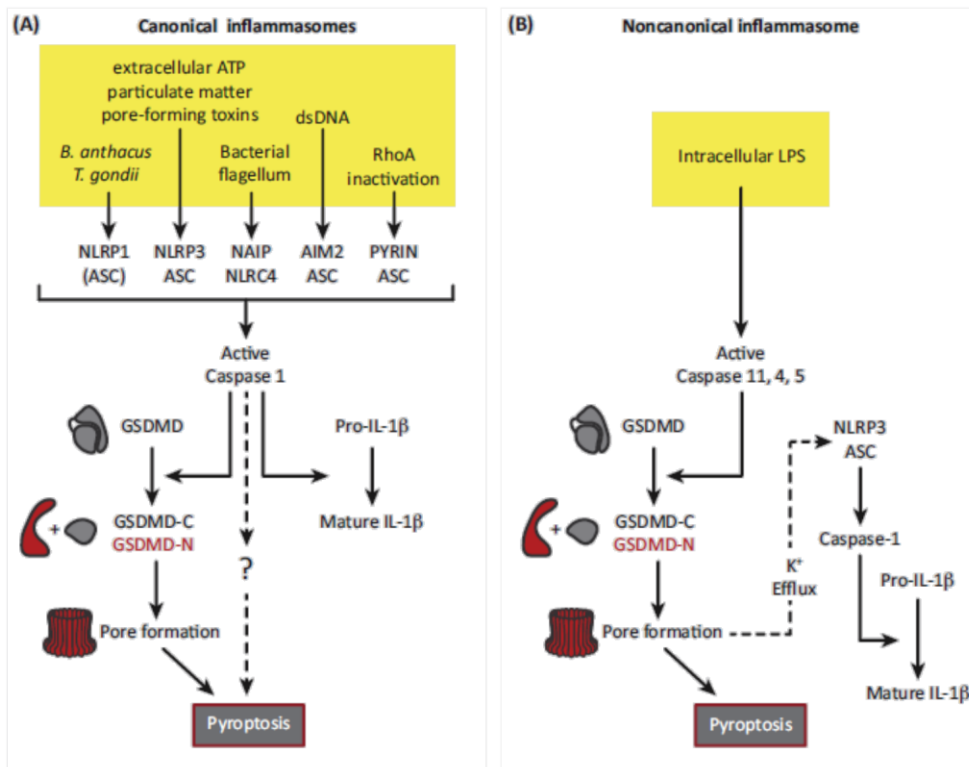


Fig.III-1. The role of GSDMD in pyroptosis driven by non-canonical and canonical inflammasomes.

A and Dueber E. C. *Trends in Immunology* 38, 261-271 (2017) [104]

III-1-2. Priming of the non-canonical inflammasome

For decades, the protection of TLR4 mutant mice against LPS lethality was a cornerstone for innate immunity. Remarkably, the laboratories of Dixit (Genentech) and Miao (University of North Carolina) independently and simultaneously rewrote this dogma and showed that, when the mutant mice were first primed to induce the non-canonical caspase-4 and -5 inflammasome, they were then susceptible to LPS lethality even in the absence of TLR4 [211]. Caspase-4 and -5 can directly detect cytosolic LPS and, intriguingly, this also requires a priming step. Whereas NLRP3 inflammasome priming for canonical caspase-1 inflammasomes is mediated by the TLR4/MyD88 axis, priming of non-canonical caspase-4 and

-5 challenge is mediated by TLR4/TRIF [213]. Principally, this seems to be due to a requirement for IFN signaling to induce the expression of the caspase-4 and -5 genes. Hence, type I IFNs seems to play a prominent role in the transcriptional regulation of the caspase-4 and -5 genes. The transcription of the caspase-4 and -5 genes are also upregulated by type I IFN or IFN- γ .

III-1-3. Non-canonical pathway interacts with UPR

Bian and Elner [214] explained that the ER is a major site for protein synthesis and folding and also functions as a major cellular storage site for calcium ion [215]. Perturbation of Ca²⁺ homeostasis, hyperproduction of ROS, impairment of protein glycosylation, and accumulation of misfolded proteins in the ER are able to induce cellular stress responses, particularly ER stress signals, to protect cells against changes in the subcellular Ca²⁺ levels and toxic buildup of misfolded proteins [215–217]. Calcium ion as second messenger has ability to control various cell functions. Intracellular calcium ion levels are buffered by ER. Calcium ion plays a regulatory role in metabolism of glucose, bile secretion, cell proliferation and programmed cell death [218]. A study in rat hepatocytes showed that intracellular calcium was involved in cell death [219]. During this biological phenomenon, various mechanisms are involved in calcium-mediated cell death including calcium-dependent endonuclease and calpains activation [220]. Calpains belong to a family of cytosolic cysteine proteases that depend on intracellular calcium concentrations in the activity of the cell and involved in cell death process [221].

Additionally, accumulating evidence suggests the involvement of caspase-4 activity in ER

stress-induced cell death. First, caspase-4 is predominantly located in the ER [222]. Second, caspase-4 is closely associated with a number of essential proteins in ER stress-induced cell death pathways, including BiP/GRP78, a well-known chaperone working during ER stress [223]; CARD-only protein, a negative regulator of procaspase-1 [224]; APAF1 (apoptotic protease-activating factor 1), a protein involved in assembly of apoptosome during death protease-mediated cell death [225]; and TRAF6, a member of the TNF receptor-associated factor [226]. Third, caspase-4 inhibitor Z-LEVD-FMK (benzoxy-Leu-Glu-Val-Asp-fluoromethylketone) selectively and effectively blocks ER stress-induced cell death in many cancer cells, including Jurkat [227], and melanoma cells [228]. Fourth, knocking down of caspase-4 expression by siRNA in multiple myeloma cells [229], leukemia cells [230], glioma cell lines [231], and neuroblastoma cells [222], expressing catalytically inactive caspase-4, and microinjecting of anti-caspase-4 antibodies into HeLa [232] all abolished ER stress-induced cell death. In this context, one can reasonably speculate that activation of caspase-4 (or -5) is essential for ER-stress-induced (or UPR-mediated) cell death, which may be transmitted by LPS.

In chapter III, we investigated that the non-canonical inflammasome pathway in HuH-7 cells might be linked to GGA-induced pyroptosis.

III-2. Results

III-2-1. GGA-induced pyroptosis via non-canonical inflammasome pathway in HuH-7 cells

In chapter II, to clarify a molecular mechanism of GGA-induced cell death as pyroptosis through canonical pathway, we found GGA upregulated caspase-1 activity, resulting in a cleavage of GSDMD to produce a pore-forming GSDMD-N. Although we showed caspase-1 activation and GSDMD cleavage occurred in 10 h after GGA treatment, the migration of GSDMD from the nucleus to the plasma membrane was clearly observed already at 3 h after addition of GGA (**Fig.III-2A**), when caspase-1 activity was not so much activated. As shown in Fig.II-5A of Chapter II, the cellular caspase-1 activity was only 1.5 times increased at 3 h after GGA treatment, but we detected the amino-terminal GSDMD-N fragment on the immunoblot as early as 1 h after GGA addition. Besides caspase-1 protease, GSDMD is known to be an efficient substrate for both caspase-4 and -5 [233]. Hence, we analyzed GGA-induced changes in the cellular mRNA levels of the *caspase-4* and *-5* genes. As a result, the mRNA levels of both genes were time-dependently increased after GGA treatment; the expression of the *caspase-4* gene almost doubled and the expression of the *caspase-5* gene increased 55-fold at 24 h (**Fig.III-2B and C**). However, they did not change so much until 5 h after addition of GGA.

Since a baseline cellular mRNA level of the *caspase-4* gene relative to 28s rRNA level was 200 times or more than that of the *caspase-5* gene, we decided to measure the cellular protein levels of caspase-4 after GGA treatment. In accordance with the changes in the *caspase-4* mRNA level, the pro-caspase-4 protein level almost doubled at 24 h after GGA treatment (**Fig.III-2D**). More importantly, active caspase-4

bands were detected from 1 to 5 h after addition of GGA, indicating that GGA quickly induced activation of caspase-4.

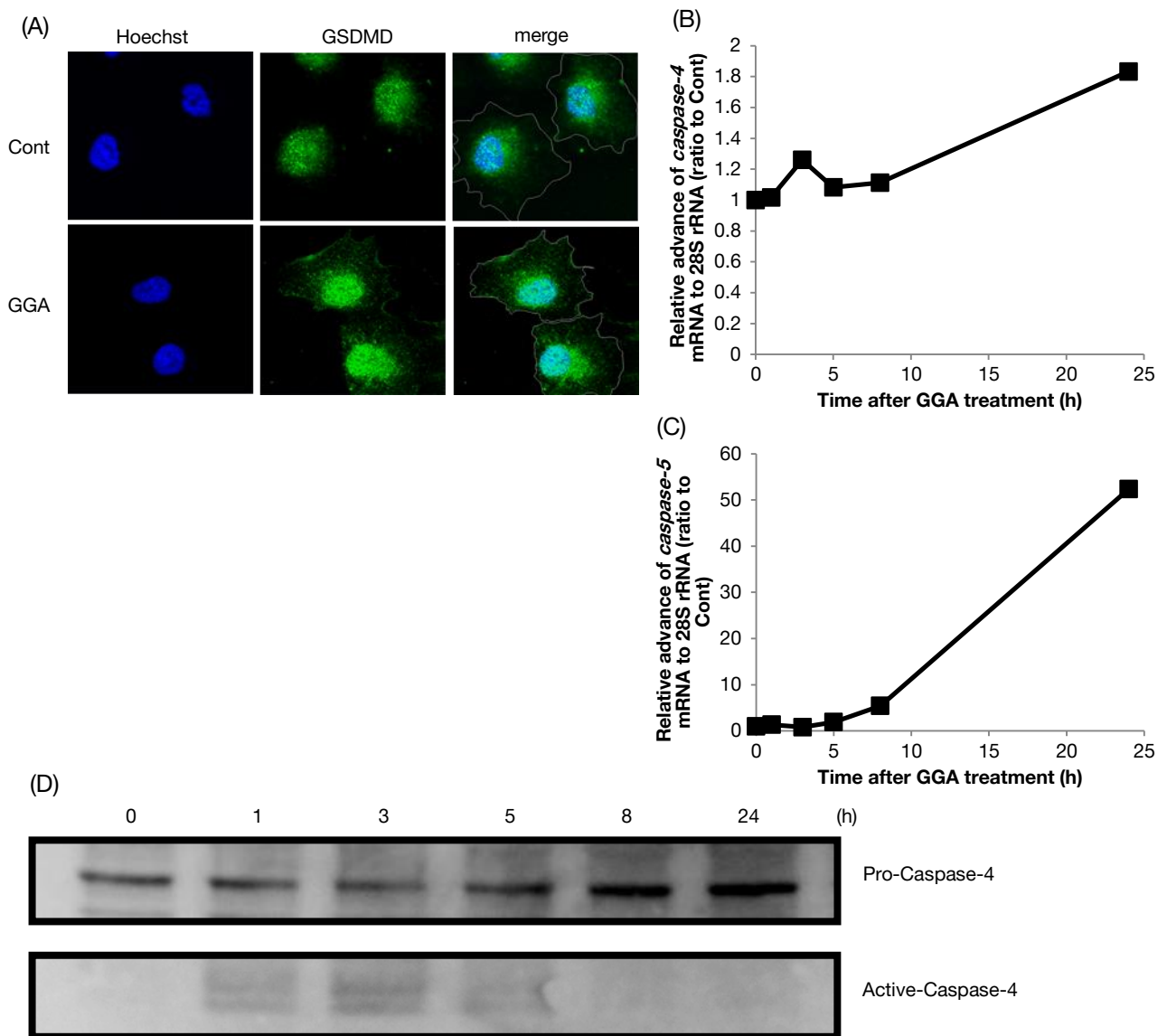


Fig.III-2. GGA-induced pyroptosis via non-canonical inflammasome pathway in HuH-7 cells.

(A) HuH-7 cells were cultured under the following conditions: vehicle control (Cont), 20 μ M GGA for 3 h (GGA). Green fluorescence indicates the distribution of GSDMD. (B, C) HuH-7 cells were treated with 20 μ M GGA for 0, 1, 3, 5, 8, or 24. Total RNA was extracted to measure the cellular level of *caspase-4* (B) and *-5* (C) mRNA by RT-qPCR. (D) HuH-7 cells were treated with 20 μ M GGA for 0, 1, 3, 5, 8, and 24 h. Whole-cell lysates were prepared, 40 μ g of total protein per line and caspase-4 levels were analyzed by immunoblotting.

III-2-2. UPR induces the activation of caspase-4

Caspase-4 is localized to the ER membrane, and several studies reported caspase-4 was cleaved to be activated when cells were treated with ER stress-inducing reagents [222]. We examined the *caspase-4* and *-5* mRNA levels upregulation through UPR by tunicamycin (TM) or thapsigargin (TG) treatment (**Fig.III-3A – 3C**). Fig.III-3A repeatedly showed either GGA, TM or TG treatment resulted in upregulation of the *XBPIs* mRNA level as an indicator of UPR signaling in HuH-7 cells. Accordingly, *caspase-4* and *-5* mRNA expression levels were increased (Fig.III-3B and 3C). Cellular protein levels of active caspase-4 were further assessed after GGA, TG, or TM treatment. **Fig.III-3D** clearly showed GGA or TM-induced activation of caspase-4 protein for 5 h, but no induction was observed by TM, as in the case of TM treatment UPR was late induced in comparison with GGA or TG.

We reported GGA-induced *XBPI* mRNA splicing and upregulation of *DDIT3* mRNA level were both efficiently and dose-dependently suppressed by co-treatment with OA, while TM-induced upregulation of *XBPIs* and *DDIT3* mRNA levels were both unaffected by co-treatment with OA [77]. Additionally, we previously described UPR triggered by GGA was suppressed by co-treatment with VIPER (Fig.II-9H and 9I). To determine whether GGA-induced UPR occurs via a similar mechanism underlying TG-induced UPR, we performed the inhibition experiment that TG-induced UPR can be also prevented by co-treatment with OA or VIPER. **Fig.III-3E and 3F** show that TG-induced upregulation of *XBPIs* and *DDIT3* mRNA levels were both unaffected, similar to TM. By the way, TM or TG cannot induce cell death (**Fig.III-3G**).

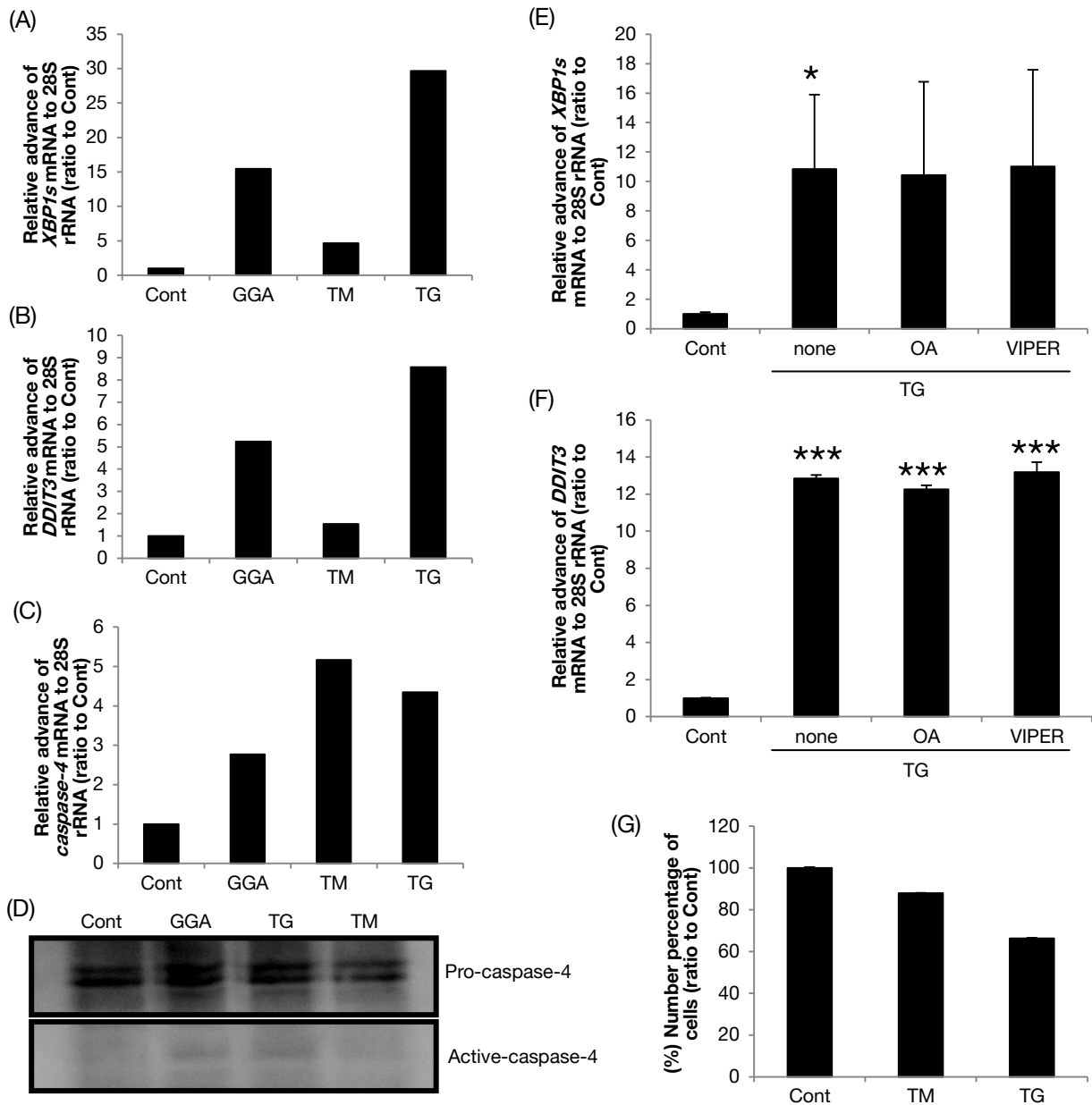


Fig.III-3. UPR induces the activation of caspase-4.

(A-C) HuH-7 cells were treated with 20 μ M GGA (GGA), 0.25 μ g/mL tunicamycin (TM), 25 ng/mL thapsigargin (TG) or ethanol vehicle alone (Cont) for 8 h. Then total RNA was extracted to analyze the cellular levels of *XBP1s* (A) and *caspase-5* (B) mRNA by RT-qPCR. HuH-7 cells were treated with 20 μ M GGA (GGA), 0.25 μ g/mL TM, 25 ng/mL TG or ethanol vehicle alone (Cont) for 24 h, and total RNA was extracted to analyze *caspase-4* mRNA expression (C). (D) HuH-7 cells were treated with 20 μ M GGA, 25 ng/mL TG, or 0.25 μ g/mL TM for 5 h. Whole-cell lysates were prepared, 18 μ g of total protein per line and caspase-4 levels were analyzed by immunoblotting. (E, F) HuH-7 cells were treated with 25 ng/mL TG for 3 h in the absence or presence of OA or VIPER (50 or 5 μ M, respectively). Total RNA was extracted to measure the cellular level of *XBP1s* (E) or *DDIT3* (F) mRNA by RT-qPCR. The asterisks (*, ***) indicate statistical significance ($p < 0.05$, 0.001, respectively), compared with each relevant as determined by Student's *t*-test.

III-2-3. Increase of intracellular calcium concentration via UPR in HuH-7 cells

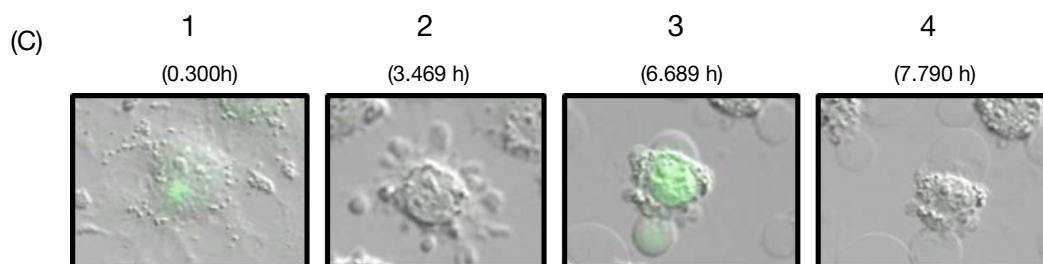
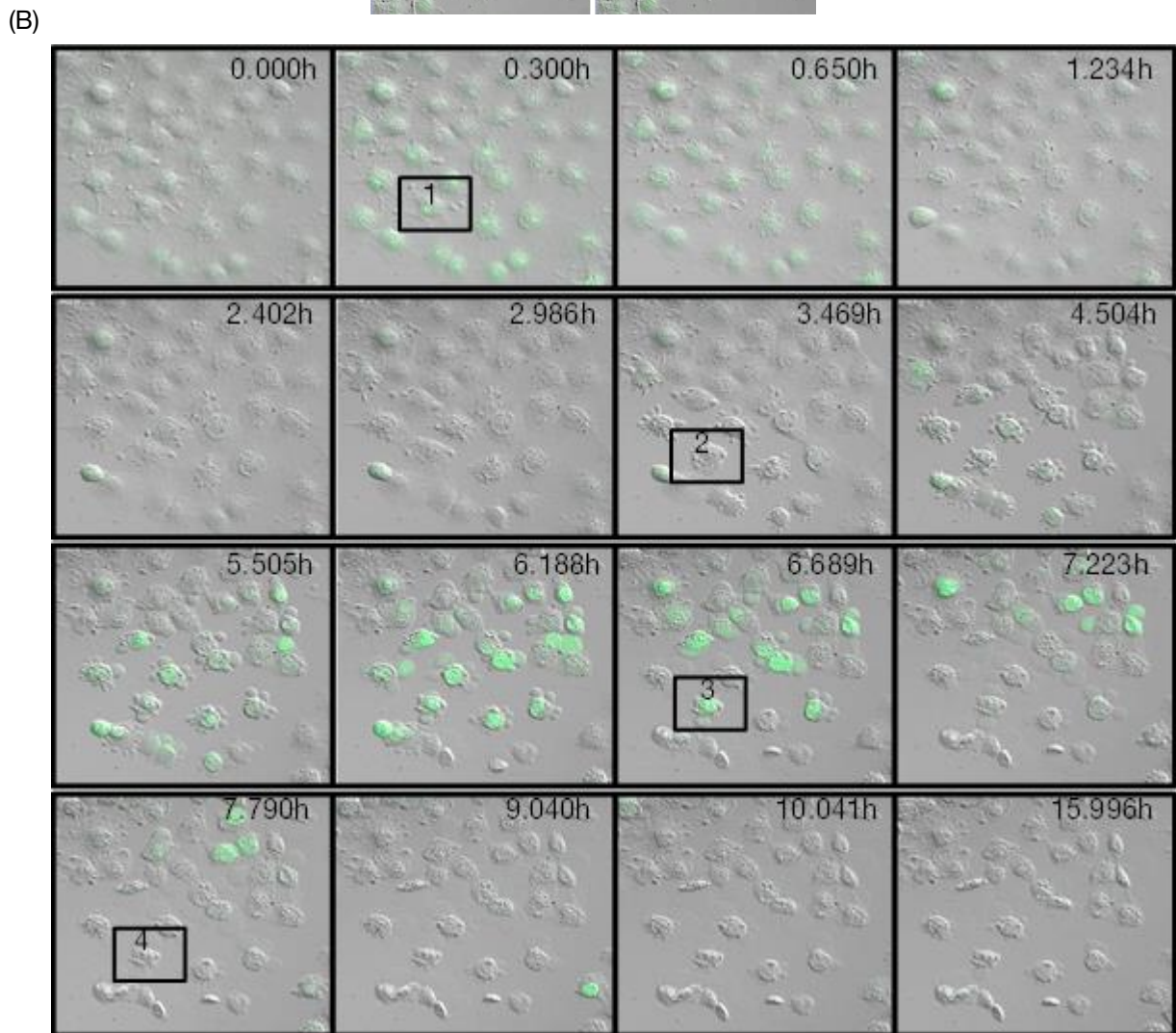
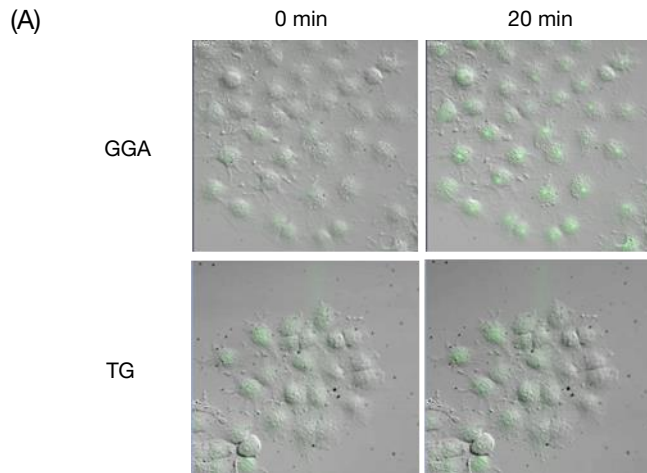
Fig.III-4A shows that GGA or TG induced Ca^{2+} release from ER to the cytoplasmic fluid via UPR, because intracellular Ca^{2+} is stored mainly in the ER. Treatment with GGA rapidly detected a transient increase in the green fluorescence in Fluo-4 AM-preloaded (Ca^{2+} -dependent fluorogenic) HuH-7 cells. Following addition of 10 μM GGA to the culture medium, the level of Fluo4 fluorescence was immediately decreased (**Fig.III-4A**). Conversely, the effect of treatment with 25 ng/mL TG on Fluo-4 fluorescence appeared unchanged during the experiment. Further time-series analysis was conducted with live-cell imaging frames of Fluo-4 AM-preloaded cells from 0 to 20 h of GGA treatment. By judging morphological changes in differential interfering contrast (DIC) images, some of the treated cells lost cell-cell adhesion and began to contract to make the cell body smaller in 2-3 h after GGA addition. A clear morphological change was detected after 3 h of adding GGA to the medium, which is shown in a 3.469 h panel of **Fig.III-4B**. As you can see in a panel 2 of **Fig.III-4C**, many irregular bulges are protruded in the plasma membrane of a cell, some of them appear to be apart from the cell like as apoptotic bodies. Then after 6 h, these irregular bulges fuse together and still stick to the cell membrane as two or three large balloon-shaped bulges as seen in a panel 3 of **Fig.III-4C**. These balloons become larger than their own cell body after 7 h (panel 4) and last until 16 h.

Time-series analysis of the cellular Ca^{2+} concentration revealed an interesting phenomenon that two calcium concentration peaks appeared after GGA addition of the medium. The first immediate peak comes out in 16 min and the second relatively broader peak occurs at around 6 h after addition of GGA

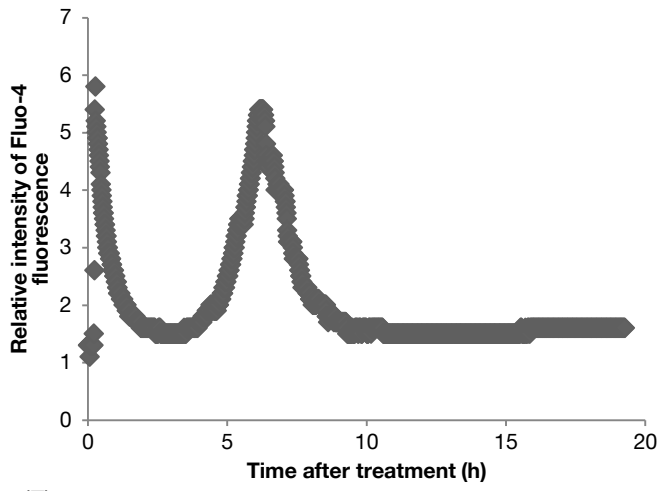
(**Fig.III-4D**). And when we observe this in individual cells, the first peak appears in 16 min in every cell, but the time at which the second peak appeared varies from cell to cell; the earliest was detected at 4.5 h, the latest was at 10.5 h, as shown in **Fig.III-4E**. If you look closely at the second peak, the average of the fluctuations over time of the fluorescence measured the entire field of view is observed as a symmetrical peak at around 6 h after GGA treatment (**Fig.III-4D**), but in the observation of individual cells the second each peak gradually ascends and when it reaches the peak, it descends all of a sudden, resulting in formation of an asymmetric peak (**Fig.III-4E**).

When the cells were exposed to GGA cultured in Ca^{2+} -free D-MEM, an early peak was detected within 1 h after GGA treatment, but no second peak appeared (**Fig.III-4F**). The first peak of cytoplasmic Ca^{2+} concentration of cells cultured in Ca^{2+} -free D-MEM was detected later as a wider form compared with cells cultured in Ca^{2+} -containing D-MEM (**Fig.III-4G**).

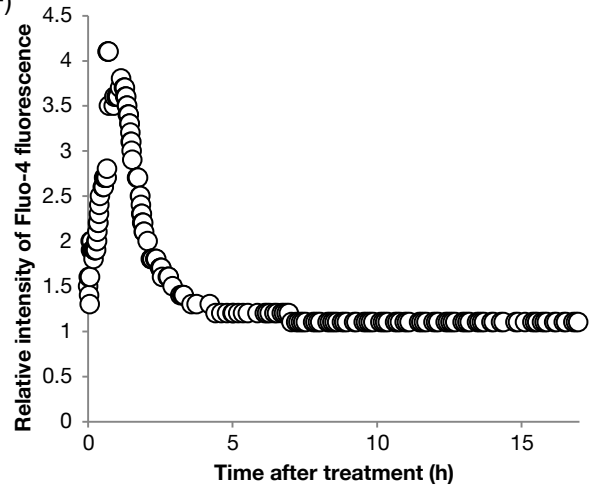
We next examined whether calpain inhibitors were able to rescue the cells from GGA-induced cell death, because calpains belong to family of cytosolic cysteine proteases that depend on intracellular Ca^{2+} and may be involved in activation of caspase-4. Furthermore, calpain inhibition has been reported to reduce neutrophil infiltration and liver pathology [221]. GGA (20 μM)- induced cell death was not suppressed by co-treatment with 6.25 μM calpain inhibitor I or II in 96-well plates measured by CellTiterGlo assay (**Fig.III-4H**). Further, GGA-induced cell death was dose-dependently advanced by co-treatment with calpain inhibitor I or II (**Fig.III-4I and 4J**).



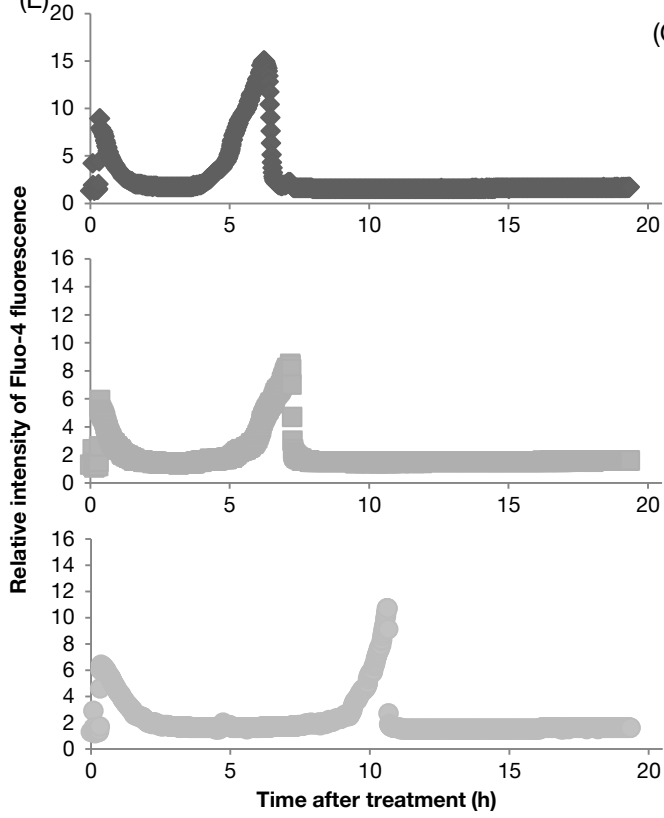
(D)



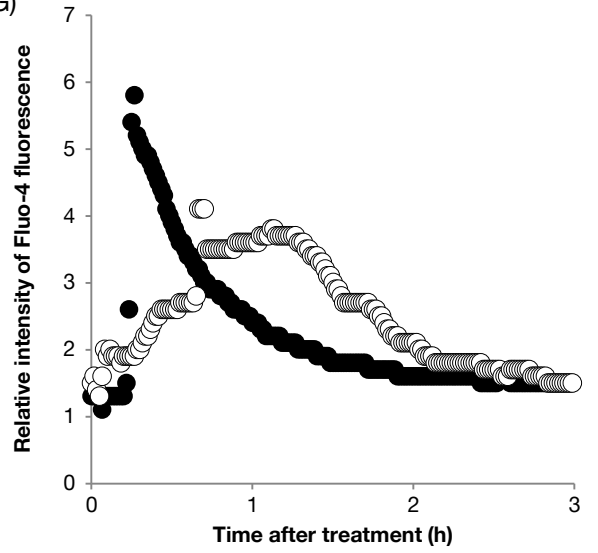
(F)



(E)



(G)



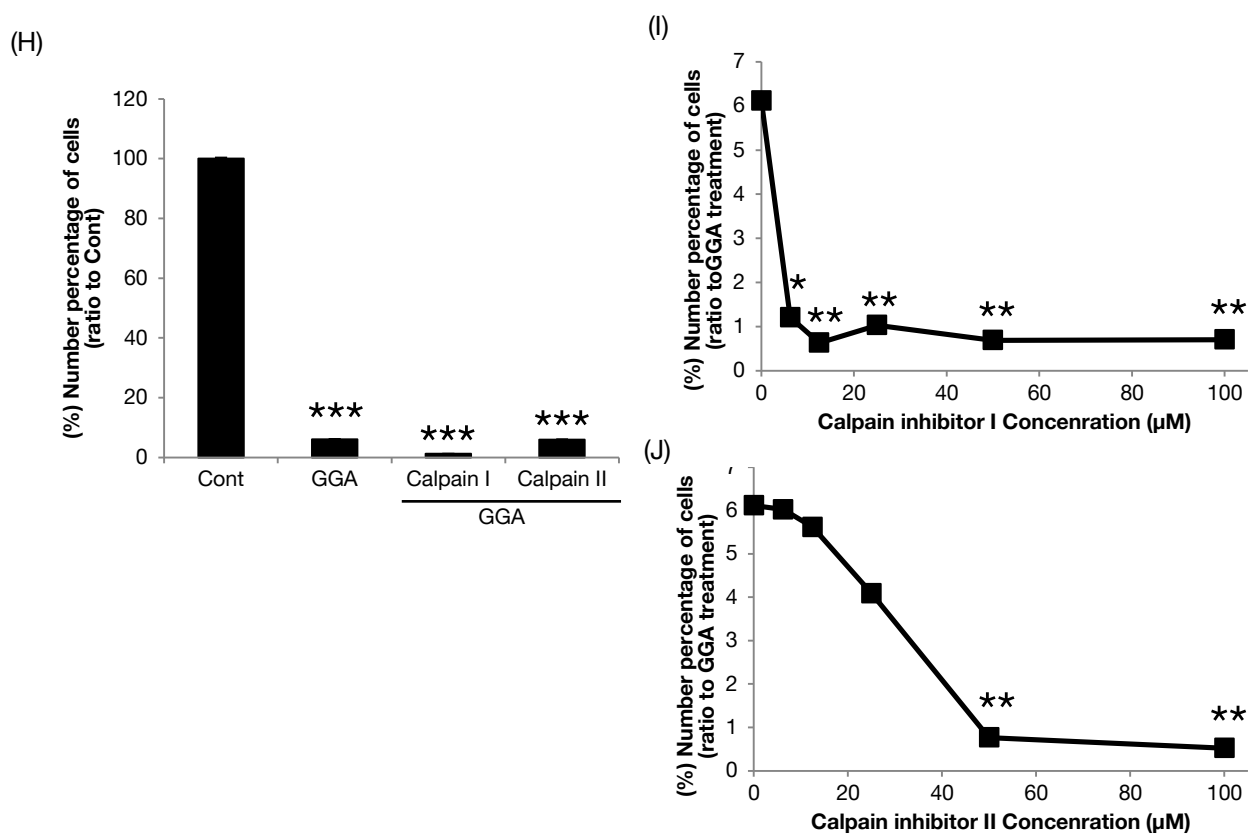


Fig.III-4 Increase of intracellular calcium via UPR in HuH-7 cells.

(A) HuH-7 cells were treated with 10 μM GGA (GGA) or 25 ng/mL thapsigargin (TG) overnight. Live-cell imaging was performed with the green fluorescence for Fluo4 on the LSM700 confocal laser-scanning fluorescence microscope. (B, C) Immediately after treatment with 10 μM GGA, live-cell imaging was performed with the green fluorescence of Fluo-4 AM with HuH-7 cells cultured in a chamber unit in a LSM700 confocal laser-scanning fluorescence microscope. Snap shots at each time point shown in each frame were time-dependently arrayed from 0 to 16 h. Rectangles numbered 1 to 4 containing the same cell are enlarged and shown in B. (D, E) Total green fluorescence intensity was monitored in each microscopic field (D), or in each cell (E) and was plotted up to 18 h every minute after GGA addition. (F, G) Total green fluorescence intensity was monitored in each microscopic field, and was plotted up to 16 h every minute after GGA addition with Ca²⁺-free medium (F). Early changes in the fluorescence intensity of cells cultured in Ca²⁺-free medium (open circle) are shown from 0 to 3 h compared with HuH-7 cells (closed circle) cultured in D-MEM containing Ca²⁺ (G). (H) HuH-7 cells were treated with 20 μM GGA (GGA) in the presence or absence of 6.25 μM calpain inhibitor I or II (Calpain I/II) for 24 h. Viable cells were measured using the CellTiter-Glo assay kit. (I, J) HuH-7 cells were treated with 20 μM GGA (GGA) in the co-treatment of 6.25, 12.5, 25, 50 or 100 μM calpain inhibitor I (I) or II (J) for 24 h. Viable cells were measured using the CellTiter-Glo assay kit. Values are the means ± SE (n=6). The asterisks (*, **, ***) indicate statistical significance (p<0.05, 0.01, 0.001, respectively), compared with GGA alone as determined by Student's *t*-test.

III-3. Discussion

Pyroptosis is characterized by membrane blebbing and produces apoptotic body-like cell protrusions (termed pyroptotic bodies), which fuse to a size as large as the cell body prior to plasma membrane rupture [234]. These morphological alterations were confirmed by time-series recordings of live-cell imaging (Fig.III-4). Membrane blebbing and pyroptotic bodies appeared 1-3 h after GGA addition and the fused balloons were detected after 6 h. It is noteworthy to mention that a transient increase in cytoplasmic Ca^{2+} concentration was observed after and before these morphological changes of membrane blebbing/pyroptotic bodies and their fused balloons, respectively. Because the first Ca^{2+} peak was detected in GGA-treated cells cultured in Ca^{2+} -free medium, we believe that the first peak was caused by Ca^{2+} leakage from cellular Ca^{2+} -storage organelles such as the ER. This is supported by our previous finding that GGA induced an ER stress response/UPR in 15 min [77]. The second peak was not detected in GGA-treated cells with Ca^{2+} -free medium, indicating that cellular Ca^{2+} in the second peak must be from the medium.

One of the most important findings about GGA-induced pyroptosis is the GGA-induced translocation of GSDMD to the plasma membrane (Figs.II-8A and III-2A). Recent intensive studies on pyroptosis have revealed that the N-terminal fragment of GSDMD is the sole executor of pyroptotic cell death by its intrinsic pore-forming activity in the plasma membrane [173,177,233,235]. We found that the nuclear- and perinuclear-localized GSDMD was distributed throughout the cytoplasm of untreated cells and at first that part of the GSDMD reached the cell membrane at 10 h after GGA addition. Interestingly, cytoplasmic

caspase-1 moved into the nuclear space upon GGA treatment, suggesting active caspase-1 may produce the N-terminal fragment of GSDMD in the nuclear space. However, we found N-terminal fragments of GSDMD-N on immunoblots as early as 1 h after GGA addition, when caspase-1 was not yet activated (Fig.II-5). Consistent with these data, we clearly detected the plasma membrane translocation of GSDMD 3 h after GGA addition prior to caspase-1 activation, and the GSDMD signals were particularly eminent in the concave parts of the plasma membrane (Fig.III-2A). GSDMD is an efficient substrate for caspase-1 as well as caspase-4/5 (human equivalents of rodent caspase-11) [236]. As mentioned above, an active form of caspase-4 was found as early as 1 h after GGA treatment, which may explain why GSDMD was present in the plasma membrane 3 h after GGA addition.

How does GGA treatment activate caspase-4 activity? For LPS, a well-known TLR4 ligand, caspase-4 directly binds to LPS and undergoes oligomerization, resulting in the self-activation of enzyme activity [112], termed non-canonical inflammasome activation [104]. Although we have not examined the direct binding of GGA to caspase-4 or its resultant oligomerization, in the present paper we present experimental evidence that GGA-induced UPR activates caspase-4, by demonstrating that TG induces an active form of caspase-4 (Fig.III-3D), which is consistent with previous reports [237–239]. TG is a non-competitive inhibitor of the ER Ca^{2+} -ATPase and induces UPR by causing Ca^{2+} release from the ER. TG-induced UPR was not inhibited by co-treatment with oleic acid or VIPER (Fig.III-3E, F). Since Hitomi et al. first reported that UPR activated caspase-4 activity [222], many research groups have confirmed the UPR-mediated activation of caspase-4 [240,241] and suggested a possible molecular mechanism involving

caspase-4 cleavage by Ca^{2+} -activated calpain [242,243]. Therefore, it is reasonable to speculate that GGA might be activated by caspase-4, which is cleaved by calpain enzymes activated by the first Ca^{2+} peak at 1 h after GGA addition (Fig.III-4D).

In conclusion, we show that a non-canonical inflammasome pathway via UPR in HuH-7 cells might enhance GGA-induced pyroptosis through activation of NF- κ B pathway. Furthermore, GGA induced the cytosolic release of calcium stored in the ER, probably due to GGA-induced UPR, suggesting that GGA may be not only able to induce canonical pathway in pyroptosis, but also induce non-canonical pathway in HuH-7 human hepatoma cells.

Chapter IV

Epigenetic aspect of cancer chemoprevention with GGA

Suemi Yabuta

Molecular and Cellular Biology, Graduate School of Human Health Science,

University of Nagasaki, Nagasaki, Japan

Abstract

Histone-modifiable lysine-specific demethylase-1 (LSD1/KDM1A) is often upregulated in many cancers, including hepatoma, and is regarded as oncoprotein. We previously reported that the hepatoma-preventive compound GGA inhibits KDM1A activity at the same IC_{50} as that of the clinically used drug tranylcypromine, a verified inhibitor of KDM1A. Here, we report that these inhibitors induced cytoplasmic translocation of nuclear KDM1A in a human hepatoma-derived cell line. Immunofluorescence studies revealed cytoplasmic localization of KDM1A, usually a nuclear marker protein, 3 h after addition of GGA or tranylcypromine in HuH-7 cells. Similar isoprenoids, geranylgeraniol, farnesoic acid and ATRA, were all unable to induce translocation of nuclear KDM1A under the same conditions. Furthermore, GGA did not affect subcellular localization of another histone lysine-specific demethylase, KDM5A, which remained in the nucleus 3 h after GGA treatment. This suggests that the inhibitor-induced translocation of KDM1A from the nucleus to the cytoplasm is specific for KDM1A. When the nuclear fraction was incubated with GGA, KDM1A was detected in the supernatant after centrifugation. These data demonstrate for the first time that KDM1A inhibitors specifically induce translocation of nuclear KDM1A to the cytoplasm.

IV-1. Introduction

IV-1-1. Epigenetic regulatory mechanisms

Epigenetic alterations often promote or even drive cancer development by activating and sustaining cancer-promoting gene expression [244]. Among epigenetic changes in cancer cells, histone lysine methylation/demethylation has gained substantial attention as a possible target in therapeutic drug development [245]. Histone lysine methylation/demethylation is extensively involved in nucleosome remodeling and gene expression. Lysine residue methylation is reversibly regulated by histone lysine methyltransferases and histone lysine demethylase 1 (KDM1A/LSD1) has received increasing attention since its identification in 2004 [246]. Overexpression of KDM1A is frequently observed in prostate, breast, and bladder cancers, neuroblastoma, and especially hepatoma [247], where it correlates directly with adverse clinical outcome and inversely with differentiation [248]. Thus, KDM1A inhibitors are of clinical interest for their anticancer role as well as their potential application in other human diseases that exhibit deregulated gene expression [249].

IV-1-2. Histone modification

Karch et al. [250] explained nucleosomes, the basic repeating unit of chromatin, consist of ~147 bp DNA wound around a histone core containing two copies of the histone proteins H2A, H2B, H3, and H4 [251]. Histones undergo dynamic post-translational modifications (PTMs) on specific residues, most of which are contained in the flexible N-terminal tail that protrudes from the nucleosomal surface [252]. It has been

hypothesized that PTMs may form a “histone code” in which particular marks or combinations of marks elicit a specific physiological response by regulating chromatin structure [253]. PTMs may perform these tasks by directly altering the chemical environment of the surrounding chromatin or through the action of other proteins that bind to these marks, termed readers. Readers may contain or recruit effector proteins, modify chromatin function and consequently form signaling scaffolds that mediate processes such as gene expression, apoptosis, and DNA damage repair [253].

Furthermore, Oike et al. [254] described in human cells, many activities essential for cell survival, such as DNA transcription, synthesis and repair, are mediated by dynamic changes in nucleosome structure that facilitate access of DNA-binding proteins to double-stranded DNA [255]. Proteins that control change in nucleosome structure are called chromatin-regulating proteins. These proteins can be categorized into two groups that take part in distinct mechanisms: histone modification and chromatin remodeling. Some histone modifiers agents bind substrates, such as phosphate, poly-ADP-ribosyl, acetyl, methyl, SUMOyl and ubiquityl groups to histone tails by covalent interaction, whereas other histone modifying agents bind these groups from previously modified histones. Chromatin remodelers usually function as complexes that alter nucleosome assembly (e.g. by forming a DNA-loop or sliding a nucleosome) in an ATP-dependent manner.

Gu and Lee [256] introduced that histone lysine methylation has been widely accepted as a major epigenetic modification. Whereas acetylation of lysine residues causes neutralization of the basic amine group, the methylation does not alter the charge of lysine residues and thus has a minimal direct charge

effect on DNA-histone bonds. Rather, the different methylation status of specific histone lysine can serve as a unique platform for engaging methylation “reader” proteins that activate or repress genes’ transcriptional activity through hydrophobic interaction. In general, histone H3 lysine-4 (H3K4), H3K36, and H3K79 methylation are gene activation marks, whereas H3K9 and H4K27 methylation are gene-repressive modifications [257].

Additionally, they [256] have described H3K4me3 accounts for 75% of all human gene promoters in several cell types (e.g., ES cells), indicating that it plays a critical role in mammalian gene expression [258,259]. Indeed, H3K4me3 is required to induce important developmental genes in animals, including several mammals, and is essential for animal embryonic development [260]. H3K4me3 levels are positively correlated with gene expression levels [259].

IV-1-3. Lysine-specific demethylase 1A (LSD1/KDM1A)

Gu and Lee also explained the biological significance of KDM1A-mediated histone modification as follows [256]. Although H3K4me3 is clearly associated with actively transcribed genes, some studies have demonstrated that H3K4me3 is localized around the transcription initiation sites of numerous unexpressed genes in human ES cells, primary hepatocytes, and several other cell types [261]. In particular, it frequently coexists with the repressive mark H3K27me3 in the promoters of important differentiation-specific genes [e.g., *homeobox (HOX)* gene clusters] that are transcriptionally inactive in ES cells [261,262]. It has been proposed that the “bivalent” domains, consisting of H3K4me3 and H3K27me3,

may maintain differentiation-specific gene promoters in a inhibitory status in self-renewing stem cells but may be prepared for prompt gene activation upon differentiation stimuli [263]. Consistent with this, many bivalent genes have increased H3K4me3 levels and decreased H3K27me3 levels while being transcriptionally activated during differentiation. Interestingly, a couple of studies demonstrated that most bivalent domains were occupied by KDM1A [264,265], indicating that it plays a role in maintaining low levels of dimethylated H3K4 (H3K4me2) that often coincides with H3K4me3 (**Fig.IV-1**). For these reasons, H3K4me3 is classified as a chromatin sign of transcriptionally active genes in ES cells [261].

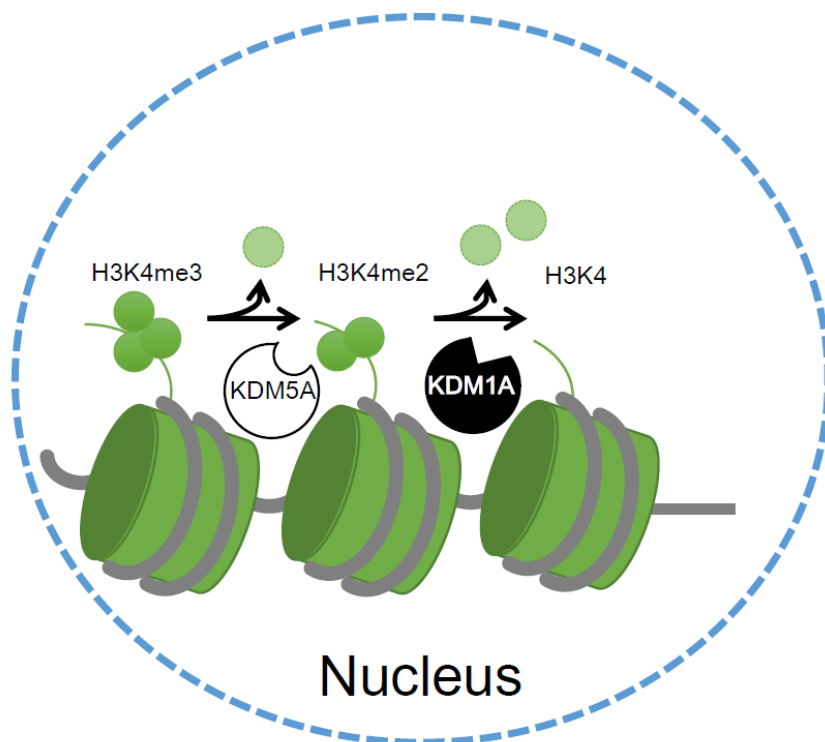


Fig.IV-1. Characteristic of histone H3K4 demethylase KDM1A.

Additionally, they [256] described most H3K4me3-containing promoters are also occupied by H3K9/H3K14 acetylation [261]. In transcriptionally active genes, H3K36me3 and H3K79me2 are significantly enriched downstream of H3K4me3-containing promoters: H3K36me3 peaks toward the 3'

end of genes, whereas H3K79me2 is located at the 5' end [261]. Therefore, H3K4me3 seems to cooperate with other histone marks for gene activation. The combination of H3K4me3 with other histone marks may support, at least in part, the “histone code” hypothesis [253].

And they stated [256] that H3K4me2 modifies genomic regions independently of H3K4me3, although most of it overlaps with H3K4me3 near the transcription start sites [266]. H3K4me2 may have an antagonistic effect on DNA methylation [267]. Mono-methylated H3K4 (H3K4me1) also co-occupies regions near the start sites with H3K4me3. Apart from the transcription start sites, H3K4me1, together with H3K27 acetylation, specifies enhancer regions [268,269]. In summary, H3K4me1, H3K4me2 and H3K4me3 have harmony in gene activation, although their subsets play different roles in regulating chromatin function.

Historically, the reversibility of histone methylation was not clear until the discovery of the first histone demethylase KDM1A (also known as LSD1) in 2004 [246]. Subsequently, more than a dozen of human histone lysine-specific demethylase genes have been cloned. A new class of the F-box protein family was reported as KDM2A that specifically demethylates both mono- and di-methylated lysine-36 of histone H3 (H3K36me1/me2). Another new class of zinc finger proteins containing JmjC-domain was identified that KDM3A/JMJD1A can demethylate methylated lysine residues in histone (H3K9me3) [270], KDM4A/JMJD2A for methylated lysine residues H3K9/36 [271], KDM5C/JARID1C for H3K4me3 [272], and KDM6A/JMJD3 for H3K27 [273]. These members of KDM superfamily play important roles in gene transcription in various cells during development and homeostasis.

IV-1-4. Another lysine-specific demethylase for histone H3 (KDM5A)

Among other members of the KDM family, KDM5A/JARID1A is of particular interest because it specifically removes a methyl group from the trimethylated lysine 4 of histone H3 to produce dimethylated lysine 4. This produces a substrate for KDM1A, which is cooperatively capable of removing dimethyl and monomethyl groups from lysine 4 of histone H3 [249,274]. KDM1A and KDM5A are recruited to chromatin through the corepressor for element 1-silencing transcription factor (CoREST) [249] and origin recognition complex 2 (ORC2)- small ubiquitin-like modifier 2 (SUMO2) [275] complexes, respectively. Hence, these KDMs are generally recognized as nuclear-localized proteins [276,277].

IV-1-5. Aim of the present study in this chapter

KDM1A is a flavin adenine dinucleotide-containing enzyme belonging to the amine oxidase superfamily [278]. Structural homology between KDM1A and monoamine oxidase-B, a clinically validated pharmacological target, suggests that KDM1A is a druggable target. Indeed, screening of known monoamine oxidase inhibitors has uncovered KDM1A inhibitors that are effective at sub-millimolar concentrations, among which the best known is the clinically used antidepressant drug *trans*-2-phenylcyclopropylamine (TCP). Multiple clinical trials have begun to investigate the antitumor effect of TCP [279].

Recently, we reported that all-*trans* GGA inhibits KDM1A activity at the same IC_{50} as that of TCP [20]. To our knowledge, no studies have yet reported KDM1A inhibitor-induced changes in the subcellular

distribution of the enzyme. When studying the effects of GGA on hepatoma cells, we found that GGA altered the subcellular localization of KDM1A, which could be important for both KDM1A-inhibitor screening and understanding KDM1A biology. Here, we report that some KDM1A-inhibitors can remove KDM1A from chromatin and move it to the cytoplasmic space in human hepatoma cells.

IV-2. Results

IV-2-1. Cytoplasmic translocation of nuclear KDM1A induced by GGA or TCP

First, nuclear localization of the chromatin protein KDM1A was confirmed in non-treated control cells by immunofluorescence. The upper row of images in **Fig.IV-2A** clearly indicates a strict colocalization of KDM1A with Hoechst 33258-stained chromatin DNA. However, 3 h after treatment of HuH-7 cells with the KDM1A inhibitors GGA or TCP, the subcellular localization of KDM1A appeared to have shifted from the nucleus to the cytoplasmic space, as shown in the lower two rows of images in Fig.IV-2A. This indicates that exclusion of nuclear KDM1A was induced by both KDM1A inhibitors. Quantitative analysis of the green fluorescence intensity of KDM1A clearly shows that both inhibitors significantly affected the subcellular localization of KDM1A (**Fig.IV-2B**). This indicates that exclusion of nuclear KDM1A was induced by both KDM1A inhibitors.

The exclusion of nuclear KDM1A by treatment with its inhibitors was further confirmed by Z-axis projections (top and right parts of each image in **Fig.IV-2C**). Three-dimensional rendering of the three images using z-stacks clearly illustrates that the KDM1A protein was localized outside the nuclei 3 h after treatment with GGA or TCP, whereas most of the KDM1A protein was sequestered in the nuclei of the control cells (Fig.IV-2C).

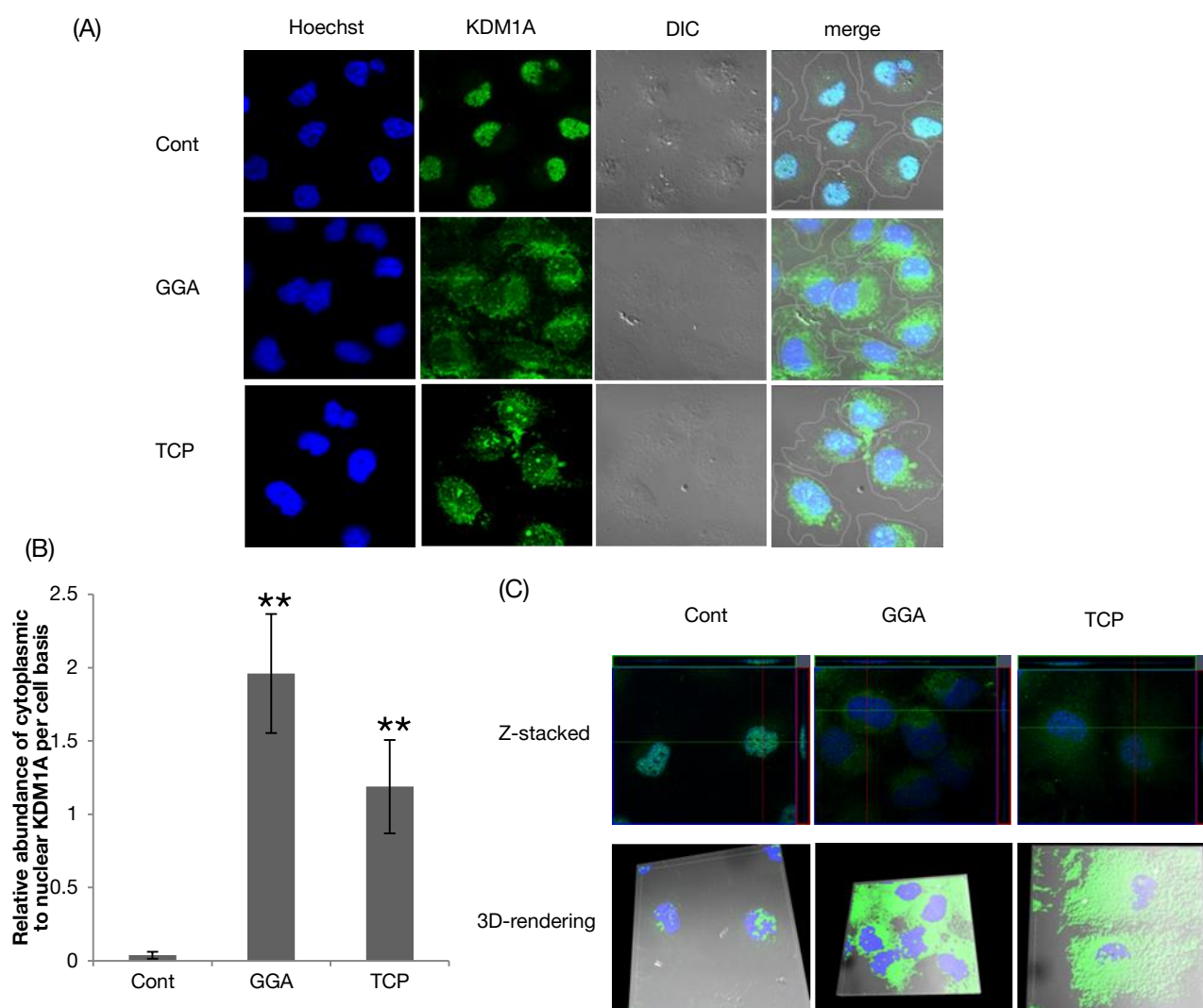


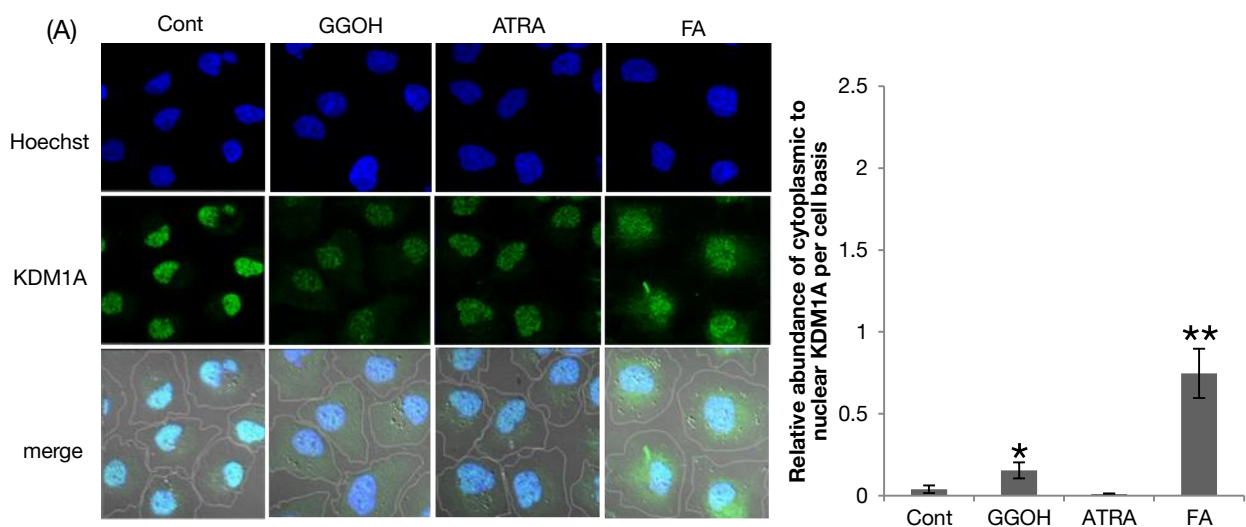
Fig.IV-2. Cytoplasmic translocation of nuclear KDM1A induced by either GGA or TCP treatment.

HuH-7 cells were incubated for 3 h with GGA (20 μ M), TCP (5 μ M) or vehicle alone as a control. (A) Images were obtained of immunofluorescence staining with anti-KDM1A primary antibody and anti-rabbit IgG-Alexa488 secondary antibody (green); nuclei were counter-stained with Hoechst 33258 (blue). Merged images (Merge) were constructed using differential interference contrast (DIC) images. (B) Quantitative analysis was performed on a cellular basis with the green fluorescent images in panel (A) and relative abundance of the cytoplasmic to the nuclear fluorescence intensity was calculated. ** indicate statistical significance ($p < 0.01$), compared with control. (C) In the merged Z-stacked images of KDDM1A (green) with nucleus (blue), orthogonal hairlines show the XZ (green line and upper green box) and YZ (pink line and right pink box) planes in each panel. Z-stacked images were processed to obtain three-dimensional renderings using Imaris software. The solid view of the three-dimensional renderings allows confirmation of the cytoplasmic export of KDM1A (green) from the nucleus (blue) in GGA- and TCP-treated cells, whereas in control cells the majority of KDM1A is located in the nucleus.

IV-2-2. Specificity for KDM1A inhibitors and nuclear KDMs

Having identified GGA-induced translocation of nuclear KDM1A for the first time, we next considered whether this cytoplasmic translocation could be induced by treatment with similar isoprenoids that lack KDM1A-inhibitory activity, such as GGOH, ATRA and farnesoic acid (FA) [20]. GGOH, ATRA and FA did not induce cytoplasmic translocation of nuclear KDM1A (**Fig.IV-3A**), suggesting that the translocation response of nuclear KDM1A is specific to its inhibitors.

Next, we tested whether GGA or TCP could induce cytoplasmic translocation of another nuclear KDM, KDM5A, which acts cooperatively with KDM1A to remove methyl groups from histone H3K4me3. As shown in the upper images in **Fig.IV-3B**, KDM5A was localized only in the nuclei of non-treated control cells. Neither GGA nor TCP, inhibitors of KDM1A but not of KDM5A, induced cytoplasmic translocation of the nuclear KDM5A; this was further confirmed by Z-axis projections (top and right parts of each image in **Fig.IV-3C**).



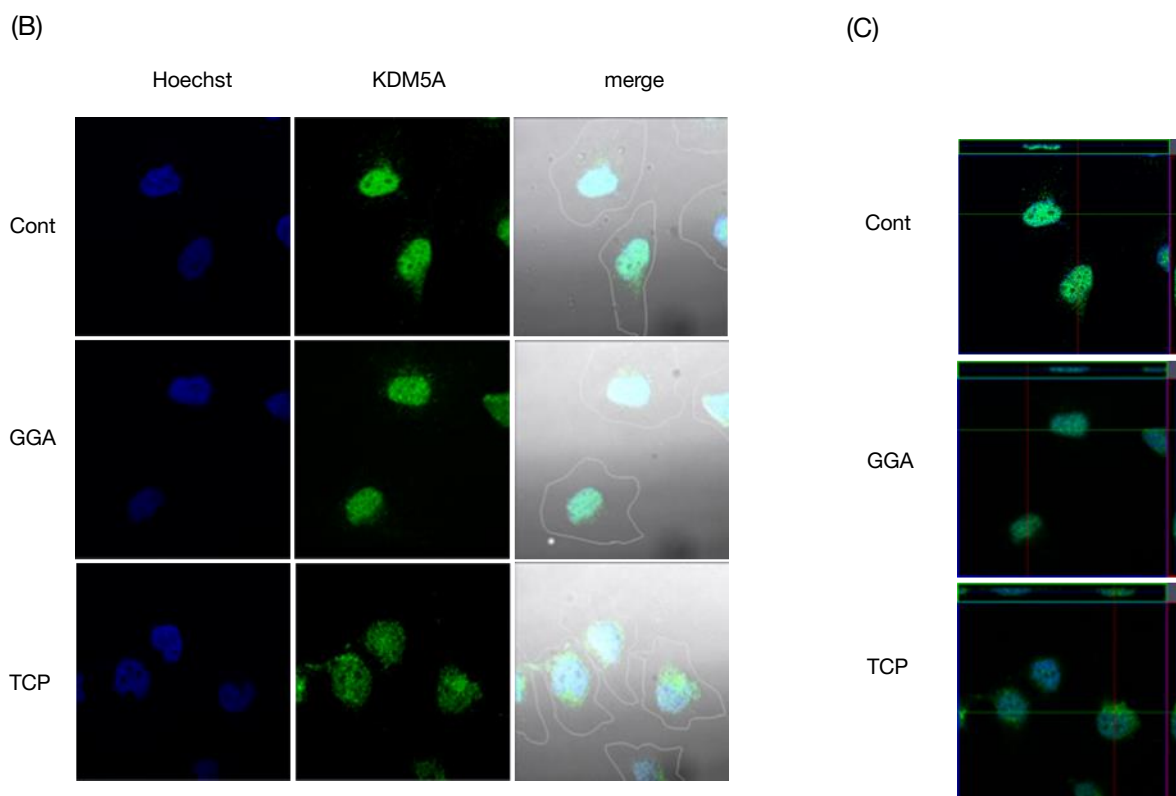


Fig.IV-3. Nuclear localization of KDM1A and KDM5A after 3 h treatment with non-inhibitory isoprenoids and KDM1A-inhibitors.

(A) Immunofluorescence staining of KDM1A (green) and counter-staining with Hoechst 33258 (blue) in HuH-7 cells treated for 3 h with the GGA-analogous isoprenoids GGOH, ATRA, and FA. Each isoprenoid was used at a final concentration of 20 μ M. Quantitative analysis was performed on a cellular basis with the green fluorescent images and relative abundance of the cytoplasmic to the nuclear fluorescence intensity was calculated. *, ** indicate statistical significance ($p < 0.05$, 0.01, respectively), compared with control. (B) After GGA or TCP treatment, cells were immunostained for KDM5A (green), another lysine-specific demethylase, and the nuclei were counter-stained with Hoechst 33258 (blue). (C) In the merged images of KDM5A (green) and nucleus (blue) staining, orthogonal hairlines show the XZ (green line and upper green box) and YZ (pink line and right pink box) planes in each panel.

IV-2.3. Subcellular distribution of KDM1A in M-phase cells

Nair et al [280] have reported that KDM1A is recruited to the chromatin of rodent embryonic stem cells in the G1/S/G2 phases and is displaced from the chromatin of M-phase cells. Therefore, we next examined whether this was the case also in human hepatoma-derived HuH-7 cells. As shown in the upper row of images in **Fig.IV-4**, in anti-pHH3-stained M-phase cells, KDM1A protein was distributed throughout the inside of the cell, whereas in the other two cells on the right side of the M-phase cell the protein was retained in the nucleus. However, in cells treated with a KDM1A inhibitor (GGA or TCP), the protein was distributed throughout the whole cell or outside the nucleus not only in M-phase cells, but in the other remaining cells (images in lower two rows of Fig.IV-4).

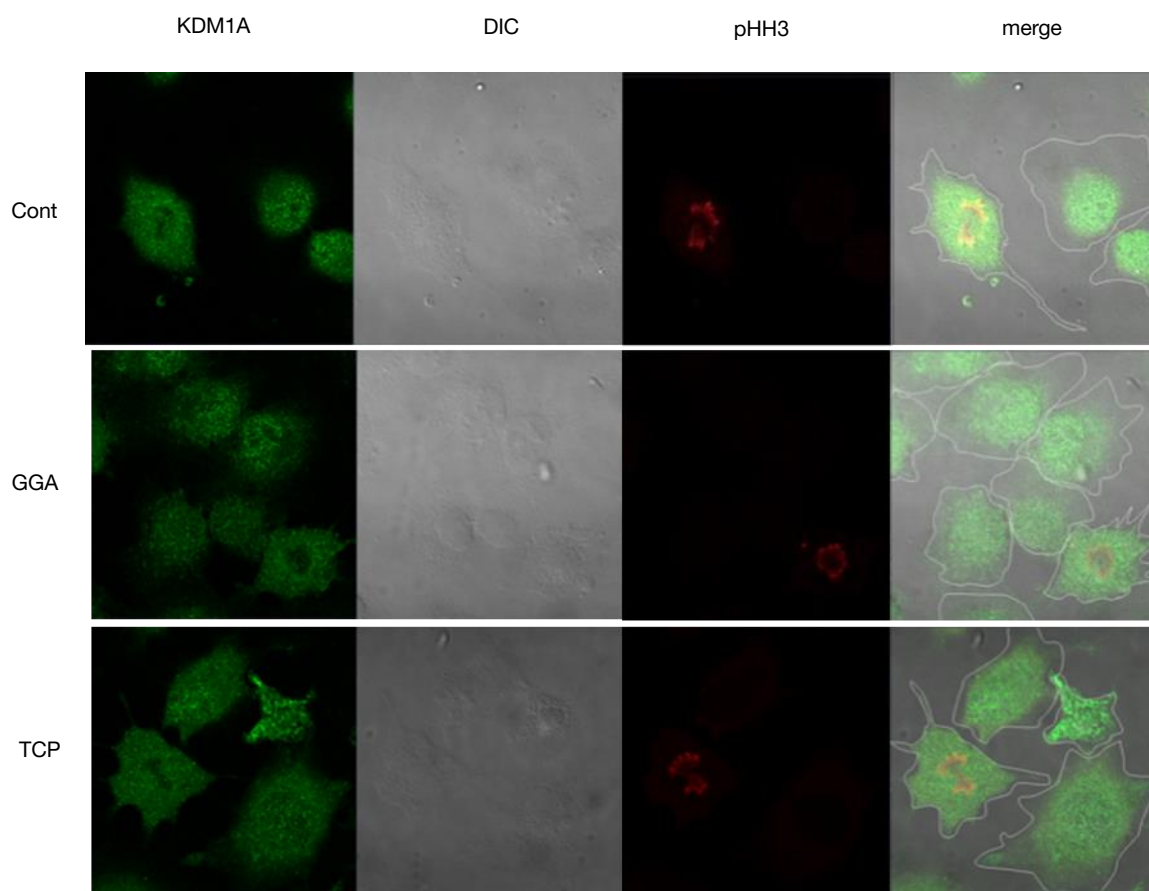


Fig.IV-4. Subcellular distribution of KDM1A in M-phase cells.

Immunofluorescence staining of KDM1A (green) and staining of M-phase nuclei with anti-pHH3 (Ser10) antibody (red) in HuH-7 cells after treatment for 3 h with GGA (20 μ M), TCP (5 μ M) or vehicle alone as a control. White lines in the merged images mark the peripheries of cells.

IV-2-4. Release of nuclear KDM1A by GGA or TCP under cell-free conditions

We recently reported that GGA directly inhibits recombinant human KDM1A [20]. And TCP acts as an irreversible inhibitor forming a covalent adduct with the FAD cofactor of the KDM1A enzyme [281]. In the present study, we examined the direct effect of these two inhibitors on the release of KDM1A protein from the nucleus. Dose-dependent release of the protein from the nuclear fraction was observed with either GGA or TCP (**Fig.IV-5A**).

Finally, we investigated GGA-induced changes in the cellular level of KDM1A protein to understand why KDM1A translocates out of the nucleus upon GGA treatment. **Fig.IV-5B** clearly shows that cellular levels of KDM1A decreased in a time-dependent manner after GGA treatment, which suggests that GGA may induce KDM1A protein degradation, because the *KDM1A* gene transcript level did not change during GGA treatment (**Fig.IV-5C**).

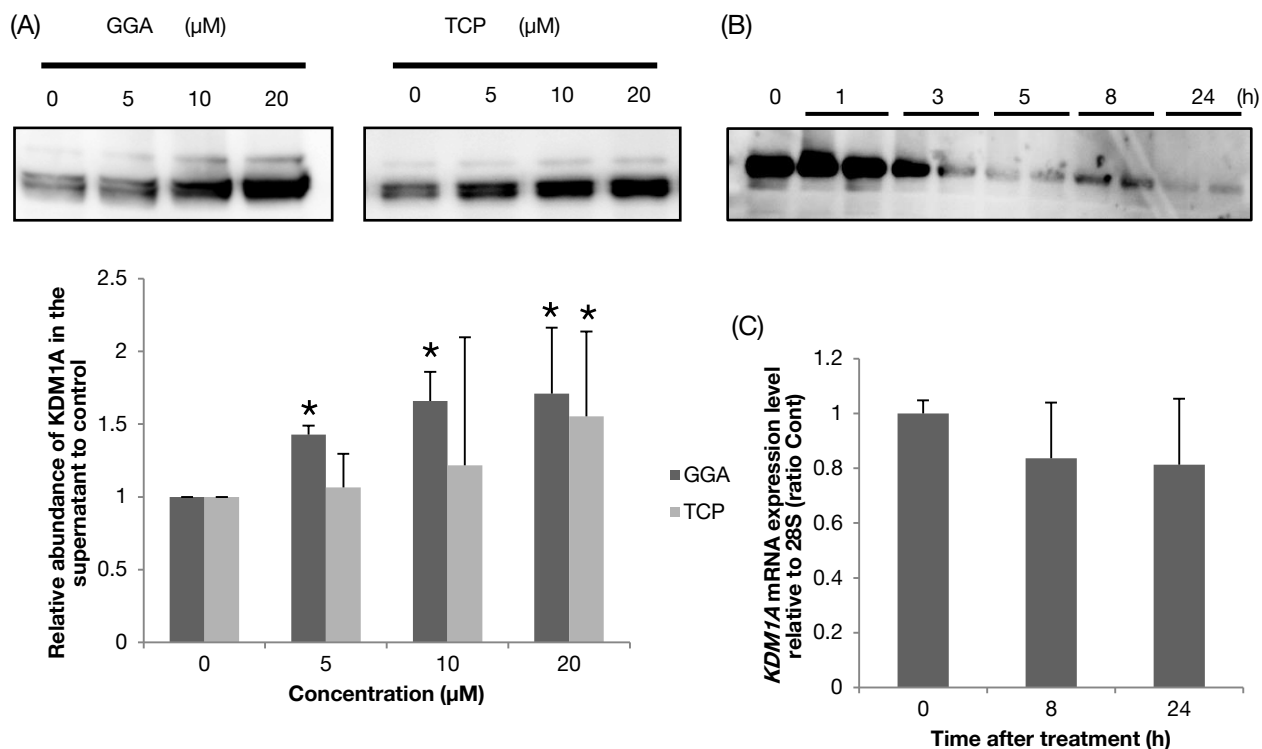


Fig.IV-5. Release of nuclear KDM1A after incubation of the nuclear fraction with GGA or TCP.

(A) GGA and TCP directly released KDM1A from the nuclear fraction in a concentration-dependent manner. The nuclear fractions were treated with either GGA (5 to 20 μM) or TCP (5 to 20 μM) at 4°C for 24 h. After centrifugation, the supernatant was analyzed SDS-PAGE and immunoblotting. The lower bar graph shows densitometric analysis of the KDM1A bands on the blots ($n=3$). * indicate statistical significance ($p < 0.05$), compared with control). (B) Immunoblot KDM1A protein in whole cell lysates of HuH-7 cells treated 20 μM GGA for the indicated times. (C) KDM1A mRNA levels were analyzed by RT-qPCR after 8 or 24 h treatment with 20 μM GGA.

IV-3. Discussion

The present study demonstrates for the first time that small chemical inhibitors of KDM1A, GGA and TCP, induce cytoplasmic translocation of nuclear KDM1A protein from the nucleus in human hepatoma-derived cells. Taking into account the fact that KDM1A has been identified as a component of the CoREST corepressor complex [282] and is a recognized nuclear marker protein [283], the present finding of KDM1A inhibitor-induced translocation of KDM1A from the nucleus to the cytoplasm may be important both for inhibitor screening and for understanding the biology of KDM1A. In this paper, we propose and discuss the biological significance of the transfer of KDM1A protein from the nucleus to the cytoplasm in response to KDM1A inhibitors.

In the present study, we confirmed strict nuclear localization of KDM1A protein in control human hepatoma-derived HuH-7 cells (Fig.IV-2). KDM1A was first discovered in 2004 as a nuclear homolog of amine oxidases that functions as a histone demethylase and transcriptional corepressor [246], which indicates that the enzyme originally resides in chromatin and plays a role in the repression of gene expression through epigenetic mechanisms. Here, however, we describe the striking finding that the KDM1A inhibitors GGA and TCP immediately dislodged KDM1A from the nucleus to the cytoplasm, suggesting that these inhibitors not only inhibited enzyme activity, but moved the enzyme itself to a location where epigenetic regulation was not possible. Therefore, these two inhibitors block the function of the enzyme via a dual mechanism.

The question then arises as to what types of compounds can induce this transfer of the KDM1A

enzyme from the nucleus to the cytoplasm. We tested the ability of the GGA-analogous compounds GGOH (an alcoholic derivative of GGA), ATRA (a monocyclic and conjugated derivative of GGA) and FA (an acyclic sesquiterpenoid acid, whereas GGA is an acyclic diterpenoid acid) to induce the cytoplasmic translocation of nuclear KDM1A. All of these isoprenoids, which exhibit minimal KDM1A-inhibitory activity [20] failed to induce translocation of the enzyme, suggesting that the activity of the inhibitors may be associated with the dislodging activity. Hence, one can reasonably speculate that an assay for drug-induced translocation of nuclear KDM1A could be developed to screen for KDM1A inhibitors without the need for measurement of the enzyme activity.

A second question is whether these enzyme inhibitors dislodge only KDM1A from the chromatin. We investigated another lysine-specific demethylase, KDM5A, which plays a cooperative role in H3K4me3 in conjunction with KDM1A [284]. We confirmed that KDM5A localized to the nucleus. Neither GGA nor TCP induced translocation of the nuclear KDM5A to the cytoplasm under the same conditions as those under which these inhibitors dislodged nuclear KDM1A. This indicates that the inhibitors' effect on subcellular localization is specific for KDM1A. However, it currently remains unclear whether other components, such as HDAC1/2, may be released from the CoREST complex by GGA or TCP treatment.

Recruitment of KDM1A to chromatin has been extensively and thoroughly explored [285–289], but little research has been conducted on the unloading of KDM1A from chromatin. Particularly relevant among the previous studies on the subcellular distribution of KDM1A is a report by Nair et al, which describes cell cycle-dependent association and dissociation of KDM1A with chromatin [280]. Specifically,

KDM1A is recruited to the chromatin of cells in the G1/S/G2 phases and is displaced from the chromatin of M-phase cells. We confirmed that in M-phase cells stained with pHH3 antibody, KDM1A protein was distributed throughout the cell, whereas in the other non-M-phase cells KDM1A protein remained in the nucleus. However, in cells treated with GGA or TCP, KDM1A was distributed throughout the whole cell interior as in control M-phase cells, regardless of cell cycle stage. We can therefore conclude that GGA and TCP did not increase the number of cells in M-phase, and did act on cells in the G1/S/G2 phases to induce translocation of nuclear KDM1A to the cytoplasm. Taking these findings together with the fact that anti-pHH3 antibody recognizes phosphorylated Ser-10 on histone H3 and that introduction of a negatively charged phosphate group on Ser 10 completely abolishes KDM1A activity [290], one can reasonably speculate that a KDM1A inhibitor may unload the enzyme from chromatin.

Finally, we should discuss how GGA and TCP specifically dislodged KDM1A from the nucleus. We speculated that direct binding of GGA or TCP to nuclear KDM1A might cause release of the enzyme from the chromatin. By analyzing the nuclear fraction containing KDM1A, we demonstrated that GGA- and TCP-mediated release of KDM1A from the nuclear fraction to the supernatant was dose-dependent. Both GGA [20] and TCP [281] directly inhibit recombinant KDM1A enzyme activity and are thought to bind to the substrate-binding site of the enzyme. The structures of free and CoREST-bound KDM1A are virtually identical, with only a small difference in the orientations of two α -helices of the tower domain relative to the amine oxidase domain of KDM1A [291]. In this context, it is difficult to speculate as to whether direct binding of GGA or TCP to the substrate-binding site in the amine oxidase domain of KDM1A would affect

interaction between the enzyme and the CoREST protein. Other inhibitor-induced conformational changes of KDM1A may be involved in its unloading from the nuclear fraction in the cell-free experiment. We should also consider the metabolic fate of the KDM1A exported in response to treatment with its inhibitor. Fig.IV-5B clearly shows that GGA-induced downregulation of the cellular KDM1A level was time-dependent. This may potentially be explained by polyubiquitination and efficient degradation by the proteasome system of cytoplasmic KDM1A [292].

In conclusion, the present study clearly demonstrates that the KDM1A inhibitors GGA and TCP induce cytoplasmic translocation of nuclear KDM1A. This biological process has potential to be useful for screening promising cancer-preventive epigenetic therapeutic agents targeting KDM1A, and further work to this end is warranted.

Chapter V

General Discussion

Suemi Yabuta

*Molecular and Cellular Biology, Graduate School of Human Health Science,
University of Nagasaki, Nagasaki, Japan*

A previous study reported that daily intake (600 mg/day) of 4,5-didehydroGGA for 1 year significantly increased a 5-year survival rate after a radical therapy of primary hepatoma in post-operative hepatoma patients [39]. Recent larger-size and longer-period (2 years) clinical trial conducted according to a single protocol but at more than one site and, therefore, carried out by more than one investigator further confirmed the previous findings of the preventive effects on second primary hepatoma [208]. These results of the clinical trials strongly suggest that daily intake of 4, 5-didehydroGGA for 1 - 2 years might extinguish premalignant cells from the post-operative patients to prevent recurrence of hepatoma for at least 5 years.

V-1. How does GGA induce cell death in HuH-7 cells?

V-1-1. Previous studies on GGA-induced cell death in HuH-7 cells.

GGA has been repeatedly reported to induce cell death in HuH-7 cells [30,37]. Historically, Nakamura et al first described in 1995 that 4,5-didehydroGGA induced apoptotic cell death in human hepatoma cells by showing nucleosomal fragmentation of genomic DNA and chromatin condensation [30]. Thereafter, our laboratory had tried to find other evidence for apoptosis such as a formation of apoptosome and activation of caspase cascade (caspase-9/3), but they failed to show any further evidence for apoptosis. But, they have reported various cell-death related effects of GGA at micro-molar concentrations in HuH-7 cells, including 1) dissipation of mitochondrial membrane potential, 2) hyperproduction of superoxide in mitochondria, 3) incomplete autophagic response with massive accumulation of autophagosomes and 4) immediate

induction of UPR [47,77]. Although most of them are thought to be linked to cell death in the literature, none of them is a direct mechanism of cell death. In this thesis, however, we could show for the first time GGA-induced cell death was associated with inflammation and we propose that the inflammatory cell death is a direct mechanism of GGA-induced cell death. Here, we address a basic and final question why inflammatory cell death can contribute to hepatoma prevention in this chapter.

V-1-2. Anti-tumorigenic effects of GGA other than inflammatory cell death.

In Chapter 0, we investigated GGA clearly showed a time-dependent downregulation of the cellular *TERRA* level. In addition to this finding, in Chapter IV, we reported that GGA induced cytoplasmic translocation of nuclear KDM1A, an epigenetic enzyme of which interacts with *TERRA*. As described in Chapter 0, Porro et al. showed that *TERRA* upregulation correlates with telomeric recruitment of the KDM1A [21]. Elevated *TERRA* levels in TRF2-depleted cells promote nucleolytic processing of uncapped telomeres by favoring the recruitment of a KDM1A-MRE11 complex at telomeres [21]. We showed cytoplasmic localization of KDM1A or downregulation of *TERRA* at 3 or 8 h after addition of GGA in HuH-7 cells. Thus, these results strongly suggested that GGA-induced export of KDM1A from nuclear space might affect the *TERRA*-mediated maintenance of telomeric integrity. Besides the telomere maintenance, KDM1A is known to play roles in epigenetic transcriptional regulation such as activation of oncogenes and suppression of anti-oncogenes, and therefore excess KDM1A works oncogenic. Taking account that GGA directly inhibits KDM1A [20], it is reasonable to consider that GGA may be

anti-carcinogenic in tri-modal way through KDM1A as follows; 1) down-regulation of *TERRA* level, 2) export of nuclear KDM1A and 3) inhibition of KDM1A activity.

V-2. Inflammation

Prior to intensive discussion on GGA-induced inflammatory cell death, we have to describe a biological significance of inflammation itself in a cancer science field. In general, chronic inflammation is known to contribute to carcinogenesis. Indeed, most studies have so far reported the effectiveness of some anti-inflammatory drugs to prevent against clinical cancers [293–295]. Originally, inflammation is part of the complex biological response of body tissues to harmful stimuli, such as pathogens [296], entry of foreign matter into a body (for example, asbestos and silica) [297,298], exposition of heavy metal [299], and radiation of UV or radial rays [300,301]. Recently, however, some studies reported that inflammation was induced by abnormal accumulation of metabolite (e.g., urate crystal and lipid peroxide) [302,303], hyperglycemia [304], obesity [305], nucleic acid from necrotic cells [306], or cytokine-like biologically active agents [307].

Inflammation is a generic response, and therefore it is considered as a mechanism of innate immunity, which is specific for profiles of each pathogen [308]. Too much inflammation could lead to progressive tissue destruction by the harmful stimulus and compromise the survival of the organism, but it is also useful to induce cell death in premalignant and malignant cells. In contrast, chronic inflammation may lead to a host of diseases, such as cancer (e. g., gallbladder carcinoma or hepatoma). Chronic inflammation may

supply continuous exposure of neighboring cells to ROS such as superoxide, which will lastly cause genomic instability to produce tumor cells. Therefore, inflammation is a double-edged sword against carcinogenesis.

V-2-1. GGA-induced inflammatory response with UPR and autophagy.

Now, we are ready to discuss about GGA-induced inflammatory cell death. Then, first of all, we would like to see what happens in GGA-induced inflammatory cell death in a timeline. UPR or ER stress response can be observed as the earliest cellular event after GGA treatment. Indeed, enhanced splicing of *XBPI* mRNA is detected within 5 min after GGA treatment [77]. The second cellular event is detected as upregulation of the intracellular Ca^{2+} concentration, a peak of which is recorded in 16 min after GGA treatment. The next major cellular event is an incomplete response of autophagy. In other words, the third cellular events are hyperproduction of mitochondrial superoxide, appearance of autophagosomal puncta and conversion of LC3-I to LC3-II, all of which are detectable in 30 min. After these events including UPR and autophagy, GGA induces several phenomena that appear as a sign of inflammation; nuclear translocation of the cytoplasmic NF- κ B, then priming and activation of NLRP3 inflammasome, the resultant activation of caspase-1, plasma membrane localization of GSDMD, the second upregulation of the intracellular Ca^{2+} concentration at 6 h and finally pyroptotic cell death. These inflammatory events could be achieved via intracellular signaling from TLR4 that is a cell-surface sensor in innate immune system. As mentioned above, inflammation is a generic response, which is one of protective, defense,

biological, and adaptive response to certain cytotoxicity, has the role of eliminating both cytotoxic factors and damaged tissues, and lastly repairs the wound tissues. Therefore, the inflammatory transcription factor of NF- κ B has multiple target genes of cell division such as cyclin D1 and *c-myc*, so that inflammation can also be regarded as a proliferative response. However, if cells have other concomitant events such UPR and an incomplete response of autophagy, the inflammatory response may become a destructive response to conduct the cell suicide of pyroptosis. It is exactly the case, when we treat human hepatoma-derived cell lines with GGA. In this case, GGA-induced inflammatory response acts destructively rather than proliferating on tumor cells.

V-2-2. GGA-induced pyroptosis occurred in hepatoma cells.

Here, we described GGA induced inflammation in human hepatoma cells. Does it mean GGA is a cytotoxic compound? But, of note, GGA does not show any effect on survival of primary hepatocytes, because mouse primary cultured hepatocytes were resistant to GGA treatment and kept the mitochondrial membrane potential intact and did not produce any excessive ROS [37]. We have demonstrated that TLR4-mediated pyroptosis plays an important role in GGA-induced cell death. Considering that cell death by GGA is performed through TLR4 signaling, GGA should not be able to induce cell death for cells that express TLR4 only slightly. TLR4 is expressed at a lower level in primary hepatocytes than hepatoma cells [309].

We will discuss about TLR4 highly expressing cells in detail later.

V-2-3. GGA in comparison with LPS, in terms of TLR4 signaling

Then, why do hepatoma cells become highly expressing the *TLR4* gene? TLR4 is generally recognized as a receptor protein for foreign materials such as LPS of gram-negative bacteria to transduce inflammation signals in host cells. The most prominent task of LPS-binding protein (LBP) is its role as part of the sensing apparatus for LPS [310]. Upon binding to LBP in serum delivered from hepatocytes, LPS is transported via soluble and membrane-anchored cluster of differentiation 14 (CD14) to the TLR4/MD2 signaling complex [311–314]. In general, however, TLR4 signaling via LPS alone cannot induce pyroptosis. What does TLR4 signaling make in TLR4-expressing hepatoma cells?

In normal hepatic tissues, Kupffer cells express TLR4 and low levels of CD14, and are responsive to LPS. Hepatocytes, most likely in concert with Kupffer cells, serve to remove LPS from systemic circulation and, for this reason, express low levels of TLR4 and only weakly respond to LPS. Activated human hepatic stellate cells (HSCs) express both TLR4 and CD14 and respond to LPS with the activation of NF- κ B as well as the secretion of proinflammatory cytokines. Seki et al confirmed that LPS/TLR4 signaling promoted liver fibrosis through two independent mechanisms. LPS/TLR4 induced HSCs to secrete chemokines that promote the chemotaxis of Kupffer cells, while TLR4-dependent signaling enhanced TGF- β signaling [315], suggesting that LPS/TLR4 signaling may provide the basis for hepatocarcinogenesis.

A recent systematic review has concluded that TLR4 is an innate immunity receptor which plays a pathogenic role during chronic inflammation and can induce hepatoma in humans [207]. During

hepatocarcinogenesis, it was reported that the expression of the *TLR4* gene in hepatocytes gradually increased. TLR4 and LPS were required not for hepatoma initiation but for hepatoma promotion, mediating increased proliferation, expression of the hepatomitogen epiregulin, and prevention of apoptosis [316].

A study reported no PI uptake in response to LPS alone but demonstrated similar kinetics in pyroptotic pore formation as measured by PI uptake when LPS-primed and then stimulated with nigericin or ATP [317]. Thus, LPS promotes tumor growth by activation of NF- κ B signaling, which induces transcriptional activation of the cyclin D1 and *c-myc* genes, unless second signals, for example, activation of P2X7 receptor or efflux of K⁺ occur.

On the other hand, we have demonstrated GGA-induced TLR4 signaling is responsible for GGA-induced cell death, but does not cause inflammation-mediated proliferation. Indeed, GGA via TLR4 signaling not only induced pyroptotic cell death in hepatoma cells, but also produced ROS in mitochondria and induced UPR and an incomplete autophagic response. These are essential intracellular processes important for cells to conduct pyroptosis. As far as scrutinized in the literature, we cannot confirm the occurrence of UPR and induction of mitochondrial ROS production induced by treatment with LPS alone.

V-3. How does GGA work in highly TLR4-expressing cells such as macrophage?

So, what about other normal cells with high *TLR4* gene expression? It is well known that macrophage and dendritic cells, major players of innate immune system, have high expression level of TLR4. Then,

does GGA induce inflammatory response in macrophage and dendritic cells? If GGA shows the same effect via TLR4 signaling in macrophages as in hepatoma cells, GGA might be able to induce immunological defects of patients in the clinical trial with the polyphenoic acid [23], but it did not occur. So, we would suppose that GGA might induce inflammatory cell death only in cells expressing *TLR4* gene in pathologically high levels such as hepatoma cells. And, in TLR4-expressed cells in physiologically high, GGA may not stimulate TLR4 signaling or even stimulate proliferative TLR4 signaling.

V-4. To be, or not to be in inflammation

We have to return to the first question, is inflammation our friend or foe during carcinogenesis?

Perhaps it is non-canonical inflammasome activation to decide it.

During GGA-induced canonical inflammasome activation, as described in Chapter III, non-canonical inflammasome activation occurs to activate caspase-4 to release GSDMDN, which might make a fate of cell to die. Early studies linking IL-1 β responses to addition of exogenous ATP or the *Streptomyces hygroscopicus*-derived potassium ion-pore forming nigericin [318], non-canonical inflammasome activation occurred before inflammasome components were identified and the term of ‘non-canonical’ was introduced. Although LPS itself can cleavage caspase-4, 5, once it is internalized, which we wrote in chapter III, plasma membrane pore-formation through this non-canonical inflammasome activation does not arise in response to LPS alone [317]. It suggests one possibility that pyroptotic cell death cannot occur only due to cleavage of caspase-4 or -5. Indeed, active caspase-4 and -5 can cleavage GSDMD to produce

GSDMDN, which is a pore-forming fragment of GSDMD. Then, where is a point of no-return in pyroptosis, canonical or non-canonical inflammasome pathway in each? Pyroptosis is a form of programmed lytic cell death associated with innate immunity during inflammation. Inflammation is a complex and fine-tuned mechanism. Insufficient response may cause immunodeficiency resulting in infection and cancer, while overactive response may result in diseases like inflammatory bowel disease but may also result in cell death or pyroptosis in malignant cells. Anyhow, we would like to highlight a preventive role of GGA in carcinogenesis through induction of pyroptosis specifically in malignant hepatocytes and not in differentiated hepatocytes, by inducing both canonical and non-canonical inflammasome activation.

V-5. Cancer prevention with GGA

V-5-1. Between secondary and tertiary prevention by using GGA

Finally, we think about cancer prevention with GGA. Shidoji and Ogawa found natural GGA in medicinal herbs [31]. For example, turmeric contains 2.9 $\mu\text{g/g}$ GGA. Twenty years ago, GGA-analogous compound synthetic polyprenoic acid or peretinoin was shown to prevent second primary hepatoma in a double-blinded and randomized phase II clinical trial with post-operative hepatoma patients [24]. In this study 600 mg/day of peretinoin were orally ingested by post-operative hepatoma-free patients. If they try to intake the same amount of GGA only from dietary origins, they might be required to ingest several hundred kg of ordinary foods, which sounds unrealistic.

On the other hand, there is a way to increase endogenous GGA without using exogenous one. For example, one can reasonably speculate that mammalian cells may be able to produce GGA from endogenous or even exogenous GGPP [33]. Therefore, Mitake and Shidoji examined 1) bioavailability of plant GGPP in humans [34], 2) possible conversion of ingested GGPP to GGOH in mammalian cells [35], and 3) possibility of synthesis of GGA from GGOH in mammalian cells [35]. Thus, in vitro administration of squalene synthesis inhibitors of squalenstatin increased the cellular levels of FPP, GGPP, and GGA in human hepatoma-derived cell lines (unpublished results). Indeed, it will be also evident to induce cell death in the hepatoma cells by squalenstatin treatment in vitro. Furthermore, GGA is further metabolized and converted to 2, 3-dihydroGGA. In this regard, it is possible to increase intracellular GGA concentration by treatment with CYP26A1 inhibitor of liarozole. Therefore, in the future, not only direct administration of GGA but it also can be expected to use medicine to perturb GGA metabolism in high-risk group of liver cancer such as patients after surgical removal of primary hepatoma.

V-5-2. Primary prevention with GGA

The amount of 600 mg/day GGA is certainly required for prevention of hepatoma recurrence for hepatoma-high risk group. In the general population (here show as healthy subjects), however, it is considered that hepatoma prevention may be possible with the dietary GGA. We now know a few foods containing GGA, but the amount is very small. However, as mentioned earlier, GGA can be produced from precursor GGPP or GGOH, in vivo. For example, rice, which is a Japanese staple food, does not contain

detectable amount of GGA, but a significant amount of GGPP is present in polished rice [34]. It is expected that the ingested GGPP may be converted to GGA in our body, which should efficiently work to prevent spontaneous hepatocarcinogenesis. Furthermore, there is another possibility that ingested or in vivo produced GGA can be stored as ester forms in our cells, and it can be supplied as need from the storage site. The prevention of liver cancer by GGA or induction of TLR4-mediated cell death in hepatoma cells is thought to be a promising mechanism that can remove premalignant hepatocytes before the conversion to cancer cells. Due to the presence of endogenous GGA in normal hepatocytes, we speculate that at some stage of developing liver cancer, some hepatocytes must reduce GGA biosynthetic capacity.

In conclusion, currently there are no available foods that can compensate for the amount necessary to prevent hepatoma recurrence, so we cannot help relying on drug treatment for high-risk group patients. However, a possible primary prevention, an idea with combination of various foods containing GGA and its precursors, can be applicable for a general population.

At the end of my thesis:

While I had been researching about GGA and cancer, I thought like this. Research on cancer prevention is difficult. Metabolic studies of GGA are boring. So, it seems impossible to combine both. Anyway, basic research is tough to pursue. When it gets hard to do, it makes me desire to do what is fashionable. When I have performed what is fashionable and it leads to what I wanted to know, new ideas are born and some articles are written.

Until I started this research, I had no idea about the word "pyroptosis". Now, I know pyroptosis is inflammatory cell death and during pyroptosis caspase-1 is activated via inflammasome. Activated caspase-1 can convert interleukin-1, an inflammatory cytokine, into its mature form. In this way, the inflammatory response diffuses throughout the surrounding cells. As a result, inflammation spreads to the surroundings.

Caspase-1 is a proteolytic enzyme, which cleaves not only cytokines but also gasdermin D. N-terminal fragment of the cleaved gasdermin D pierces the plasma membrane of the cancer cell and opens holes on the membrane. Naturally, cancer cells that have been punctured by gasdermin D will die. It is a way of dying called pyroptosis. In this context, inflammation is on my side.

Prior to starting my doctoral thesis study, it was unlikely to predict that GGA, which has been thought to have cancer prevention effect, causes inflammation in advance. There is a traditional theory that cancer occurs as a result of chronic inflammation. Inflammatory response is a proliferative response. In this case, chronic inflammation becomes enemy during carcinogenesis. At last, however, I have sincerely realized that successful use and control of inflammation is fatally important for cancer prevention.

Chapter VI

Materials and methods

SuemiYabuta

Molecular and Cellular Biology, Graduate School of Human Health Science,

University of Nagasaki, Nagasaki, Japan

VI. Materials and methods

VI-1. Materials

VI-1-1. Instruments

24-well plate (ThermoFisher Science, Nunc, Tokyo, Japan)

3-cm culture dish (Nunc)

6-well plate (Nunc)

96-well plate (Nunc)

ABI PRISM 7300 Sequence Detection System (Applied Biosystems, Life Technology Japan, Tokyo, Japan)

Carousel centrifuge (Roche, Diagnostics GmbH, Mannheim, Germany)

Centrifuge (GILSON, M & S Instruments Inc., Osaka, Japan)

Centro XS3 LB960 (Berthold Technologies, Berthold Japan K.K., Tokyo, Japan)

Clean Bench (ASTECC, Fukuoka, Japan)

CO₂ incubator (ASTECC)

Confocal LSM700 (Carl Zeiss, Tokyo, Japan)

*Eiyokun*FFQ (KENPAKUSHA, Tokyo, Japan)

Falcon™ single polyester fiber-tipped applicator swab (Becton Dickinson, East Rutherford, NJ)

glass-bottomed dish (Matsunami, Osaka, Japan)

high-performance liquid chromatography (HPLC) column (Kanto Kagaku, Tokyo, Japan)

Image J software (National Institutes of Health, Bethesda, MD, USA)

Imaris x64 version 7.1.0 (Bitplane Scientific Software, Zurich, Switzerland)

LAS4000 (GE Healthcare Japan, Tokyo, Japan)

NanoDrop spectrophotometer (Thermo Fisher Scientific Inc., Waltham, MA, USA)

QIAamp spin column in a 2-mL collection tube (QIAGEN K.K., Tokyo, Japan)

pH meter (Fisher Scientific, Thermo Fisher Scientific, Tokyo, Japan)

Polyester Fiber-Tipped Applicator Swab (Becton Dickinson, NJ, USA)

Prominence HPLC apparatus (Shimadzu, Kyoto, Japan)

PVDF (Bio-Rad, Tokyo, Japan)

Real-Time PCR System (Roche Diagnostics GmbH)

SPD-20A (Shimadzu)

SPSS/PC statistical software package (IBM, Tokyo, Japan)

Thermal cycle (ASTEC)

Vortex (Mylab)

Water Bath (SANSYO, Tokyo, Japan)

Zen 2010B SP1 software (LSM700 version 6.0, Carl Zeiss)

VI-1-2. Chemical reagents

Acetic acid (Wako Pure Chemical Industries, Osaka, Japan)

Acrylamide / Bis (Bio-Rad)

All-*trans* retinoic acid (ATRA) (Wako Pure Chemical)

Ammonium persulfate (APS) (Bio-Rad)

Arachidonic acid (AA) (Sigma Aldrich)

α -tocopherol (Sigma Aldrich)

Bromophenolblue (Sigma Aldrich)

C34 (TLR4 inhibitor) (Sigma Aldrich)

Calpain inhibitor I and II (Nacalai tesque, Kyoto, Japan)

Dimethylsulfoxide (DMSO) (Wako Pure Chemical)

Ethanol (Wako Pure Chemical)

Farnesoic acid (FA) (Kuraray, Okayama, Japan)

Fast SYBR Master Mix (Roche Diagnostics GmbH)

Formaldehyde (KANTO CHEMICAL, Tokyo, Japan)

10% Formalin neutral buffer solution (Wako Pure Chemicals)

Geranylgeranoic acid (GGA) (Kuraray)

Geranylgeraniol (GGOH) (Sigma Aldrich)

Glycerol (Sigma Aldrich)

Glycine (Sigma Aldrich)

Hoechst 33258 (Sigma Aldrich)

HEPES (Nacalai tesque)

Hydrochloric acid (HCl) (Wako Pure Chemical)

Lipoteicoic acid (LTA; TLR2 ligand) from *Bacillus subtilis* (InvivoGen, Nacalai tesque)

Methanol (Wako Pure Chemical)

Nonidet P-40 substitute (Sigma Aldrich)

Oleic acid (OA) (Sigma Aldrich)

Quick-CBB PLUS (Wako Pure Chemical)

Paraformaldehyde (PFA) (Wako Pure Chemicals)

PermaFluor (Beckman Coulter Japan, Tokyo, Japan)

Phosphate-buffered saline (PBS) (Sigma Aldrich)

Prestained XL-ladder (APRO life Science Institute, Inc., Tokushima, Japan)

Protein assay reagent (Bio-Rad)

Skim milk powder (Megmilk snow brand, Hokkaido, Japan)

Sodium chloride (Wako Pure Chemical)

Sodium deoxycholate (Sigma Aldrich)

Sodium dodecyl sulfate (SDS) (Wako Pure Chemical)

Sodium hydroxide (NaOH) (Wako Pure Chemical)

Sucrose (Nacalai tesque)

TAK242 (TLR4 inhibitor) (Chemscene, Funakoshi, Tokyo, Japan)

TCP hydrochloride (Sigma Aldrich)

Thapsigargin (Sigma Aldrich)

Tris-(hydroxymethyl)-aminomethane (Tris) (Nacalai tesque)

Triton-X100 (Sigma Aldrich)

Trypan blue (0.4%) (Sigma Aldrich)

Tunicamycin (Sigma Aldrich)

Tween20 (Sigma Aldrich)

o-vanillin (TLR2 inhibitor) (Tokyo Chemical Industry; TCI, Tokyo, Japan)

VIPER (TLR4 inhibitor) (NOVUS, Funakoshi)

VI-1-3. Cell culture compounds

Dulbecco's modified eagle's medium (DMEM) (Wako Pure Chemical)

Fetal bovine serum (FBS) (biowest, Funakoshi)

Trypsin-EDTA (Sigma Aldrich)

VI-1-4. Kits

Caspase-Glo1 assay (Promega, Madison, WI, USA)

CellLytic nuclear kit (Sigma Aldrich)

CellTiter-Glo (Promega)

Fluo 4-AM (DOJINDO, Kumamoto, Japan)

High Pure RNA Isolation Kit (Roche Diagnostics GmbH)

Cytotoxicity detection kit (Roche Diagnostics GmbH)

MitoSOX (Invitrogen, Thermo Fisher Scientific)

Qiagen Blood DNA Mini kit (QIAGEN)

Transcriptor[®] first strand cDNA synthesis kit (Roche Diagnostics GmbH)

VI-1-5. Antibodies

ASC	Medical and Biological Laboratories
Caspase-1	Cell Signaling Technology
Caspase-4	Cell Signaling Technology
GSDMD	abcam / GeneTex, Funakoshi
Hoechst33258	Invitrogen, Thermo Fisher Scientific
JARID1A	Cell Signaling Technology
LSD1	Cell Signaling Technology

LC3	Medical and Biological Laboratories
NF- κ B	Cell Signaling Technology
NLRP3	Cell Signaling Technology
pHH3-Alexa Fluor® 647	Cell Signaling Technology
Anti-goat IgG HRP-linked antibody	GE Healthcare
Alexa-488-labeled goat anti-rabbit IgG antibody	Invitrogen, Molecular Probes
*Cell Signaling Technology; Danvers, MA, USA Abcam; Tokyo, Japan	

VI-1-6. Cell line

HuH-7	RIKEN BioResource Center
HepG2	RIKEN BioResource Center
PLC/PRF/5	RIKEN BioResource Center
Hep3B	DS Pharma Biomedical

*RIKEN BioResource Center; Tsukuba, Japan
DS Pharma Biomedical; Osaka, Japan

VI-1-7. Solutions and Buffers

4% PFA:

4% PFA

1 × PBS

5N NaOH

13.7% HEPES

2% Sucrose

Fixing solution:

40% Methanol

10% Acetic acid

RIPA buffer:

50 mM Tris-HCl, pH 8.5

150 mM NaCl

0.5% Sodium deoxycholate

0.1% Sodium dodecyl sulfate

1.0% Nonidet P-40 substitute

1× Transfer buffer:

25 mM Tris

192 mM Glycine

10-20% Methanol

SDS-PAGE stacking-gel buffer:

500 mM Tris

0.1% Sodium dodecyl sulfate

Adjust pH to 6.8 with HCl

SDS-PAGE resolving buffer:

1.5 M Tris

0.1% Sodium dodecyl sulfate

Adjust pH 8.8 with HCl

10×SDS-PAGE running buffer:

25 mM Tris

192 mM Glycine

1% SDS

Permeabilization solution:

PBS

0.3% Triton X-100

6× SDS / Sample buffer:

31 mM Tris-HCl (pH 7.4)

1% Sodium dodecyl sulfate

5% Glycerol

0.05% Bromophenol blue

0.5% Triton X-100:

H₂O

0.5% Triton X-100

0.1% PBS-T:

PBS

0.1% Tween 20

VI-2. Methods

VI-2-1. Study population

Seventy or ninety-two subjects, who were working in a city office, enrolled in a previous study carried out in Japan (*Masaki et al, manuscript in preparation*), have been involved in the current study. Detailed information about diet and lifestyle habits and DNA sample in buccal cells were collected from each participant, after they had signed an informed consent form. The analyses were carried out on anonymously coded samples. The study-design was approved by our university ethics committee for genome research.

VI-2-2. Food frequency questionnaire (FFQ)

The data of habitual food intakes were collected and processed by using Excel *Eiyokun*FFQ that gave information about demographics, lifestyle and dietary intake. FFQ was comprised of 91 food items which were divided into nine food groups of the same nutrient profiles (cereals and cereal products; meat and meat products; fish and seafood; eggs, legumes and legume products; milk and milk products; vegetables and fruits; beverages; alcoholic beverages; and confectionaries, spreads and spices/miscellaneous items) with five categories of consumption frequency over 1 year.

VI-2-3. DNA-preparation

To collect a buccal cell sample, the inside of both cheeks was firmly scraped three times with a Falcon™ single polyester fiber-tipped applicator swab. The swab was air-dried for at least 1 h after collection. DNA was extracted using Qiagen Blood DNA Mini kit according to the manufacturer's instructions. Preparation of DNA was conducted according to a manual provided by the manufacture as shown in detail below.

After being separated from the stick by hand, buccal swab was placed in a 1.5-mL microcentrifuge tube containing 400 µL phosphate-buffered saline (PBS). The sample was added 20 µL QIAGEN Protease stock solution and 400 µL Buffer AL and mixed immediately by vortexing for 15 s. The sample was incubated at 56°C for 10 min and briefly centrifuged to remove drops from inside of the lid. The sample was added 400 µL ethanol and mixed again by vortexing and briefly centrifuged to remove drops from inside of the lid. Seven hundreds µL of the resultant mixture were carefully applied to the QIAamp spin column in a 2-mL collection tube and were centrifuged at 6,000 x g for 2min. The column was placed in a clean 2-mL collection tube. This was repeated by applying up to 700 µL of the remaining mixture to the spin column. The column was added 500 µL Buffer AW1 without wetting the rim, and centrifuged at 6,000 x g for 2 min. The column was placed in a clean 2-mL collection tube, was added 500 µL Buffer AW2, and was centrifuged at 6,000 x g for 3 min. The column was placed in a clean 1.5-mL microcentrifuge tube, added 200 µL Buffer AE, incubated at room temperature for 1min, and then centrifuged at 6,000 x g for 1 min to collect the DNA solution. The DNA preparations were frozen at -20 °C until use.

VI-2-4. RTLs determination

RTLs determination was performed essentially by Cawthon's method [4]. In details, PCR reactions were set up by aliquoting 5 µL of 1x Fast SYBR Master Mix into each reaction capillary equipped in a carousel with capacity for 32 samples with the LightCycler 1.5 instrument, followed by adding 1.2 µL of each experimental DNA sample, for a final volume of 11 µL per reaction. Telomere primer sequences were

telg (ACACTAAGGTTTGGGTTTGGGTTTGGGTTTGGGTTAGTGT),

telc (TGTTAGGTATCCCTATCCCTATCCCTATCCCTAACA), and *ALB* was used as the *scg* reference using primers modified with the addition of a 5'-GC clamp to shift melting temperature:

albu (CGGCGGCGGCGGCGGCGGGCTGGGCGGaaatgctgcacagaatccttg) and

albd (GCCCCGCCCCGCGCGCCCGTCCCGCCGaaagcatggtgcctgtt). The reagent components and

final concentrations were 900 nM each primer, 1 M betaine, 1x Fast SYBR Master Mix in 11 µL. The

thermal cycling profile was Stage 1: 15 min at 95°C; Stage 2: 2 cycles of 15 s at 94 °C, 15 s at 49°C; and

Stage 3: 32 cycles of 15 s at 94 °C, 10 s at 62°C, 15 s at 74 °C with signal acquisition, 10 s at 84 °C, 15 s at

88 °C with signal acquisition. The 74 °C reads provided the Ct values for the amplification of the telomere

template (in early cycles when the *scg* signal is still at baseline); the 88 °C reads provided the Ct values for

the amplification of the *scg* template (at this temperature there is no signal from the telomere PCR product,

because it is fully melted).

After thermal cycling and raw data collection were completed, the LightCycler software 3.5.3 was used

to generate two standard curves for each signal, one for the telomere signal and one for the *scg* (*ALB*)

signal. As each experimental sample was assayed in duplicate, two T/A results were obtained for each sample; the final reported result for a sample in a given run is the average of the two T/A values. Average T/A is expected to be proportional to the average telomere length per cell.

VI-2-5. Genotyping

Two common SNPs of rs6564851 and rs362090 were genotyped. The corresponding probes were obtained from Applied Biosystems (Foster City, CA, USA). Allelic discrimination (AD) using Taqman[®] probes was chosen for genotyping on the ABI PRISM 7300 Sequence Detection System and we performed the allelic discrimination assay. The primer and probe sequences were designed and provided by Applied Biosystems. Assuming that allele 1 (G in rs6564851 near the *BCO1* gene or A in rs362090 of the *ISX* gene) and allele 2 (T or G, respectively), the TaqMan probes specific for allele 1 were labeled with FAM[™] and those of allele 2 were with VIC[™]. The probes for alleles 1 and 2 were mixed with the PCR reagents and PCR reaction was conducted. MMqPCR was conducted with Applied Biosystems 7300 Real-Time PCR System. Automatic allele calling was selected to determine each genotype for AD post-read run according to AD guide from Applied Biosystems.

VI-2-6. Measurement of serum β -carotene

Tubes containing frozen serum were thawed and extracted within 30 min. A mixture of serum (100 μ L) and ethanol (500 μ L) was vortexed for 30 s, and then water (2 mL) and butylated hydroxytoluene with

hexane (5 mL) were successively pipetted into 10-mL Pyrex tubes. After centrifugation at 150 x g for 10 min, the upper hexane phase (4 mL) was transferred into brown glass vials and dried under a nitrogen stream. The residue was dissolved in 100 μ L of acetonitrile-dichloromethane-methanol (7:2:1 v/v/v), and 20 μ L of the resultant solution were injected into a high-performance liquid chromatography (HPLC) column (5 μ m, 250 x 4.6 mm, Mightysil PR-18; Kanto Kagaku, Tokyo, Japan). The effluent was monitored for the detection of carotenoids using an ultraviolet-vis detector of SPD-20A equipped with Prominence HPLC apparatus at 450 nm.

VI-2-7. Cell culture

Human hepatoma-derived HuH-7, HepG2 and PLC/PRF/5 cells were cultured in high-glucose Dulbecco's modified Eagle's medium (D-MEM) supplemented with 5% fetal bovine serum (FBS). The Hep3B cells were obtained from DS Pharma Biomedical, Osaka, Japan, and maintained in D-MEM containing 10% FBS and MEM nonessential amino acid solution. Cells were cultured with DMEM containing 5% or 10% FBS for 2 days followed by replacement with FBS-free D-MEM for a further 2 days before drug treatment. GGA, other diterpenoids or other lipids (in ethanol) were dispersed in FBS-free medium.

VI.2-8. Sodium dodecyl sulfate polyacrylamide gel electrophoresis (SDS-PAGE) and immunoblotting

For SDS-PAGE and immunoblot analysis, cells were washed twice with PBS, and lysed with RIPA buffer. The cell lysates were collected in centrifuge tubes, sonicated, centrifuged at 15,000 x g for 20 min at 4°C,

and the supernatant was collected. Protein concentrations were determined using the Bradford method.

Proteins can be separated on the basis of their mass by electrophoresis in a polyacrylamide gel under denaturing conditions. Proteins (5 or 30 – 50 µg) from a lysate were denatured in SDS sample buffer by boiling for 5min. Polyacrylamide gels were prepared by pouring gel solutions between two glass plates and letting it polymerize. Gels were composed of two layers: a 10% resolving gel (pH 8.8), which separates proteins by their size, and a 4% stacking gel (pH 6.8) on top that ensures the simultaneous entry of proteins into the separating gel.

Resolving gel (10%)		Stacking gel (4%)	
H ₂ O	4.0mL	H ₂ O	3.05 mL
Acrylamide / Bis (30%)	3.4 mL	Acrylamide / Bis (30%)	0.65 mL
TEMED	5 µl	TEMED	5 µl
10% APS	50 µl	10% APS	25 µl

After the separation of the samples by SDS-PAGE, proteins were transferred by electroblotting to PVDF membranes for immunoblotting. The PVDF membrane was then blocked in 0.1% PBS-T containing 5% skim milk for 15 min at room temperature. The primary antibody solution was applied for an overnight incubation at 4°C to ensure the specific binding to the antigen on the PVDF membrane. Then, the membrane was rinsed three times for 5 min in 0.1% PBS-T and incubated for 45 min at room temperature with the respective peroxidase-coupled secondary antibody solution (1: 2,000 in PBS-T containing 1% skim milk). After three further rinsing steps the antibody-antigen complexes were detected with Immunoblot Chemiluminescent HRP substrate using an ImageQuant LAS4000.

VI-2-9. Cell-free analysis

Nuclear fraction of HuH-7 cells was prepared using a CellLytic nuclear kit. The nuclear pellets were gently suspended in PBS-T, then treatment to each nuclear suspension (60 µg protein/tube), and samples were gently vortexed and incubated overnight at 4°C. The supernatants were centrifuges at 1000 × g for 10 min, separated by SDS-PAGE.

VI-2-10. Isolation of total cellular RNA

Total RNA was isolated from cells by using High Pure RNA Isolation Kit. Cells in 3-cm dishes were washed with 1 mL of PBS (-), scraped off with lysis buffer of the kit, and transferred into each 1.5-mL tube.

Total RNA was quantified by absorbance at 260 nm with NanoDrop[®] spectrophotometer ND-1000, and 260:280 nm ratio was used as index of purity. After confirmation of the integrity, a preparation of total RNA was kept frozen at -20°C until use for reverse transcription polymerase chain reaction (RT-PCR).

VI-2-11. Reverse transcription for cDNA synthesis

The aliquot corresponding to 250 to 300 ng of total cellular RNA of each sample, water (PCR-grade) and random hexamer primer included in Transcriptor[®] first strand cDNA synthesis kit were incubated at 65°C for 10 min. To the mixture 5 × Transcriptor[®] RT reaction buffer, Protector[®] RNase inhibitor, deoxynucleotide mix and Transcriptor[®] reverse transcriptase were added and incubated at 25°C for 10 min, at 55 °C for 60 min, at 85 °C for 5min and at 4 °C for over 10min.

VI-2-12. Real-time PCR

Nucleotide sequences of the primers are listed in **Table VI-1**. Real-time PCR was performed in a LightCycler[®] platform 1.5 or 96 with 20 μ l glass capillaries or 96-well plate, respectively, using 4 μ L reaction mixture containing 0.5 μ L of primer solution (0.5 μ M, the stock solution was diluted by 1:10), 1 μ L of 5 \times Roche Faststart DNA Master SYBR Green I and 1 μ L of cDNA containing solution under condition described in Table VI-1.

Table VI-1. The nucleotide sequences of each primers used for real time RT-PCR.

Genes		Sequence (5'-3')	Temp. (°C)	Amplicon (bp)
<i>Caspase-1</i>	F	TGCCTGTTXXTGTGATGTGG	58	132
	R	TGTCCTGGGAAGAGGTAGAAACATC		
<i>Caspase-4</i>	F	TTGCTTTCTGCTCTTCAACG	62	72
	R	GTGTGATGAAGATAGAGCCCATT		
<i>Caspase-5</i>	F	GTCTAAAGGACAAACCCAAGG	57	109
	R	TGTGAAGAGATGAGTGCCAAG		
<i>NLRP3</i>	F	GTGTTTCGAATCCCCTGTG	60	143
	R	TCTGCTTCTCACGTA CTTTCTG		
<i>IL-1β</i>	F	CCACAGACCTTCCAGGAGAA	57	121
	R	GTGATCGTACAGGTGCATCG		
<i>GSDMD</i>	F	TGGGTCTTGCTGGACGAGTGT	62	98
	R	GCGTAGAGTGCACACATGCGG		
<i>TLR1</i>	F	CCTAGCAGTTATCACAAGCTCAA	57	70
	R	TCTTTTCCTTGGGCCATTC		
<i>TLR2</i>	F	CGTTCTCTCAGGTGACTGCTC	58	66
	R	TCTCCTTTGGATCCTGCTTG		
<i>TLR4</i>	F	CTGCCACATGTCAGGCCTTAT	59	138
	R	AATGCCACCTGGAAGACTCT		
<i>TLR6</i>	F	TGAAACAGTCTCTTTTGAGTAAATGC	59	72
	R	CAGAATCCATTTGGGAAAGC		
<i>TLR9</i>	F	CCAGACCCTCTGGAGAAGC	56	133
	R	GTAGGAAGGCAGGCAAGGT		

Table VI-1. continued,

Genes	Sequence (5'-3')		Temp. (°C)	Amplicon (bp)
<i>ASC</i>	F	CTGACGGATGAGCAGTACCA	57	108
	R	CAAGTCCTTGCAGGTCCAGT		
<i>IFNα</i>	F	TCGCCCTTTGCTTTACTGAT	60	82
	R	GGGTCTCAGGGAGATCACAG		
<i>IFNβ</i>	F	CTTTGCTATTTTCAGACAAGATTCA	56	69
	R	GCCAGGAGGTTCTCAACAAT		
<i>XBP1s</i>	F	TGCTGAGTCCGCAGCAGGTG	62	169
	R	GCTGGCAGGCTCTGGGGAAG		
<i>DDIT3</i>	F	ATGGCAGCTGAGTCATTGCCTTTC	54	177
	R	AGAAGCAGGGTCAAGAGTGGTGAA		
<i>KDM1A</i>	F	CCAGGTGCCCCACAGCCGAT	63	161
	R	GCCTGGCGAGGCAGCGTATA		
<i>28S rRNA</i>	F	TTAGTGACGCGCATGAATGG	55	67
	R	TGTGGTTTCGCTGGATAGTAGGT		

F: forward primer, R: reverse primer

VI-2-13. ROS detection

HuH-7 cells were seeded at a density of 1.0×10^4 cells per well into glass-bottomed dishes, and then incubated in a humidified atmosphere of 95% air and 5% CO₂ at 37°C. Cells were cultured with D-MEM containing 5% FBS for 2 days followed by replacement with FBS-free D-MEM for a further 2 days before drug treatment. The cell cultures were placed in a MitoSOX experiment was started. MitoSOX was added in culture media at 10 min before the compound treatment. Fluorescence was measured using a Carl Zeiss LSM700 inverted laser-scanning confocal, live-cell images were time course for treated.

VI-2-14. Ca²⁺ fluorescence imaging

HuH-7 cells were seeded at a density of 1.0×10^4 cells per well into glass-bottomed dishes, and then incubated in a humidified atmosphere of 95% air and 5% CO₂ at 37°C. Cells were cultured with D-MEM containing 5% FBS for 2 days followed by replacement with FBS-free D-MEM for a further 2 days before drug treatment. Fluo 4-AM was added in culture media at 1 h before the compound treatment. Fluorescence was measured using a Carl Zeiss LSM700 inverted laser-scanning confocal, live-cell images were time course for treated.

VI-2-15. Fluorescent immunostaining

HuH-7 cells grown on glass inserts in a 24-well plate were rinsed with PBS (-) and fixed for 40min with 4% paraformaldehyde containing 2% sucrose in PBS (-), and then rinsed with PBS (-). Cells were then

permeabilized with 0.5% triton X-100 and nonspecific binding blocked with 10% FBS. Next, cells were incubated at 4°C overnight with polyclonal antibody, following by 1 h incubation with Alexa-488-labeled goat anti-rabbit IgG antibody. After rinsing PBS (-), cells were mounted in PermaFluor, covered on a glass slide, and observed under a confocal laser scanning fluorescence microscope, LSM700 2Ch URGB equipped with Axio Observer Z1 Bio. Microscopic images were acquired and quantitatively analyzed using Zen 2010B SP1 software. A Z-stack procedure was employed, and the acquired images were processed with Zen 2010B SP1 and three-dimensional rendering was performed with Imaris x64 version 7.1.0.

VI-2-16. Caspase-Glo1 assay

Cells (100 cells/well) were seeded into a 96-well plate and cultured with D-MEM containing 5% FBS for 2 days before replacing the medium with FBS-free D-MEM for a further 2 days prior to treatments with GGA. The Caspase-Glo[®] 1 was then used to measure the activity of caspase-1. The luminescence was recorded by using Centro XS3 LB960.

VI-2-17. Cell viability assay

Cells (100 cells/well) were seeded into a 96-well plate and cultured with D-MEM containing 5% FBS for 2 days before replacing the medium with FBS-free D-MEM for a further 2 days prior to 24 h treatments with GGA or other compounds. The CellTiter-Glo was then used to measure cell viability by ATP levels as per

manufacturer's instructions. The luminescence was recorded by using Centro XS3 LB960.

VI-2-18. LDH assay

Cells (1000 cells/well) were seeded into a 96-well plate and cultured with D-MEM containing 5% FBS for 2 days before replacing the medium with FBS-free D-MEM for a further 2 days prior to 24 h treatments with GGA or other compounds. The cytotoxicity detection kit was then used to measure cell death by LDH levels. The luminescence was recorded by using Prestained XL-ladder.

VI-2-19. Statistical analysis

The analyses were based on data reported by the dietary questionnaire administered at the beginning of the study. The influence of each dietary factor on buccal RTL was estimated by logistic multivariate analysis adjusted for age, gender and energy intake. The correlation between the biomarkers investigated was evaluated by Pearson correlation analysis. The level of statistical significance was set at $p < 0.05$. The SPSS/PC statistical software package was used for the analyses.

Notes

I made this dissertation by referring to the following papers.

1) S. Yabuta, M. Masaki, and Y. Shidoji. Associations of buccal cell telomere length with daily intakes of β -carotene or α -tocopherol are dependent on carotenoid-metabolism related gene genotypes in healthy

Japanese adults. *The Journal of Nutrition, Health and Aging* (2015)

2) S. Yabuta, M. Urata, R. Y. Kun, M. Masaki, and Y. Shidoji. Common SNP rs6564851 in the *BCO1* gene affects the Circulating Levels of β -carotene and the daily intake of carotenoids in healthy Japanese women.

PLOS ONE (2016)

3) S. Yabuta and Y. Shidoji. TLR4-mediated pyroptosis in human hepatoma cells with a branched-chain

PUFA, geranylgeranoic acid. (submitted)

4) S. Yabuta and Y. Shidoji. Cytoplasmic translocation of nuclear lysine-specific demethylase-1

(LSD1/KDM1A) in human hepatoma cells is induced by its inhibitors. *bioRxiv*

(doi:<http://doi.org/10.1101/274050>)

Acknowledgments

A part of the study was supported by a Project Research Funds from the University of Nagasaki.

I am delighted to thank the following people, and describe their contributions to this study.

Professor Yoshihiro Shidoji, head of the Laboratory of Molecular and Cellular Biology. He has been laying foundation of cell biological studies for a molecular mechanism of chemopreventive geranylgeranoic acid, and providing spatiotemporal, physical and intellectual source to the study. I am extremely grateful for all that he has done for me as my supervisor, especially his philosophical guidance.

Dr. Chiharu Sakane and Dr. Chieko Iwao, former graduate students of the Shidoji research group, I thank for their support. Especially, Chiharu gave me a lot of fun during my graduate student life with each life supported.

Finally, I would like to thank all the present and former members of the Shidoji's party for all their help and kindness.

At the end, I owe my deepest gratitude to my parents, my sisters and my brothers for their understanding and generous support. I never ever thank you enough.

March 2018

Sincerely,

Suemi Yabuta

References

- [1] C. Fehrer, R. Voglauer, M. Wieser, G. Pfister, R. Brunauer, D. Cioca, B. Grubeck-Loebenstien, G. Lepperdinger, Techniques in gerontology: Cell lines as standards for telomere length and telomerase activity assessment, *Exp. Gerontol.* 41 (2006) 648–651. doi:10.1016/j.exger.2006.03.016.
- [2] A. Müezziner, A.K. Zaineddin, H. Brenner, A systematic review of leukocyte telomere length and age in adults, *Ageing Res. Rev.* 12 (2013) 509–519. doi:10.1016/j.arr.2013.01.003.
- [3] R.M. Cawthon, Telomere measurement by quantitative PCR, *Nucleic Acids Res.* 30 (2002) 47e–47. doi:10.1093/nar/30.10.e47.
- [4] R.M. Cawthon, Telomere length measurement by a novel monochrome multiplex quantitative PCR method, *Nucleic Acids Res.* 37 (2009) e21. doi:10.1093/nar/gkn1027.
- [5] M. Shen, R. Cawthon, N. Rothman, S.J. Weinstein, J. Virtamo, H.D. Hosgood, W. Hu, U. Lim, D. Albanes, Q. Lan, A prospective study of telomere length measured by monochrome multiplex quantitative PCR and risk of lung cancer, *Lung Cancer.* 73 (2011) 133–137. doi:10.1016/j.lungcan.2010.11.009.
- [6] J.M.J. Houben, H.J.J. Moonen, F.J. van Schooten, G.J. Hageman, Telomere length assessment: Biomarker of chronic oxidative stress?, *Free Radic. Biol. Med.* 44 (2008) 235–246. doi:10.1016/j.freeradbiomed.2007.10.001.
- [7] J.K. Kiecolt-Glaser, E.S. Epel, M.A. Belury, R. Andridge, J. Lin, R. Glaser, W.B. Malarkey, B.S. Hwang, E. Blackburn, Omega-3 fatty acids, oxidative stress, and leukocyte telomere length: A randomized controlled trial, *Brain. Behav. Immun.* 28 (2013) 16–24. doi:10.1016/j.bbi.2012.09.004.
- [8] D. Ornish, J. Lin, J. Daubenmier, G. Weidner, E. Epel, C. Kemp, M.J.M. Magbanua, R. Marlin, L. Yglecias, P.R. Carroll, E.H. Blackburn, Increased telomerase activity and comprehensive lifestyle changes: a pilot study, *Lancet Oncol.* 9 (2008) 1048–1057. doi:10.1016/S1470-2045(08)70234-1.
- [9] R. Farzaneh-Far, J. Lin, E.S. Epel, W.S. Harris, E.H. Blackburn, M. a Whooley, Association of

- marine omega-3 fatty acid levels with telomeric aging in patients with coronary heart disease., *JAMA*. 303 (2010) 250–257. doi:10.1001/jama.2009.2008.
- [10] N. O’Callaghan, N. Parletta, C.M. Milte, B. Benassi-Evans, M. Fenech, P.R.C. Howe, Telomere shortening in elderly individuals with mild cognitive impairment may be attenuated with omega-3 fatty acid supplementation: A randomized controlled pilot study, *Nutrition*. 30 (2014) 489–491. doi:10.1016/j.nut.2013.09.013.
- [11] L. Ferrucci, J.R.B. Perry, A. Matteini, M. Perola, T. Tanaka, K. Silander, N. Rice, D. Melzer, A. Murray, C. Cluett, L.P. Fried, D. Albanes, A.-M. Corsi, A. Cherubini, J. Guralnik, S. Bandinelli, A. Singleton, J. Virtamo, J. Walston, R.D. Semba, T.M. Frayling, Common variation in the beta-carotene 15,15'-monooxygenase 1 gene affects circulating levels of carotenoids: a genome-wide association study., *Am. J. Hum. Genet.* 84 (2009) 123–133. doi:10.1016/j.ajhg.2008.12.019.
- [12] W.C. Leung, S. Hessel, C. Méplan, J. Flint, V. Oberhauser, F. Tourniaire, J.E. Hesketh, J. von Lintig, G. Lietz, Two common single nucleotide polymorphisms in the gene encoding beta-carotene 15,15'-monooxygenase alter beta-carotene metabolism in female volunteers., *FASEB J.* 23 (2009) 1041–1053. doi:10.1096/fj.08-121962.
- [13] G.P. Lobo, J. Amengual, H.N.M. Li, M. Golczak, M.L. Bonet, K. Palczewski, J. Von Lintig, beta,beta-carotene decreases peroxisome proliferator receptor gamma activity and reduces lipid storage capacity of adipocytes in a beta,beta-carotene oxygenase 1-dependent manner, *J. Biol. Chem.* 285 (2010) 27891–27899. doi:10.1074/jbc.M110.132571.
- [14] G.P. Lobo, S. Hessel, A. Eichinger, N. Noy, A.R. Moise, A. Wyss, K. Palczewski, J. von Lintig, ISX is a retinoic acid-sensitive gatekeeper that controls intestinal beta,beta-carotene absorption and vitamin A production, *FASEB J.* 24 (2010) 1656–1666. doi:10.1096/fj.09-150995.
- [15] S. Yabuta, M. Masaki, Y. Shidoji, β -Carotene requirement for anti-aging depends on genetic background, *Atlas Sci.* (2016).
<https://atlasofscience.org/beta-carotene-requirement-for-anti-aging-depends-on-genetic-background/>.

- [16] L. Ferrucci, J.R.B. Perry, A. Matteini, M. Perola, T. Tanaka, K. Silander, N. Rice, D. Melzer, A. Murray, C. Cluett, L.P. Fried, D. Albanes, A.M. Corsi, A. Cherubini, J. Guralnik, S. Bandinelli, A. Singleton, J. Virtamo, J. Walston, R.D. Semba, T.M. Frayling, Common variation in the β -carotene 15,15'-monooxygenase 1 gene affects circulating levels of carotenoids: A genome-wide association study, *Am. J. Hum. Genet.* 84 (2008) 123–133. doi:10.1016/j.ajhg.2008.12.019.
- [17] S. Yabuta, M. Urata, R.Y.W. Kun, M. Masaki, Y. Shidoji, Common SNP rs6564851 in the BCO1 gene affects the circulating levels of beta-Carotene and the daily intake of carotenoids in healthy Japanese women, *PLoS One.* 11 (2016) e0168857. doi:10.1371/journal.pone.0168857.
- [18] I. Yasuda, Y. Shiratori, S. Adachi, A. Obora, M. Takemura, M. Okuno, Y. Shidoji, M. Seishima, Y. Muto, H. Moriwaki, Acyclic retinoid induces partial differentiation, down-regulates telomerase reverse transcriptase mRNA expression and telomerase activity, and induces apoptosis in human hepatoma-derived cell lines, *J. Hepatol.* 36 (2002) 660–671. doi:10.1016/S0168-8278(02)00044-2.
- [19] W.-J. Liu, Y.-W. Zhang, Z.-X. Zhang, J. Ding, Alternative splicing of human telomerase reverse transcriptase may not be involved in telomerase regulation during all-trans-retinoic acid-induced HL-60 cell differentiation., *J. Pharmacol. Sci.* 96 (2004) 106–114. doi:10.1254/jphs.FP0030600.
- [20] C. Sakane, T. Okitsu, A. Wada, H. Sagami, Y. Shidoji, Inhibition of lysine-specific demethylase 1 by the acyclic diterpenoid geranylgeranoic acid and its derivatives, *Biochem. Biophys. Res. Commun.* 444 (2014) 24–29. doi:10.1016/j.bbrc.2013.12.144.
- [21] A. Porro, S. Feuerhahn, J. Lingner, TERRA-Reinforced Association of LSD1 with MRE11 Promotes Processing of Uncapped Telomeres, *Cell Rep.* 6 (2014) 765–776. doi:10.1016/j.celrep.2014.01.022.
- [22] C.C. Coombs, M. Tavakkoli, M.S. Tallman, Acute promyelocytic leukemia: where did we start, where are we now, and the future, *Blood Cancer J.* 5 (2015) e304. doi:10.1038/bcj.2015.25.
- [23] Y. Muto, H. Moriwaki, M. Ninomiya, S. Adachi, A. Saito, K.T. Takasaki, T. Tanaka, K. Tsurumi, M. Okuno, E. Tomita, T. Nakamura, T. Kojima, Prevention of second primary tumors by an acyclic retinoid, polyprenoic acid, in patients with hepatocellular carcinoma. Hepatoma Prevention Study

- Group., *N. Engl. J. Med.* 334 (1996) 1561–1567. doi: 10.1056/NEJM199606133342402
- [24] Y. Muto, H. Moriwaki, A. Saito, Prevention of second primary tumors by an acyclic retinoid in patients with hepatocellular carcinoma., *N. Engl. J. Med.* 340 (1999) 1046–1047.
doi:10.1056/NEJM199904013401315.
- [25] Y. Muto, H. Moriwaki, M. Omori, In vitro binding affinity of novel synthetic polyprenoids (polyprenolic acids) to cellular retinoid-binding proteins., *Japanese J. Cancer Res.* 72 (1991) 974–977.
- [26] H. Araki, Y. Shidoji, Y. Yamada, H. Moriwaki, Y. Muto, Retinoid agonist activities of synthetic geranylgeranoic acid derivatives, *Biochem. Biophys. Res. Commun.* 209 (1995) 66–72.
doi:10.1006/bbrc.1995.1471.
- [27] Y. Yamada, Y. Shidoji, Y. Fukutomi, T. Ishikawa, T. Kaneko, H. Nakagama, M. Imawari, H. Moriwaki, Y. Muto, Positive and negative regulations of albumin gene expression by retinoids in human hepatoma cell lines., *Mol. Carcinog.* 10 (1994) 151–158. doi: 10.1002/mc.2940100306.
- [28] Y. Muto, H. Moriwaki, Antitumor activity of vitamin A and Its derivatives, *J. Natl. Cancer Inst.* 73 (1984) 1389–1393. doi:10.1093/jnci/73.6.1389.
- [29] Y. Muto, H. Moriwaki, Acyclic retinoids and cancer chemoprevention, *Pure Appl. Chem.* 63 (1991) 157–160. doi:10.1351/pac199163010157.
- [30] Nakamura N, Shidoji Y, Yamada Y, Hatakeyama H, Moriwaki H, Muto Y, Induction of apoptosis by acyclic retinoid in the human hepatoma derived cell line, HuH 7., *Biochem. Biophys. Res. Commun.* 207 (1995) 382–388. doi:10.1006/bbrc.1995.1199.
- [31] Y. Shidoji, H. Ogawa, Natural occurrence of cancer-preventive geranylgeranoic acid in medicinal herbs, *J. Lipid Res.* 45 (2004) 1092–1103. doi:10.1194/jlr.M300502-JLR200.
- [32] Y. Kodaira, K. Usui, I. Kon, H. Sagami, Formation of (R)-2,3-dihydrogeranylgeranoic acid from geranylgeraniol in rat thymocytes, *J. Biochem.* 132 (2002) 327–334.
- [33] H. Sagami, T. Korenaga, A. Kurisaki, K. Ogura, Biosynthesis of prenyl diphosphates by cell-free extracts from mammalian tissues, *J. Biochem.* 114 (1993) 112–117.

- [34] T. Muraguchi, K. Okamoto, M. Mitake, H. Ogawa, Y. Shidoji, Polished rice as natural sources of cancer-preventing geranylgeranoic acid., *J. Clin. Biochem. Nutr.* 49 (2011) 8–15.
doi:10.3164/jcbn.10-110.
- [35] M. Mitake, Y. Shidoji, Geranylgeraniol oxidase activity involved in oxidative formation of geranylgeranoic acid in human hepatoma cells., *Biomed. Res.* 33 (2012) 15–24.
doi:10.2220/biomedres.33.15.
- [36] V.S. Bansal, S. Vaidya, Characterization of two distinct allyl pyrophosphatase activities from rat liver microsomes, *Arch. Biochem. Biophys.* 315 (1994) 393–399. doi:10.1006/abbi.1994.1516.
- [37] Y. Shidoji, N. Nakamura, H. Moriwaki, Y. Muto, Rapid Loss in the Mitochondrial Membrane Potential during Geranylgeranoic Acid-Induced Apoptosis, *Biochem. Biophys. Res. Commun.* 230 (1997) 58–63. doi:10.1006/bbrc.1996.5883.
- [38] Y. Fukutomi, M. Omori, Y. Muto, M. Ninomiya, M. Okuno, H. Moriwaki, Inhibitory Effects of Acyclic Retinoid (Polyprenoic Acid) and Its Hydroxy Derivative on Cell Growth and on Secretion of alpha-Fetoprotein in Human Hepatoma-derived Cell Line (PLC/PRF/5), *Japanese J. Cancer Res.* 81 (1990) 1281–1285. doi:10.1111/j.1349-7006.1990.tb02691.x.
- [39] Y. Muto, H. Moriwaki, M. Ninomiya, S. Adachi, a Saito, K.T. Takasaki, T. Tanaka, K. Tsurumi, M. Okuno, E. Tomita, T. Nakamura, T. Kojima, Prevention of second primary tumors by an acyclic retinoid, polyprenoic acid, in patients with hepatocellular carcinoma. Hepatoma Prevention Study Group., *N. Engl. J. Med.* 334 (1996) 1561–1567. doi:10.1056/NEJM199606133342402.
- [40] Y. Yamada, Y. Shidoji, Y. Fukutomi, T. Ishikawa, T. Kaneko, H. Nakagama, M. Imawari, H. Moriwaki, Y. Muto, Positive and negative regulations of albumin gene expression by retinoids in human hepatoma cell lines., *Mol. Carcinog.* 10 (1994) 151–158. doi:10.1002/mc.2940100306.
- [41] H. Nakabayashi, K. Taketa, T. Yamane, M. Miyazaki, K. Miyano, J. Sato, Phenotypical stability of a human hepatoma cell line, HuH-7, in long-term culture with chemically defined medium., *Gann.* 75 (1984) 151–158.

- [42] M. Enari, R. Talanian, W. Wong, S. Nagata, Sequential activation of ICE-like and CPP32-like proteases during Fas-mediated apoptosis., *Nature*. 25 (1996) 723–726. doi:10.1038/380723a0.
- [43] K. Orth, K. O'Rourke, G.S. Salvesen, V.M. Dixit, Molecular ordering of apoptotic mammalian CED-3/ICE-like proteases, *J. Biol. Chem.* 271 (1996) 20977–20980. doi:10.1074/jbc.271.35.20977.
- [44] P. Marchetti, S.A. Susin, D. Decaudin, S. Gamen, M. Castedo, T. Hirsch, N. Zamzami, J. Naval, A. Senik, G. Kroemer, Apoptosis-associated derangement of mitochondrial function in cells lacking mitochondrial DNA, *Cancer Res.* 56 (1996) 2033–2038.
- [45] X. Liu, C.N. Kim, J. Yang, R. Jemmerson, X. Wang, Induction of apoptotic program in cell-free extracts: Requirement for dATP and cytochrome c, *Cell*. 86 (1996) 147–157. doi:10.1016/S0092-8674(00)80085-9.
- [46] A.H. Goodall, D. Fisher, J.A. Lucy, Cell fusion, haemolysis and mitochondrial swelling induced by retinol and derivatives, *BBA - Biomembr.* 595 (1980) 9–14. doi:10.1016/0005-2736(80)90242-4.
- [47] K. Okamoto, Y. Sakimoto, K. Imai, H. Senoo, Y. Shidoji, Induction of an incomplete autophagic response by cancer-preventive geranylgeranoic acid (GGA) in a human hepatoma-derived cell line, *Biochem. J.* 440 (2011) 63–71. doi:10.1042/BJ20110610.
- [48] S. Kumagai, R. Narasaki, K. Hasumi, Glucose-dependent active ATP depletion by koniginic acid kills high-glycolytic cells, *Biochem. Biophys. Res. Commun.* 365 (2008) 362–368. doi:10.1016/j.bbrc.2007.10.199.
- [49] S.W. Lowe, a W. Lin, Apoptosis in cancer., *Carcinogenesis*. 21 (2000) 485–495. doi:10.1093/carcin/21.3.485.
- [50] A. Ashkenazi, V.M. Dixit, Death receptors: signaling and modulation., *Science*. 281 (1998) 1305–1308. doi:10.1126/science.281.5381.1305.
- [51] S. Bates, K.H. Vousden, Mechanisms of p53-mediated apoptosis, *Cell. Mol. Life Sci.* 55 (1999) 28–37. doi:10.1007/s000180050267.
- [52] F. Toledo, G.M. Wahl, Regulating the p53 pathway: in vitro hypotheses, in vivo veritas, *Nat. Rev.*

- Cancer. 6 (2006) 909–923. doi:10.1038/nrc2012.
- [53] P.A.J. Muller, K.H. Vousden, J.C. Norman, p53 and its mutants in tumor cell migration and invasion, *J. Cell Biol.* 192 (2011) 209–218. doi:10.1083/jcb.201009059.
- [54] C.F. Cheok, C.S. Verma, J. Baselga, D.P. Lane, Translating p53 into the clinic, *Nat. Rev. Clin. Oncol.* 8 (2011) 25–37. doi:10.1038/nrclinonc.2010.174.
- [55] K. Bensaad, K.H. Vousden, p53: new roles in metabolism, *Trends Cell Biol.* 17 (2007) 286–291. doi:10.1016/j.tcb.2007.04.004.
- [56] J.E. Chipuk, D.R. Green, Dissecting p53-dependent apoptosis, *Cell Death Differ.* 13 (2006) 994–1002. doi:10.1038/sj.cdd.4401908.
- [57] J. Yu, L. Zhang, PUMA, a potent killer with or without p53, *Oncogene.* 27 (2008) S71–S83. doi:10.1038/onc.2009.45.
- [58] K.S. Yee, S. Wilkinson, J. James, K.M. Ryan, K.H. Vousden, PUMA- and Bax-induced autophagy contributes to apoptosis., *Cell Death Differ.* 16 (2009) 1135–1145. doi:10.1038/cdd.2009.28.
- [59] L. Kaustov, J. Lukin, A. Lemak, S. Duan, M. Ho, R. Doherty, L.Z. Penn, C.H. Arrowsmith, The conserved CPH domains of Cul7 and PARC are protein-protein interaction modules that bind the tetramerization domain of p53, *J. Biol. Chem.* 282 (2007) 11300–11307. doi:10.1074/jbc.M611297200.
- [60] X.H. Pei, F. Bai, Z. Li, M.D. Smith, G. Whitewolf, R. Jin, Y. Xiong, Cytoplasmic CUL9/PARC ubiquitin ligase is a tumor suppressor and promotes p53-dependent apoptosis, *Cancer Res.* 71 (2011) 2969–2977. doi:10.1158/0008-5472.CAN-10-4300.
- [61] K.H. Vousden, K.M. Ryan, p53 and metabolism, *Nat. Rev. Cancer.* 9 (2009) 691–700. doi:10.1038/nrc2715.
- [62] D. Crighton, S. Wilkinson, J. O’Prey, N. Syed, P. Smith, P.R. Harrison, M. Gasco, O. Garrone, T. Crook, K.M. Ryan, DRAM, a p53-Induced Modulator of Autophagy, Is Critical for Apoptosis, *Cell.* 126 (2006) 121–134. doi:10.1016/j.cell.2006.05.034.

- [63] L.Y. Mah, J. O'Prey, A.D. Baudot, A. Hoekstra, K.M. Ryan, DRAM-1 encodes multiple isoforms that regulate autophagy, *Autophagy*. 8 (2012) 18–28. doi:10.4161/auto.8.1.18077.
- [64] M.C. Maiuri, L. Galluzzi, E. Morselli, O. Kepp, S.A. Malik, G. Kroemer, Autophagy regulation by p53, *Curr. Opin. Cell Biol.* 22 (2010) 181–185. doi:10.1016/j.ceb.2009.12.001.
- [65] C. Iwao, Y. Shidoji, Induction of nuclear translocation of mutant cytoplasmic p53 by geranylgeranoic acid in a human hepatoma cell line., *Sci. Rep.* 4 (2014) 4419. doi:10.1038/srep04419.
- [66] N. Mizushima, Y. Ohsumi, T. Yoshimori, Autophagosome Formation in Mammalian Cells, *Cell Struct. Funct.* 27 (2002) 421–429. doi:10.1247/csf.27.421.
- [67] M. Hochstrasser, UBIQUITIN-DEPENDENT PROTEIN DEGRADATION, *Annu. Rev. Genet.* 30 (1996) 405–439. doi:10.1146/annurev.genet.30.1.405.
- [68] G. Mortimore, Intracellular Protein Catabolism And Its Control During Nutrient Deprivation And Supply, *Annu. Rev. Nutr.* 7 (1987) 539–564. doi:10.1146/annurev.nutr.7.1.539.
- [69] P.O. Seglen, P. Bohley, Autophagy and other vacuolar protein degradation mechanisms, *Experientia*. 48 (1992) 158–172. doi:10.1007/BF01923509.
- [70] D.J. Klionsky, Autophagy: From phenomenology to molecular understanding in less than a decade, *Nat. Rev. Mol. Cell Biol.* 8 (2007) 931–937. doi:10.1038/nrm2245.
- [71] Y. Kabeya, LC3, a mammalian homologue of yeast Apg8p, is localized in autophagosome membranes after processing, *EMBO J.* 19 (2000) 5720–5728. doi:10.1093/emboj/19.21.5720.
- [72] B. Levine, D.J. Klionsky, Development by self-digestion: Molecular mechanisms and biological functions of autophagy, *Dev. Cell.* 6 (2004) 463–477. doi:10.1016/S1534-5807(04)00099-1.
- [73] T. Hara, K. Nakamura, M. Matsui, A. Yamamoto, Y. Nakahara, R. Suzuki-Migishima, M. Yokoyama, K. Mishima, I. Saito, H. Okano, N. Mizushima, Suppression of basal autophagy in neural cells causes neurodegenerative disease in mice., *Nature*. 441 (2006) 885–889. doi:10.1038/nature04724.
- [74] M. Komatsu, S. Waguri, T. Chiba, S. Murata, J. Iwata, I. Tanida, T. Ueno, M. Koike, Y. Uchiyama, E. Kominami, K. Tanaka, Loss of autophagy in the central nervous system causes neurodegeneration in

- mice, *Nature*. 441 (2006) 880–884. doi:10.1038/nature04723.
- [75] M. Komatsu, T. Ueno, S. Waguri, Y. Uchiyama, E. Kominami, K. Tanaka, Constitutive autophagy: vital role in clearance of unfavorable proteins in neurons, *Cell Death Differ.* (2007). doi:10.1038/sj.cdd.4402120.
- [76] M. Komatsu, S. Waguri, T. Ueno, J. Iwata, S. Murata, I. Tanida, J. Ezaki, N. Mizushima, Y. Ohsumi, Y. Uchiyama, E. Kominami, K. Tanaka, T. Chiba, Impairment of starvation-induced and constitutive autophagy in Atg7-deficient mice, *J. Cell Biol.* 169 (2005) 425–434. doi:10.1083/jcb.200412022.
- [77] C. Iwao, Y. Shidoji, Polyunsaturated branched-chain fatty acid geranylgeranoic acid induces unfolded protein response in human hepatoma cells, *PLoS One*. 10 (2015) e0132761. doi:10.1371/journal.pone.0132761.
- [78] Y. Kitai, H. Ariyama, N. Kono, D. Oikawa, T. Iwawaki, H. Arai, Membrane lipid saturation activates IRE1alpha without inducing clustering., *Genes to Cells*. 18 (2013) 798–809. doi:10.1111/gtc.12074.
- [79] P. Walter, D. Ron, The unfolded protein response: from stress pathway to homeostatic regulation., *Science*. 334 (2011) 1081–1086. doi:10.1126/science.1209038.
- [80] H. Urrea, C. Hetz, The ER in 4D: a novel stress pathway controlling endoplasmic reticulum membrane remodeling, *Cell Death Differ.* 19 (2012) 1893–1895. doi:10.1038/cdd.2012.127.
- [81] R. Liu-Bryan, R. Terkeltaub, Emerging regulators of the inflammatory process in osteoarthritis, *Nat. Rev. Rheumatol.* 11 (2015) 35–44. doi:10.1038/nrrheum.2014.162.
- [82] H. Malhi, R.J. Kaufman, Endoplasmic reticulum stress in liver disease, *J. Hepatol.* 54 (2011) 795–809. doi:10.1016/j.jhep.2010.11.005.
- [83] R. Volmer, K. van der Ploeg, D. Ron, Membrane lipid saturation activates endoplasmic reticulum unfolded protein response transducers through their transmembrane domains, *Proc. Natl. Acad. Sci. U. S. A.* 110 (2013) 4628–4633. doi:10.1073/pnas.1217611110.
- [84] L.L. Listenberger, X. Han, S.E. Lewis, S. Cases, R. V Farese, D.S. Ory, J.E. Schaffer, Triglyceride accumulation protects against fatty acid-induced lipotoxicity., *Proc. Natl. Acad. Sci. U. S. A.* 100

(2003) 3077–3082. doi:10.1073/pnas.0630588100.

- [85] M. Bosma, D.H. Dapito, Z. Drosatos-Tampakaki, N. Huiping-Son, L.S. Huang, S. Kersten, K. Drosatos, I.J. Goldberg, Sequestration of fatty acids in triglycerides prevents endoplasmic reticulum stress in an in vitro model of cardiomyocyte lipotoxicity, *Biochim. Biophys. Acta - Mol. Cell Biol. Lipids.* 1841 (2014) 1648–1655. doi:10.1016/j.bbaliip.2014.09.012.
- [86] Y. Shidoji, K. Okamoto, Y. Muto, S. Komura, N. Ohishi, K. Yagi, Prevention of geranylgeranoic acid-induced apoptosis by phospholipid hydroperoxide glutathione peroxidase gene, *J. Cell. Biochem.* 97 (2006) 178–187. doi:10.1002/jcb.20627.
- [87] S. Shimonishi, T. Muraguchi, M. Mitake, C. Sakane, K. Okamoto, Y. Shidoji, Rapid Downregulation of Cyclin D1 Induced by Geranylgeranoic Acid in Human Hepatoma Cells, *Nutr. Cancer.* 64 (2012) 473–480. doi:10.1080/01635581.2012.655401.
- [88] L. Hartwell, T. Weinert, Checkpoints: controls that ensure the order of cell cycle events, *Science* 246 (1989) 629–634. doi:10.1126/science.2683079.
- [89] C. Sakane, Non-genomic Actions of Diterpenoid Acids : with Special Reference to Differentiation Induction of Human Neuroblastoma and Hepatoma Cells, (2014). <http://hdl.handle.net/10561/1114>.
- [90] A.P. Bracken, M. Ciro, A. Cocito, K. Helin, E2F target genes: Unraveling the biology, *Trends Biochem. Sci.* 29 (2004) 409–417. doi:10.1016/j.tibs.2004.06.006.
- [91] N. Hosokawa, T. Hara, T. Kaizuka, C. Kishi, A. Takamura, Y. Miura, S. -i. Iemura, T. Natsume, K. Takehana, N. Yamada, J.-L. Guan, N. Oshiro, N. Mizushima, Nutrient-dependent mTORC1 Association with the ULK1-Atg13-FIP200 Complex Required for Autophagy, *Mol. Biol. Cell.* 20 (2009) 1981–1991. doi:10.1091/mbc.E08-12-1248.
- [92] R. Malaviya, J.D. Laskin, D.L. Laskin, Oxidative stress-induced autophagy: Role in pulmonary toxicity, *Toxicol. Appl. Pharmacol.* 275 (2014) 145–151. doi:10.1016/j.taap.2013.12.022.
- [93] T.J. Biden, E. Boslem, K.Y. Chu, N. Sue, Lipotoxic endoplasmic reticulum stress, β cell failure, and type 2 diabetes mellitus., *Trends Endocrinol. Metab.* 25 (2014) 389–398.

doi:10.1016/j.tem.2014.02.003.

- [94] J.W. Brewer, J.A. Diehl, PERK mediates cell-cycle exit during the mammalian unfolded protein response., *Proc. Natl. Acad. Sci. U. S. A.* 97 (2000) 12625–12630. doi:10.1073/pnas.220247197.
- [95] R. Liu, L. Zhang, J. Yang, X. Zhang, R. Mikkelsen, S. Song, H. Zhou, HIV protease inhibitors sensitize human head and neck squamous carcinoma cells to radiation by activating endoplasmic reticulum stress, *PLoS One*. 10 (2015). doi:10.1371/journal.pone.0125928.
- [96] M. Lamkanfi, V.M. Dixit, Manipulation of host cell death pathways during microbial infections, *Cell Host Microbe*. 8 (2010) 44–54. doi:10.1016/j.chom.2010.06.007.
- [97] S. Grootjans, T. Vanden Berghe, P. Vandenabeele, Initiation and execution mechanisms of necroptosis: an overview., *Cell Death Differ.* 24 (2017) 1184–1195. doi: 10.1038/cdd.2017.65.
- [98] T. Bergsbaken, S.L. Fink, B.T. Cookson, Pyroptosis: host cell death and inflammation, *Nat. Rev. Microbiol.* 7 (2009) 99–109. doi:10.1038/nrmicro2070.
- [99] S.J. Dixon, K.M. Lemberg, M.R. Lamprecht, R. Skouta, E.M. Zaitsev, C.E. Gleason, D.N. Patel, A.J. Bauer, A.M. Cantley, W.S. Yang, B. Morrison, B.R. Stockwell, Ferroptosis: An iron-dependent form of nonapoptotic cell death, *Cell*. 149 (2012) 1060–1072. doi:10.1016/j.cell.2012.03.042.
- [100] A. Bergmann, Autophagy and Cell Death: No Longer at Odds, *Cell*. 131 (2007) 1032–1034. doi:10.1016/j.cell.2007.11.027.
- [101] Q. Remijnsen, T.W. Kuijpers, E. Wirawan, S. Lippens, P. Vandenabeele, T. Vanden Berghe, Dying for a cause: NETosis, mechanisms behind an antimicrobial cell death modality, *Cell Death Differ.* 18 (2011) 581–588. doi:10.1038/cdd.2011.1.
- [102] M. Tanaka, Preface; How cells die and what they do?, *Exp. Med.* 34 (2016).
- [103] A. Wree, L. Broderick, A. Canbay, H.M. Hoffman, A.E. Feldstein, From NAFLD to NASH to cirrhosis-new insights into disease mechanisms, *Nat. Rev. Gastroenterol. Hepatol.* 10 (2013) 627–636. doi:10.1038/nrgastro.2013.149.
- [104] R.A. Aglietti, E.C. Dueber, Recent Insights into the Molecular Mechanisms Underlying Pyroptosis

- and Gasdermin Family Functions, *Trends Immunol.* 38 (2017) 261–271. doi:10.1016/j.it.2017.01.003.
- [105] E. Latz, T.S. Xiao, A. Stutz, Activation and regulation of the inflammasomes, *Nat. Rev. Immunol.* 13 (2013) 397–411. doi:10.1038/nri3452.
- [106] J. von Moltke, J.S. Ayres, E.M. Kofoed, J. Chavarría-Smith, R.E. Vance, Recognition of Bacteria by Inflammasomes, *Annu. Rev. Immunol.* 31 (2013) 73–106. doi:10.1146/annurev-immunol-032712-095944.
- [107] L. Sborgi, S. Rühl, E. Mulvihill, J. Pipercevic, R. Heilig, H. Stahlberg, C.J. Farady, D.J. Müller, P. Broz, S. Hiller, GSDMD membrane pore formation constitutes the mechanism of pyroptotic cell death, *EMBO J.* 35 (2016) 1766–1778. doi:10.15252/embj.201694696.
- [108] M. Lamkanfi, Emerging inflammasome effector mechanisms, *Nat. Rev. Immunol.* 11 (2011) 213–220. doi:10.1038/nri2936.
- [109] N.A. Thornberry, H.G. Bull, J.R. Calaycay, K.T. Chapman, A.D. Howard, M.J. Kostura, D.K. Miller, S.M. Molineaux, J.R. Weidner, J. Aunins, et al., A novel heterodimeric cysteine protease is required for interleukin-1 beta processing in monocytes, *Nature.* 356 (1992) 768–774. doi:10.1038/356768a0.
- [110] S.L. Fink, B.T. Cookson, Pyroptosis and host cell death responses during *Salmonella* infection, *Cell. Microbiol.* 9 (2007) 2562–2570. doi:10.1111/j.1462-5822.2007.01036.x.
- [111] N. Kayagaki, S. Warming, M. Lamkanfi, L. Vande Walle, S. Louie, J. Dong, K. Newton, Y. Qu, J. Liu, S. Heldens, J. Zhang, W.P. Lee, M. Roose-Girma, V.M. Dixit, Non-canonical inflammasome activation targets caspase-11, *Nature.* 479 (2011) 117–121. doi:10.1038/nature10558.
- [112] J. Shi, Y. Zhao, Y. Wang, W. Gao, J. Ding, P. Li, L. Hu, F. Shao, Inflammatory caspases are innate immune receptors for intracellular LPS, *Nature.* (2014). doi:10.1038/nature13683.
- [113] S.L. Fink, T. Bergsbaken, B.T. Cookson, Anthrax lethal toxin and *Salmonella* elicit the common cell death pathway of caspase-1-dependent pyroptosis via distinct mechanisms, *Proc. Natl. Acad. Sci. U. S. A.* 105 (2008) 4312–4317. doi:10.1073/pnas.0707370105.
- [114] E.A. Miao, I.A. Leaf, P.M. Treuting, D.P. Mao, M. Dors, A. Sarkar, S.E. Warren, M.D. Wewers, A.

Aderem, Caspase-1-induced pyroptosis is an innate immune effector mechanism against intracellular bacteria, *Nat. Immunol.* 11 (2010) 1136–1142. doi:10.1038/ni.1960.

- [115] S.K. Vanaja, V.A.K. Rathinam, K.A. Fitzgerald, Mechanisms of inflammasome activation: Recent advances and novel insights, *Trends Cell Biol.* 25 (2015) 308–315. doi:10.1016/j.tcb.2014.12.009.
- [116] H.M. Hoffman, F.A. Wright, D.H. Broide, A.A. Wanderer, R.D. Kolodner, Identification of a locus on chromosome 1q44 for familial cold urticaria., *Am. J. Hum. Genet.* 66 (2000) 1693–1698. doi:10.1086/302874.
- [117] B.K. Davis, H. Wen, J.P.-Y. Ting, The Inflammasome NLRs in Immunity, Inflammation, and Associated Diseases, *Annu. Rev. Immunol.* 29 (2011) 707–735. doi:10.1146/annurev-immunol-031210-101405.
- [118] J. Tschopp, K. Schroder, NLRP3 inflammasome activation: the convergence of multiple signalling pathways on ROS production?, *Nat. Rev. Immunol.* 10 (2010) 210–215. doi:10.1038/nri2725.
- [119] H. Wen, D. Gris, Y. Lei, S. Jha, L. Zhang, M.T.-H. Huang, W.J. Brickey, J.P.-Y. Ting, Fatty acid-induced NLRP3-ASC inflammasome activation interferes with insulin signaling, *Nat. Immunol.* 12 (2011) 408–415. doi:10.1038/ni.2022.
- [120] L. Shen, Y. Yang, T. Ou, C.-C.C. Key, S.H. Tong, R.C. Sequeira, J.M. Nelson, Y. Nie, Z. Wang, E. Boudyguina, S. V. Shewale, X. Zhu, Dietary PUFAs attenuate NLRP3 inflammasome activation via enhancing macrophage autophagy., *J. Lipid Res.* 58 (2017) 1808–1821. doi:10.1194/jlr.M075879.
- [121] H. Guo, J.B. Callaway, J.P.-Y. Ting, Inflammasomes: mechanism of action, role in disease, and therapeutics, *Nat. Med.* 21 (2015) 677–687. doi:10.1038/nm.3893.
- [122] M. Lamkanfi, V.M. Dixit, Mechanisms and functions of inflammasomes, *Cell.* 157 (2014) 1013–1022. doi:10.1016/j.cell.2014.04.007.
- [123] F.S. Sutterwala, S. Haasken, S.L. Cassel, Mechanism of NLRP3 inflammasome activation, *Ann. N. Y. Acad. Sci.* 1319 (2014) 82–95. doi:10.1111/nyas.12458.
- [124] R.A. Ratsimandresy, A. Dorfleutner, C. Stehlik, An update on PYRIN domain-containing pattern

recognition receptors: From immunity to pathology, *Front. Immunol.* 4 (2013) 440.

doi:10.3389/fimmu.2013.00440.

- [125] V.A.K. Rathinam, S.K. Vanaja, K.A. Fitzgerald, Regulation of inflammasome signaling, *Nat. Immunol.* 13 (2012) 333–332. doi:10.1038/ni.2237.
- [126] T. Murakami, J. Ockinger, J. Yu, V. Byles, A. McColl, A.M. Hofer, T. Horng, Critical role for calcium mobilization in activation of the NLRP3 inflammasome., *Proc. Natl. Acad. Sci. U. S. A.* 109 (2012) 11282–11287. doi:10.1073/pnas.1117765109.
- [127] G.-S. Lee, N. Subramanian, A.I. Kim, I. Aksentijevich, R. Goldbach-Mansky, D.B. Sacks, R.N. Germain, D.L. Kastner, J.J. Chae, The calcium-sensing receptor regulates the NLRP3 inflammasome through Ca^{2+} and cAMP, *Nature.* 492 (2012) 123–127. doi:10.1038/nature11588.
- [128] M.A. Katsnelson, L.G. Rucker, H.M. Russo, G.R. Dubyak, K^+ efflux agonists induce NLRP3 inflammasome activation independently of Ca^{2+} signaling., *J. Immunol.* 194 (2015) 3937–3952. doi:10.4049/jimmunol.1402658.
- [129] C. Dostert, G. Guarda, J.F. Romero, P. Menu, O. Gross, A. Tardivel, M.L. Suva, J.C. Stehle, M. Kopf, I. Stamenkovic, G. Corradin, J. Tschopp, Malarial hemozoin is a Nalp3 inflammasome activating danger signal, *PLoS One.* 4 (2009) e6510. doi:10.1371/journal.pone.0006510.
- [130] H. Guo, J.B. Callaway, J.P. Ting, Inflammasomes: mechanism of action, role in disease, and therapeutics, *Nat Med.* 21 (2015) 677–687. doi:10.1038/nm.3893.
- [131] F.G. Bauernfeind, G. Horvath, A. Stutz, E.S. Alnemri, K. MacDonald, D. Speert, T. Fernandes-Alnemri, J. Wu, B.G. Monks, K.A. Fitzgerald, V. Hornung, E. Latz, Cutting Edge: NF- κ B Activating Pattern Recognition and Cytokine Receptors License NLRP3 Inflammasome Activation by Regulating NLRP3 Expression, *J. Immunol.* 183 (2009) 787–791. doi:10.4049/jimmunol.0901363.
- [132] C. Juliana, T. Fernandes-Alnemri, S. Kang, A. Farias, F. Qin, E.S. Alnemri, Non-transcriptional priming and deubiquitination regulate NLRP3 inflammasome activation, *J. Biol. Chem.* 287 (2012) 36617–36622. doi:10.1074/jbc.M112.407130.

- [133] B.F. Py, M.S. Kim, H. Vakifahmetoglu-Norberg, J. Yuan, Deubiquitination of NLRP3 by BRCC3 Critically Regulates Inflammasome Activity, *Mol. Cell.* 49 (2013) 331–338. doi:10.1016/j.molcel.2012.11.009.
- [134] M.A. Rodgers, J.W. Bowman, H. Fujita, N. Orazio, M. Shi, Q. Liang, R. Amatya, T.J. Kelly, K. Iwai, J. Ting, J.U. Jung, The linear ubiquitin assembly complex (LUBAC) is essential for NLRP3 inflammasome activation, *J. Exp. Med.* 211 (2014) 1333–1347. doi:10.1084/jem.20132486.
- [135] A. Lu, V.G. Magupalli, J. Ruan, Q. Yin, M.K. Atianand, M.R. Vos, G.F. Schroeder, K.A. Fitzgerald, H. Wu, E.H. Egelman, Unified polymerization mechanism for the assembly of asc-dependent inflammasomes, *Cell.* 156 (2014) 1193–1206. doi:10.1016/j.cell.2014.02.008.
- [136] X. Cai, J. Chen, H. Xu, S. Liu, Q.X. Jiang, R. Halfmann, Z.J. Chen, Prion-like polymerization underlies signal transduction in antiviral immune defense and inflammasome activation, *Cell.* 156 (2014) 1207–1222. doi:10.1016/j.cell.2014.01.063.
- [137] M.N. Patel, R.G. Carroll, S. Galván-Peña, E.L. Mills, R. Olden, M. Triantafilou, A.I. Wolf, C.E. Bryant, K. Triantafilou, S.L. Masters, Inflammasome Priming in Sterile Inflammatory Disease, *Trends Mol. Med.* 23 (2017) 165–180. doi:10.1016/j.molmed.2016.12.007.
- [138] Y. He, H. Hara, G. Nunez, Mechanism and Regulation of NLRP3 Inflammasome Activation, *Trends Biochem. Sci.* 41 (2016) 1012–1021. doi:10.1016/j.tibs.2016.09.002.
- [139] L. Franchi, R. Muñoz-Planillo, G. Núñez, Sensing and reacting to microbes through the inflammasomes, *Nat. Immunol.* 13 (2012) 325–332. doi:10.1038/ni.2231.
- [140] C. Bryant, K.A. Fitzgerald, Molecular mechanisms involved in inflammasome activation, *Trends Cell Biol.* 19 (2009) 455–464. doi:10.1016/j.tcb.2009.06.002.
- [141] A.J. Puren, G. Fantuzzi, C.A. Dinarello, Gene expression, synthesis, and secretion of interleukin 18 and interleukin 1beta are differentially regulated in human blood mononuclear cells and mouse spleen cells., *Proc. Natl. Acad. Sci. U. S. A.* 96 (1999) 2256–2261. doi:DOI 10.1073/pnas.96.5.2256.
- [142] P. Godwin, A.M. Baird, S. Heavey, M.P. Barr, K.J. O’Byrne, K. Gately, Targeting Nuclear

Factor-Kappa B to Overcome Resistance to Chemotherapy, *Front. Oncol.* 3 (2013).

doi:10.3389/fonc.2013.00120.

- [143] S. Ghosh, M.J. May, E.B. Kopp, NF- κ B AND REL PROTEINS : Evolutionarily Conserved Mediators of Immune Responses, *Annu. Rev. Immunology.* 16 (1998) 225–260.
doi:10.1146/annurev.immunol.16.1.225.
- [144] H.L. Pahl, Activators and target genes of Rel/NF-kappaB transcription factors., *Oncogene.* 18 (1999) 6853–6866. doi:10.1038/sj.onc.1203239.
- [145] S.G. Boaru, E. Borkham-Kamphorst, E. Van De Leur, E. Lehnen, C. Liedtke, R. Weiskirchen, NLRP3 inflammasome expression is driven by NF-kappaB in cultured hepatocytes, *Biochem. Biophys. Res. Commun.* 458 (2015) 700–706. doi:10.1016/j.bbrc.2015.02.029.
- [146] S. Akira, K. Takeda, Toll-like receptor signalling, *Nat. Rev. Immunol.* 4 (2004) 499–511.
doi:10.1038/nri1391.
- [147] C. Hashimoto, K.L. Hudson, K. V. Anderson, The Toll gene of drosophila, required for dorsal-ventral embryonic polarity, appears to encode a transmembrane protein, *Cell.* 52 (1988) 269–279.
doi:10.1016/0092-8674(88)90516-8.
- [148] B. Lemaitre, E. Nicolas, L. Michaut, J. Reichhart, J. Hoffmann, The Dorsoventral Regulatory Gene Cassette spaetzle/Toll/cactus Controls the spa Potent Antifungal Response in Drosophila Adults, *Cell.* 86 (1996) 973–983. doi:10.1016/S0092-8674(00)80172-5.
- [149] C. a Janeway, R. Medzhitov, Innate immune recognition., *Annu. Rev. Immunol.* 20 (2002) 197–216.
doi:10.1146/annurev.immunol.20.083001.084359.
- [150] R. Medzhitov, Toll-like receptors and innate immunity., *Nat. Rev. Immunol.* 1 (2001) 135–145.
doi:10.1038/35100529.
- [151] S. Akira, K. Takeda, T. Kaisho, Toll-like receptors : critical proteins linking inante and acquired immunity, *Nat. Immunol.* 2 (2001) 675–680. doi:10.1038/90609.
- [152] P. Ahmad-Nejad, H. Häcker, M. Rutz, S. Bauer, R.M. Vabulas, H. Wagner, Bacterial CpG-DNA and

- lipopolysaccharides activate toll-like receptors at distinct cellular compartments, *Eur. J. Immunol.* 32 (2002) 1958–1968. doi:10.1002/1521-4141(200207)32:7<1958::AID-IMMU1958>3.0.CO;2-U.
- [153] F. Heil, P. Ahmad-Nejad, H. Hemmi, H. Hochrein, F. Ampenberger, T. Gellert, H. Dietrich, G. Lipford, K. Takeda, S. Akira, H. Wagner, S. Bauer, The Toll-like receptor 7 (TLR7)-specific stimulus loxoribine uncovers a strong relationship within the TLR7, 8 and 9 subfamily, *Eur. J. Immunol.* 33 (2003) 2987–2997. doi:10.1002/eji.200324238.
- [154] M. Matsumoto, K. Funami, M. Tanabe, H. Oshiumi, M. Shingai, Y. Seto, A. Yamamoto, T. Seya, Subcellular localization of Toll-like receptor 3 in human dendritic cells., *J. Immunol. (Baltimore, Md 1950)*. 171 (2003) 3154–3162. doi:10.4049/jimmunol.171.6.3154.
- [155] E. Latz, A. Schoenemeyer, A. Visintin, K.A. Fitzgerald, B.G. Monks, C.F. Knetter, E. Lien, N.J. Nilsen, T. Espevik, D.T. Golenbock, TLR9 signals after translocating from the ER to CpG DNA in the lysosome, *Nat. Immunol.* 5 (2004) 190–198. doi:10.1038/ni1028.
- [156] K. Takeda, S. Akira, TLR signaling pathways, *Semin. Immunol.* 16 (2004) 3–9. doi:10.1016/j.smim.2003.10.003.
- [157] L.A.J. O’Neill, D. Golenbock, A.G. Bowie, The history of Toll-like receptors — redefining innate immunity, *Nat. Rev. Immunol.* 13 (2013) 453–460. doi:10.1038/nri3446.
- [158] K. Takeda, T. Kaisho, S. Akira, Toll-Like Receptors, *Annu. Rev. Immunol.* 21 (2003) 335–376. doi:10.1146/annurev.immunol.21.120601.141126.
- [159] A. Dunne, L.A.J. O’Neill, The interleukin-1 receptor/Toll-like receptor superfamily: signal transduction during inflammation and host defense., *Sci. STKE.* 2003 (2003) re3. doi:10.1126/stke.2003.171.re3.
- [160] O. Tufanli, P. Telkoparan Akillilar, D. Acosta-Alvear, B. Kocaturk, U.I. Onat, S.M. Hamid, I. Çimen, P. Walter, C. Weber, E. Erbay, Targeting IRE1 with small molecules counteracts progression of atherosclerosis., *Proc. Natl. Acad. Sci. U. S. A.* 114 (2017) E1395–E1404. doi:10.1073/pnas.1621188114.

- [161] I. Cimen, B. Kocaturk, S. Koyuncu, O. Tufanl, U.I. Onat, A.D. Yildirim, O. Apaydin, E. Demirsoy, Z.G. Aykut, U.T. Nguyen, S.M. Watkins, G.S. Hotamisligil, E. Erbay, Prevention of atherosclerosis by bioactive palmitoleate through suppression of organelle stress and inflammasome activation, *Sci. Transl. Med.* 8 (2016) 358ra126. doi:10.1126/scitranslmed.aaf9087.
- [162] M.M. Robblee, C.C. Kim, J.P. Abate, M. Valdearcos, K.L.M. Sandlund, M.K. Shenoy, R. Volmer, T. Iwawaki, S.K. Koliwad, Saturated Fatty Acids Engage an IRE1 α -Dependent Pathway to Activate the NLRP3 Inflammasome in Myeloid Cells, *Cell Rep.* 14 (2016) 2611–2623. doi:10.1016/j.celrep.2016.02.053.
- [163] S. Janssens, B. Pulendran, B.N. Lambrecht, Emerging functions of the unfolded protein response in immunity, *Nat. Immunol.* 15 (2014) 910–919. doi:10.1038/ni.2991.
- [164] F. Osorio, S.J. Tavernier, E. Hoffmann, Y. Saeys, L. Martens, J. Veters, I. Delrue, R. De Rycke, E. Parthoens, P. Pouliot, T. Iwawaki, S. Janssens, B.N. Lambrecht, The unfolded-protein-response sensor IRE-1 α regulates the function of CD8 α ⁺ dendritic cells, *Nat. Immunol.* 15 (2014) 248–257. doi:10.1038/ni.2808.
- [165] R. Brunsing, S.A. Omori, F. Weber, A. Bicknell, L. Friend, R. Rickert, M. Niwa, B- and T-cell development both involve activity of the unfolded protein response pathway, *J. Biol. Chem.* 283 (2008) 17954–17961. doi:10.1074/jbc.M801395200.
- [166] F. Martinon, X. Chen, A.-H. Lee, L.H. Glimcher, TLR activation of the transcription factor XBP1 regulates innate immune responses in macrophages, *Nat. Immunol.* 11 (2010) 411–418. doi:10.1038/ni.1857.
- [167] C.W. Woo, L. Kutzler, S.R. Kimball, I. Tabas, Toll-like receptor activation suppresses ER stress factor CHOP and translation inhibition through activation of eIF2B, *Nat. Cell Biol.* 14 (2012) 192–200. doi:10.1038/ncb2408.
- [168] R.L. Wiseman, Y. Zhang, K.P.K. Lee, H.P. Harding, C.M. Haynes, J. Price, F. Sicheri, D. Ron, Flavonol Activation Defines an Unanticipated Ligand-Binding Site in the Kinase-RNase Domain of

- IRE1, *Mol. Cell.* 38 (2010) 291–304. doi:10.1016/j.molcel.2010.04.001.
- [169] M. Okla, W. Wang, I. Kang, A. Pashaj, T. Carr, S. Chung, Activation of Toll-like receptor 4 (TLR4) attenuates adaptive thermogenesis via endoplasmic reticulum stress, *J. Biol. Chem.* 290 (2015) 26476–26490. doi:10.1074/jbc.M115.677724.
- [170] J.D. Huang, J. Amaral, J.W. Lee, I.R. Rodriguez, 7-Ketocholesterol-induced inflammation signals mostly through the TLR4 receptor both in vitro and in vivo, *PLoS One.* 9 (2014). doi:10.1371/journal.pone.0100985.
- [171] I. Tabas, The role of endoplasmic reticulum stress in the progression of atherosclerosis, *Circ. Res.* 107 (2010) 839–850. doi:10.1161/CIRCRESAHA.110.224766.
- [172] W. He, H. Wan, L. Hu, P. Chen, X. Wang, Z. Huang, Z.-H. Yang, C.-Q. Zhong, J. Han, Gasdermin D is an executor of pyroptosis and required for interleukin-1 β secretion, *Cell Res.* 25 (2015) 1285–1298. doi:10.1038/cr.2015.139.
- [173] J. Shi, Y. Zhao, K. Wang, X. Shi, Y. Wang, H. Huang, Y. Zhuang, T. Cai, F. Wang, F. Shao, Cleavage of GSDMD by inflammatory caspases determines pyroptotic cell death, *Nature.* 526 (2015) 660–665. doi:10.1038/nature15514.
- [174] P. Broz, Immunology: Caspase target drives pyroptosis, *Nature.* 526 (2015) 642–643. doi:10.1038/nature15632.
- [175] J. Ding, K. Wang, W. Liu, Y. She, Q. Sun, J. Shi, H. Sun, D.-C. Wang, F. Shao, Erratum: Pore-forming activity and structural autoinhibition of the gasdermin family, *Nature.* 540 (2016) 150–150. doi:10.1038/nature20106.
- [176] X. Liu, Z. Zhang, J. Ruan, Y. Pan, V.G. Magupalli, H. Wu, J. Lieberman, Inflammasome-activated gasdermin D causes pyroptosis by forming membrane pores, *Nature.* 535 (2016) 153–158. doi:10.1038/nature18629.
- [177] J. Ding, K. Wang, W. Liu, Y. She, Q. Sun, J. Shi, H. Sun, D. Wang, F. Shao, Pore-forming activity and structural autoinhibition of the gasdermin family, *Nature.* 535 (2016) 111–116.

doi:10.1038/nature18590.

- [178] P.V. Borges, K.H. Moret, N.M. Raghavendra, T.E. Maramaldo Costa, A.P. Monteiro, A.B. Carneiro, P. Pacheco, J.R. Temerozo, D.C. Bou-Habib, M. das Graças Henriques, C. Penido, Protective effect of gedunin on TLR-mediated inflammation by modulation of inflammasome activation and cytokine production: Evidence of a multitarget compound, *Pharmacol. Res.* 115 (2017) 65–77.
doi:10.1016/j.phrs.2016.09.015.
- [179] R.C. Coll, A.A.B. Robertson, J.J. Chae, S.C. Higgins, R. Muñoz-Planillo, M.C. Insserra, I. Vetter, L.S. Dungan, B.G. Monks, A. Stutz, D.E. Croker, M.S. Butler, M. Haneklaus, C.E. Sutton, G. Núñez, E. Latz, D.L. Kastner, K.H.G. Mills, S.L. Masters, K. Schroder, M.A. Cooper, L.A.J. O’Neill, A small-molecule inhibitor of the NLRP3 inflammasome for the treatment of inflammatory diseases., *Nat. Med.* 21 (2015) 248–255. doi:10.1038/nm.3806.
- [180] S. Shimasaki, T. Koga, T. Shuto, M.A. Suico, T. Sato, K. Watanabe, S. Morino-Koga, M. Taura, S. Okada, K. Mori, H. Kai, Endoplasmic reticulum stress increases the expression and function of toll-like receptor-2 in epithelial cells, *Biochem. Biophys. Res. Commun.* 402 (2010) 235–240.
doi:10.1016/j.bbrc.2010.09.132.
- [181] J. van Bergenhenegouwen, T.S. Plantinga, L. a B. Joosten, M.G. Netea, G. Folkerts, A.D. Kraneveld, J. Garssen, A.P. Vos, TLR2 & Co: a critical analysis of the complex interactions between TLR2 and coreceptors., *J. Leukoc. Biol.* 94 (2013) 885–902. doi:10.1189/jlb.0113003.
- [182] P. Mistry, M.H.W. Laird, R.S. Schwarz, S. Greene, T. Dyson, G.A. Snyder, T.S. Xiao, J. Chauhan, S. Fletcher, V.Y. Toshchakov, A.D. MacKerell, S.N. Vogel, Inhibition of TLR2 signaling by small molecule inhibitors targeting a pocket within the TLR2 TIR domain, *Proc Natl Acad Sci U S A.* 112 (2015) 5455–5460. doi:10.1073/pnas.1422576112.
- [183] M.R. Dasu, I. Jialal, Free fatty acids in the presence of high glucose amplify monocyte inflammation via Toll-like receptors, *Am. J. Physiol. - Endocrinol. Metab.* 300 (2011) E145–E154.
doi:10.1152/ajpendo.00490.2010.

- [184] J. Peng, H. Zheng, X. Wang, Z. Cheng, Upregulation of TLR4 via PKC activation contributes to impaired wound healing in high-glucose-treated kidney proximal tubular cells, *PLoS One*. 12 (2017) e0178147. doi:10.1371/journal.pone.0178147.
- [185] L. Wang, J. Wang, J. Fang, H. Zhou, X. Liu, S.B. Su, High glucose induces and activates Toll - like receptor 4 in endothelial cells of diabetic retinopathy, *Diabetol. Metab. Syndr.* 7 (2015) 89. doi:10.1186/s13098-015-0086-4.
- [186] J.-A. Kim, H.-J. Jang, D.H. Hwang, Toll-like receptor 4-induced endoplasmic reticulum stress contributes to impairment of vasodilator action of insulin., *Am. J. Physiol. Endocrinol. Metab.* 309 (2015) E767-E776. doi:10.1152/ajpendo.00369.2015.
- [187] S. Savic, L. Ouboussad, L.J. Dickie, J. Geiler, C. Wong, G.M. Doody, S.M. Churchman, F. Ponchel, P. Emery, G.P. Cook, M.H. Buch, R.M. Tooze, M.F. McDermott, TLR dependent XBP-1 activation induces an autocrine loop in rheumatoid arthritis synoviocytes, *J. Autoimmun.* 50 (2014) 59–66. doi:10.1016/j.jaut.2013.11.002.
- [188] N.J. Bernard, L.A. O'Neill, Mal, more than a bridge to MyD88, *IUBMB Life*. 65 (2013) 777–786. doi:10.1002/iub.1201.
- [189] Y. Yang, J. Lv, S. Jiang, Z. Ma, D. Wang, W. Hu, C. Deng, C. Fan, S. Di, Y. Sun, W. Yi, The emerging role of Toll-like receptor 4 in myocardial inflammation., *Cell Death Dis.* 7 (2016) e2234. doi:10.1038/cddis.2016.140.
- [190] T. Lysakova-Devine, B. Keogh, B. Harrington, K. Nagpal, A. Halle, D.T. Golenbock, T. Monie, A.G. Bowie, Viral Inhibitory Peptide of TLR4, a Peptide Derived from Vaccinia Protein A46, Specifically Inhibits TLR4 by Directly Targeting MyD88 Adaptor-Like and TRIF-Related Adaptor Molecule, *J. Immunol.* 185 (2010) 4261–4271. doi:10.4049/jimmunol.1002013.
- [191] E. Guven-Maiorov, O. Keskin, A. GURSOY, C. VanWaes, Z. Chen, C.-J. Tsai, R. Nussinov, The Architecture of the TIR Domain Signalosome in the Toll-like Receptor-4 Signaling Pathway., *Sci. Rep.* 5 (2015) 13128. doi:10.1038/srep13128.

- [192] M.D. Neal, H. Jia, B. Eyer, M. Good, C.J. Guerriero, C.P. Sodhi, A. Afrazi, T. Prindle, C. Ma, M. Branca, J. Ozolek, J.L. Brodsky, P. Wipf, D.J. Hackam, Discovery and Validation of a New Class of Small Molecule Toll-Like Receptor 4 (TLR4) Inhibitors, *PLoS One*. 8 (2013).
doi:10.1371/journal.pone.0065779.
- [193] A.J. Scott, B.L. Oyler, D.R. Goodlett, R.K. Ernst, Lipid A structural modifications in extreme conditions and identification of unique modifying enzymes to define the Toll-like receptor 4 structure-activity relationship, *Biochim. Biophys. Acta - Mol. Cell Biol. Lipids*. 1862 (2016) 1439–1450. doi:10.1016/j.bbalip.2017.01.004.
- [194] S. Yao, N. Yang, G. Song, H. Sang, H. Tian, C. Miao, Y. Zhang, S. Qin, Minimally modified low-density lipoprotein induces macrophage endoplasmic reticulum stress via toll-like receptor 4, *Biochim. Biophys. Acta - Mol. Cell Biol. Lipids*. 1821 (2012) 954–963.
doi:10.1016/j.bbalip.2012.03.003.
- [195] D.M. Rocha, A.P. Caldas, L.L. Oliveira, J. Bressan, H.H. Hermsdorff, Saturated fatty acids trigger TLR4-mediated inflammatory response, *Atherosclerosis*. 244 (2016) 211–215.
doi:10.1016/j.atherosclerosis.2015.11.015.
- [196] J.Y. Lee, J. Ye, Z. Gao, H.S. Youn, W.H. Lee, L. Zhao, N. Sizemore, D.H. Hwang, Reciprocal modulation of toll-like receptor-4 signaling pathways involving MyD88 and phosphatidylinositol 3-kinase/AKT by saturated and polyunsaturated fatty acids, *J. Biol. Chem*. 278 (2003) 37041–37051.
doi:10.1074/jbc.M305213200.
- [197] D.A. Nicholas, K. Zhang, C. Hung, S. Glasgow, A.W. Aruni, J. Unternaehrer, K.J. Payne, W.H.R. Langridge, M. De Leon, Palmitic acid is a toll-like receptor 4 ligand that induces human dendritic cell secretion of IL-1 β , *PLoS One*. 12 (2017) e0176793. doi:10.1371/journal.pone.0176793.
- [198] A. Schaeffler, P. Gross, R. Buettner, C. Bollheimer, C. Buechler, M. Neumeier, A. Kopp, J. Schoelmerich, W. Falk, Fatty acid-induced induction of Toll-like receptor-4/nuclear factor-kappaB pathway in adipocytes links nutritional signalling with innate immunity, *Immunology*. 126 (2009)

233–245. doi:10.1111/j.1365-2567.2008.02892.x.

- [199] B.S. Park, D.H. Song, H.M. Kim, B.-S. Choi, H. Lee, J.-O. Lee, The structural basis of lipopolysaccharide recognition by the TLR4–MD-2 complex, *Nature*. 458 (2009) 1191–1195. doi:10.1038/nature07830.
- [200] H. Yamada, T. Umemoto, M. Kawano, M. Kawakami, M. Kakei, S. ichi Momomura, S. e. Ishikawa, K. Hara, High-density lipoprotein and apolipoprotein A-I inhibit palmitate-induced translocation of toll-like receptor 4 into lipid rafts and inflammatory cytokines in 3T3-L1 adipocytes, *Biochem. Biophys. Res. Commun.* 484 (2017) 403–408. doi:10.1016/j.bbrc.2017.01.138.
- [201] A.M. Cheng, P. Handa, S. Tateya, J. Schwartz, C. Tang, P. Mitra, J.F. Oram, A. Chait, F. Kim, Apolipoprotein A-I attenuates palmitate-mediated NF- κ B activation by reducing toll-like receptor-4 recruitment into lipid rafts, *PLoS One*. 7 (2012). doi:10.1371/journal.pone.0033917.
- [202] C.R. Stewart, L.M. Stuart, K. Wilkinson, J.M. Van Gils, A. Halle, K.J. Rayner, L. Boyer, R. Zhong, W. A, A. Lacy-hulbert, J. El Khoury, D.T. Golenbock, K. J, CD36 ligands promote sterile inflammation through assembly of a Toll-like receptor 4 and 6 heterodimer., *Nat. Immunol.* 11 (2010) 155–161. doi:10.1038/ni.1836.CD36.
- [203] A. Płóciennikowska, A. Hromada-Judycka, K. Borzęcka, K. Kwiatkowska, Co-operation of TLR4 and raft proteins in LPS-induced pro-inflammatory signaling, *Cell. Mol. Life Sci.* 72 (2015) 557–581. doi:10.1007/s00018-014-1762-5.
- [204] H. Kamiyama, K. Kakoki, S. Shigematsu, M. Izumida, Y. Yashima, Y. Tanaka, H. Hayashi, T. Matsuyama, H. Sato, N. Yamamoto, T. Sano, Y. Shidoji, Y. Kubo, CXCR4-Tropic, But Not CCR5-Tropic, Human Immunodeficiency Virus Infection Is Inhibited by the Lipid Raft-Associated Factors, Acyclic Retinoid Analogs, and Cholera Toxin B Subunit, *AIDS Res. Hum. Retroviruses*. 29 (2013) 279–288. doi:10.1089/AID.2012.0174.
- [205] A.P. West, I.E. Brodsky, C. Rahner, D.K. Woo, H. Erdjument-Bromage, P. Tempst, M.C. Walsh, Y. Choi, G.S. Shadel, S. Ghosh, TLR signaling augments macrophage bactericidal activity through

mitochondrial ROS, *Nature*. 472 (2011) 476–480. doi:10.1038/nature09973.

- [206] Y. Min, S.M. Wi, D. Shin, E. Chun, K.-Y. Lee, Peroxiredoxin-6 Negatively Regulates Bactericidal Activity and NF- κ B Activity by Interrupting TRAF6-ECSIT Complex, *Front. Cell. Infect. Microbiol.* 7 (2017) 94. doi:10.3389/fcimb.2017.00094.
- [207] Z. Sepehri, Z. Kiani, F. Kohan, S.M. Alavian, S. Ghavami, Toll like receptor 4 and hepatocellular carcinoma; A systematic review, *Life Sci.* 179 (2017) 80–87. doi:10.1016/j.lfs.2017.04.025.
- [208] K. Okita, N. Izumi, K. Ikeda, Y. Osaki, K. Numata, M. Ikeda, N. Kokudo, K. Imanaka, S. Nishiguchi, S. Kondo, Y. Nishigaki, S. Shiomi, K. Ueshima, N. Isoda, Y. Karino, M. Kudo, K. Tanaka, S. Kaneko, H. Moriwaki, M. Makuuchi, T. Okusaka, N. Hayashi, Y. Ohashi, H. Kumada, Survey of survival among patients with hepatitis C virus-related hepatocellular carcinoma treated with peretinoin, an acyclic retinoid, after the completion of a randomized, placebo-controlled trial, *J. Gastroenterol.* 50 (2015) 667–674. doi:10.1007/s00535-014-0996-1.
- [209] K. Schroder, J. Tschopp, The Inflammasomes, *Cell*. 140 (2010) 821–832. doi:10.1016/j.cell.2010.01.040.
- [210] J.A.S. Roberts, Özlem Yilmaz, Dangerous liaisons: Caspase-11 and reactive oxygen species crosstalk in pathogen elimination, *Int. J. Mol. Sci.* 16 (2015) 23337–23354. doi:10.3390/ijms161023337.
- [211] N. Kayagaki, M.T. Wong, I.B. Stowe, S.R. Ramani, L.C. Gonzalez, S. Akashi-Takamura, K. Miyake, J. Zhang, W.P. Lee, A. Muszynski, L.S. Forsberg, R.W. Carlson, V.M. Dixit, Noncanonical Inflammasome Activation by Intracellular LPS Independent of TLR4., *Science*. 341 (2013) 1246–1249. doi:10.1126/science.1240248.
- [212] J.A. Hagar, D.A. Powell, Y. Aachoui, R.K. Ernst, E.A. Miao, Cytoplasmic LPS Activates Caspase-11: Implications in TLR4-Independent Endotoxic Shock, *Science*. 341 (2013) 1250–1253. doi:10.1126/science.1240988.
- [213] P. Broz, T. Ruby, K. Belhocine, D.M. Bouley, N. Kayagaki, V.M. Dixit, D.M. Monack, Caspase-11

- increases susceptibility to Salmonella infection in the absence of caspase-1, *Nature*. 490 (2012) 288–291. doi:10.1038/nature11419.
- [214] Z.M. Bian, S.G. Elner, V.M. Elner, Dual involvement of caspase-4 in inflammatory and ER stress-induced apoptotic responses in human retinal pigment epithelial cells, *Investig. Ophthalmol. Vis. Sci.* 50 (2009) 6006–6014. doi:10.1167/iovs.09-3628.
- [215] W. Paschen, Dependence of vital cell function on endoplasmic reticulum calcium levels: implications for the mechanisms underlying neuronal cell injury in different pathological states, *Cell Calcium*. 29 (2001) 1–11. doi:10.1054/ceca.2000.0162.
- [216] R.J. Kaufman, Stress signaling from the lumen of the endoplasmic reticulum: coordination of gene transcriptional and translational controls, *Genes Dev.* 13 (1999) 1211–1233. doi:10.1101/gad.13.10.1211.
- [217] M.P. Mattson, F.M. LaFerla, S.L. Chan, M. a Leissring, P.N. Shepel, J.D. Geiger, Calcium signaling in the ER: its role in neuronal plasticity and neurodegenerative disorders., *Trends Neurosci.* 23 (2000) 222–229. doi:10.1016/S0166-2236(00)01548-4.
- [218] M.J. Amaya, M.H. Nathanson, Calcium signaling in the liver, *Compr. Physiol.* 3 (2013) 515–539. doi:10.1002/cphy.c120013.
- [219] S. Tsuchiya, M. Tsuji, Y. Morio, K. Oguchi, Involvement of endoplasmic reticulum in glycochenodeoxycholic acid-induced apoptosis in rat hepatocytes, *Toxicol. Lett.* 166 (2006) 140–149. doi:10.1016/j.toxlet.2006.06.006.
- [220] N. Dejeans, N. Tajeddine, R. Beck, J. Verrax, H. Taper, P. Gailly, P.B. Calderon, Endoplasmic reticulum calcium release potentiates the ER stress and cell death caused by an oxidative stress in MCF-7 cells, *Biochem. Pharmacol.* 79 (2010) 1221–1230. doi:10.1016/j.bcp.2009.12.009.
- [221] S.K. Ray, M. Fidan, M.W. Nowak, G.G. Wilford, E.L. Hogan, N.L. Banik, Oxidative stress and Ca²⁺ influx upregulate calpain and induce apoptosis in PC12 cells, *Brain Res.* 852 (2000) 326–334. doi:10.1016/S0006-8993(99)02148-4.

- [222] J. Hitomi, T. Katayama, Y. Eguchi, T. Kudo, M. Taniguchi, Y. Koyama, T. Manabe, S. Yamagishi, Y. Bando, K. Imaizumi, Y. Tsujimoto, M. Tohyama, Involvement of caspase-4 in endoplasmic reticulum stress-induced apoptosis and Abeta-induced cell death., *J. Cell Biol.* 165 (2004) 347–56.
doi:10.1083/jcb.200310015.
- [223] C.C. Jiang, L.H. Chen, S. Gillespie, Y.F. Wang, K. a Kiejda, X.D. Zhang, P. Hersey, Inhibition of MEK sensitizes human melanoma cells to endoplasmic reticulum stress-induced apoptosis., *Cancer Res.* 67 (2007) 9750–9761. doi:10.1158/0008-5472.CAN-07-2047.
- [224] X. Wang, M. Narayanan, J.M. Bruey, D. Rigamonti, E. Cattaneo, J.C. Reed, R.M. Friedlander, Protective role of Cop in Rip2/Caspase-1/Caspase-4-mediated HeLa cell death, *Biochim. Biophys. Acta - Mol. Basis Dis.* 1762 (2006) 742–754. doi:10.1016/j.bbadis.2006.06.015.
- [225] Y. Hu, M.A. Benedict, D. Wu, N. Inohara, G. Nunez, Bcl-XL interacts with Apaf-1 and inhibits Apaf-1-dependent caspase-9 activation., *Proc. Natl. Acad. Sci. U. S. A.* 95 (1998) 4386–4391.
doi:10.1073/pnas.95.8.4386.
- [226] U. Lakshmanan, A.G. Porter, Caspase-4 interacts with TNF receptor-associated factor 6 and mediates lipopolysaccharide-induced NF-kappaB-dependent production of IL-8 and CC chemokine ligand 4 (macrophage-inflammatory protein-1), *J. Immunol.* 179 (2007) 8480–8490.
doi:10.4049/jimmunol.179.12.8480.
- [227] N. López-Antón, A. Rudy, N. Barth, L.M. Schmitz, G.R. Pettit, K. Schulze-Osthoff, V.M. Dirsch, A.M. Vollmar, The marine product cephalostatin 1 activates an endoplasmic reticulum stress-specific and apoptosome-independent apoptotic signaling pathway, *J. Biol. Chem.* 281 (2006) 33078–33086.
doi:10.1074/jbc.M607904200.
- [228] H.C. Li, C.J. Chen, R. Watts, R.F. Thorne, K.A. Kiejda, D.Z. Xu, P. Hersey, Inhibition of endoplasmic reticulum stress-induced apoptosis of melanoma cells by the ARC protein, *Cancer Res.* 68 (2008) 834–842. doi:10.1158/0008-5472.CAN-07-5056.
- [229] S.T. Nawrocki, J.S. Carew, K.H. Maclean, J.F. Courage, P. Huang, J.A. Houghton, J.L. Cleveland,

F.J. Giles, D.J. McConkey, Myc regulates aggresome formation, the induction of Noxa, and apoptosis in response to the combination of bortezomib and SAHA, *Blood*. 112 (2008) 2917–2926.

doi:10.1182/blood-2007-12-130823.

- [230] M. Rahmani, E.M. Davis, T.R. Crabtree, J.R. Habibi, T.K. Nguyen, P. Dent, S. Grant, The kinase inhibitor sorafenib induces cell death through a process involving induction of endoplasmic reticulum stress., *Mol. Cell. Biol.* 27 (2007) 5499–5513. doi:10.1128/MCB.01080-06.
- [231] P. Pyrko, A. Kardosh, W. Wang, W. Xiong, A.H. Schönthal, T.C. Chen, HIV-1 protease inhibitors nelfinavir and atazanavir induce malignant glioma death by triggering endoplasmic reticulum stress, *Cancer Res.* 67 (2007) 10920–10928. doi:10.1158/0008-5472.CAN-07-0796.
- [232] S. Kamada, M. Washida, J. Hasegawa, H. Kusano, Y. Funahashi, Y. Tsujimoto, Involvement of caspase-4(-like) protease in Fas-mediated apoptotic pathway., *Oncogene*. 15 (1997) 285–290. doi:10.1038/sj.onc.1201192.
- [233] S.B. Kovacs, E.A. Miao, Gasdermins: Effectors of Pyroptosis, *Trends Cell Biol.* 27 (2017) 673–684. doi:10.1016/j.tcb.2017.05.005.
- [234] X. Chen, W. He, L. Hu, J. Li, Y. Fang, X. Wang, X. Xu, Z. Wang, K. Huang, J. Han, Pyroptosis is driven by non-selective gasdermin-D pore and its morphology is different from MLKL channel-mediated necroptosis, *Cell Res.* 26 (2016) 1007–1020. doi:10.1038/cr.2016.100.
- [235] S. Rühl, P. Broz, GSDMD membrane pore formation constitutes the mechanism of pyroptotic cell death, *EMBO J.* (2016) e201694696-13. doi:10.15252/emboj.201694696.
- [236] N. Kayagaki, I.B. Stowe, B.L. Lee, K. O'Rourke, K. Anderson, S. Warming, T. Cuellar, B. Haley, M. Roose-Girma, Q.T. Phung, P.S. Liu, J.R. Lill, H. Li, J. Wu, S. Kummerfeld, J. Zhang, W.P. Lee, S.J. Snipas, G.S. Salvesen, L.X. Morris, L. Fitzgerald, Y. Zhang, E.M. Bertram, C.C. Goodnow, V.M. Dixit, Caspase-11 cleaves gasdermin D for non-canonical inflammasome signalling., *Nature*. 526 (2015) 666–671. doi:10.1038/nature15541.
- [237] R.O. Costa, E. Ferreira, I. Martins, I. Santana, S.M. Cardoso, C.R. Oliveira, C.M.F. Pereira, Amyloid

- β -induced ER stress is enhanced under mitochondrial dysfunction conditions, *Neurobiol. Aging*. 33 (2012) 824.e5-824.e16. doi:10.1016/j.neurobiolaging.2011.04.011.
- [238] A. Nakajima, M. Tsuji, M. Inagaki, Y. Tamura, M. Kato, A. Niiya, Y. Usui, K. Oguchi, Neuroprotective effects of propofol on ER stress-mediated apoptosis in neuroblastoma SH-SY5Y cells, *Eur. J. Pharmacol.* 725 (2014) 47–54. doi:10.1016/j.ejphar.2014.01.003.
- [239] Z. Shigemi, K. Manabe, N. Hara, Y. Baba, K. Hosokawa, H. Kagawa, T. Watanabe, M. Fujimuro, Methylseleninic acid and sodium selenite induce severe ER stress and subsequent apoptosis through UPR activation in PEL cells, *Chem. Biol. Interact.* 266 (2017) 28–37. doi:10.1016/j.cbi.2017.01.027.
- [240] A. Koramagazi, D. Wang, B. Yousef, M. Guerram, F. Yu, Rhein triggers apoptosis via induction of endoplasmic reticulum stress, caspase-4 and intracellular calcium in primary human hepatic HL-7702 cells, *Biochem. Biophys. Res. Commun.* 473 (2016) 230–236. doi:10.1016/j.bbrc.2016.03.084.
- [241] A. El-Khattouti, D. Selimovic, M. Hannig, E.B. Taylor, Z.Y. Abd Elmageed, S.Y. Hassan, Y. Haikel, E. Kandil, M. Leverkus, R.T. Brodell, M. Megahed, M. Hassan, Imiquimod-induced apoptosis of melanoma cells is mediated by ER stress-dependent Noxa induction and enhanced by NF- κ B inhibition, *J. Cell. Mol. Med.* 20 (2016) 266–286. doi:10.1111/jcmm.12718.
- [242] C.C. Jiang, Z.G. Mao, K.A. Avery-Kiejda, M. Wade, P. Hersey, X.D. Zhang, Glucose-regulated protein 78 antagonizes cisplatin and adriamycin in human melanoma cells, *Carcinogenesis*. 30 (2009) 197–204. doi:10.1093/carcin/bgn220.
- [243] S. Matsuzaki, T. Hiratsuka, R. Kuwahara, T. Katayama, M. Tohyama, Caspase-4 is partially cleaved by calpain via the impairment of Ca²⁺ homeostasis under the ER stress, *Neurochem. Int.* 56 (2010) 352–356. doi:10.1016/j.neuint.2009.11.007.
- [244] M. Buschbeck, S.B. Hake, Variants of core histones and their roles in cell fate decisions, development and cancer, *Nat. Rev. Mol. Cell Biol.* 18 (2017) 299–314. doi:10.1038/nrm.2016.166.
- [245] Z. Feng, Y. Yao, C. Zhou, F. Chen, F. Wu, L. Wei, W. Liu, S. Dong, M. Redell, Q. Mo, Y. Song, Pharmacological inhibition of LSD1 for the treatment of MLL-rearranged leukemia, *J. Hematol.*

Oncol. 9 (2016) 24. doi:10.1186/s13045-016-0252-7.

- [246] Y. Shi, F. Lan, C. Matson, P. Mulligan, J.R. Whetstone, P.A. Cole, R.A. Casero, Y. Shi, Histone demethylation mediated by the nuclear amine oxidase homolog LSD1, *Cell*. 119 (2004) 941–953. doi:10.1016/j.cell.2004.12.012.
- [247] A. Sakamoto, S. Hino, K. Nagaoka, K. Anan, R. Takase, H. Matsumori, H. Ojima, Y. Kanai, K. Arita, M. Nakao, Lysine demethylase LSD1 coordinates glycolytic and mitochondrial metabolism in hepatocellular carcinoma cells, *Cancer Res*. 75 (2015) 1445–1456. doi:10.1158/0008-5472.CAN-14-1560.
- [248] Z.K. Zhao, H.F. Yu, D.R. Wang, P. Dong, L. Chen, W.G. Wu, W.J. Ding, Y. Bin Liu, Overexpression of lysine specific demethylase 1 predicts worse prognosis in primary hepatocellular carcinoma patients, *World J. Gastroenterol*. 18 (2012) 6651–6656. doi:10.3748/wjg.v18.i45.6651.
- [249] D. Duteil, M. Tomic, F. Lausecker, H.Z. Nenseth, J.M. Müller, S. Urban, D. Willmann, K. Petroll, N. Messaddeq, L. Arrigoni, T. Manke, J.W. Kornfeld, J.C. Brüning, V. Zagoriy, M. Meret, J. Dengjel, T. Kanouni, R. Schüle, Lsd1 Ablation Triggers Metabolic Reprogramming of Brown Adipose Tissue, *Cell Rep*. 17 (2016) 1008–1021. doi:10.1016/j.celrep.2016.09.053.
- [250] K.R. Karch, J.E. DeNizio, B.E. Black, B.A. Garcia, Identification and interrogation of combinatorial histone modifications, *Front. Genet*. 4 (2013). doi:10.3389/fgene.2013.00264.
- [251] K. Luger, a W. Mäder, R.K. Richmond, D.F. Sargent, T.J. Richmond, Crystal structure of the nucleosome core particle at 2.8 Å resolution., *Nature*. 389 (1997) 251–260. doi:10.1038/38444.
- [252] M.S. Cosgrove, Histone proteomics and the epigenetic regulation of nucleosome mobility., *Expert Rev. Proteomics*. 4 (2007) 465–478. doi:10.1586/14789450.4.4.465.
- [253] T. Jenuwein, C.D. Allis, Translating the histone code., *Science*. 293 (2001) 1074–1080. doi:10.1126/science.1063127.
- [254] T. Oike, H. Ogiwara, N. Amornwichee, T. Nakano, T. Kohno, Chromatin-regulating proteins as targets for cancer therapy, *J. Radiat. Res*. 55 (2014) 613–628. doi:10.1093/jrr/rrt227.

- [255] C.R. Clapier, B.R. Cairns, The Biology of Chromatin Remodeling Complexes, *Annu. Rev. Biochem.* 78 (2009) 273–304. doi:10.1146/annurev.biochem.77.062706.153223.
- [256] B. Gu, M.G. Lee, Histone H3 lysine 4 methyltransferases and demethylases in self-renewal and differentiation of stem cells., *Cell Biosci.* 3 (2013) 39. doi:10.1186/2045-3701-3-39.
- [257] G.G. Wozniak, B.D. Strahl, Hitting the “mark”: Interpreting lysine methylation in the context of active transcription, *Biochim. Biophys. Acta - Gene Regul. Mech.* 1839 (2014) 1353–1361. doi:10.1016/j.bbagr.2014.03.002.
- [258] G. Pan, S. Tian, J. Nie, C. Yang, V. Ruotti, H. Wei, G.A. Jonsdottir, R. Stewart, J.A. Thomson, Whole-Genome Analysis of Histone H3 Lysine 4 and Lysine 27 Methylation in Human Embryonic Stem Cells, *Cell Stem Cell.* 1 (2007) 299–312. doi:10.1016/j.stem.2007.08.003.
- [259] A. Barski, S. Cuddapah, K. Cui, T.Y. Roh, D.E. Schones, Z. Wang, G. Wei, I. Chepelev, K. Zhao, High-Resolution Profiling of Histone Methylations in the Human Genome, *Cell.* 129 (2007) 823–837. doi:10.1016/j.cell.2007.05.009.
- [260] H.M. Herz, M. Mohan, A.S. Garruss, K. Liang, Y. hei Takahashi, K. Mickey, O. Voets, C.P. Verrijzer, A. Shilatifard, Enhancer-associated H3K4 monomethylation by trithorax-related, the drosophila homolog of mammalian MLL3/MLL4, *Genes Dev.* 26 (2012) 2604–2620. doi:10.1101/gad.201327.112.
- [261] M.G. Guenther, S.S. Levine, L.A. Boyer, R. Jaenisch, R.A. Young, A Chromatin Landmark and Transcription Initiation at Most Promoters in Human Cells, *Cell.* 130 (2007) 77–88. doi:10.1016/j.cell.2007.05.042.
- [262] T.S. Mikkelsen, J. Hanna, X. Zhang, M. Ku, M. Wernig, P. Schorderet, B.E. Bernstein, R. Jaenisch, E.S. Lander, A. Meissner, Dissecting direct reprogramming through integrative genomic analysis, *Nature.* 454 (2008) 49–55. doi:10.1038/nature07056.
- [263] B.E. Bernstein, A. Meissner, E.S. Lander, The Mammalian Epigenome, *Cell.* 128 (2007) 669–681. doi:10.1016/j.cell.2007.01.033.

- [264] A. Adamo, B. Sesé, S. Boue, J. Castaño, I. Paramonov, M.J. Barrero, J.C.I. Belmonte, LSD1 regulates the balance between self-renewal and differentiation in human embryonic stem cells, *Nat. Cell Biol.* 13 (2011) 652–660. doi:10.1038/ncb2246.
- [265] W.A. Whyte, S. Bilodeau, D.A. Orlando, H.A. Hoke, G.M. Frampton, C.T. Foster, S.M. Cowley, R.A. Young, Enhancer decommissioning by LSD1 during embryonic stem cell differentiation., *Nature.* 482 (2012) 221–225. doi:10.1038/nature10805.
- [266] B.E. Bernstein, M. Kamal, K. Lindblad-Toh, S. Bekiranov, D.K. Bailey, D.J. Huebert, S. McMahon, E.K. Karlsson, E.J. Kulbokas, T.R. Gingeras, S.L. Schreiber, E.S. Lander, Genomic maps and comparative analysis of histone modifications in human and mouse, *Cell.* 120 (2005) 169–181. doi:10.1016/j.cell.2005.01.001.
- [267] M. Weber, I. Hellmann, M.B. Stadler, L. Ramos, S. Pääbo, M. Rebhan, D. Schübeler, Distribution, silencing potential and evolutionary impact of promoter DNA methylation in the human genome, *Nat. Genet.* 39 (2007) 457–466. doi:10.1038/ng1990.
- [268] A. Visel, M.J. Blow, Z. Li, T. Zhang, J.A. Akiyama, A. Holt, I. Plajzer-Frick, M. Shoukry, C. Wright, F. Chen, V. Afzal, B. Ren, E.M. Rubin, L.A. Pennacchio, ChIP-seq accurately predicts tissue-specific activity of enhancers, *Nature.* 457 (2009) 854–858. doi:10.1038/nature07730.
- [269] N.D. Heintzman, G.C. Hon, R.D. Hawkins, P. Kheradpour, A. Stark, L.F. Harp, Z. Ye, L.K. Lee, R.K. Stuart, C.W. Ching, K.A. Ching, J.E. Antosiewicz-Bourget, H. Liu, X. Zhang, R.D. Green, V. V. Lobanenkov, R. Stewart, J.A. Thomson, G.E. Crawford, M. Kellis, B. Ren, Histone modifications at human enhancers reflect global cell-type-specific gene expression, *Nature.* 459 (2009) 108–112. doi:10.1038/nature07829.
- [270] S. Goda, T. Isagawa, Y. Chikaoka, T. Kawamura, H. Aburatani, Control of histone H3 lysine 9 (H3K9) methylation state via cooperative two-step demethylation by jumonji domain containing 1A (JMJD1A) homodimer, *J. Biol. Chem.* 288 (2013) 36948–36956. doi:10.1074/jbc.M113.492595.
- [271] J.C. Black, J.R. Whetstine, Tipping the lysine methylation balance in disease, *Biopolymers.* 99 (2013)

127–135. doi:10.1002/bip.22136.

- [272] D. Grafodatskaya, B.H.Y. Chung, D.T. Butcher, A.L. Turinsky, S.J. Goodman, S. Choufani, Y.-A. Chen, Y. Lou, C. Zhao, R. Rajendram, F.E. Abidi, C. Skinner, J. Stavropoulos, C. a Bondy, J. Hamilton, S. Wodak, S.W. Scherer, C.E. Schwartz, R. Weksberg, Multilocus loss of DNA methylation in individuals with mutations in the histone H3 lysine 4 demethylase KDM5C., *BMC Med. Genomics*. 6 (2013) 1. doi:10.1186/1755-8794-6-1.
- [273] M. Shahhoseini, Z. Taghizadeh, M. Hatami, H. Baharvand, Retinoic acid dependent histone 3 demethylation of the clustered HOX genes during neural differentiation of human embryonic stem cells., *Biochem. Cell Biol.* 91 (2013) 116–122. doi:10.1139/bcb-2012-0049.
- [274] E. Shen, H. Shulha, Z. Weng, S. Akbarian, Regulation of histone H3K4 methylation in brain development and disease, *Philos. Trans. R. Soc. B Biol. Sci.* 369 (2014) 20130514. doi:10.1098/rstb.2013.0514.
- [275] C. Huang, J. Cheng, T. Bawa-Khalfe, X. Yao, Y.E. Chin, E.T.H. Yeh, SUMOylated ORC2 Recruits a Histone Demethylase to Regulate Centromeric Histone Modification and Genomic Stability, *Cell Rep.* 15 (2016) 147–157. doi:10.1016/j.celrep.2016.02.091.
- [276] V. Kashuba, a Protopopov, R. Podowski, R. Gizatullin, J. Li, G. Klein, C. Wahlestedt, E. Zabarovsky, Isolation and chromosomal localization of a new human retinoblastoma binding protein 2 homologue 1a (RBBP2H1A)., *Eur. J. Hum. Genet.* 8 (2000) 407–413. doi:10.1038/sj.ejhg.5200474.
- [277] Y. Jin, T.Y. Kim, M.S. Kim, M.A. Kim, S.H. Park, Y.K. Jang, Nuclear import of human histone lysine-specific demethylase LSD1, *J. Biochem.* 156 (2014) 305–313. doi:10.1093/jb/mvu042.
- [278] T. Maes, E. Carceller, J. Salas, A. Ortega, C. Buesa, Advances in the development of histone lysine demethylase inhibitors, *Curr. Opin. Pharmacol.* 23 (2015) 52–60. doi:10.1016/j.coph.2015.05.009.
- [279] National Institutes of Health, National Institutes of Health Sleep Disorders Research Plan, 2011. doi:Report No. DOT HS 808 707.
- [280] V.D. Nair, Y. Ge, N. Balasubramaniyan, J. Kim, Y. Okawa, M. Chikina, O. Troyanskaya, S.C.

- Sealfon, Involvement of histone demethylase LSD1 in short-time-scale gene expression changes during cell cycle progression in embryonic stem cells., *Mol. Cell. Biol.* 32 (2012) 4861–4876.
doi:10.1128/MCB.00816-12.
- [281] D. Hayward, P.A. Cole, LSD1 Histone Demethylase Assays and Inhibition, in: *Methods Enzymol.*, 2016: pp. 261–278. doi:10.1016/bs.mie.2016.01.020.
- [282] K. Meier, A. Brehm, Chromatin regulation: How complex does it get?, *Epigenetics.* 9 (2014) 1485–1495. doi:10.4161/15592294.2014.971580.
- [283] X. Lai, Reproducible method to enrich membrane proteins with high purity and high yield for an LC-MS/MS approach in quantitative membrane proteomics, *Electrophoresis.* 34 (2013) 809–817. doi:10.1002/elps.201200503.
- [284] C.N. Vallianatos, S. Iwase, Disrupted intricacy of histone H3K4 methylation in neurodevelopmental disorders., *Epigenomics.* 7 (2015) 503–519. doi:10.2217/epi.15.1.
- [285] I. Scionti, S. Hayashi, S. Mouradian, E. Girard, J. Esteves de Lima, V. Morel, T. Simonet, M. Wurmser, P. Maire, K. Ancelin, E. Metzger, R. Schüle, E. Goillot, F. Relax, L. Schaeffer, LSD1 Controls Timely MyoD Expression via MyoD Core Enhancer Transcription, *Cell Rep.* 18 (2017) 1996–2006. doi:10.1016/j.celrep.2017.01.078.
- [286] M. Kuppaswamy, S. Vijayalingam, L.-J. Zhao, Y. Zhou, T. Subramanian, J. Ryerse, G. Chinnadurai, Role of the PLDLS-Binding Cleft Region of CtBP1 in Recruitment of Core and Auxiliary Components of the Corepressor Complex, *Mol. Cell. Biol.* 28 (2008) 269–281. doi:10.1128/MCB.01077-07.
- [287] M.J. Gamble, W.L. Kraus, Visualizing the Histone Code on LSD1, *Cell.* 128 (2007) 433–434. doi:10.1016/j.cell.2007.01.017.
- [288] C. Cai, H.H. He, S. Chen, I. Coleman, H. Wang, Z. Fang, S. Chen, P.S. Nelson, X.S. Liu, M. Brown, S.P. Balk, Androgen Receptor Gene Expression in Prostate Cancer Is Directly Suppressed by the Androgen Receptor Through Recruitment of Lysine-Specific Demethylase 1, *Cancer Cell.* 20 (2011)

457–471. doi:10.1016/j.ccr.2011.09.001.

- [289] G. Sun, K. Alzayady, R. Stewart, P. Ye, S. Yang, W. Li, Y. Shi, Histone demethylase LSD1 regulates neural stem cell proliferation., *Mol. Cell. Biol.* 30 (2010) 1997–2005. doi:10.1128/MCB.01116-09.
- [290] F. Forneris, C. Binda, M.A. Vanoni, E. Battaglioli, A. Mattevi, Human histone demethylase LSD1 reads the histone code, *J. Biol. Chem.* 280 (2005) 41360–41365. doi:10.1074/jbc.M509549200.
- [291] M. Yang, C.B. Gocke, X. Luo, D. Borek, D.R. Tomchick, M. Machius, Z. Otwinowski, H. Yu, Structural Basis for CoREST-Dependent Demethylation of Nucleosomes by the Human LSD1 Histone Demethylase, *Mol. Cell.* 23 (2006) 377–387. doi:10.1016/j.molcel.2006.07.012.
- [292] L. Piao, T. Suzuki, N. Dohmae, Y. Nakamura, R. Hamamoto, SUV39H2 methylates and stabilizes LSD1 by inhibiting polyubiquitination in human cancer cells., *Oncotarget.* 6 (2015) 16939–16950. doi:10.18632/oncotarget.4760.
- [293] S.K. Veetil, N. Teerawattanapong, S.M. Ching, K.G. Lim, S. Saokaew, P. Phisalprapa, N. Chaiyakunapruk, Effects of chemopreventive agents on the incidence of recurrent colorectal adenomas: A systematic review with network meta-analysis of randomized controlled trials, *Onco. Targets. Ther.* 17 (2017) 763. doi:10.2147/OTT.S127335.
- [294] V. Ramesh, K. Selvarasu, J. Pandian, S. Myilsamy, C. Shanmugasundaram, K. Ganesan, NFκB activation demarcates a subset of hepatocellular carcinoma patients for targeted therapy, *Cell. Oncol.* 39 (2016) 523–536. doi:10.1007/s13402-016-0294-4.
- [295] E.I. Marks, N.S. Yee, Molecular Genetics and Targeted Therapy in Hepatocellular Carcinoma., *Curr. Cancer Drug Targets.* 16 (2016) 53–70. doi:10.2174/1568009615666150916092903.
- [296] C. Hayashi, C. V. Gudino, F.C. Gibson, C.A. Genco, Pathogen-induced inflammation at sites distant from oral infection: Bacterial persistence and induction of cell-specific innate immune inflammatory pathways, *Mol. Oral Microbiol.* 25 (2010) 305–316. doi:10.1111/j.2041-1014.2010.00582.x.
- [297] M. Rola-Pleszczynski, S. Gouin, R. Bégin, Asbestos-induced lung inflammation - Role of local macrophage-derived chemotactic factors in accumulation of neutrophils in the lungs, *Inflammation.* 8

(1984) 53–62. doi:10.1007/BF00918353.

- [298] J.M. Carter, K.E. Driscoll, The role of inflammation, oxidative stress, and proliferation in silica-induced lung disease: a species comparison., *J. Environ. Pathol. Toxicol. Oncol.* 20 Suppl 1 (2001) 33–43. doi: 10.1615/JEnvironPatholToxicolOncol.
- [299] V. Stejskal, K. Öckert, G. Bjørklund, Metal-induced inflammation triggers fibromyalgia in metal-allergic patients, *Neuroendocrinol. Lett.* 34 (2013) 559–565.
- [300] L.L. Hruza, A.P. Pentland, Mechanisms of UV-Induced Inflammation, *J. Invest. Dermatol.* 100 (1993) S35–S41. doi:10.1038/jid.1993.21.
- [301] D. Schaeue, E.D. Micewicz, J.A. Ratikan, M.W. Xie, G. Cheng, W.H. McBride, Radiation and Inflammation, *Semin. Radiat. Oncol.* 25 (2015) 4–10. doi:10.1016/j.semradonc.2014.07.007.
- [302] L.J. Moilanen, M. Hämäläinen, L. Lehtimäki, R.M. Nieminen, E. Moilanen, Urate crystal induced inflammation and joint pain are reduced in transient receptor potential ankyrin 1 deficient mice - Potential role for transient receptor potential ankyrin1 in gout, *PLoS One.* 10 (2015). doi:10.1371/journal.pone.0117770.
- [303] P. Hirsova, S.H. Ibrahim, A. Krishnan, V.K. Verma, S.F. Bronk, N.W. Werneburg, M.R. Charlton, V.H. Shah, H. Malhi, G.J. Gores, Lipid-Induced Signaling Causes Release of Inflammatory Extracellular Vesicles from Hepatocytes, *Gastroenterology.* 150 (2016) 956–967. doi:10.1053/j.gastro.2015.12.037.
- [304] Y. Lin, A.H. Berg, P. Iyengar, T.K.T. Lam, A. Giacca, T.P. Combs, M.W. Rajala, X. Du, B. Rollman, W. Li, M. Hawkins, N. Barzilai, C.J. Rhodes, I.G. Fantus, M. Brownlee, P.E. Scherer, The hyperglycemia-induced inflammatory response in adipocytes: the role of reactive oxygen species., *J. Biol. Chem.* 280 (2005) 4617–4626. doi:10.1074/jbc.M411863200.
- [305] M.A. McArdle, O.M. Finucane, R.M. Connaughton, A.M. McMorrow, H.M. Roche, Mechanisms of obesity-induced inflammation and insulin resistance: Insights into the emerging role of nutritional strategies, *Front. Endocrinol. (Lausanne).* 4 (2013). doi:10.3389/fendo.2013.00052.

- [306] Y. Liu, K. Kimura, T. Orita, K.H. Sonoda, Necrosis-induced sterile inflammation mediated by interleukin-1 α in retinal pigment epithelial cells, *PLoS One*. 10 (2015).
doi:10.1371/journal.pone.0144460.
- [307] H. Tsutsui, K. Adachi, E. Seki, K. Nakanishi, Cytokine-induced inflammatory liver injuries., *Curr. Mol. Med.* 3 (2003) 545–559. doi:10.2174/1566524033479618.
- [308] A.K. Abbas, A.H. Lichtman, S. Pillai, Basic immunology: functions and disorders of the immune system, in: *Basic Immunol. Funct. Disord. Immune Syst.*, 2012: pp. 303–305.
doi:10.1007/978-1-62703-589-7_1.
- [309] J. Li, M. Setiawan, H. Wu, R.W. Beuerman, P. Zhao, Regulation of toll-like receptor expression in human conjunctival epithelial cells, *Mediators Inflamm.* 2014 (2014). doi:10.1155/2014/493596.
- [310] B. Beutler, E.T. Rietschel, Innate immune sensing and its roots: the story of endotoxin., *Nat. Rev. Immunol.* 3 (2003) 169–176. doi:10.1038/nri1004.
- [311] P.S. Tobias, K. Soldau, R.J. Ulevitch, Isolation of a lipopolysaccharide-binding acute phase reactant from rabbit serum., *J. Exp. Med.* 164 (1986) 777–793. doi:10.1084/jem.164.3.777.
- [312] A. Poltorak, X. He, I. Smirnova, M.Y. Liu, C. Van Huffel, X. Du, D. Birdwell, E. Alejos, M. Silva, C. Galanos, M. Freudenberg, P. Ricciardi-Castagnoli, B. Layton, B. Beutler, Defective LPS signaling in C3H/HeJ and C57BL/10ScCr mice: Mutations in Tlr4 gene, *Science* (80-.). 282 (1998) 2085–2088.
doi:10.1126/science.282.5396.2085.
- [313] R. Shimazu, S. Akashi, H. Ogata, Y. Nagai, K. Fukudome, K. Miyake, M. Kimoto, MD-2, a Molecule that Confers Lipopolysaccharide Responsiveness on Toll-like Receptor 4, *J. Exp. Med.* 189 (1999) 1777–1782. doi:10.1084/jem.189.11.1777.
- [314] S. Wright, R. Ramos, P. Tobias, R. Ulevitch, J. Mathison, CD14, a receptor for complexes of lipopolysaccharide (LPS) and LPS binding protein, *Science* (80-.). 249 (1990) 1431–1433.
doi:10.1126/science.1698311.
- [315] J. Yang, M. Li, Q.C. Zheng, Emerging role of Toll-like receptor 4 in hepatocellular carcinoma., *J.*

Hepatocell. Carcinoma. 2 (2015) 11–17. doi:10.2147/JHC.S44515.

- [316] D.H. Dapito, A. Mencin, G.Y. Gwak, J.P. Pradere, M.K. Jang, I. Mederacke, J.M. Caviglia, H. Khiabani, A. Adeyemi, R. Bataller, J.H. Lefkowitz, M. Bower, R. Friedman, R.B. Sartor, R. Rabadan, R.F. Schwabe, Promotion of Hepatocellular Carcinoma by the Intestinal Microbiota and TLR4, *Cancer Cell*. 21 (2012) 504–516. doi:10.1016/j.ccr.2012.02.007.
- [317] J.K. Rathkey, B.L. Benson, S.M. Chirieleison, J. Yang, T.S. Xiao, G.R. Dubyak, A.Y. Huang, D.W. Abbott, Live-cell visualization of gasdermin D-driven pyroptotic cell death, *J. Biol. Chem.* 292 (2017) 14649–14658. doi:10.1074/jbc.M117.797217.
- [318] D. Perregaux, C.A. Gabel, Interleukin-1 β maturation and release in response to ATP and nigericin. Evidence that potassium depletion mediated by these agents is a necessary and common feature of their activity, *J. Biol. Chem.* 269 (1994) 15195–15203.